

Joint Downlink Beamforming and Discrete Resource Allocation Using Mixed-Integer Programming

Vom Fachbereich 18
Elektrotechnik und Informationstechnik
der Technischen Universität Darmstadt
zur Erlangung der Würde eines
Doktor-Ingenieurs (Dr.-Ing.)
genehmigte Dissertation

von

Yong Cheng, M.Phil.

Geboren am 03. Sep. 1983 in Anhui, P. R. China

Referent:	Prof. Dr. Marius Pesavento
Korreferent:	Prof. Dr. Stefan Ulbrich
Tag der Einreichung:	15. Oct. 2013
Tag der mündlichen Prüfung:	13. Dec. 2013

D17

Darmstädter Dissertation

2013

Declaration

I, the undersigned, hereby declare that this dissertation is my original work and has not been submitted or accepted for the award of any other degree in any institution.

Erklärung laut §9 der Promotionsordnung

Ich versichere hiermit dass ich die vorliegende Dissertation allein und nur unter Verwendung der angegebenen Literatur verfasst habe. Die Arbeit hat bisher noch nicht zu Prüfungszwecken gedient.

Signature/Unterschrift:

Your name here

Place/Ort:

Date/Datum:

Abstract

Multi-antenna processing is widely adopted as one of the key enabling technologies for current and future cellular networks. Particularly, multiuser downlink beamforming (also known as space-division multiple access), in which multiple users are simultaneously served with spatial transmit beams in the same time and frequency resource, achieves high spectral efficiency with reduced energy consumption. To harvest the potential of multiuser downlink beamforming in practical systems, optimal beamformer design shall be carried out jointly with network resource allocation. Due to the specifications of cellular standards and/or implementation constraints, resource allocation in practice naturally necessitates discrete decision makings, e.g., base station (BS) association, user scheduling and admission control, adaptive modulation and coding, and codebook-based beamforming (precoding).

This dissertation focuses on the joint optimization of multiuser downlink beamforming and discrete resource allocation in modern cellular networks. The problems studied in this thesis involve both continuous and discrete decision variables and are thus formulated as mixed-integer programs (MIPs). A systematic MIP framework is developed to address the problems. The MIP framework consists of four components: (i) MIP formulations that support the commercial solver based approach for computing the optimal solutions, (ii) analytic comparisons of the MIP formulations, (iii) customizing techniques for speeding up the MIP solvers, and (iv) low-complexity heuristic algorithms for practical applications.

We consider first joint network topology optimization and multi-cell downlink beamforming (JNOB) for coordinated multi-point transmission. The objective is to minimize the overall power consumption of all BSs while guaranteeing the quality-of-service (QoS) requirements of the mobile stations (MSs). A standard mixed-integer second-order cone program (MISOCP) formulation and an extended MISOCP formulation are developed, both of which support the branch-and-cut (BnC) method. Analysis shows that the extended formulation admits tighter continuous relaxations (and hence less computational complexity) than that of the standard formulation. Effective strategies are proposed to customize the BnC method in the MIP solver CPLEX when applying it to the JNOB problem. Low-complexity inflation and deflation procedures are devised for large-scale applications. The simulations show that our design results in sparse network topologies and partial BS cooperation.

We study next the joint optimization of discrete rate adaptation and downlink beamforming (DRAB), in which rate adaptation is carried out via modulation and coding scheme (MCS) assignment and admission control is embedded in the MCS assignment procedure. The objective is to achieve the maximum sum-rate with the minimum transmitted BS power. As in the JNOB problem, a standard and an extended MISOCP formulations are developed,

and analytic comparisons of the two formulations are carried out. The analysis also leads to efficient customizing strategies for the BnC method in CPLEX. We also develop fast inflation and deflation procedures for applications in large-scale networks. Our numerical results show that the heuristic algorithms yield sum-rates that are very close to the optimal ones.

We then turn our attention to codebook-based downlink beamforming. Codebook-based beamforming is employed in the latest cellular standards, e.g., in long-term evolution advanced (LTE-A), to simplify the signaling procedure of beamformers with reduced signaling overhead. We consider first the standard codebook-based downlink beamforming (SCBF) problem, in which precoding vector assignment and power allocation are jointly optimized. The objective is to minimize the total transmitted BS power while ensuring the prescribed QoS targets of the MSs. We introduce a virtual uplink (VUL) problem, which is proved to be equivalent to the SCBF problem. A customized power iteration method is developed to solve optimally the VUL problem and hence the SCBF problem. To improve the performance of codebook-based downlink beamforming, we propose a channel predistortion mechanism that does not introduce any additional signalling overhead or require modification of the mobile receivers. The joint codebook-based downlink beamforming and channel predistortion (CBCP) problem represents a non-convex MIP. An alternating optimization algorithm and an alternating feasibility search algorithm are devised to approximately solve the CBCP problem. The simulation results confirm the efficiency of the channel predistortion scheme, e.g., achieving significant reductions of the total transmitted BS power.

We study finally the worst-case robust codebook-based downlink beamforming when only estimated channel covariance matrices are available at the BS. Similar to the DRAB problem, user admission control is embedded in the precoding vector assignment procedure. In the robust codebook-based downlink beamforming and admission control (RCBA) problem, the objective is to achieve the maximum number of admitted MSs with the minimum transmitted BS power. We develop a conservative mixed-integer linear program (MILP) approximation and an exact MISOCP formulation of the RCBA problem. We further propose a low-complexity inflation procedure. Our simulations show that the three approaches yield almost the same average number of admitted MSs, while the MILP based approach requires much more transmitted BS power than the other two to support the admitted MSs.

The MIP framework developed in this thesis can be applied to address various discrete resource allocation problems in interference limited cellular networks. Both optimal solutions, i.e., performance benchmarks, and low-complexity practical algorithms are considered in our MIP framework. Conventional approaches often did not adopt the exact discrete models and approximated the discrete variables by (quantized) continuous ones, which could lead to highly suboptimal solutions or infeasible problem instances.

Zusammenfassung

Mehrantennensignalverarbeitung ist als eine der Schlüsseltechnologien für moderne und zukünftige Mobilfunknetze weit verbreitet. Insbesondere das Multiuser Downlink Beamforming (auch bekannt als Space-Division Multiple Access), bei dem mehrere Teilnehmer mit räumlichen Sendestrahlenbündeln (oder Sendebestrahlungen) in derselben Zeit- und Frequenzressource gleichzeitig bedient werden, erreicht eine hohe spektrale Effizienz bei gleichzeitig reduzierter Sendeleistung. Um das Potential von Multiuser Downlink Beamforming in der Praxis nutzbar zu machen, soll der optimale Beamforming Entwurf gemeinsam mit der Netzwerkressourcenvergabe durchgeführt werden. Aufgrund der Spezifikationen in Mobilfunkstandards und/oder Einschränkungen bei der Implementierung erfordert die Ressourcenvergabe diskrete Entscheidungen wie z.B. die Basisstationszuordnung (BS Zuordnung), das Scheduling der Teilnehmer und die Zugangskontrolle, adaptive Modulation und Kodierung sowie *Codebuch-basiertes* Beamforming (Vorkodierung).

Diese Dissertation legt den Schwerpunkt auf die gemeinsame Optimierung von Multiuser Downlink Beamforming und diskreter Ressourcenvergabe in modernen zellularen Mobilfunknetzen. Die Probleme, die in dieser Arbeit untersucht werden, beinhalten sowohl kontinuierliche als auch diskrete Entscheidungsvariablen und werden daher als gemischt ganzzahlige Programme (engl. *mixed-integer programs*, MIPs) formuliert. Ein systematisches MIP Rahmenwerk wird entwickelt, um die Probleme anzugehen. Es besteht aus den folgenden vier Komponenten: (i) den MIP Formulierungen, die den Ansatz unterstützen, optimale Lösungen mittels kommerzieller Software-Löser zu berechnen (Leistungsfähigkeits-Benchmarks), (ii) verschiedener analytischer Leistungsfähigkeitsuntersuchungen, (iii) der individuellen Anpassung der Verfahren, um die MIP Löser zu beschleunigen, und (iv) heuristische Algorithmen, die insbesondere für den Einsatz in praktischen Anwendungen eine geringe Rechenkomplexität aufweisen.

Zunächst betrachten wir die simultane Optimierung, Netzwerktopologie und Multi-Cell Downlink Beamformings (JNOB) für *Coordinated Multi-Point Übertragung*. Ziel ist es, den gesamten Leistungsverbrauch aller BSs zu minimieren und gleichzeitig die Anforderungen an die Service-Qualität (engl. *Quality-of-Service*, QoS) der mobilen Teilnehmer (MSs) zu gewährleisten. Eine herkömmliche *Mixed-Integer Second-Order Cone Program* Formulierung (MISOCP Formulierung) sowie eine erweiterte MISOCP Formulierung werden entwickelt, die beide das *Branch-and-Cut* Verfahren (BnC Verfahren) unterstützen. Analysen zeigen, dass die erweiterte Formulierung engere kontinuierliche Relaxierungen zulässt (und somit einen geringeren Rechenaufwand), als die der herkömmlichen Formulierung. Es werden darüber hinaus effektive Strategien entwickelt, um das BnC Verfahren in den Software-

Lösen CPLEX für die Anwendung des JNOB Problems individuell anzupassen. Rechengünstige Inflations- und Deflationsverfahren werden für groß dimensionierte Anwendungen entwickelt. Die Simulationen zeigen, dass unser Entwurf im Ergebnis dünn besetzte Netzwerktopologien und Teil BS Kooperation hervorbringt.

Wir untersuchen als Nächstes die gemeinsame optimierte diskrete Ratenanpassung und das Downlink Beamforming (DRAB), bei dem die Ratenanpassung mittels Modulations- und Kodierungsverfahrenzuweisung (engl. *Modulation and Coding*, MCS Zuweisung) erfolgt. Bei diesem Ansatz ist die Teilnehmerauswahl auf natürliche Weise in MCS Zuweisung eingebettet. Ziel ist es, die maximale Summenrate mit einem Minimum an abgestrahlter BS Leistung zu erreichen. Wie für das JNOB Problem, werden eine herkömmliche und eine erweiterte MISOCP Formulierung entwickelt, und anschließend analytische Vergleiche angestellt. Die Analyse führt auch zu effizienten Anpassungsstrategien für das BnC Verfahren in CPLEX. Wir entwickeln außerdem schnelle Inflations- und Deflationsverfahren für die Anwendung in groß dimensionierten Netzwerken. Unsere numerischen Ergebnisse zeigen, dass die heuristischen Algorithmen Summenraten liefern, die sehr nahe an den optimal möglichen Summenraten liegen.

Wir richten unsere Aufmerksamkeit dann auf den Codebuch-basierten Downlink Beamformer Entwurf. Codebuch-basiertes Beamforming kommt in den neuesten Mobilfunkstandards zum Einsatz, z.B. in Long Term Evolution Advanced (LTE-A), um die Signalisierung des gewählten Beamformers zu vereinfachen. Wir betrachten als Erstes das herkömmliche Codebuch-basierte Downlink Beamforming Problem (SCBF Problem), bei dem die Zuweisung der Precodingvektoren und die Sendeleistung gemeinsam optimiert werden. Ziel ist es, die Gesamtsendeleistung der BS zu minimieren, während die vorgegebenen QoS Anforderungen der MSs einzuhalten sind. In unserem Ansatz greifen wir auf ein Virtuelles Uplink Problem (VUL Problem) zurück, welches mathematisch equivalent zu dem betrachteten SCBF Problem ist. Ein individuell angepasstes Potenzverfahren wird entwickelt, um das Optimum des VUL Problems, und somit das des SCBF Problems, zu finden. Um die Leistungsfähigkeit des Codebuch-basierten Downlink Beamformings zu verbessern, schlagen wir ein Kanalvorverzerrungsverfahren vor, das ohne zusätzliche Signalisierung oder Modifizierung der mobilen Empfänger eingesetzt werden kann. Das gemeinsame Codebuch-basierte Downlink Beamforming- und Kanalvorverzerrungs Problem (CBCP Problem) stellt ein nicht-konvexes MIP dar. Ein alternativer Optimierungsalgorithmus und ein alternatives Zulässigkeitsverfahren werden entwickelt um das CBCP Problem näherungsweise zu lösen. Die Simulationsergebnisse bestätigen die Effizienz des Kanalvorverzerrungsschritts. So wird numerisch gezeigt, dass sich mit dem Verfahren eine erhebliche Reduzierung der Gesamtsendeleistung der BS erreichen lässt.

Wir untersuchen zuletzt das robuste Codebuch-basierte Worst-Case Downlink Beamforming wobei angenommen wird, dass sich die Kanalinformation an der BS lediglich auf geschätzte Kanalkovarianzmatrizen beschränkt. Ähnlich wie bei dem DRAB Problem ist die Teilnehmerauswahl in die Auswahl der Precodingvektoren eingebettet. In dem robusten Codebuch-basierten Downlink Beamforming und Zugangskontroll Problem (RCBA Problem) ist es das Ziel, die maximale Anzahl an ausgewählten MSs bei minimaler Sendeleistung der BS zu erreichen. Wir entwickeln eine konservative Mixed-Integer Linear Program Approximierung (MILP Approximierung) des RCBA Problems, sowie eine exakte MISOCP Umformulierung. Ferner entwickeln wir ein recheneffizientes Inflationsverfahren für das RCBA Problem. Unsere Simulationen zeigen, dass die drei Ansätze nahezu die gleiche durchschnittliche Anzahl an zugelassenen MSs erzielen, wobei die BS bei dem MILP-basierten Ansatz dafür jedoch wesentlich mehr Sendeleistung aufwenden muss, als bei den anderen beiden Ansätzen.

Das MIP Rahmenkonzept, das in dieser Dissertation entwickelt wird, kann auf eine Vielzahl von diskreten Ressourcenvergabeproblemen in Interferenz begrenzten Mobilfunknetzen angewendet werden. Sowohl optimale Leistungsfähigkeits-Benchmarks als auch praxistaugliche Algorithmen mit geringer Komplexität werden in unserem MIP Rahmenwerk berücksichtigt. Herkömmliche Ansätze haben sich oftmals nicht mit den exakten diskreten Modellen auseinandergesetzt, sondern die diskreten Variablen mit kontinuierlichen angenähert, was zu hochgradig suboptimalen Lösungen oder unzulässigen Probleminstanzen führen kann.

Acknowledgment

Foremost, I would like to thank Prof. Marius Pesavento, without whom this thesis can never be possible. He has been very supportive throughout my doctoral studies. He has been constantly feeding me with innovative ideas and painstakingly guiding me towards “a great mind and a perfect gentleman”. I have been enjoying the numerous brainstormings and discussions with him, which have helped me a lot with my Ph.D. work. I am thankful to his great efforts in revising my paper and thesis drafts and I appreciate his incredible sharpness. I have been learning a lot from Prof. Marius Pesavento and I am deeply grateful to him.

I give sincere thanks to my co-supervisor Prof. Stefan Ulbrich for his interest and time in my work. I particularly appreciate his efforts in reviewing my Ph.D. dissertation.

I thank Dr. Sarah Drewes for introducing me to the field of mixed-integer programming. She equipped me with a warm-start of my Ph.D. program, which saved me a lot of time. I am also thankful to Anne Philipp. She has been a cooperator of my research. Anne and I had a large number of productive discussions, and she also helped me with writing.

I am thankful to all colleagues in the Communication Systems Group. I benefit largely from the discussions with them, and the interesting discussions during our group lunch have made my Ph.D. program a pleasant journey. Particularly, I thank Nils Bornhorst and Dr. Ka Lung Law for the wonderful discussions that we had when we were sharing one office. I very much appreciate the efforts of my colleagues in proofreading my Ph.D. thesis draft. I am grateful to the Germans (Adrian Schad, Christian Steffens, and Nils Bornhorst) in our group for their German language assistances. They make my life in Darmstadt easier.

I thank Marlis Gorecki for taking care of the administrative issues. She has been very helpful with my teaching duties and my conference trips. I also thank her for helping my wife and me with the applications of VISAs.

Most importantly, I am indebted and grateful to all my family members, especially my wife, my mother, and my parents-in-law. Their love, support, encouragement, and criticism have made me what I am today.

Yong Cheng

Mathematical notation

Sets:

\mathbb{R}	Real numbers
$\mathbb{R}^{m \times n}$	Real matrices (vectors)
\mathbb{C}	Complex numbers
$\mathbb{C}^{m \times n}$	Complex matrices (vectors)
\emptyset	The empty set

Vectors and matrices:

$\mathbf{0}$	Matrix (vector) of zeros with conformable dimensions
$\mathbf{1}$	Matrix (vector) of ones with conformable dimensions
\mathbf{I}	Identity matrix with conformable dimensions
$(\cdot)^T$	Transpose
$(\cdot)^H$	Hermitian (conjugate transpose)
$\text{Tr}\{\cdot\}$	Trace of a square matrix
$\text{vec}\{\cdot\}$	Vectorization of a matrix by stacking the columns on top of each other

Norms:

$\ \cdot\ _2$	Euclidean (l_2) norm of a vector
$\ \cdot\ _F$	Frobenius norm of a matrix

Miscellaneous:

$\operatorname{Re}\{\cdot\}$	Real part of a variable
$\operatorname{Im}\{\cdot\}$	Imaginary part of a variable
$E\{\cdot\}$	Statistical expectation
\triangleq	Defined as
\forall	For all
\exists	Exists/exist
$\mathbf{A} \succeq \mathbf{0}$	Matrix \mathbf{A} is positive semidefinite
$\mathbf{a} \geq \mathbf{b}$	Element-wise inequalities of vectors \mathbf{a} and \mathbf{b}
$\mathbf{a} > \mathbf{b}$	Element-wise strict inequalities of vectors \mathbf{a} and \mathbf{b}

Table of contents

1	Introduction	1
1.1	Joint downlink beamforming and discrete resource allocation	1
1.2	Overview and contributions	6
2	Network optimization and multi-cell beamforming for CoMP transmission	11
2.1	Introduction	11
2.2	System model and problem statement	13
2.2.1	Network model	13
2.2.2	BS power consumption model	15
2.2.3	The standard big-M formulation of the JNOB problem	17
2.3	Optimal solutions via the BnC method	19
2.3.1	The continuous relaxation of the big-M formulation	19
2.3.2	Overview of the BnC method and the solver CPLEX	21
2.4	The extended formulation and analytic studies	24
2.4.1	The extended MISOCP formulation	24
2.4.2	Analytic comparison of the two formulations	26
2.5	Techniques for customizing the BnC method	29
2.5.1	Customized optimality criterion	29
2.5.2	Customized node selection and branching rules	30
2.5.3	Integer-feasible initializations	32
2.6	The low-complexity heuristic algorithms	33
2.6.1	The SOCP based inflation procedure	33
2.6.2	The SOCP based deflation procedure	34
2.7	Simulation results	36
2.7.1	Performance of the low-complexity algorithms	37
2.7.2	Comparison of the two MISOCP formulations	41
2.8	Summary	44

3	Discrete rate adaptation, admission control, and downlink beamforming	45
3.1	Introduction	45
3.2	System model	48
3.3	The standard big-M formulation of the DRAB problem	51
3.3.1	The big-M MISOCP formulation	51
3.3.2	The continuous relaxation of the big-M formulation	55
3.4	The extended formulation and analytic studies	56
3.4.1	The extended MISOCP formulation	56
3.4.2	Analytic comparison of the two formulations	58
3.5	Techniques for customizing the BnC method	62
3.5.1	Customized optimality criterion	62
3.5.2	Customized node selection and branching rules	62
3.5.3	Preprocessing	64
3.6	The low-complexity heuristic algorithms	65
3.6.1	The SOCP based inflation procedure	65
3.6.2	The SOCP based deflation procedure	66
3.7	Simulation results	68
3.7.1	Performance of the low-complexity algorithms	68
3.7.2	Comparison of the two MISOCP formulations	71
3.8	Summary	74
4	Codebook-based downlink beamforming and channel predistortion	75
4.1	Introduction	75
4.2	System model	78
4.3	The standard codebook-based downlink beamforming problem	79
4.3.1	The SCBF problem formulation	79
4.3.2	The customized power iteration method	82
4.3.3	Optimality of the power iteration method	85
4.4	Channel predistortion for performance improvement	87
4.4.1	The CBCP problem formulation	87
4.4.2	The alternating optimization algorithm	91
4.4.3	The alternating feasibility search algorithm	96
4.5	Simulation results	99
4.5.1	Performance of the power iteration method	99
4.5.2	Performance of the alternating optimization approach	101
4.6	Summary	104

5	Robust codebook-based downlink beamforming and admission control	105
5.1	Introduction	105
5.2	System model and problem statement	107
5.3	The conservative MILP approximation	112
5.4	The equivalent MISOCP reformulation	115
5.5	Techniques for customizing the BnC method	120
5.5.1	Customized optimality criterion	121
5.5.2	Customized node selection and branching rules	121
5.5.3	Preprocessing	122
5.6	The SOCP based inflation procedure	122
5.7	Simulation results	124
5.7.1	Performance with different SINR targets	125
5.7.2	Performance with different numbers of admissible MSs	128
5.7.3	Further comparison with large numbers of admissible MSs	131
5.8	Summary	133
6	Conclusions and outlook	135
A	Appendices of Chapters 2 and 3	139
A.1	Proof of <i>Theorem 2.1</i>	139
A.2	Proof of <i>Theorem 2.2</i>	140
A.3	Proof of <i>Theorem 2.3</i>	140
A.4	Proof of <i>Lemma 3.1</i>	141
A.5	Proof of <i>Lemma 3.2</i>	142
A.6	Proof of <i>Theorem 3.1</i>	142
A.7	Sample branching priorities in the DRAB problem	143
	Bibliography	145
	List of abbreviations	159
	Curriculum vitae	161
	Supervision and teaching	163

Chapter 1

Introduction

1.1 Joint downlink beamforming and discrete resource allocation

The information and communications technology (ICT) contributes a notable percentage to global greenhouse gas emissions [1, 2], and therefore the cellular network operators are encouraged to employ green (energy-efficient) communications technologies by regulatory bodies and governmental associations. Further, the wireless data traffic has been growing exponentially in recently years, due to, e.g., the prevailing of smartphones and tablet personal computers (PCs) for mobile web-browsing, audio- and video-streaming [3–5]. Given the limited spectrum resource, the unprecedented mobile data explosion compels the cellular network operators to seek for more energy- and spectrum-efficient wireless technologies [6–10]. Furthermore, it has long been known that energy- and spectrum-efficient wireless communications technologies are the essential apparatuses for the cellular operators to reduce the capital expenditures (CAPEX) and the operational expenditures (OPEX) [1, 2, 6–11].

Transmit beamforming with smart antennas is widely recognized as a promising technique to realize energy- and spectrum-efficient wireless communications. In multiuser downlink transmit beamforming, the base station (BS) forms a very narrow transmission beam (in baseband processing) towards each intended mobile station (MS). Hence, transmit beamforming is more energy-efficient, as compared to omnidirectional transmissions and analog directional radiations with directional antennas [7–10, 12–14]. Moreover, in multiuser downlink beamforming, the BS is able to generate nulls towards the unintended MSs to minimize the co-channel interference, e.g., by employing multiuser zero-forcing beamforming [15–17]. As a result, multiple MSs can be served jointly on the same time and frequency resources, resulting in the so-called space-division multiple access (SDMA) schemes [18, 19].

Through concurrently serving multiple MSs with SDMA, multiuser downlink beamforming achieves high spectrum efficiency. In light of the potential advancement towards energy- and spectrum-efficient mobile communications, multiuser downlink beamforming has been adopted into modern third generation (3G) and fourth generation (4G) cellular standards, e.g., in long-term evolution (LTE) and LTE-advanced (LTE-A) of the third generation partnership project (3GPP) [7–10, 20].

In multiuser downlink beamforming, when the BS applies the beamforming vector (also called beamformer) to transmit data to a MS, the MS sees the composite channel, i.e., the inner product of the beamformer and the original downlink channel vector. While the optimal beamformers generally need to be computed at the BS, the MSs require the information of the respective composite channels for coherent data symbols detection. Additional signaling procedures have to be introduced for the MSs to acquire the knowledge of the composite channels [7, 8, 14]. Depending on how the composite channels are made available at the MSs, downlink beamforming techniques can be classified into two categories, namely non-codebook-based beamforming and codebook-based beamforming [7, 8, 12, 13]. Both non-codebook-based and codebook-based beamforming schemes are adopted in the most recent cellular standards, e.g., in 3GPP LTE and LTE-A [7–10, 20].

In non-codebook-based multiuser downlink beamforming (also called conventional adaptive beamforming [14]), the optimal beamforming vectors (i.e., the beamformers) of the MSs are taken from a continuous complex vector space [7, 12–14]. After computing the optimal beamformers, including transmission power allocations, at the BS, the BS applies the optimal beamformers to transmit user-specific reference signals. A MS can estimate the corresponding composite channel (also known as precoded channel) using the predefined user-specific reference signals sent by the BS [7, 8, 20].

In contrast to non-codebook-based beamforming, in codebook-based downlink beamforming (also known as switched beamforming) [7, 8, 14, 20, 21], the BS and the MSs share the information of a codebook that consists of a finite number of predetermined beam patterns, i.e., a predefined precoding vector codebook of unit-norm precoding vectors (beamformers). The BS assigns the precoding vectors from the precoding vector codebook to the MSs, together with proper transmission power allocations. The BS then signals the indices of the assigned precoding vectors and the allocated transmission powers to the respective MSs [7, 8, 14, 20–22]. Note that codebook-based beamforming is referred to as codebook-based single-layer-per-user precoding in cellular standards, e.g., in 3GPP LTE and LTE-A [7, 8, 20].

In the open technical literature, there is a large volume of technical contributions dealing with non-codebook-based multiuser downlink beamforming. The standard quality-of-

service (QoS) based downlink beamformer design problem, in which the total transmitted BS power is minimized while guaranteeing the received signal-to-interference-plus-noise ratio (SINR) targets (representing the QoS requirements [23]) of the admitted MSs, has been extensively investigated, see, e.g., [12, 13, 18, 24–33]. Since the standard SINR-constrained multiuser downlink beamforming problem can be formulated as (or can be equivalently converted to) a convex program [12, 24, 31, 34], both efficient convex optimization techniques (e.g., the interior-point method [34]) and low-complexity optimal iterative algorithms (e.g., the power iteration method [26, 35, 36]) have been developed to solve the problem (see, e.g., [12, 13, 26, 31]).

Due to the limited channel training and/or feedback resources, the downlink channel state information (CSI), in terms of either the downlink channel vectors, i.e., instantaneous CSI in slow-fading scenarios, or the downlink channel covariance matrices, i.e., statistical CSI in fast-fading scenarios, may not be perfectly known at the BS, e.g., in frequency-division duplex (FDD) systems. To accommodate the scenarios that only estimated and/or erroneous CSI is available at the BS, various robust downlink beamforming schemes have been proposed, see, e.g., [12, 37–48]. The existing contributions on robust beamforming can generally be categorized into two classes, namely the deterministic (worst-case) design, see, e.g., [12, 37–42], and the probabilistic design (also known as chance-constrained approach and outage-constrained approach), see, e.g., [43–48]. Unlike multiuser downlink beamforming with perfect CSI [12, 13, 18, 25–33], the robust multiuser downlink beamforming problem cannot be efficiently solved to optimality and convex approximation methods are widely applied (see, e.g., [38, 42, 48]).

Different from the SINR-constrained multiuser downlink beamforming problem [12, 13, 18, 25–33, 37–42], in the sum-rate maximization based multiuser downlink beamforming, the objective is to maximize the (weighted) sum-rate of the downlink system under the given transmission power budget of the BS, see, e.g., [13, 49–59]. In contrast to the standard SINR-constrained downlink beamforming problem [12, 24, 28, 31], the sum-rate maximization based downlink beamforming problem has been proved to be non-deterministic polynomial-time (NP) hard and thus cannot be efficiently solved to global optimality [55–58]. In addition to carrying out local search for suboptimal solutions [50–53], global optimization techniques, e.g., the branch-and-bound (BnB) method and its variations [60], have also been proposed to solve the problem of multiuser downlink beamforming for (weighted) sum-rate maximization, see, e.g., [54–56].

There are much fewer technical contributions dealing with codebook-based multiuser downlink beamforming, as compared to non-codebook-based multiuser downlink beamforming. The codebook-based beamforming (also known as single-layer-per-user precod-

ing) is mainly studied within the standardization bodies, e.g., within 3GPP [7, 8, 20]. Recently, the authors of [22] have considered codebook-based beamforming for sum-rate maximization in a multi-group multi-casting scenario. Since the beamformers have to be selected from a predetermined precoding vector codebook and precoding vector assignments of different MSs are coupled through co-channel interference in the downlink SINR constraints, the codebook-based multiuser downlink beamforming problem inherently involves integer (binary) decision variables and naturally leads to combinatorial optimization problems [7, 8, 14, 20–22]. Further, effective convex approximations are not directly applicable because of the constraints that at most one of the candidate precoding vectors can possibly be assigned to each MS. Due to the integer (binary) decision variables and the combinatorial precoding vector assignments, codebook-based multiuser downlink beamforming problem is generally more challenging than non-codebook-based multiuser downlink beamforming problem.

Besides codebook-based multiuser downlink beamforming, a lot of resource allocation problems in practical telecommunications networks involve discrete (integer) decision variables. Since the MSs are coupled by co-channel interference when they are served in the same time and frequency resources, the discrete resource allocation problems in practice naturally result in combinatorial discrete (mixed-integer) optimization programs [61–66]. For instance, the joint optimization of adaptive modulating and coding (AMC) and multiuser downlink beamforming, as illustrated in Fig. 1.1, inherently involve binary decision markings, i.e., assigning at most one of the candidate modulation and coding schemes (MCSs) to each MS (cf. Chapter 3). Since MCS assignments of different MSs are coupled through the co-channel interference in the downlink received SINRs, the problem of joint discrete rate adaptation and downlink beamforming represents a combinatorial mixed-integer nonlinear program (MINLP) [60, 67–69].

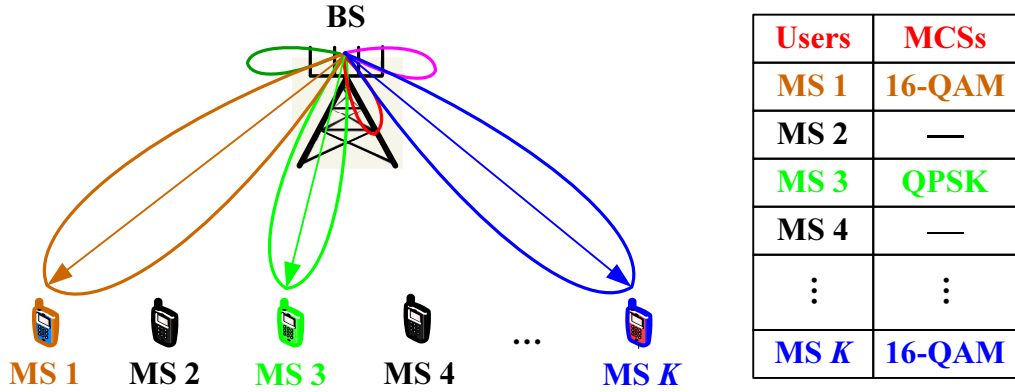


Figure 1.1: Illustration of joint adaptive modulating and coding (AMC) and multiuser downlink beamforming, e.g., MS 1 is admitted and assigned the MCS 16-QAM, while MS 2 is not admitted.

Another well-known example is the problem of BS clustering, i.e., BS association, for coordinated multi-point (CoMP) processing, in which a subset of the total BSs are assigned to each MS jointly with beamformer design (see, e.g., [70–78]). Since the MSs are coupled through co-channel interference under SDMA, the BSs clustering problem also belongs to the class of combinatorial MINLPs (cf. Chapter 2). The joint optimization of multiuser downlink beamforming and discrete resource allocation usually results in superior performance than the separate approaches in practical telecommunications systems (see, e.g., [77–80]). Readers are referred to the works of [61–66] for more detailed examples of combinatorial discrete resource allocation problems in practical wireless networks.

In this dissertation, we propose to address the discrete resource allocation problems using the exact discrete models. That is, we start with exact mixed-integer program (MIP) formulations. The MIP formulations provide a way to compute the optimal solutions of the discrete resource allocation problems. The optimal solutions serve as performance benchmarks for the low-complexity practical algorithms and can be used for network planning and system performance predictions. Most of the existing approaches (see, e.g., [75–77]) do not adopt the exact discrete models and the discrete decision variables are approximated by (quantized) continuous variables, which generally cannot reach the optimal solutions of the discrete resource allocation problems. The existing approximation and quantization based approaches may also result in infeasible problem instances due to quantization operations even if the original discrete problems are feasible.

However, due to the challenges of discrete (mixed-integer) optimization problems, limited attention has been devoted to the joint optimization of multiuser downlink beamforming and discrete resource allocation even though they are practically relevant. To promote practical applications of multiuser downlink beamforming techniques, we consider in this thesis

the joint optimization of (multi-cell) multiuser downlink beamforming and discrete resource allocation in modern cellular networks. Both non-codebook-based and codebook-based multiuser downlink beamforming are covered, and the problems are addressed within the developed systematic MIP framework. In our MIP framework, we consider (i) MIP based problem formulations that support the commercial solver (e.g., IBM ILOG CPLEX [81]) based approach for computing the optimal solutions (performance benchmarks), (ii) analytic comparisons of different MIP problem formulations, (iii) customizing techniques for speeding up the standard branch-and-cut (BnC) method [67–69, 81, 82] for reaching the optimality certificates, and (iv) low-complexity practical algorithms for large-scale applications. Particularly, by analyzing the characteristics of the considered problems, we propose efficient strategies to specifically customize the standard BnC method implemented in the MIP solver CPLEX for each problem. Thanks to the mathematical advancement of MIP techniques and the fast development of commercial MIP solvers [67–69, 81, 82], applying MIP based approaches to address practical discrete resource allocation problems in wireless networks is gaining wider interests of the research community (see, e.g., [61–66]). The next section presents an overview and the contributions of this thesis.

1.2 Overview and contributions

The technical contributions of this dissertation can be divided into two parts. The first technical part of this thesis, including Chapters 2 and 3, deals with the joint optimization of non-codebook-based multiuser downlink beamforming and discrete resource allocation. The second technical part of this thesis, consisting of Chapters 4 and 5, considers the joint optimization of codebook-based multiuser downlink beamforming and discrete resource allocation. The problems are addressed within the developed systematic MIP framework. Several efficient customizing strategies are introduced to customize the standard BnC method implemented in the MIP solver CPLEX [67–69, 81, 82] when applying CPLEX to the respective problems. It is assumed in Chapters 2, 3, and 4 that the perfect CSI in terms of the instantaneous downlink channel vectors is available at the BSs. Only erroneous statistical CSI in terms of the estimated downlink channel covariance matrices is assumed to be known at the BS in Chapter 5. Furthermore, Chapter 2 considers the multi-cell case, while Chapters 3, 4, and 5 focus on the single-cell and signal-BS scenario.

In Chapter 2, we address the joint optimization of network topology and multi-cell downlink beamforming (JNOB) for CoMP transmission (see, e.g., [70–78]), with the objective to minimize the overall BSs power consumption (including the operational overhead of

CoMP transmission) while guaranteeing the QoS requirements (expressed through the received SINR targets) of the MSs. The JNOB problem is addressed within the mixed integer second-order cone program (MISOCP) framework [82]. We first develop a standard big-M MISOCP formulation of the JNOB problem, which can be solved using, e.g., the BnC method [67–69, 81, 82]. To reduce the computational complexity of the BnC method, we further propose an improved extended MISOCP formulation of the JNOB problem. Analytic studies show that the extended MISOCP formulation admits tighter continuous relaxations (and hence lower computational complexity) than that of the big-M MISOCP formulation. For practical applications in large-scale networks, we also develop low-complexity SOCP based inflation and deflation procedures [83, 84]. The simulation results show that the inflation and deflation procedures yield total BSs power consumptions that are very close to the lower bounds computed by the MIP solver CPLEX (and therefore very close to that of the optimal solutions). The numerical results also confirm that minimizing the total BSs power consumption results in partial BSs cooperation and sparse network topologies for CoMP transmission and some of the BSs are powered off for further reduction of the unnecessary power expenditures.

Chapter 3 deals with the joint optimization of discrete rate adaptation and downlink beamforming (DRAB) in the scenarios employing discrete rate adaptation in the form of AMC [7, 8, 20, 85–90]. In the DRAB problem, the discrete rate adaptation, i.e., modulation and coding scheme (MCS) assignment, is jointly optimized along with the multiuser beamformer design, with the objective to achieve the maximum downlink sum-rate with minimum total transmitted BS power. User admission control is naturally embedded in the discrete rate assignment procedure. As in Chapter 2, we address the DRAB problem using the MISOCP based approach, developing a standard big-M MISOCP formulation and an improved extended MISOCP formulation. We analytically show that the extended formulation generally admits strictly tighter continuous relaxations (and hence less computational complexity) than that of the big-M formulation. Effective customizing strategies for the standard BnC method implemented in the MIP solver CPLEX are adopted when applying CPLEX on the DRAB problem. As in Chapter 2, we also devise low-complexity SOCP based inflation and deflation procedures to find near-optimal solutions of the DRAB problem for applications in large-scale networks. Our simulation results demonstrate that the inflation and deflation procedures yield sum-rates that are very close to that of the optimal solutions computed by CPLEX. The numerical results also confirm that when applying the solver CPLEX to the DRAB problem, the extended MISOCP formulation requires much less runtime to solve than the standard big-M MISOCP formulation.

In Chapter 4, we study the codebook-based multiuser downlink beamforming. We con-

sider first the standard codebook-based downlink beamforming (SCBF) problem, in which precoding vector assignment and power allocation are jointly optimized to minimize the total transmitted BS power while guaranteeing the prescribed QoS targets (SINR constraints) of the MSs. We propose a mixed-integer linear program (MILP) formulation of the SCBF problem, which can be solved using, e.g., the BnC method [67–69, 81, 82]. To derive low-complexity solutions, we introduce a virtual uplink problem, in which precoding vector assignments of different MSs are nicely decoupled. We establish the uplink-downlink duality properties of the two problems and develop a customized power iteration method for the SCBF problem. Analytic studies show that the customized iterative algorithm yields either optimal solutions of the SCBF problem (when it is feasible), or infeasibility certificates (when it is infeasible). To enhance the performance of the codebook-based downlink beamforming, we further propose a linear adaptive channel predistortion mechanism, by applying a common predistortion on the downlink channel vectors. The channel predistortion scheme does not involve any additional signalling overhead or modifications of the mobile receivers. We propose to jointly optimize codebook-based downlink beamforming and channel predistortion (CBCP), taking into account the smoothness constraints on the predistorted channel processes. The CBCP problem represents a non-convex MIP. An alternating optimization algorithm (ATO) and an alternating feasibility search algorithm (AFSA) are developed to approximately solve the CBCP problem. The simulation results verify that the proposed customized power iteration method either optimally solves the SCBF problem or detects its infeasibility. Our numerical results also demonstrate the superior performance of the channel predistortion procedure in terms of, e.g., achieving significant reductions of the total transmitted BS power and substantial increases of the percentage of feasible Monte Carlo runs, as compared to the standard codebook-based beamforming (without channel predistortion). This practically means that with channel predistortion, a significant reduction of transmitted BS power can be realized and more MSs can be jointly served in the same time and frequency resources. That is, the proposed channel predistortion design effectively alleviates the performance degradation of codebook-based beamforming, as compared to non-codebook-based beamforming.

Finally, we investigate in Chapter 5 the worst-case robust codebook-based downlink beamforming problem in the scenarios where only estimated (and thus erroneous) downlink channel covariance matrices are available at the BS. In this thesis, robustness refers to that the minimum SINR requirements of the admitted MSs are guaranteed to be satisfied, regardless of the quality of the CSI known at the BSs. Similar to Chapter 3, user admission control is naturally embedded in the precoding vector assignment procedure. In the robust codebook-based downlink beamforming and admission control (RCBA) problem, the

objective is to achieve the maximum number of admitted MSs (representing revenue) with the minimum total transmitted BS power (representing expenditure). Due to the worst-case SINR constraints, the RCBA problem leads to a bi-level MIP (BL-MIP). We first adopt the conservative approach as presented in [12, 37] and develop a MILP approximation of the RCBA problem. While the MILP approximation can be efficiently solved using, e.g., the BnC method [67–69, 81, 82], it yields solutions with unnecessarily increased total transmitted BS power (see, e.g., [38]). We then follow a similar procedure as given in [38] and convert the RCBA problem into an equivalent MISOCP. Based on the exact MISOCP reformulation, a low-complexity SOCP based inflation procedure (i.e., a greedy algorithm) is further devised to compute near-optimal solutions of the RCBA problem for applications in large-scale systems. Our simulation results show that the MILP based approach, the MISOCP based approach, and the inflation procedure achieve almost the same average number of admitted MSs. However, the total transmitted BS power required for ensuring the SINR targets of the admitted MSs in the MILP based approach is significantly larger than that of the other two methods. Furthermore, the inflation procedure has much less computational complexity than the MILP based approach when the number of admissible MSs is large. The MISOCP based approach yields the least total transmitted BS power, but with the highest computational complexity.

This dissertation is based on the following publications, which have been published or submitted during the course of my doctoral studies:

Journal articles:

- Y. Cheng and M. Pesavento, “Joint rate adaptation and downlink beamforming using mixed integer conic programming,” submitted to *IEEE Trans. Signal Process.*, Jun. 2013.
- Y. Cheng and M. Pesavento, “An optimal iterative algorithm for codebook-based downlink beamforming,” *IEEE Signal Process. Lett.*, vol. 20, no. 8, pp. 775–778, Aug. 2013.
- Y. Cheng, M. Pesavento, and A. Philipp, “Joint network optimization and downlink beamforming for CoMP transmissions using mixed integer conic programming,” *IEEE Trans. Signal Process.*, vol. 61, no. 16, pp. 3972–3987, Aug. 2013.
- Y. Cheng and M. Pesavento, “Joint optimization of source power allocation and distributed relay beamforming in multiuser peer-to-peer relay networks,” *IEEE Trans. Signal Process.*, vol. 60, no. 6, pp. 2962–2973, Jun. 2012.

Conference papers:

- Y. Cheng and M. Pesavento, “Predistortion and precoding vector assignment in codebook-based downlink beamforming,” in *Proc. IEEE Int. Workshop on Signal Process. Advances for Wireless Commun. (SPAWC)*, Jun. 2013, pp. 440–444.
- Y. Cheng and M. Pesavento, “Robust codebook-based downlink beamforming using mixed integer conic programming,” in *Proc. IEEE Int. Conf. on Acoustics, Speech and Signal Process. (ICASSP)*, May 2013, pp. 4187–4191.
- Y. Cheng, A. Philipp, and M. Pesavento, “Dynamic rate adaptation and multiuser downlink beamforming using mixed integer conic programming,” in *Proc. European Signal Process. Conf. (EUSIPCO)*, Aug. 2012, pp. 824–828.
- Y. Cheng, S. Drewes, A. Philipp, and M. Pesavento, “Joint network optimization and beamforming for coordinated multi-point transmission using mixed integer conic programming,” in *Proc. IEEE Int. Conf. on Acoustics, Speech and Signal Process. (ICASSP)*, Mar. 2012, pp. 3217–3220.
- Y. Cheng, S. Drewes, A. Philipp, and M. Pesavento, “Joint network topology optimization and multicell beamforming using mixed integer conic programming,” in *Proc. Int. ITG Workshop on Smart Antennas (WSA)*, Mar. 2012, pp. 187–192.

Chapter 2

Network optimization and multi-cell beamforming for CoMP transmission

2.1 Introduction

Coordinated multi-point (CoMP) processing is widely recognized as an effective mechanism for managing inter-cell interference (ICI) and improving system throughput in cellular networks with universal frequency reuse (see, e.g., [7, 33, 70–78, 91–96]). The potential of CoMP transmission has been validated in both theoretic studies [71, 91, 92] and field trials [71, 94, 95], and CoMP processing has therefore already been included in the emerging cellular standards, e.g., in the third generation partnership project (3GPP) long-term evolution advanced (LTE-A) [7, 71, 93]. While CoMP operation with full cooperation between all base stations (BSs) that jointly serve the mobile stations (MSs) offers significant increases in network capacity and cell-edge throughput, it induces also considerable operational overhead, such as power expended in collecting and exchanging CSI among multiple BSs and MSs, signaling beamforming weights and forwarding user payload data to multiple cooperating BSs [71, 75].

To balance the benefits and the operational costs, CoMP processing shall be carried out among a limited number of cooperating BSs, resulting in the so-called partial BS cooperation designs. Several partial BS cooperation schemes have been proposed in the literature, see, e.g., [33, 71–78, 96]. These existing contributions can generally be categorized into two classes, namely coordinated beamforming [33, 71, 96] and clustered BSs cooperation [71–78]. In the coordinated downlink beamforming designs, the beamforming weights of the MSs are jointly designed across the network, but each MS is served by a single BS and therefore there is no need to route payload data or control information, e.g., beamforming

weights, corresponding to one MS over the backhaul network to multiple serving BSs [33, 71, 96]. In the clustered BS cooperation frameworks, CoMP processing is implemented within clusters of BSs, with full BSs cooperation inside each cluster and no cooperation between clusters [71–78]. Since the CoMP operation is restricted to a small number of BSs in each cluster, the communication overhead of CoMP processing is bounded by the size of the cooperating BSs clusters.

While the existing approaches [33, 71–78, 96] can alleviate the additional expenses in CoMP transmission to a certain extent, several important issues remain open. For instance, in coordinated beamforming [33, 71, 96], the performance of cell-edge MSs may still suffer from ICI and large pathloss, as in conventional cellular systems. Even though cell-edge MSs can enjoy the performance gain from CoMP processing in the clustered BSs cooperation frameworks [71–78], the MSs located at the cluster edges still suffer from ICI and large path-loss. In addition, determining the optimal size of the BSs clusters is a very challenging open problem [71–78].

More recently, mechanisms to jointly optimize BS selection and multi-cell beamforming are proposed in [75–77] to reduce the overhead of CoMP transmission, in which the BS selection is carried out based on the solution of an optimization problem that gives preference to sparse beamforming vectors [74–77]. However, the sparsity patterns of the beamformers are more appropriate for antenna selection, rather than for BS selection or network topology optimization.

In contrast to the existing contributions [70–78], we propose in this chapter a systematic approach to find the optimal tradeoff between the gain and the overhead of CoMP transmission. Specifically, we consider the problem of joint network topology optimization and multi-cell downlink beamforming (JNOB), with the objective to minimize the overall BSs power consumption (including the overhead of CoMP operation) while guaranteeing the quality-of-service (QoS) requirements of the admitted MSs. The JNOB problem under consideration includes coordinated beamforming [33, 71, 96], partial BS cooperation [71–78], and full BS cooperation [71, 91, 92] as special cases. In our systematic approach, the number of cooperating BSs that transmit to each MS is optimally determined on-the-fly according to the system parameters and the channel conditions. In addition, we consider the possibility of switching off the power amplifiers (PAs) of the BSs in the JNOB problem formulation to further reduce unnecessary BSs power dissipations, which has not been considered in the previous works [33, 71–78, 96].

We address the JNOB problem using the mixed-integer second order cone program (MISOCP) approach [82], proposing a standard big-M MISOCP formulation that supports the convex continuous relaxation based BnC method [67–69, 81, 82]. Based on the big-M

formulation, we introduce auxiliary variables and develop an extended MISOCP formulation [67–69], also known as perspective formulation [68, 97] and lifting [68, 82], which exhibits several appealing properties that are exploited in the numerical algorithms. Analytic studies are carried out. The analysis shows that the extended MISOCP formulation admits tighter continuous relaxations than that of the big-M MISOCP formulation and thus yields significantly reduced computational complexity when applying the standard branch-and-cut (BnC) method. The insights of the analysis allow us to introduce several customizing techniques (e.g., customized node selection rules and branching priorities) to further speed up the BnC method by generating tighter lower bounds of the minimum total BSs power consumptions. We develop low-complexity second-order cone program (SOCP) based inflation and deflation procedures [83, 84] that yield with very low computational complexity high-quality solutions of the JNOB problem. The fast heuristic algorithms are suitable for practical applications in large-scale networks.

Extensive simulations are carried out to evaluate the developed algorithms and to confirm the analytic studies. The commercial mixed-integer program (MIP) solver IBM ILOG CPLEX [81] is employed in our numerical experiments. The simulation results show that the proposed fast inflation and deflation procedures achieve total BSs power consumptions that are very close to the lower bounds computed by CPLEX (and hence very close to that of the optimal solutions). The proposed heuristic algorithms outperform the BS clustering schemes of [75–78] in terms of the achieved total BSs power consumptions. The reduction in the computational complexity of the extended MISOCP formulation over the standard big-M MISOCP formulation when applying the BnC method is also confirmed in the simulations. Our numerical results further show that minimizing the total BSs power consumption results in sparse network topologies rather than full BSs cooperation. The network topologies become sparser as the power consumption overhead associated with CoMP transmission is increased, and some of the BSs are switched off when possible to further reduce the overall BSs power consumption.

This chapter is based on my original work that has been published in [98–100].

2.2 System model and problem statement

2.2.1 Network model

Consider a cellular network consisting of L multiple-antenna BSs and K single-antenna MSs, where the l th BS is equipped with $M_l \geq 1$ transmit antennas, $\forall l \in \mathcal{L} \triangleq \{1, 2, \dots, L\}$, as illustrated in Fig. 2.1. The K MSs are admitted with the prescribed QoS requirements.

Similar to [70–78, 91, 92], it is assumed that the BSs are mutually connected over a BS network interface (e.g., the X2-type interface in LTE-A systems [93]), and therefore the data of a MS can be made available at the cooperating BSs with associated backhauling cost [71, 75]. The L BSs are assumed to be synchronized so that CoMP processing can possibly be employed for downlink data transmissions [7, 71], as shown in Fig. 2.1.

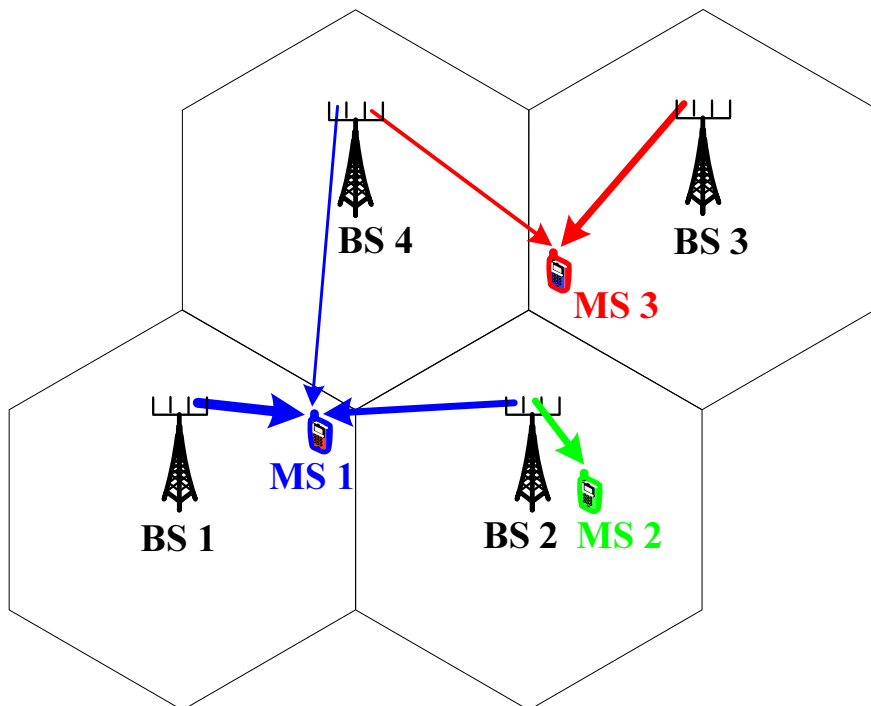


Figure 2.1: Downlink CoMP transmission, with $L = 4$ BSs, each of which equipped with $M_l = 4$ transmit antennas, and $K = 3$ single-antenna MSs. MS 1 is jointly served by BS 1, BS 2, and BS 3. MS 3 is jointly served by BS 3 and BS 4.

Let $\mathbf{h}_{k,l}^H \in \mathbb{C}^{1 \times M_l}$ denote the frequency-flat channel vector between the l th BS and the k th MS, $\forall l \in \mathcal{L}, k \in \mathcal{K} \triangleq \{1, 2, \dots, K\}$, and define $\mathbf{h}_k^H \triangleq [\mathbf{h}_{k,1}^H, \mathbf{h}_{k,2}^H, \dots, \mathbf{h}_{k,L}^H] \in \mathbb{C}^{1 \times M}$ as the aggregate channel vector of the k th MS, $\forall k \in \mathcal{K}$, with $M \triangleq \sum_{l=1}^L M_l$. Accordingly, we denote $\mathbf{w}_{k,l} \in \mathbb{C}^{M_l \times 1}$ as the beamforming vector (i.e., the antenna weights) used at the l th BS for transmitting data to the k th MS, $\forall l \in \mathcal{L}, k \in \mathcal{K}$, and we define $\mathbf{w}_k \triangleq [\mathbf{w}_{k,1}^T, \mathbf{w}_{k,2}^T, \dots, \mathbf{w}_{k,L}^T]^T \in \mathbb{C}^{M \times 1}$ as the collection of all beamforming weights corresponding to the k th MS, $\forall k \in \mathcal{K}$. When all BSs share the same frequency bands and CoMP processing is employed in the downlink data transmission, the received signal $y_k \in \mathbb{C}$ at the

k th MS can be written as (see, e.g., [70, 71, 73–78])

$$y_k = \mathbf{h}_k^H \mathbf{w}_k x_k + \sum_{j=1, j \neq k}^K \mathbf{h}_k^H \mathbf{w}_j x_j + z_k, \forall k \in \mathcal{K} \quad (2.1)$$

where $x_k \in \mathbb{C}$ denotes the normalized data symbol designated for the k th MS with unit-power, i.e., $\mathbb{E}\{|x_k|^2\} = 1$, and $z_k \in \mathbb{C}$ stands for the additive circularly-symmetric white Gaussian noise [19] at the k th MS, with zero mean and variance σ_k^2 , $\forall k \in \mathcal{K}$.

Similar to the existing works [33, 71–78, 91, 92, 96], it is assumed that the data symbols for different MSs are mutually statistically independent and also independent from the noise, and single user detection is adopted at the MSs, i.e., the co-channel interference in (2.1) is treated as noise. When the channel vectors $\{\mathbf{h}_k, \forall k \in \mathcal{K}\}$ are quasi-static and the beamformers $\{\mathbf{w}_k, \forall k \in \mathcal{K}\}$ are adaptive only to the instantaneous channel vectors, the received SINR at the k th MS, denoted by SINR_k , can be expressed as (see, e.g., [70, 71, 73–78])

$$\text{SINR}_k \triangleq \frac{|\mathbf{h}_k^H \mathbf{w}_k|^2}{\sum_{j=1, j \neq k}^K |\mathbf{h}_k^H \mathbf{w}_j|^2 + \sigma_k^2}, \forall k \in \mathcal{K}. \quad (2.2)$$

We remark that when the l th BS does not participate in transmitting data to the k th MS in CoMP transmission, i.e., when the l th BS is not assigned to the k th MS, for some $l \in \mathcal{L}$ and $k \in \mathcal{K}$, then the equality $\mathbf{w}_{k,l} = \mathbf{0}$ shall hold.

As in the prior contributions [7, 33, 70–78, 91, 92, 94–96], it is assumed in this chapter that the l th BS has perfect knowledge of the instantaneous channel vectors $\{\mathbf{h}_{k,l}^H, \forall k \in \mathcal{K}\}$, $\forall l \in \mathcal{L}$. This assumption can practically be realized, e.g., in time-division duplex (TDD) systems by exploiting uplink-downlink channel reciprocity and channel calibration techniques at the BSs [7, 19]. The l th BS reports the channel vectors $\{\mathbf{h}_{k,l}^H, \forall k \in \mathcal{K}\}$ to the central processing node (CPN), $\forall l \in \mathcal{L}$. The CPN, which can be implemented on one of the L BSs, assigns one or multiple BSs to each MS and computes the optimal beamformers for the K MSs.

2.2.2 BS power consumption model

According to the prior works [71, 101–104], the power consumption of a cellular BS can be categorized into non-transmission related power dissipations (e.g., battery backup costs) and transmission related power consumptions (e.g., signal processing overhead and power amplifier costs). The non-transmission related power consumption, i.e., the offset power, can be treated as a constant [71, 101–104], while the transmission related power consumption of a BS depends on the activities of the power amplifier (PA). The PA (and also the RF chain) of

a BS may be in one of the three states, namely (i) powered off (OFF), (ii) powered on but not transmitting, i.e., idle (IDL), and (iii) powered on and transmitting. We introduce the *binary* variable $b_l \in \{0, 1\}$ to indicate that the PA of the l th BS is switched on with $b_l = 1$, and $b_l = 0$ otherwise, $\forall l \in \mathcal{L}$. Furthermore, we adopt the *binary* indicators $\{a_{k,l} \in \{0, 1\}, \forall k \in \mathcal{K}, \forall l \in \mathcal{L}\}$ to represent BS assignments, with $a_{k,l} = 1$ meaning that the l th BS is assigned to the k th MS, and $a_{k,l} = 0$ otherwise. In case that $a_{k,l} = 0$, the equalities $\mathbf{w}_{k,l} = \mathbf{0}$ shall hold. When the PA of the l th BS is powered off, i.e., when $b_l = 0$, the l th BS cannot be assigned to any MSs, i.e., it shall hold $a_{k,l} = 0, \forall k \in \mathcal{K}$. Hence, the case of $b_l = 0$ implies that $\{a_{k,l} = 0, \mathbf{w}_{k,l} = \mathbf{0}, \forall k \in \mathcal{K}\}$. The aforementioned properties regarding the binary integer variables $\{a_{k,l}, b_l, \forall k \in \mathcal{K}, \forall l \in \mathcal{L}\}$ can be summarized into the following conventions:

$$\mathbf{w}_{k,l} = a_{k,l} \mathbf{w}_{k,l}, \forall k \in \mathcal{K}, \forall l \in \mathcal{L} \quad (2.3)$$

$$b_l \sum_{k=1}^K \|\mathbf{w}_{k,l}\|_2^2 = \sum_{k=1}^K \|\mathbf{w}_{k,l}\|_2^2, \forall l \in \mathcal{L} \quad (2.4)$$

$$b_l \sum_{k=1}^K a_{k,l} P_{k,l}^{(\text{CMP})} = \sum_{k=1}^K a_{k,l} P_{k,l}^{(\text{CMP})}, \forall l \in \mathcal{L} \quad (2.5)$$

where the user-specific constant $P_{k,l}^{(\text{CMP})}$ represents the fixed power consumption associated with forwarding the payload data and the beamforming weights $\mathbf{w}_{k,l}$ of the k th MS to the l th BS. That is, the constants $\{P_{k,l}^{(\text{CMP})}, \forall k \in \mathcal{K}, \forall l \in \mathcal{L}\}$ model the operational overhead associated with CoMP transmission.

Let the constants $P_l^{(\text{OFT})}$, $P_l^{(\text{IDL})}$, and $P_l^{(\text{TPA})}$ denote the offset power, the idle-state PA power consumption, and the power required to turn off and turn on the PA, respectively, of the l th BS, $\forall l \in \mathcal{L}$. We consider in this chapter the scenarios that $P_l^{(\text{TPA})} < P_l^{(\text{IDL})}$, $\forall l \in \mathcal{L}$, so that powering off an idle-state PA can indeed save power [101–103]. With the constant $1/\Lambda_l$ denoting the PA efficiency, the total power consumption of the l th BS, denoted by $P_l^{(\text{TOT})}$, can then be expressed as (see, e.g., [71, 101–104]):

$$\begin{aligned} P_l^{(\text{TOT})} &\triangleq P_l^{(\text{OFT})} + b_l \left(P_l^{(\text{IDL})} + \Lambda_l \sum_{k=1}^K \|\mathbf{w}_{k,l}\|_2^2 \right) + (1 - b_l) P_l^{(\text{TPA})} + b_l \sum_{k=1}^K a_{k,l} P_{k,l}^{(\text{CMP})} \\ &= \tilde{P}_l^{(\text{OFT})} + b_l \tilde{P}_l^{(\text{IDL})} + \Lambda_l \sum_{k=1}^K \|\mathbf{w}_{k,l}\|_2^2 + \sum_{k=1}^K a_{k,l} P_{k,l}^{(\text{CMP})}, \forall l \in \mathcal{L} \end{aligned} \quad (2.6)$$

where Eqs. (2.4) and (2.5) are used in the development of Eq. (2.6), with the new constants $\tilde{P}_l^{(\text{OFT})} \triangleq P_l^{(\text{OFT})} + P_l^{(\text{TPA})}$ and $\tilde{P}_l^{(\text{IDL})} \triangleq P_l^{(\text{IDL})} - P_l^{(\text{TPA})} > 0$. Since the constants $\{\tilde{P}_l^{(\text{OFT})}, \forall l \in \mathcal{L}\}$ are immaterial to the network optimization problem, for ease of elabo-

ration, it is assumed without loss of generality that $\tilde{P}_l^{(\text{OFT})} = 0, \forall l \in \mathcal{L}$, and we define the total BSs power consumption function $f(\{a_{k,l}\}, \{b_l\}, \{\mathbf{w}_{k,l}\})$ as

$$f(\{a_{k,l}\}, \{b_l\}, \{\mathbf{w}_{k,l}\}) \triangleq \sum_{l=1}^L b_l \tilde{P}_l^{(\text{IDL})} + \sum_{l=1}^L \left(\Lambda_l \sum_{k=1}^K \|\mathbf{w}_{k,l}\|_2^2 + \sum_{k=1}^K a_{k,l} P_{k,l}^{(\text{CMP})} \right). \quad (2.7)$$

2.2.3 The standard big-M formulation of the JNOB problem

In order to limit the overall power dissipations, the cellular network shall be operated in a power-efficient way. Towards this end, we consider in this chapter the network optimization problem with the objective to minimize the overall power consumptions of the L BSs while guaranteeing the minimum QoS requirements of the K MSs. Similar to [12, 23, 33, 71, 75], we adopt the following QoS constraints for the K MSs:

$$\text{SINR}_k = \frac{|\mathbf{h}_k^H \mathbf{w}_k|^2}{\sum_{j=1, j \neq k}^K |\mathbf{h}_k^H \mathbf{w}_j|^2 + \sigma_k^2} \geq \Gamma_k^{(\text{MIN})}, \forall k \in \mathcal{K} \quad (2.8)$$

where the constant $\Gamma_k^{(\text{MIN})} > 0$ denotes the minimum SINR requirement of the k th MS, and SINR_k is defined in Eq. (2.2).

We observe from Eqs. (2.6) and (2.8) that the beamformers are phase-invariant in the sense that if the beamformers $\{\mathbf{w}_k, \forall k \in \mathcal{K}\}$ are feasible for the SINR constraints (2.8), the beamformers $\{\mathbf{w}_k e^{j\theta_k \sqrt{-1}}, \forall k \in \mathcal{K}\}$ also satisfy the SINR requirements (2.8), $\forall \theta_k \in [0, 2\pi)$, $\forall k \in \mathcal{K}$. Further, the beamformers $\{\mathbf{w}_k, \forall k \in \mathcal{K}\}$ and $\{\mathbf{w}_k e^{j\theta_k \sqrt{-1}}, \forall k \in \mathcal{K}\}$ result in the same total per-BS power consumption in (2.6) and the same received SINRs at the MSs. Hence, without loss of generality, the phase of the beamformer \mathbf{w}_k can be chosen such that the term $\mathbf{h}_k^H \mathbf{w}_k$ is real and non-negative, $\forall k \in \mathcal{K}$, and the SINR constraints defined in (2.8) can be rewritten as the second-order cone (SOC) constraints (see, e.g., [12, 31, 75, 83]):

$$\text{Im}\{\mathbf{h}_k^H \mathbf{w}_k\} = 0, \forall k \in \mathcal{K} \quad (2.9a)$$

$$\|[\mathbf{h}_k^H \mathbf{W}, \sigma_k]\|_2 \leq \gamma_k \text{Re}\{\mathbf{h}_k^H \mathbf{w}_k\}, \forall k \in \mathcal{K} \quad (2.9b)$$

where the beamformer matrix $\mathbf{W} \in \mathbb{C}^{M \times K}$ and the constant $\gamma_k > 1$ are defined, respectively, as

$$\mathbf{W} \triangleq [\mathbf{w}_1, \mathbf{w}_2, \dots, \mathbf{w}_K] \quad (2.10)$$

$$\gamma_k \triangleq \sqrt{1 + 1/\Gamma_k^{(\text{MIN})}}, \forall k \in \mathcal{K}. \quad (2.11)$$

With the BS power consumption model in (2.6) and the SINR constraints in (2.9), the JNOB problem can be formulated as the following MISOCP (see, e.g., [82]):

$$\Phi^{(\text{BMI})} \triangleq \min_{\{\mathbf{w}_{k,l}, a_{k,l}, b_l\}} f(\{a_{k,l}\}, \{b_l\}, \{\mathbf{w}_{k,l}\}) \quad (2.12a)$$

$$\text{s.t. (2.9a): } \text{Im}\{\mathbf{h}_k^H \mathbf{w}_k\} = 0, \forall k \in \mathcal{K}$$

$$(2.9b): \left\| [\mathbf{h}_k^H \mathbf{W}, \sigma_k] \right\|_2 \leq \gamma_k \text{Re}\{\mathbf{h}_k^H \mathbf{w}_k\}, \forall k \in \mathcal{K}$$

$$\sqrt{\sum_{k=1}^K \|\mathbf{w}_{k,l}\|_2^2} \leq b_l \sqrt{P_l^{(\text{MAX})}}, \forall l \in \mathcal{L} \quad (2.12b)$$

$$\|\mathbf{w}_{k,l}\|_2 \leq a_{k,l} \sqrt{P_l^{(\text{MAX})}}, \forall k \in \mathcal{K}, \forall l \in \mathcal{L} \quad (2.12c)$$

$$a_{k,l} \leq b_l, \forall k \in \mathcal{K}, \forall l \in \mathcal{L} \quad (2.12d)$$

$$\sum_{l=1}^L a_{k,l} \geq 1, \forall k \in \mathcal{K} \quad (2.12e)$$

$$a_{k,l} \in \{0, 1\}, b_l \in \{0, 1\}, \forall k \in \mathcal{K}, \forall l \in \mathcal{L} \quad (2.12f)$$

where the constraints in (2.12b) denote the per-BS sum-power constraints, with the constant $P_l^{(\text{MAX})}$ denoting the maximum transmission power of the l th BS, and the objective function $f(\{a_{k,l}\}, \{b_l\}, \{\mathbf{w}_{k,l}\})$ is defined in (2.7). The constraints in (2.12d) and (2.12e) are redundant and can be removed, i.e., Eqs. (2.12d) and (2.12e) represent problem-specific cuts, which will be discussed in detail in Section 2.3.2. Note that the on-off constraints in (2.12c) implement the well-known big-M method [67–69] that is used in problem (2.12) to ensure that the beamforming vector $\mathbf{w}_{k,l} = \mathbf{0}$ if the indicator $a_{k,l} = 0$ (see Eq. (2.3)), and that no additional constraint is enforced on the beamforming vector $\mathbf{w}_{k,l}$ in problem (2.12) when $a_{k,l} = 1$. The latter property follows because the per-BS sum-power budget $P_l^{(\text{MAX})}$ represents an upper bound on the term $\|\mathbf{w}_{k,l}\|_2^2$ according to Eq. (2.12b). In the following we refer to problem (2.12) as the big-M integer (BMI) JNOB problem formulation.

We remark that the JNOB problem (2.12) includes as special cases the coordinated beamforming designs [33, 71, 96], clustered BS cooperation schemes [71–78], and full BS cooperation scenarios [71, 91, 92]. Specifically, by introducing the constraints $\{\sum_{l=1}^L a_{k,l} = 1, \forall k \in \mathcal{K}\}$, $\{1 < \sum_{l=1}^L a_{k,l} < L, \forall k \in \mathcal{K}\}$, and $\{\sum_{l=1}^L a_{k,l} = L, \forall k \in \mathcal{K}\}$, the proposed JNOB problem formulation (2.12) can be reduced into the problems of coordinated beamforming [33, 71, 96], (dynamically) clustered BS cooperation [71–78], and full BS cooperation [71, 91, 92], respectively. Moreover, the proposed JNOB problem formulation (2.12) considers powering off the PAs of the BSs to further reduce unnecessary power dissipations,

which has not been considered in CoMP transmission in prior works [71].

2.3 Optimal solutions via the BnC method

2.3.1 The continuous relaxation of the big-M formulation

The formulated JNOB problem (2.12) and other general MISOCPs, can be solved using the convex continuous relaxation based BnC method [67–69, 81, 82]. The continuous relaxation of a MISOCP is the SOCP obtained by relaxing all the integer constraints. The convex continuous relaxation of the formulated JNOB problem in (2.12) can be expressed as the following SOCP, which is referred to as the big-M continuous relaxation (BMC) in the sequel:

$$\Phi^{(\text{BMC})} \triangleq \min_{\{\mathbf{w}_{k,l}, a_{k,l}, b_l\}} f(\{a_{k,l}\}, \{b_l\}, \{\mathbf{w}_{k,l}\}) \quad (2.13a)$$

$$\text{s.t. (2.9a): } \text{Im}\{\mathbf{h}_k^H \mathbf{w}_k\} = 0, \forall k \in \mathcal{K}$$

$$(2.9b): \left\| [\mathbf{h}_k^H \mathbf{W}, \sigma_k] \right\|_2 \leq \gamma_k \text{Re}\{\mathbf{h}_k^H \mathbf{w}_k\}, \forall k \in \mathcal{K}$$

$$(2.12b): \sqrt{\sum_{k=1}^K \|\mathbf{w}_{k,l}\|_2^2} \leq b_l \sqrt{P_l^{(\text{MAX})}}, \forall l \in \mathcal{L}$$

$$(2.12c): \|\mathbf{w}_{k,l}\|_2 \leq a_{k,l} \sqrt{P_l^{(\text{MAX})}}, \forall k \in \mathcal{K}, \forall l \in \mathcal{L}$$

$$(2.12d): a_{k,l} \leq b_l, \forall k \in \mathcal{K}, \forall l \in \mathcal{L}$$

$$(2.12e): \sum_{l=1}^L a_{k,l} \geq 1, \forall k \in \mathcal{K}$$

$$0 \leq a_{k,l} \leq 1, 0 \leq b_l \leq 1, \forall k \in \mathcal{K}, \forall l \in \mathcal{L} \quad (2.13b)$$

where the variables $\{a_{k,l}, b_l, \forall k \in \mathcal{K}, \forall l \in \mathcal{L}\}$, originally constrained to take integer values in (2.12f), are relaxed to continuous variables in the closed interval $[0, 1]$ in (2.13b).

We assume that the point characterized by the parameter tuple $\{\mathbf{w}_{k,l}^{(\text{BMC})}, a_{k,l}^{(\text{BMC})}, b_l^{(\text{BMC})}, \forall k \in \mathcal{K}, \forall l \in \mathcal{L}\}$ is an optimal (not necessarily unique) solution of the SOCP in (2.13). Since the objective function in (2.13a) is minimized, we can easily prove by contradicting

argument the following properties:

$$\sum_{l=1}^L b_l^{(\text{BMC})} \geq 1 \quad (2.14)$$

$$\sum_{k=1}^K a_{k,l}^{(\text{BMC})} \geq b_l^{(\text{BMC})}, \quad \forall l \in \mathcal{L}. \quad (2.15)$$

Assume that the point $\{\mathbf{w}_{k,l}^{(\text{BMI})}, a_{k,l}^{(\text{BMI})}, b_l^{(\text{BMI})}, \forall k \in \mathcal{K}, \forall l \in \mathcal{L}\}$ is an optimal (unnecessarily unique) solution of the JNOB problem in (2.12). We show next that the optimal objective value of the continuous relaxation in (2.13) is *strictly smaller* than that of the JNOB problem (2.12) for practical systems with CoMP transmission. Towards this end, we first present the *necessary* conditions for which the JNOB problem (2.12) and the associated continuous relaxation (2.13) achieve the same optimal objective value, as summarized in the following theorem.

Theorem 2.1 (Necessary Conditions). *If the JNOB problem in (2.12) and the associated continuous relaxation in (2.13) achieve the same optimal objective value, i.e., if $\Phi^{(\text{BMI})} = \Phi^{(\text{BMC})}$, the following conditions must hold:*

$$\sum_{j=1}^K a_{j,l}^{(\text{BMI})} = \sum_{j=1}^K a_{j,m}^{(\text{BMI})} = 1, \text{ if } a_{k,l}^{(\text{BMI})} = a_{k,m}^{(\text{BMI})} = 1, \quad (2.16)$$

for some $k \in \mathcal{K}$, $l \neq m, \forall l, m \in \mathcal{L}$.

That is if the l th BS cooperates with the m th BS to serve the k th MS, then the l th and the m th BSs exclusively serve the k th MS in the case that $\Phi^{(\text{BMI})} = \Phi^{(\text{BMC})}$.

Proof 2.1. *Please refer to Appendix A.1 for the proof.*

We know from *Theorem 2.1* that the special case of $\Phi^{(\text{BMI})} = \Phi^{(\text{BMC})}$ may happen if each of the cooperating BSs (i.e., the BSs that jointly serve MSs in CoMP transmission) serves exclusively a single MS. However, in practical cellular networks employing CoMP transmission, the necessary conditions in (2.16) generally do not hold, since cooperating BSs usually serve multiple MSs to suppress ICI and to improve spectral efficiency. As a result, the following corollary represents a direct application of *Theorem 2.1*.

Corollary 2.1. *In cellular networks with multiple MSs served jointly by cooperating BSs in CoMP transmission, the optimal objective value of the continuous relaxation (2.13) is strictly*

smaller than that of the JNOB problem (2.12), i.e.,

$$\Phi^{(\text{BMC})} < \Phi^{(\text{BMI})}. \quad (2.17)$$

We further observe that we can set $a_{k,l} = 1$ and $b_l = 1$, $\forall k \in \mathcal{K}, \forall l \in \mathcal{L}$, for testing the feasibility of the JNOB problem (2.12). If the JNOB problem (2.12) is feasible, then a fully connected network is a feasible network topology. This suggests that if the SOCP in (2.13) is feasible, e.g., with a feasible solution given by the parameter tuple $\{\mathbf{w}_{k,l}^{(\text{FES})}, a_{k,l}^{(\text{FES})}, b_l^{(\text{FES})}, \forall k \in \mathcal{K}, \forall l \in \mathcal{L}\}$, then the point $\{\mathbf{w}_{k,l}^{(\text{FES})}, a_{k,l} = 1, b_l = 1, \forall k \in \mathcal{K}, \forall l \in \mathcal{L}\}$ is a feasible solution of the JNOB problem (2.12). As a result, the JNOB problem (2.12) is feasible if and only if the associated continuous relaxation in (2.13) is feasible.

2.3.2 Overview of the BnC method and the solver CPLEX

Thanks to the vast advancement of parallel computing, the convex continuous relaxation based BnC method [67–69, 81, 82] is widely adopted for solving MISOCPs and is implemented in the commercial solvers, e.g., in IBM ILOG CPLEX [81]. We present here a brief overview of the continuous relaxation based BnC method, based on the JNOB problem in (2.12) and the associated continuous relaxation in (2.13).

The BnC method is a combination of the branch-and-bound (BnB) procedure and the cutting plane (CP) algorithm [67–69, 81, 82]. As in the BnB procedure, a binary search tree that consists of nodes is constructed in the BnC algorithm, as shown in Fig. 2.2. Each node on the search tree represents the continuous relaxation, which is a SOCP as that of the SOCP in (2.13), of a subproblem resulted from fixing one or more binary integer variables in the original MISOCP (2.12) [67–69, 81, 82]. The BnC search tree is initialized with one node, e.g., the root node that represents the continuous relaxation in (2.13) of the JNOB problem (2.12), as illustrated in Fig. 2.2. If the solution of the SOCP represented by a node is not integer-feasible, the BnC procedure chooses one relaxed binary variable that is not integer-valued in the solution to perform a branching step. As a result, parting from the current node, two subproblems are created by fixing the chosen variable to be one and zero, respectively, which are represented by two descendant nodes of the current node (cf. Fig. 2.2). This branching process is carried out recursively at each node on the BnC search tree. Considering a minimization problem such as the JNOB problem in (2.12), a node and its descendants (i.e., the subtree rooted at that node) can be removed from the BnC search tree if one of the following pruning conditions is satisfied [67–69, 81, 82]:

(C1) The continuous relaxation represented by the node is infeasible (deleting the node).

- (C2) The solution of the continuous relaxation at the node is integer-feasible (deleting the node and recording the integer-feasible solution).
- (C3) The optimal objective value of the continuous relaxation at the node is larger than that of the incumbent solution (deleting the node and its descendants). The incumbent solution is the best-known integer-feasible solution, i.e., the one with the smallest objective value among the recorded integer-feasible solutions.

The pruning conditions (C1) – (C3) are also displayed in Fig. 2.2.

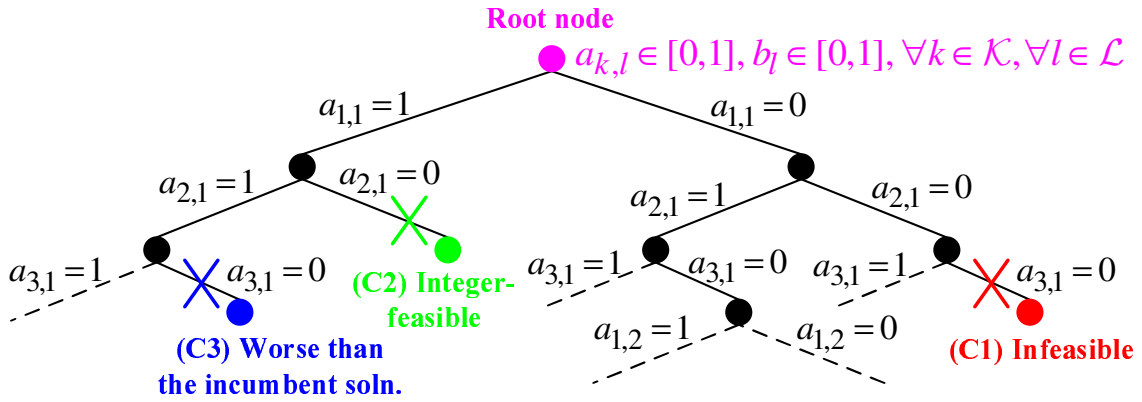


Figure 2.2: Illustration of the BnC solution process and the pruning conditions.

Further, we know from the pruning conditions (C1) – (C3) that the size of the search tree and the computational complexity of the BnC algorithm depend critically on the formulation of the MISOCP, as well as the tightness of the continuous relaxation of the sub-MISOCP at each node [67–69, 81, 82]. Throughout this thesis, the tightness of a continuous relaxation refers to the absolute gap between the optimal objective value of a MISOCP and that of the associated continuous relaxation. For instance, the term $|\Phi^{(\text{BMI})} - \Phi^{(\text{BMC})}|$ represents the tightness of the continuous relaxation in (2.13). In this sense, a smaller gap of $|\Phi^{(\text{BMI})} - \Phi^{(\text{BMC})}|$ corresponds to a tighter continuous relaxation in (2.13).

The solution of the continuous relaxation at a node provides a *local* lower bound (LLB) on the optimal objective value of the corresponding sub-MISOCP at that node and its descendants. The LLBs are important for pruning nodes and reducing the size of the search tree according to the pruning condition (C3). The minimum among the LLBs of the nodes represents a global lower bound (GLB) of the optimal objective value of the JNOB problem (2.12). The GLB is important for computing optimality certificates (see Section 2.5.1) [67–69, 81, 82]. In the BnC procedure, the GLB on the optimal objective value of the original MISOCP (2.12) is successively improved due to the branching operations on some of the relaxed binary variables. Hence, the optimality certificate is eventually obtained as the branching

process continues if the runtime allows. The standard BnC method is commonly implemented with parallel processing threads as in, e.g., the commercial MIP solver IBM ILOG CPLEX [81].

During the tree-searching process of the BnC algorithm, cuts may be generated at each node. Cuts are linear (and/or convex) constraints added to a MISOCP to reduce the size of the feasible set of the associated continuous relaxations [67–69, 81, 82]. That is, cuts are constraints that are redundant (i.e., not affecting the feasible set) for the original MISOCPs, but they reduce the size of the feasible sets of the associated continuous relaxations, as illustrated in Fig. 2.3. For instance, the following constraints, i.e., the constraints in Eq. (2.12e):

$$(2.12e): \sum_{l=1}^L a_{k,l} \geq 1, \forall k \in \mathcal{K}$$

are redundant in the JNOB problem formulation in (2.12), but they are not necessarily automatically satisfied in the associated continuous relaxation in (2.13) (cf. Section 2.3.1). As a result, adding the cuts in (2.12d) and (2.12e) into the continuous relaxation (2.13) can remove some non-integer solutions and tighten the continuous relaxation in (2.13). In addition to such problem-specific cuts in (2.12e), there are also general cuts that are valid for all MISOCPs, like the Clique-cuts, and the Gomory-cuts [67–69, 81, 82].

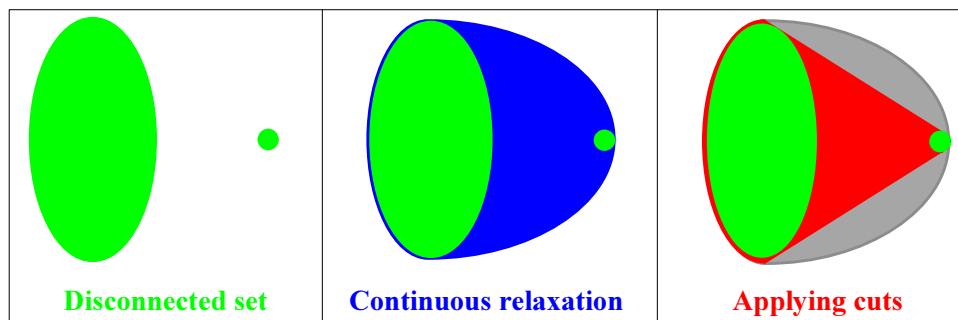


Figure 2.3: From left to right: the feasible set of a MISOCP, the feasible set of the associated continuous relaxation, and the feasible set of the associated continuous relaxation after applying cuts.

The MIP solver IBM ILOG CPLEX implements the standard parallel BnC method [67–69, 81, 82]. CPLEX offers users the full control of the BnC solution process, such as adding problem-specific cuts, and stopping the BnC tree-search when needed [81]. Control of the BnC solution process is the subject of various problem reformulations and customizing techniques discussed later in Section 2.4 and Section 2.5, respectively. The customizing strategies for the BnC method are part of the main contributions of this thesis and they will be

discussed in all the technical chapters. Moreover, the solver CPLEX also records the best-known GLB computed in the BnC procedure. The best-known GLB, or the best-known global upper bound (GUB) for maximization problems (see, e.g., Chapter 3), can be utilized to characterize the quality of the solutions found by CPLEX and to evaluate the performance of low-complexity heuristic algorithms.

2.4 The extended formulation and analytic studies

2.4.1 The extended MISOCP formulation

The standard big-M formulation (2.12) results in loose continuous relaxations (2.13) and very large BnC search trees [67–69]. To improve the standard big-M formulation (2.12), we adopt a similar approach as in [68, 97] and introduce the auxiliary variable $t_{k,l} \geq 0$ to model the power transmitted from the l th BS to the k th MS (i.e., the term $\|\mathbf{w}_{k,l}\|_2^2$), $\forall k \in \mathcal{K}, \forall l \in \mathcal{L}$. We use $t_{k,l}$ to replace the loose upper bound $P_l^{(\text{MAX})}$ used in Eq. (2.12c) and rewrite the on-off constraints in (2.12c) as

$$\|\mathbf{w}_{k,l}\|_2^2 \leq a_{k,l}t_{k,l}, \forall k \in \mathcal{K}, \forall l \in \mathcal{L}. \quad (2.18)$$

which are equivalent to (see, e.g., [34, 105])

$$\| [2\mathbf{w}_{k,l}^T, a_{k,l} - t_{k,l}] \|_2 \leq a_{k,l} + t_{k,l}, \forall k \in \mathcal{K}, \forall l \in \mathcal{L}. \quad (2.19)$$

The on-off constraints in (2.19) become SOC constraints when the binary integer variables $\{a_{k,l}, \forall k \in \mathcal{K}, \forall l \in \mathcal{L}\}$ are relaxed to be continuous variables taking values in the closed interval $[0, 1]$. We redefine accordingly the new total BSs power consumption function $g(\{a_{k,l}\}, \{b_l\}, \{t_{k,l}\})$ as

$$g(\{a_{k,l}\}, \{b_l\}, \{t_{k,l}\}) \triangleq \sum_{l=1}^L b_l \tilde{P}_l^{(\text{IDL})} + \sum_{l=1}^L \left(\Lambda_l \sum_{k=1}^K t_{k,l} + \sum_{k=1}^K a_{k,l} P_{k,l}^{(\text{CMP})} \right). \quad (2.20)$$

With the auxiliary variables $\{t_{k,l}, \forall k \in \mathcal{K}, \forall l \in \mathcal{L}\}$, the new on-off constraints in (2.19), and the new objective function in (2.20), we can convert the big-M MISOCP formulation (2.12) of the JNOB problem into the following extended MISOCP, which is labeled

as the extended integer (EXI) formulation:

$$\Phi^{(\text{EXI})} \triangleq \min_{\{\mathbf{w}_{k,l}, a_{k,l}, b_l, t_{k,l}\}} g(\{a_{k,l}\}, \{b_l\}, \{t_{k,l}\}) \quad (2.21a)$$

$$\text{s.t. (2.9a): } \text{Im}\{\mathbf{h}_k^H \mathbf{w}_k\} = 0, \forall k \in \mathcal{K}$$

$$(2.9b): \left\| [\mathbf{h}_k^H \mathbf{W}, \sigma_k] \right\|_2 \leq \gamma_k \text{Re}\{\mathbf{h}_k^H \mathbf{w}_k\}, \forall k \in \mathcal{K}$$

$$(2.12d): a_{k,l} \leq b_l, \forall k \in \mathcal{K}, \forall l \in \mathcal{L}$$

$$(2.12e): \sum_{l=1}^L a_{k,l} \geq 1, \forall k \in \mathcal{K}$$

$$(2.19): \left\| [2\mathbf{w}_{k,l}^T, a_{k,l} - t_{k,l}] \right\|_2 \leq a_{k,l} + t_{k,l}, \forall k \in \mathcal{K}, \forall l \in \mathcal{L}$$

$$\sum_{k=1}^K t_{k,l} \leq b_l P_l^{(\text{MAX})}, \forall l \in \mathcal{L} \quad (2.21b)$$

$$0 \leq t_{k,l} \leq a_{k,l} P_l^{(\text{MAX})}, \forall k \in \mathcal{K}, \forall l \in \mathcal{L} \quad (2.21c)$$

$$a_{k,l} \in \{0, 1\}, b_l \in \{0, 1\}, \forall k \in \mathcal{K}, \forall l \in \mathcal{L} \quad (2.21d)$$

where the constraints in (2.21b) denote the per-BS sum-power constraints, as that in (2.12b). Note that the constraints in (2.21c) represent problem-specific cuts added to the extended MISOCP formulation (2.21) to obtain tighter continuous relaxations. The extended MISOCP formulation in (2.21) is also known as the perspective reformulation [68, 97] and lifting [68, 82] of the standard big-M MISOCP formulation in (2.12).

Assume that the point $\{\mathbf{w}_{k,l}^{(\text{EXI})}, a_{k,l}^{(\text{EXI})}, b_l^{(\text{EXI})}, t_{k,l}^{(\text{EXI})}, \forall k \in \mathcal{K}, \forall l \in \mathcal{L}\}$ is an optimal (unnecessarily unique) solution of the extended formulation (2.21) of the JNOB problem. From the equivalence of Eqs. (2.18) and (2.19), and considering that the objective function in (2.21a) is minimized, we can straightforwardly establish by contradicting argument that

$$\left\| \mathbf{w}_{k,l}^{(\text{EXI})} \right\|_2^2 = a_{k,l}^{(\text{EXI})} t_{k,l}^{(\text{EXI})} = t_{k,l}^{(\text{EXI})}, \forall k \in \mathcal{K}, \forall l \in \mathcal{L}. \quad (2.22)$$

We know from Eq. (2.22) that adding the equality constraints $\|\mathbf{w}_{k,l}\|_2^2 = t_{k,l}, \forall k \in \mathcal{K}, \forall l \in \mathcal{L}$, will not change the optimal solution set of the extended MISOCP formulation (2.21). However, substituting the KL equalities $\{\|\mathbf{w}_{k,l}\|_2^2 = t_{k,l}, \forall k \in \mathcal{K}, \forall l \in \mathcal{L}\}$ into the extended MISOCP formulation (2.21), we obtain exactly the big-M MISOCP formulation (2.12). As a result, the extended formulation (2.21) and the big-M formulation (2.12) are equivalent in the sense that both yield the same optimal objective value, i.e., $\Phi^{(\text{EXI})} = \Phi^{(\text{BMI})}$, and from an optimal solution of the extended formulation (2.21), an optimal solution of the big-M formulation (2.12) can directly be computed, and vice versa [68, 97].

We remark that although the proposed MISOCP formulations in (2.12) and (2.21) represent the same JNOB problem, the extended formulation (2.21) admits tighter continuous relaxations than that of the big-M formulation (2.12), which shall be analyzed in the next subsection. The former admits less computational complexity than the latter when applying the BnC method, which will be demonstrated in Section 2.7.

2.4.2 Analytic comparison of the two formulations

The continuous relaxation associated with the extended MISOCP formulation (2.21) can be expressed as the following SOCP, referred as the extended continuous relaxation (EXC):

$$\Phi^{(\text{EXC})} \triangleq \min_{\{\mathbf{w}_{k,l}, a_{k,l}, b_l, t_{k,l}\}} g(\{a_{k,l}\}, \{b_l\}, \{t_{k,l}\}) \quad (2.23a)$$

$$\text{s.t. (2.9a): } \text{Im}\{\mathbf{h}_k^H \mathbf{w}_k\} = 0, \forall k \in \mathcal{K}$$

$$(2.9b): \left\| [\mathbf{h}_k^H \mathbf{W}, \sigma_k] \right\|_2 \leq \gamma_k \text{Re}\{\mathbf{h}_k^H \mathbf{w}_k\}, \forall k \in \mathcal{K}$$

$$(2.12d): a_{k,l} \leq b_l, \forall k \in \mathcal{K}, \forall l \in \mathcal{L}$$

$$(2.12e): \sum_{l=1}^L a_{k,l} \geq 1, \forall k \in \mathcal{K}$$

$$(2.19): \left\| [2\mathbf{w}_{k,l}^T, a_{k,l} - t_{k,l}] \right\|_2 \leq a_{k,l} + t_{k,l}, \forall k \in \mathcal{K}, \forall l \in \mathcal{L}$$

$$(2.21b): \sum_{k=1}^K t_{k,l} \leq b_l P_l^{(\text{MAX})}, \forall l \in \mathcal{L}$$

$$(2.21c): 0 \leq t_{k,l} \leq a_{k,l} P_l^{(\text{MAX})}, \forall k \in \mathcal{K}, \forall l \in \mathcal{L}$$

$$0 \leq a_{k,l} \leq 1, 0 \leq b_l \leq 1, \forall k \in \mathcal{K}, \forall l \in \mathcal{L}. \quad (2.23b)$$

Assume that the point $\{\mathbf{w}_{k,l}^{(\text{EXC})}, a_{k,l}^{(\text{EXC})}, b_l^{(\text{EXC})}, t_{k,l}^{(\text{EXC})}, \forall k \in \mathcal{K}, \forall l \in \mathcal{L}\}$ is an optimal (not necessarily unique) solution of the SOCP (2.23). Similar to the development of Eqs. (2.14), (2.15), and (2.22), the following results can readily be established resorting to proof-by-contradiction:

$$\sum_{l=1}^L b_l^{(\text{EXC})} \geq 1 \quad (2.24)$$

$$\sum_{k=1}^K a_{k,l}^{(\text{EXC})} \geq b_l^{(\text{BMC})}, \forall l \in \mathcal{L} \quad (2.25)$$

$$\left\| \mathbf{w}_{k,l}^{(\text{EXC})} \right\|_2^2 = a_{k,l}^{(\text{EXC})} t_{k,l}^{(\text{EXC})} \leq t_{k,l}^{(\text{EXC})}, \forall k \in \mathcal{K}, \forall l \in \mathcal{L}. \quad (2.26)$$

In case that there exist indices $j \in \mathcal{K}$ and $m \in \mathcal{L}$ such that $a_{j,m}^{(\text{EXC})}$ is non-integer valued, i.e., if $0 < a_{j,m}^{(\text{EXC})} < 1$, we know from the equalities in (2.26) and the constraints in (2.21b) that

$$\|\mathbf{w}_{j,m}^{(\text{EXC})}\|_2^2 < t_{j,m}^{(\text{EXC})} = \frac{\|\mathbf{w}_{j,m}^{(\text{EXC})}\|_2^2}{a_{j,m}^{(\text{EXC})}} \quad (2.27)$$

$$\sum_{k=1}^K \|\mathbf{w}_{k,m}^{(\text{EXC})}\|_2^2 < b_m^{(\text{EXC})} P_m^{(\text{MAX})}. \quad (2.28)$$

Eq. (2.27) suggests that if there exists a non-integer-valued variable $a_{j,m}^{(\text{EXC})}$, the objective value in (2.23a) is *strictly larger* than that of (2.13a) at the point $\{\mathbf{w}_{k,l}^{(\text{EXC})}, a_{k,l}^{(\text{EXC})}, b_l^{(\text{EXC})}, t_{k,l}^{(\text{EXC})}, \forall k \in \mathcal{K}, \forall l \in \mathcal{L}\}$. Eq. (2.28) further reveals that the feasible set described by Eqs. (2.19) and (2.21b) when projected onto the variables $\{\mathbf{w}_{k,l}, a_{k,l}, b_l, \forall k \in \mathcal{K}, \forall l \in \mathcal{L}\}$, i.e., projecting the parameter tuple $\{\mathbf{w}_{k,l}, a_{k,l}, b_l, t_{k,l}, \forall k \in \mathcal{K}, \forall l \in \mathcal{L}\}$ to the parameter tuple $\{\mathbf{w}_{k,l}, a_{k,l}, b_l, \forall k \in \mathcal{K}, \forall l \in \mathcal{L}\}$, is always contained in the corresponding feasible set defined by Eqs. (2.12b) and (2.12c).

We know directly from the constraints in (2.12d) and (2.21c) that

$$a_{k,l}^{(\text{EXC})} \leq b_l^{(\text{EXC})}, \forall k \in \mathcal{K}, \forall l \in \mathcal{L} \quad (2.29)$$

$$t_{k,l}^{(\text{EXC})} \leq a_{k,l}^{(\text{EXC})} P_l^{(\text{MAX})}, \forall k \in \mathcal{K}, \forall l \in \mathcal{L}. \quad (2.30)$$

Eqs. (2.26) and (2.30) together imply that

$$\|\mathbf{w}_{k,l}^{(\text{EXC})}\|_2^2 \leq \left(a_{k,l}^{(\text{EXC})}\right)^2 P_l^{(\text{MAX})}, \forall k \in \mathcal{K}, \forall l \in \mathcal{L} \quad (2.31)$$

and Eqs. (2.21b), (2.26), and (2.29) together suggest that

$$\sum_{k=1}^K \|\mathbf{w}_{k,l}^{(\text{EXC})}\|_2^2 \leq \left(b_l^{(\text{EXC})}\right)^2 P_l^{(\text{MAX})}, \forall l \in \mathcal{L}. \quad (2.32)$$

Eqs. (2.31) and (2.32), together with the constraints in (2.12d) and (2.12e), suggest that the point $\{\mathbf{w}_{k,l}^{(\text{EXC})}, a_{k,l}^{(\text{EXC})}, b_l^{(\text{EXC})}, \forall k \in \mathcal{K}, \forall l \in \mathcal{L}\}$, i.e., the projection of the point $\{\mathbf{w}_{k,l}^{(\text{EXC})}, a_{k,l}^{(\text{EXC})}, b_l^{(\text{EXC})}, t_{k,l}^{(\text{EXC})}, \forall k \in \mathcal{K}, \forall l \in \mathcal{L}\}$, satisfies all the constraints of the SOCP in (2.13) and therefore it is a feasible solution of the SOCP (2.13). Based on this result, we can compare the tightness of the continuous relaxations in (2.13) and (2.23), as summarized in the following theorem.

Theorem 2.2 (Tighter Continuous Relaxation). *The optimal objective value of the extended*

continuous relaxation in (2.23) is no smaller than that of the big-M continuous relaxation in (2.13), i.e., it always holds that

$$\Phi^{(\text{EXC})} \geq \Phi^{(\text{BMC})}. \quad (2.33)$$

Proof 2.2. Please refer to Appendix A.2 for the proof.

We know from *Theorem 2.2* that the extended continuous relaxation (2.23) generally provides a *larger* lower bound $\Phi^{(\text{EXC})}$ on the optimal objective value $\Phi^{(\text{EXI})} = \Phi^{(\text{BMI})}$ than the corresponding lower bound $\Phi^{(\text{BMC})}$ provided by the big-M continuous relaxation (2.13). We can further show that the optimal objective value of the continuous relaxation (2.23) is *strictly larger* than that of the continuous relaxation (2.13) for cellular networks employing CoMP transmission. To this end, we first make use of Eq. (2.26) to identify the *necessary* conditions for the special case of $\Phi^{(\text{BMC})} = \Phi^{(\text{EXC})}$ to hold, which is summarized in the following theorem.

Theorem 2.3 (Necessary Conditions). *If the continuous relaxations (2.13) and (2.23) achieve the same optimal objective value, i.e., if $\Phi^{(\text{BMC})} = \Phi^{(\text{EXC})}$, then it must hold that*

$$a_{k,l}^{(\text{EXC})} \in \{0, 1\}, b_l^{(\text{EXC})} \in \{0, 1\}, \forall k \in \mathcal{K}, \forall l \in \mathcal{L} \quad (2.34)$$

$$\Phi^{(\text{BMC})} = \Phi^{(\text{BMI})} = \Phi^{(\text{EXI})} = \Phi^{(\text{EXC})} \quad (2.35)$$

$$\sum_{j=1}^K a_{j,l}^{(\text{EXC})} = \sum_{j=1}^K a_{j,m}^{(\text{EXC})} = 1, \text{ if } a_{k,l}^{(\text{EXC})} = a_{k,m}^{(\text{EXC})} = 1, \\ \text{for some } k \in \mathcal{K}, l \neq m, \forall l, m \in \mathcal{L}. \quad (2.36)$$

That is, in the case that $\Phi^{(\text{BMC})} = \Phi^{(\text{EXC})}$, the point $\{\mathbf{w}_{k,l}^{(\text{EXC})}, a_{k,l}^{(\text{EXC})}, b_l^{(\text{EXC})}, t_{k,l}^{(\text{EXC})}, \forall k \in \mathcal{K}, \forall l \in \mathcal{L}\}$ and the projected point $\{\mathbf{w}_{k,l}^{(\text{EXC})}, a_{k,l}^{(\text{EXC})}, b_l^{(\text{EXC})}, \forall k \in \mathcal{K}, \forall l \in \mathcal{L}\}$ are optimal solutions of problems (2.21) and (2.12), respectively. Further, the special case of $\Phi^{(\text{BMC})} = \Phi^{(\text{EXC})}$ may occur if each of the cooperating BSs (i.e., the BSs that jointly serve MSs in CoMP transmission) serves only a single MS.

Proof 2.3. Please refer to Appendix A.3 for the proof.

It is important to note that in practical cellular networks employing CoMP transmission, the cooperating BSs usually serve more than one MS to mitigate ICI and to improve spectral efficiency, and therefore the necessary conditions in (2.36) practically do not hold. As a result, the following corollary can directly be concluded from *Theorem 2.3*.

Corollary 2.2. *In cellular networks with BSs collaboratively serving multiple MSs in CoMP transmission, the lower bound of the minimum total BSs power consumption provided by the SOCP (2.23) is strictly larger than that given by the SOCP (2.13), i.e.,*

$$\Phi^{(\text{BMC})} < \Phi^{(\text{EXC})} \leq \Phi^{(\text{BMI})} = \Phi^{(\text{EXI})}. \quad (2.37)$$

The advantages of the extended MISOCP formulation (2.21) over the standard big-M MISOCP formulation (2.12) in terms of computational complexity when applying the BnC method will be further demonstrated with numerical results in Section 2.7.2.

2.5 Techniques for customizing the BnC method

We introduce in this section several customizing strategies to further speed up the parallel BnC algorithm implemented in, e.g., the MIP solver CPLEX [81], to solve the JNOB problem. The customizing techniques also enable the BnC algorithm to compute tight lower bounds on the minimum total BSs power consumptions, which can be employed to evaluate the performance of fast heuristic algorithms.

2.5.1 Customized optimality criterion

Define $\Psi^{(\text{BIF})}$ and $\Psi^{(\text{GLB})}$ as the objective value of the best-known integer-feasible (BIF) solution (also called the incumbent solution [69, 81, 82]) of the JNOB problem (2.21) and the largest GLB of the optimal objective value $\Phi^{(\text{EXI})}$, respectively, computed in the BnC procedure. Since $\Psi^{(\text{BIF})}$ and $\Psi^{(\text{GLB})}$ represent the best-known global upper bound (GUB) and GLB of the optimal objective value $\Phi^{(\text{EXI})}$, respectively, we have that

$$0 < \Psi^{(\text{GLB})} \leq \Phi^{(\text{EXI})} \leq \Psi^{(\text{BIF})}. \quad (2.38)$$

A widely adopted measure of the maximum relative deviation from optimality of an incumbent solution (i.e., the best-known integer-feasible solution), is the relative MIP gap, defined as [69, 81, 82]:

$$\text{Relative MIP gap} \triangleq \frac{|\Psi^{(\text{GLB})} - \Psi^{(\text{BIF})}|}{\Psi^{(\text{BIF})}} = 1 - \frac{\Psi^{(\text{GLB})}}{\Psi^{(\text{BIF})}}. \quad (2.39)$$

However, the runtime required to establish the exact optimality certificate, i.e., $\Psi^{(\text{BIF})} = \Psi^{(\text{GLB})}$, for large-scale networks is prohibitive (even if the incumbent solution is indeed

optimal). The quality of the incumbent solution is commonly measured by the relative MIP gap defined in (2.39). According to [69, 81, 82], an incumbent solution computed in the BnC procedure is declared as an *optimal* solution of the JNOB problem (2.21) if it satisfies that

$$1 - \frac{\Psi^{(\text{GLB})}}{\Psi^{(\text{BIF})}} \leq \eta \quad (2.40)$$

where the constant $\eta \geq 0$ denotes the prescribed relative optimality tolerance, which can be customized for specific applications [69, 81, 82]. Particularly, the constant η can be set to be *strictly larger* than zero. This implies that an incumbent solution is declared as the optimal (not necessarily unique) solution of problem (2.21) if it meets the optimality criterion in (2.40), despite the fact that there may exist integer-feasible solutions with smaller objective values [69, 81, 82].

Further, we know from Eq. (2.40) that it is of great interest to find high-quality integer-feasible solutions resulting in a small GUB $\Psi^{(\text{BIF})}$ and to compute a large GLB $\Psi^{(\text{GLB})}$. Small $\Psi^{(\text{BIF})}$ and large $\Psi^{(\text{GLB})}$ are essential for speeding up the process of computing the optimality certificate in (2.40).

2.5.2 Customized node selection and branching rules

The computational complexity of solving the JNOB problem with the BnC method depends on the total number of nodes on the BnC search tree that are visited. We can reduce the number of nodes that need to be processed by customizing the BnC algorithm according to the specific characteristics of the JNOB problem (2.21). Several customizing strategies can be applied to control the execution of the BnC search process, e.g., defining the branching priorities. The customizing strategies are supported by the solver CPLEX [81].

In the BnC procedure, the node selection rule decides which node that has not been visited before on the BnC search tree will be visited after processing the current node. Several node selection strategies are supported in the solver CPLEX [81]. When applying CPLEX on the JNOB problem, we employ the *best-bound search* rule, which chooses the node that has the *smallest* objective value of the SOCP among all active nodes [67–69], i.e., the node with the smallest LLB. The best-bound search rule yields small GLB $\Psi^{(\text{GLB})}$ of the optimal objective value $\Phi^{(\text{EXI})}$ since the smallest LLB is replaced by two *larger* LLBs of the two descendant nodes after processing the current node [67–69] and therefore it speeds up computing the optimality certificate (2.40).

When the SOCP at a node of the BnC search tree is solved, a decision needs to be taken to determine which one of the non-integer-valued variable among the relaxed binary variables

in the solution to branch on, i.e., which variable to fix to integer values in the next step of the BnC algorithm. Branching variable selection at a node is carried out according to the branching priorities of the (relaxed) binary integer variables. At each branching step, the variable that has the largest branching priority among all the non-integer-valued relaxed binary variables is selected.

Recall that the point $\{\mathbf{w}_{k,l}^{(\text{EXC})}, a_{k,l}^{(\text{EXC})}, b_l^{(\text{EXC})}, t_{k,l}^{(\text{EXC})}, \forall k \in \mathcal{K}, \forall l \in \mathcal{L}\}$ represents an optimal solution of the continuous relaxation (2.23) and therefore the vectors $\{\mathbf{w}_{k,l}^{(\text{EXC})}, \forall k \in \mathcal{K}, \forall l \in \mathcal{L}\}$ can be treated as the *virtual* beamformers under a fully connected network. Due to the specific scalar ambiguity of the variables $\{a_{k,l}^{(\text{EXC})}, \forall k \in \mathcal{K}, \forall l \in \mathcal{L}\}$ and $\{t_{k,l}^{(\text{EXC})}, \forall k \in \mathcal{K}, \forall l \in \mathcal{L}\}$ expressed in the left equality of Eq. (2.26), it is generally not useful to choose a variable to branch on based solely on the values of $\{a_{k,l}^{(\text{EXC})}, \forall k \in \mathcal{K}, \forall l \in \mathcal{L}\}$. Hence, to determine proper branching priorities of the non-integer-valued relaxed binary variables, we define in this chapter the incentive measure, denoted by $\Upsilon_{k,l}$, of assigning the l th BS to serve the k th MS (i.e., setting $a_{k,l} = 1$) as

$$\Upsilon_{k,l} \triangleq \frac{\sum_{j=1}^K |\mathbf{h}_{j,l}^H \mathbf{w}_{k,l}^{(\text{EXC})}|^2}{\Lambda_l t_{k,l}^{(\text{EXC})} + P_{k,l}^{(\text{CMP})}}, \forall k \in \mathcal{K}, \forall l \in \mathcal{L}. \quad (2.41)$$

The numerator of Eq. (2.41) represents the *total power* received at the K MSs from the virtual beamformer $\mathbf{w}_{k,l}^{(\text{EXC})}$, and the denominator of Eq. (2.41) can be interpreted as the power expended to obtain this total received power. As a result, the incentive measure in Eq. (2.41) can be interpreted as the *normalized system utility* obtained from assigning the l th BS to the k th MS. In other words, the incentive measure $\Upsilon_{k,l}$ represents the *normalized importance* of the link between the l th BS and the k th MS to the entire network and to the JNOB problem (2.21).

Similarly, we define the incentive measure Ω_l of switching on the PA of the l th BS (i.e., setting $b_l = 1$) as

$$\Omega_l \triangleq \frac{\sum_{k=1}^K \sum_{j=1}^K |\mathbf{h}_{j,l}^H \mathbf{w}_{k,l}^{(\text{EXC})}|^2}{\Lambda_l \sum_{k=1}^K t_{k,l}^{(\text{EXC})} + \tilde{P}_l^{(\text{IDL})}}, \forall l \in \mathcal{L}. \quad (2.42)$$

The numerator of Eq. (2.42) represents the *total power* received at the K MSs when the l th BS is powered on and transmitting, and the denominator of Eq. (2.42) represents the total power expended at the l th BS when it is transmitting. Hence, the incentive measure Ω_l given in (2.42) can be interpreted as the *normalized system utility* that can be potentially gained from powering on the PA of the l th BS. In other words, the incentive measure Ω_l represents the *normalized importance* of the l th BS to the whole network and to the JNOB

problem (2.21).

Intuitively, the relaxed binary variables that have large impacts (i.e., large incentive measures) on the JNOB problem (2.21) shall be processed first. We propose here to carry out variable selection in the BnC procedure based on the proposed incentive measures defined in Eqs. (2.41) and (2.42). Specifically, we define the branching priority, denoted as $\bar{\Upsilon}_{k,l}$, associated with the (relaxed) binary variable $a_{k,l}$ as

$$\bar{\Upsilon}_{k,l} \triangleq \sum_{j=1}^K \sum_{m=1}^L \mathcal{I}(\Upsilon_{j,m} \leq \Upsilon_{k,l}), \forall k \in \mathcal{K}, \forall l \in \mathcal{L} \quad (2.43)$$

where the indicator function $\mathcal{I}(\Upsilon_{j,m} \leq \Upsilon_{k,l})$ is defined as

$$\mathcal{I}(\Upsilon_{j,m} \leq \Upsilon_{k,l}) = \begin{cases} 1, & \text{if } \Upsilon_{j,m} \leq \Upsilon_{k,l} \\ 0, & \text{otherwise.} \end{cases} \quad (2.44)$$

Accordingly, we define the branching priority $\bar{\Omega}_l$ of the (relaxed) binary variable b_l as

$$\bar{\Omega}_l \triangleq \max_{j \in \mathcal{K}, m \in \mathcal{L}} \bar{\Upsilon}_{j,m} + \sum_{m=1}^L \mathcal{I}(\Omega_m \leq \Omega_l), \forall l \in \mathcal{L} \quad (2.45)$$

where the term $\max_{j \in \mathcal{K}, m \in \mathcal{L}} \bar{\Upsilon}_{j,m}$ is used in (2.45) to enforce *larger* branching priorities of the variables $\{b_l, \forall l \in \mathcal{L}\}$ than that of the variables $\{a_{k,l}, \forall k \in \mathcal{K}, \forall l \in \mathcal{L}\}$, so that the PA of a BS is powered on (off) before assigning (unassigning) the BS to any MSs.

We remark that the proposed branching prioritizing principles in (2.43) and (2.45) take into account not only the channel vectors $\{\mathbf{h}_{k,l}^H, \forall k \in \mathcal{K}, \forall l \in \mathcal{L}\}$, but also the system parameters $\{\Lambda_l, \tilde{P}_l^{(\text{IDL})}, P_{k,l}^{(\text{CMP})}, \forall k \in \mathcal{K}, \forall l \in \mathcal{L}\}$. In addition, the dependence of the branching priorities (2.43) and (2.45) on the SINR requirements $\{\Gamma_k^{(\text{MIN})}, \forall k \in \mathcal{K}\}$ is implicitly incorporated through the virtual beamformers $\{\mathbf{w}_{k,l}^{(\text{EXC})}, \forall k \in \mathcal{K}, \forall l \in \mathcal{L}\}$, which are obtained from solving the SOCP in (2.23). Furthermore, fixing the branching priorities of the (relaxed) binary variables favors parallel implementations of the BnC procedure [67–69, 81, 82].

2.5.3 Integer-feasible initializations

According to the pruning conditions (C3) specified in Section 2.3.2, high-quality integer-feasible solutions can also reduce the number of visited nodes in the BnC method and therefore reduce the computational complexity of the BnC algorithm. High-quality integer-feasible initializations can be obtained through low-complexity heuristic algorithms, which

are discussed in the subsequent section.

2.6 The low-complexity heuristic algorithms

2.6.1 The SOCP based inflation procedure

We propose in this subsection a fast inflation procedure [83, 84] to compute high-quality integer-feasible solutions of the JNOB problem (2.12). Let the point $\{a_{k,l}^{(n)}, b_l^{(n)}, \forall k \in \mathcal{K}, \forall l \in \mathcal{L}\}$ denote the solution of the binary variables obtained in the n th iteration. The inflation procedure is initialized with none of the BSs assigned to any MSs, i.e., $a_{k,l}^{(0)} = 0, b_l^{(0)} = 0, \forall k \in \mathcal{K}, \forall l \in \mathcal{L}$, and a sufficiently large objective value $\Phi^{(0)}$, e.g., set $\Phi^{(0)} \triangleq \sum_{l=1}^L (\tilde{P}_l^{(\text{IDL})} + \Lambda_l P_l^{(\text{MAX})} + \sum_{k=1}^K P_{k,l}^{(\text{CMP})})$. The BSs are gradually assigned to the MSs by fixing one of the *zero-valued* variables in $\{a_{k,l}^{(n-1)}, \forall k \in \mathcal{K}, \forall l \in \mathcal{L}\}$ to one in the n th ($n \geq 1$) iteration of the inflation procedure.

It is a critical decision how to choose and fix to one a particular zero-valued variables in the set $\{a_{k,l}^{(n-1)}, \forall k \in \mathcal{K}, \forall l \in \mathcal{L}\}$ in the n th iteration. Intuitively, we shall consider the binary variables that have large impacts on the JNOB problem (2.21). Hence, we propose here to select variables according to the associated incentive measures defined in (2.41). That is, in the n th iteration, the variable that has the *largest* incentive measure (2.41) among the zero-valued variables in the set $\{a_{k,l}^{(n-1)}, \forall k \in \mathcal{K}, \forall l \in \mathcal{L}\}$ is chosen and set to one. If two or more zero-valued variables in the set $\{a_{k,l}^{(n-1)}, \forall k \in \mathcal{K}, \forall l \in \mathcal{L}\}$ have the same largest incentive measure, we randomly pick one of them. Note that according to Eqs. (2.5) and (2.12d), we need to set $b_{\bar{l}}^{(n)} = 1$ if we fix $a_{\bar{k},\bar{l}}^{(n)} = 1$, for the chosen $\bar{k} \in \mathcal{K}, \bar{l} \in \mathcal{L}$.

After obtaining the binary variables $\{a_{k,l}^{(n)}, b_l^{(n)}, \forall k \in \mathcal{K}, \forall l \in \mathcal{L}\}$ in the n th iteration of the inflation procedure, we then solve the following SOCP, which represents a subproblem of the JNOB problem in (2.12) with all the variables $\{a_{k,l}, b_l, \forall k \in \mathcal{K}, \forall l \in \mathcal{L}\}$ fixed:

$$\Phi^{(n)} \triangleq \min_{\{\mathbf{w}_{k,l}\}} f\left(\{a_{k,l}^{(n)}\}, \{b_l^{(n)}\}, \{\mathbf{w}_{k,l}\}\right) \quad (2.46a)$$

$$\text{s.t. (2.9a): } \text{Im}\{\mathbf{h}_k^H \mathbf{w}_k\} = 0, \forall k \in \mathcal{K}$$

$$(2.9b): \left\| [\mathbf{h}_k^H \mathbf{W}, \sigma_k] \right\|_2 \leq \gamma_k \text{Re}\{\mathbf{h}_k^H \mathbf{w}_k\}, \forall k \in \mathcal{K}$$

$$\sum_{k=1}^K \|\mathbf{w}_{k,l}\|_2^2 \leq P_l^{(\text{MAX})}, \text{ if } b_l^{(n)} = 1, \forall l \in \mathcal{L} \quad (2.46b)$$

$$\mathbf{w}_{k,l} = \mathbf{0}, \text{ if } a_{k,l}^{(n)} = 0, \forall k \in \mathcal{K}, \forall l \in \mathcal{L} \quad (2.46c)$$

where the total BSs power consumption function $f(\{a_{k,l}\}, \{b_l\}, \{\mathbf{w}_{k,l}\})$ is defined in (2.7).

If the SOCP in (2.46) is infeasible, we set $\Phi^{(n)} = \Phi^{(0)}$ and proceed to the next iteration. Otherwise, after solving problem (2.46), we compare the objective value $\Phi^{(n)}$ with that of $\Phi^{(n-1)}$. If $\Phi^{(n)} \leq \Phi^{(n-1)}$, we proceed to the next iteration. If $\Phi^{(n)} > \Phi^{(n-1)}$, i.e., if a worse solution is reached, we stop with one-step backtracking, i.e., stop and return the objective value $\Phi^{(n-1)}$ and the solution $\{\mathbf{w}_{k,l}^{(n-1)}, a_{k,l}^{(n-1)}, b_l^{(n-1)}, \forall k \in \mathcal{K}, \forall l \in \mathcal{L}\}$. The simple necessary conditions that: $\sum_{l=1}^L a_{k,l}^{(n)} \geq 1, \forall k \in \mathcal{K}$, can be verified before solving the SOCP (2.46) to reduce the computational efforts. The low-complexity inflation procedure is summarized in Alg. 2.1.

Init.: Set $\Phi^{(0)} \triangleq \sum_{l=1}^L (\tilde{P}_l^{(\text{IDL})} + \Lambda_l P_l^{(\text{MAX})} + \sum_{k=1}^K P_{k,l}^{(\text{CMP})})$, set $a_{k,l}^{(0)} = 0, b_l^{(0)} = 0, \forall k \in \mathcal{K}, \forall l \in \mathcal{L}$, and set the iteration number $n = 1$.

Step 1: Compute $(\bar{k}, \bar{l}) \triangleq \underset{(k,l) \in \mathcal{P}^{(n)}}{\text{argmax}} \Upsilon_{k,l}$,

with the set $\mathcal{P}^{(n)} \triangleq \{(k, l) | k \in \mathcal{K}, l \in \mathcal{L}, a_{k,l}^{(n-1)} = 0\}$.

Step 2: If no index pair (\bar{k}, \bar{l}) can be found, the inflation procedure *stops* and returns the results of the $(n-1)$ th iteration. Otherwise, copy $a_{k,l}^{(n)} = a_{k,l}^{(n-1)}, b_l^{(n)} = b_l^{(n-1)}, \forall k \in \mathcal{K}, \forall l \in \mathcal{L}$, and fix $a_{\bar{k},\bar{l}}^{(n)} = b_{\bar{l}}^{(n)} = 1$.

Step 3: Check the necessary conditions: $\sum_{l=1}^L a_{k,l}^{(n)} \geq 1, \forall k \in \mathcal{K}$. If not all of them are satisfied, update the iteration number $n \leftarrow n + 1$ and go back to **Step 1** and repeat.

Step 4: Solve the SOCP (2.46) with the obtained indicators

$\{a_{k,l}^{(n)}, b_l^{(n)}, \forall k \in \mathcal{K}, \forall l \in \mathcal{L}\}$.

Step 5: If the SOCP (2.46) is feasible and $\Phi^{(n)} > \Phi^{(n-1)}$, stop and return the results of the $(n-1)$ th iteration.

Step 6: Update $n \leftarrow n + 1$ and go back to **Step 1** and repeat.

Algorithm 2.1: The proposed SOCP based inflation procedure

Since there are in total KL binary indicators $\{a_{k,l}, \forall k \in \mathcal{K}, \forall l \in \mathcal{L}\}$, the *worst-case* computational complexity of the inflation procedure in Alg. 2.1 mainly consists in solving $K(L-1)$ instances of the SOCP (2.46) and hence the inflation procedure is a polynomial-time algorithm and it converges in finite iterations [34, 105]. We will show via numerical examples in Section 2.7 that the proposed Alg. 2.1 yields near-optimal solutions of problem (2.21) with very low computational complexity.

2.6.2 The SOCP based deflation procedure

Similar to the inflation procedure, we develop here an efficient deflation procedure to compute close-to-optimal solutions of the considered JNOB problem (2.21). In contrast to the inflation procedure in Alg. 2.1, the deflation procedure starts with a fully connected network

topology, i.e., $a_{k,l}^{(0)} = 1, b_l^{(0)} = 1, \forall k \in \mathcal{K}, \forall l \in \mathcal{L}$, which is inspired by the fact that if the JNOB problem (2.21) is feasible, then a fully-connected configuration yields a feasible solution. The sparsity of the network topology is then gradually increased via fixing one of the *one-valued* variables in the set $\{a_{k,l}^{(n-1)}, \forall k \in \mathcal{K}, \forall l \in \mathcal{L}\}$ to zero in the n th ($n \geq 1$) iteration of the deflation procedure.

The performance of the deflation procedure depends highly on the rules defining how a particular one-valued variables in the set $\{a_{k,l}^{(n-1)}, \forall k \in \mathcal{K}, \forall l \in \mathcal{L}\}$ is chosen and set to zero in the n th iteration. Similar as in Alg. 2.1, we propose here to select variables according to the associated incentive measures defined in Eq. (2.41). Specifically, in the n th iteration, the variable that has the *smallest* incentive measure (2.41) among the one-valued variables in $\{a_{k,l}^{(n-1)}, \forall k \in \mathcal{K}, \forall l \in \mathcal{L}\}$ is selected and set to zero. If multiple one-valued variables in the set $\{a_{k,l}^{(n-1)}, \forall k \in \mathcal{K}, \forall l \in \mathcal{L}\}$ have the same *smallest* incentive measure, we randomly choose one of them. Note that according to Eqs. (2.5) and (2.12d), we need to update $b_l^{(n)} = \max_{j \in \mathcal{K}} a_{j,l}^{(n)}$ after setting $a_{\tilde{k},\tilde{l}}^{(n)} = 0$, for the chosen $\tilde{k} \in \mathcal{K}, \tilde{l} \in \mathcal{L}$, in the n th iteration.

After updating the binary variables $\{a_{k,l}^{(n)}, b_l^{(n)}, \forall k \in \mathcal{K}, \forall l \in \mathcal{L}\}$ in the n th iteration, we then solve the SOCP in (2.46). If the SOCP (2.46) is feasible and $\Phi^{(n)} \leq \Phi^{(n-1)}$, i.e., a better solution is obtained, we record the results and proceed to the next iteration. Conversely, if the SOCP (2.46) is infeasible, or if it is feasible and $\Phi^{(n)} > \Phi^{(n-1)}$, we initiate a one-step backtracking procedure, i.e., we set $a_{\tilde{k},\tilde{l}}^{(n)} = 1, b_{\tilde{l}}^{(n)} = 1, \Phi^{(n)} = \Phi^{(n-1)}$, and mark $\Upsilon_{\tilde{k},\tilde{l}} = +\infty$ (for preventing infinite loop), with $a_{\tilde{k},\tilde{l}}^{(n)}$ denoting the variable that is picked up in the n th iteration. Similar to the inflation procedure, the necessary conditions that $\sum_{l=1}^L a_{k,l}^{(n)} \geq 1, \forall k \in \mathcal{K}$, can also be used here to quickly certify the feasibility of the SOCP (2.46). The

low-complexity deflation procedure is summarized in Alg. 2.2.

Init.: Set $\Phi^{(0)} \triangleq \sum_{l=1}^L (\tilde{P}_l^{(\text{IDL})} + \Lambda_l P_l^{(\text{MAX})} + \sum_{k=1}^K P_{k,l}^{(\text{CMP})})$, set $a_{k,l}^{(0)} = 1, b_l^{(0)} = 1$, $\forall k \in \mathcal{K}, \forall l \in \mathcal{L}$, and set the iteration number $n = 1$.

Step 1: Compute $(\tilde{k}, \tilde{l}) \triangleq \underset{(k,l) \in \mathcal{Q}^{(n)}}{\operatorname{argmin}} \Upsilon_{k,l}$, s.t. $\sum_{m=1}^L a_{k,m} \geq 2$, with the set $\mathcal{Q}^{(n)} \triangleq \{(k, l) | k \in \mathcal{K}, l \in \mathcal{L}, a_{k,l}^{(n-1)} = 1\}$.

Step 2: If no index pair (\tilde{k}, \tilde{l}) can be found, the deflation procedure *stops* and returns the results of the $(n - 1)$ th iteration. Otherwise, copy $a_{\tilde{k},\tilde{l}}^{(n)} = a_{\tilde{k},\tilde{l}}^{(n-1)}, b_{\tilde{l}}^{(n)} = b_{\tilde{l}}^{(n-1)}$, $\forall k \in \mathcal{K}, \forall l \in \mathcal{L}$, and fix $a_{\tilde{k},\tilde{l}}^{(n)} = 0$ and $b_{\tilde{l}}^{(n)} = \max_{j \in \mathcal{K}} a_{j,\tilde{l}}^{(n)}$.

Step 3: Solve the SOCP (2.46) with the obtained indicators $\{a_{k,l}^{(n)}, b_l^{(n)}, \forall k \in \mathcal{K}, \forall l \in \mathcal{L}\}$.

Step 4: If the SOCP (2.46) is feasible and $\Phi^{(n)} > \Phi^{(n-1)}$, or if the SOCP (2.46) is infeasible, we set $a_{\tilde{k},\tilde{l}}^{(n)} = 1, b_{\tilde{l}}^{(n)} = 1, \Phi^{(n)} = \Phi^{(n-1)}$, and mark $\Upsilon_{\tilde{k},\tilde{l}} = +\infty$.

Step 5: Update $n \leftarrow n + 1$ and go back to **Step 1** and repeat.

Algorithm 2.2: The proposed SOCP based deflation procedure

The computational complexity of the deflation procedure in Alg. 2.2 mainly consists in solving $K(L - 1)$ times the SOCP (2.46) since there are only KL binary variables of $\{a_{k,l}, \forall k \in \mathcal{K}, \forall l \in \mathcal{L}\}$ and therefore the deflation procedure is a polynomial-time algorithm [34]. In addition, we shall show via numerical results in Section 2.7 that the deflation procedure yields close-to-optimal solutions of the JNOB problem (2.21) with very low computational complexity.

2.7 Simulation results

In the simulations, we consider a cellular network comprising 13 identical hexagonal cells with one BS located at each cell-center. The layout of the 13 cells in a two-dimensional coordinate system is depicted in Fig. 2.4 with a cell-radius of 1 kilometer (km). A total of $K = 15$ MSs are randomly and uniformly dropped in the rectangular coverage area defined by the dashed lines as shown in Fig. 2.4. Similar to the existing works [72, 75–78], we consider the following channel model [106]: (i) the 3GPP LTE pathloss (PL) mode: $PL = 148.1 + 37.6 \log_{10}(d)$ (in dB), with d (in km) denoting the BS-MS distance, (ii) Log-norm shadowing with zero mean, 8 dB variance, (iii) Rayleigh fading with zero mean and unit variance, (iv) transmit antenna power gain of 9 dB and noise power $\sigma_k^2 = -143$ dB, $\forall k \in \mathcal{K}$. We adopt homogeneous parameter settings: the l th BS is equipped with $M_l = 4$ transmit antennas, the per-BS transmission power budget $P_l^{(\text{MAX})} = 10$ dB, the PA efficiency $1/\Lambda_l =$

25% [104], the system parameters $\Gamma_k^{(\text{MIN})} = 6$ dB, $\tilde{P}_l^{(\text{IDL})} = 10$ dB, and $P_{k,l}^{(\text{CMP})} = P^{(\text{CMP})}$, $\forall k \in \mathcal{K}, \forall l \in \mathcal{L}$, with the values of $P^{(\text{CMP})}$ listed in the figures and the tables. The relative optimality tolerance in (2.40) is set as $\eta = 1\%$. The simulation results are averaged over 500 Monte Carlo runs (MCRs).

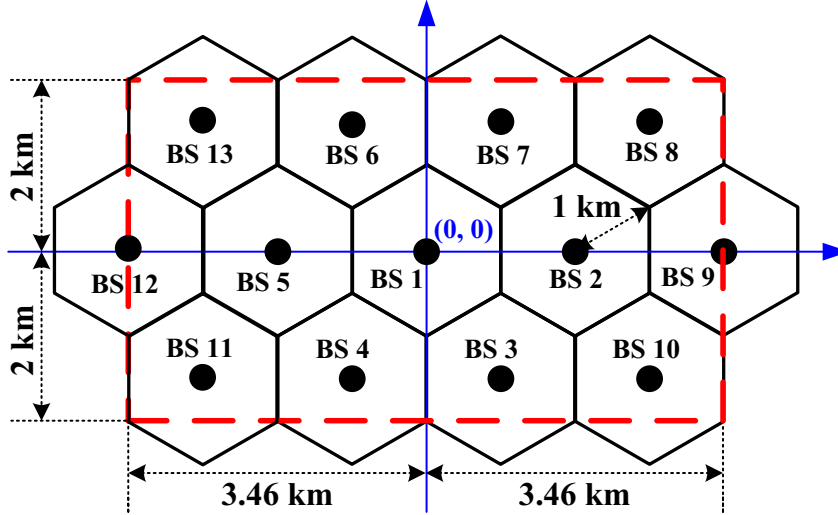


Figure 2.4: The layout of the 13 cells. The $K = 15$ admitted MSs are randomly uniformly dropped in the rectangular area defined by the red dashed lines.

2.7.1 Performance of the low-complexity algorithms

We first evaluate the performance of the proposed low-complexity algorithms in Alg. 2.1 and Alg. 2.2. To provide a fair comparison with the existing schemes [75–78] and to further motivate the proposed incentive measures in Eqs. (2.41) and (2.42), we consider two baseline schemes: employing channel gain [78] and sparsity of the beamformers [75–77] based incentive measures, respectively, in **Step 1** of the inflation and deflation procedures. The channel gain based incentive measure [78], denoted by $\hat{\Upsilon}_{k,l}$, of assigning the l th BS to the k th MS (i.e., setting $a_{k,l} = 1$) is defined as:

$$\hat{\Upsilon}_{k,l} \triangleq \|\mathbf{h}_{k,l}\|_2, \forall k \in \mathcal{K}, \forall l \in \mathcal{L}. \quad (2.47)$$

In the sparse optimization based approaches [75–77], the following regularized convex

optimization problem:

$$\{\mathbf{w}_k^{(\text{SPA})}\} \triangleq \underset{\{\mathbf{w}_k\}}{\text{argmin}} \sum_{k=1}^K \|\mathbf{w}_k\|_2^2 + \mu \sum_{k=1}^K \|\mathbf{w}_k\|_1 \quad (2.48a)$$

$$\text{s.t. (2.9a): } \text{Im}\{\mathbf{h}_k^H \mathbf{w}_k\} = 0, \forall k \in \mathcal{K}$$

$$(2.9b): \left\| [\mathbf{h}_k^H \mathbf{W}, \sigma_k] \right\|_2 \leq \gamma_k \text{Re}\{\mathbf{h}_k^H \mathbf{w}_k\}, \forall k \in \mathcal{K}$$

$$\sum_{k=1}^K \|\mathbf{w}_{k,l}\|_2^2 \leq P_l^{(\text{MAX})}, \forall l \in \mathcal{L} \quad (2.48b)$$

is firstly solved if it is feasible to obtain the sparse beamformers $\{\mathbf{w}_k^{(\text{SPA})}, \forall k \in \mathcal{K}\}$ under full BS cooperation. The large constant $\mu > 0$ in Eq. (2.48a) denotes the penalty factor on the l_1 -norm of the beamformers. We then define accordingly the sparsity based incentive measure [75–77], denoted by $\widehat{\Upsilon}_{k,l}$, of assigning the l th BS to serve the k th MS as

$$\widehat{\Upsilon}_{k,l} \triangleq \|\mathbf{w}_{k,l}^{(\text{SPA})}\|_1, \forall k \in \mathcal{K}, \forall l \in \mathcal{L}. \quad (2.49)$$

We observe in the simulations that the performance of the inflation and deflation procedures employing the incentive measure (2.49) is not sensitive to the penalty factor μ , e.g., choosing $\mu \in \{10^2, 10^3, 10^4, 10^5\}$ resulting in the same performance, and we thus fix $\mu = 10^3$ in the simulations

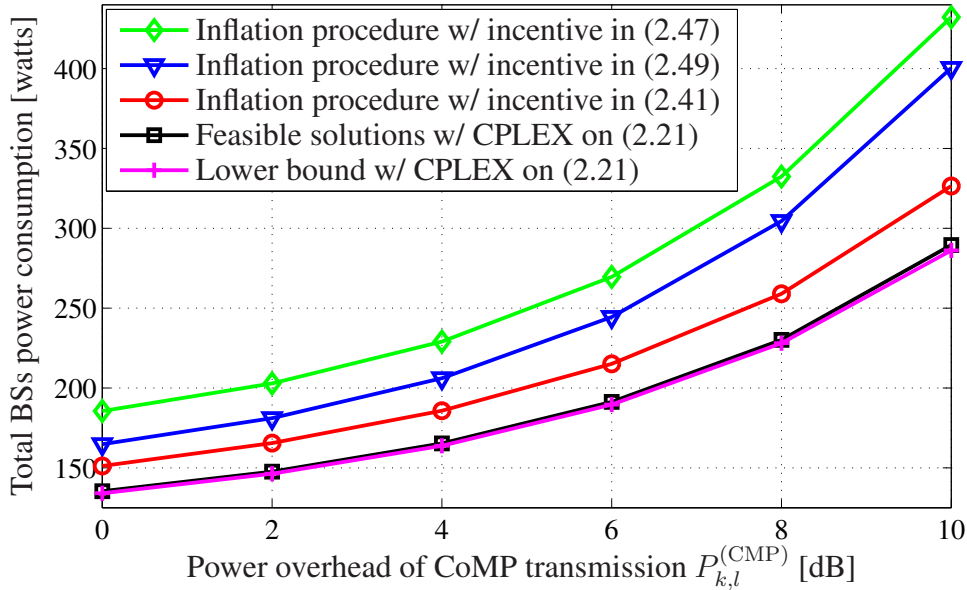


Figure 2.5: Performance evaluation of the *inflation procedure*: the total power consumption of all BSs vs. the system parameter $P_{k,l}^{(\text{CMP})}$.

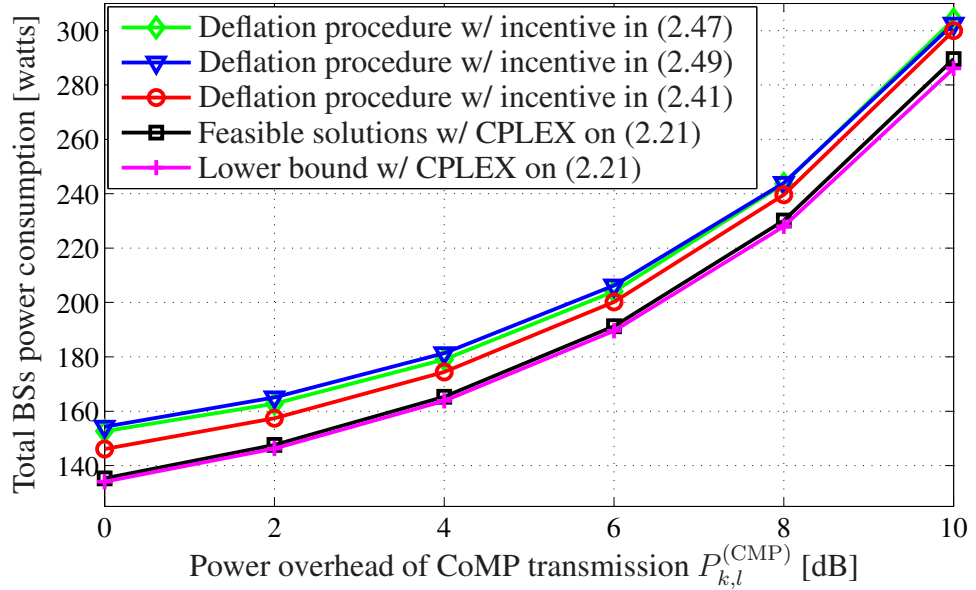


Figure 2.6: Performance evaluation of the *deflation procedure*: the total power consumption of all BSs vs. the system parameter $P_{k,l}^{(CMP)}$.

Fig. 2.5 and Fig. 2.6 display the total BSs power consumptions versus (vs.) the system parameter $P^{(CMP)}$. The curves labeled with “Lower bound w/ CPLEX on (2.21)” correspond to the largest global lower bounds computed by the solver CPLEX applied to the JNOB problem formulation (2.21) under the runtime limit of 300 seconds. The BnC algorithm implemented in CPLEX is customized according to the techniques discussed in Section 2.5 and it is initialized with the solutions found by the proposed deflation procedure in Alg. 2.2 equipped with the proposed incentive measure in Eq. (2.41).

We observe from Fig. 2.5 and Fig. 2.6 that: (i) the inflation and deflation procedures employing the proposed incentive measure in (2.41) outperform in terms of the achieved total BSs power consumptions their counterparts that adopt the channel gain based incentive measure in (2.47) [78] and the sparsity based incentive measure in (2.49) [75–77], (ii) the deflation procedure outperforms in terms of the achieved total BSs power consumptions the inflation procedure, and (iii) the average total BSs power consumptions achieved by the proposed inflation and deflation procedures are very close to the lower bounds computed by CPLEX, e.g., exceeding the lower bounds by less than 11.7% and 7.6%, respectively, for the considered settings.

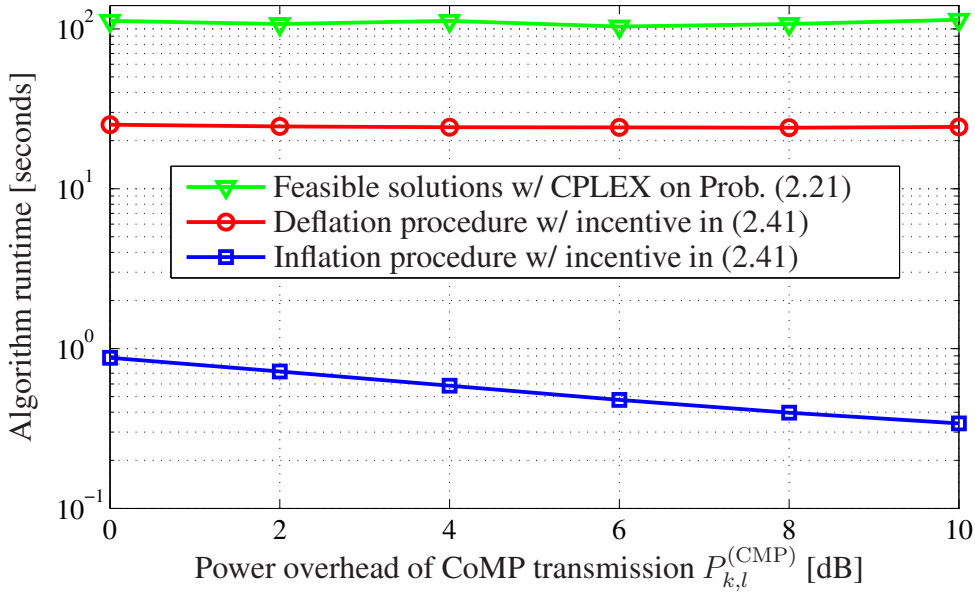


Figure 2.7: The algorithm runtime vs. the system parameter $P_{k,l}^{(CMP)}$.

Fig. 2.7 depicts the runtime of the considered schemes vs. the parameter $P^{(CMP)}$. Since almost the same runtime is required by the inflation procedure employing different incentive measures, which holds also for the deflation procedure, we plot in Fig. 2.7 only the runtime of the inflation and deflation procedures employing the proposed incentive measure in (2.41). We observe from Fig. 2.7 that, while the proposed inflation and deflation procedures yield the total BSs power consumptions that are very close to the lower bounds, the inflation and deflation procedures admit much less computational complexity and consume much less runtime, e.g., requiring respectively less than 0.46% and 21.4% of the runtime required by the customized BnC method.

Table 2.1: The number of *active* BS-MS links vs. the parameter $P_{k,l}^{(CMP)}$.

$P_{k,l}^{(CMP)}$ [dB]	0	2	4	6	8	10
Infl. proc. w/ incent. (2.47)	34.7	32.9	31.1	29.8	28.9	28.2
Infl. proc. w/ incent. (2.49)	32.5	30.7	29.3	28.1	27.2	26.7
Infl. proc. w/ incent. (2.41)	30.6	27.4	24.8	22.6	21.1	19.8
Defl. proc. w/ incent. (2.47)	18.9	17.3	16.6	16.1	15.7	15.6
Defl. proc. w/ incent. (2.49)	19.8	17.9	16.8	16.1	15.7	15.4
Defl. proc. w/ incent. (2.41)	21.0	18.9	17.5	16.8	16.2	15.9
Feas. soln. w/ CPLEX on (2.21)	21.7	19.7	18.0	17.0	16.2	15.7

Tab. 2.1 lists the number of active BS-MS links vs. the parameter $P^{(CMP)}$. Here, we

denote the BS-MS link between the l th BS and the k th MS as “active” if $a_{k,l} = 1$. We observe from Tab. 2.1 that instead of the full BS cooperation with $KL = 195$ active links, the average number of active BS-MS links obtained by applying CPLEX to the JNOB problem (2.21) ranges from 21.7 to 15.7 as the power overhead of CoMP transmission $P^{(\text{CMP})}$ is increased from 0 dB to 10 dB. This shows that partial BS cooperation and sparse network topologies are employed in the proposed CoMP transmission design to minimize the total BSs power consumption, and to balance the gain and the overhead of CoMP transmission.

Table 2.2: The average number of *powered on* BSs vs. the parameter $P^{(\text{CMP})}$.

$P_{k,l}^{(\text{CMP})}$ [dB]	0	2	4	6	8	10
Infl. proc. w/ incent. (2.47)	12.2	12.1	11.9	11.8	11.6	11.5
Infl. proc. w/ incent. (2.49)	10.9	10.9	10.8	10.8	10.8	10.8
Infl. proc. w/ incent. (2.41)	9.6	9.6	9.6	9.5	9.4	9.4
Defl. proc. w/ incent. (2.47)	10.1	9.7	9.6	9.4	9.3	9.2
Defl. proc. w/ incent. (2.49)	10.4	10.3	10.1	10.0	10.0	9.9
Defl. proc. w/ incent. (2.41)	9.4	9.2	9.1	9.1	9.0	8.9
Feas. soln. w/ CPLEX on (2.21)	7.6	7.7	7.8	7.9	8.0	8.1

Tab. 2.2 lists the average number of BSs that are switched on, i.e., the BSs that are transmitting data to the MSs, in the proposed design. We see from Tab. 2.2 that when taking into account the idle-state power consumptions of the PAs of the BSs, some of the BSs are powered off to minimize the total BSs power consumption, e.g., on average more than 37.7% of the BSs are switched off in the proposed design.

2.7.2 Comparison of the two MISOCP formulations

In this subsection, we compare the two problem formulations in (2.12) and (2.21) and the corresponding continuous relaxations in (2.13) and (2.23). We also demonstrate the effectiveness of the proposed branching priorities in (2.43) and (2.45). To provide meaningful and fair comparison, we apply the solver CPLEX to problems (2.12) and (2.21) with (w/) and without (w/o) issuing the branching priorities in Eqs. (2.43) and (2.45), respectively. The solver CPLEX is initialized with the solutions obtained by the deflation procedure equipped with the proposed incentive measure in (2.41). The BnC procedure in CPLEX terminates once a *strictly better* solution, i.e., a solution with *strictly smaller* total BSs power consumption, than the initial solution is reached within the runtime limitation of 150 seconds.

We first compare the continuous relaxations in (2.13) and (2.23). Fig. 2.8 displays the optimal objective values of the continuous relaxations in Eqs. (2.13) and (2.23) vs. the parameter $P^{(\text{CMP})}$. The figure clearly shows that the continuous relaxation (2.23) associated with the extended formulation (2.21) provides *strictly larger* lower bounds on the minimum total BSs power consumptions than that of the continuous relaxation (2.13) associated with the standard big-M formulation (2.12). The lower bounds given by the SOCP (2.23) are almost twice as large as that offered by the SOCP (2.13).

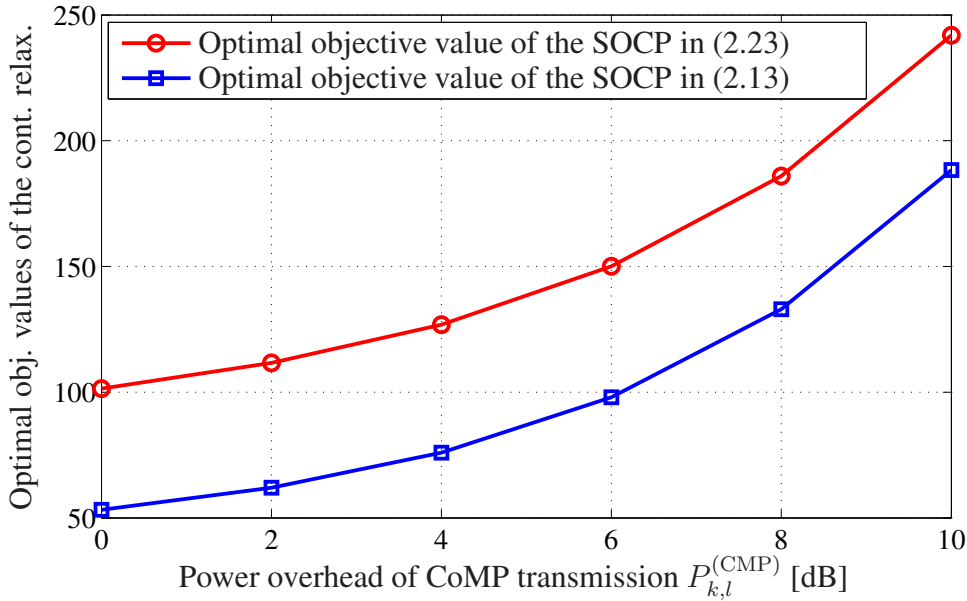


Figure 2.8: The optimal objective values of the continuous relaxations in (2.23) and (2.13) vs. the system parameter $P_{k,l}^{(\text{CMP})}$.

Fig. 2.9, Fig. 2.10, and Fig. 2.11 depict the percentages of solutions that are *strictly* better than the initializations, the *normalized* total BSs power consumptions achieved by the considered methods (normalized by the total BSs power consumptions achieved by the proposed deflation procedure), and the algorithm runtime vs. the parameter $P^{(\text{CMP})}$, respectively.

We observe from Figs. 2.9 – 2.11 that: (i) applying the BnC algorithm implemented in CPLEX to the extended formulation (2.21) yields significantly more *strictly* better solutions, i.e., solutions with *strictly* less total BSs power consumptions, than that computed by applying the BnC method to the standard big-M formulation (2.12), while the former requires *strictly* less runtime than the latter, and (ii) employing the proposed branching priorities in Eqs. (2.43) and (2.45) in the BnC method when applied to problem (2.21) achieves a larger percentage of *strictly* better solutions than the initializations with much less runtime than that without issuing the proposed branching priorities. These observations confirm that the extended formulation (2.21) admits less computational complexity than the standard big-M

formulation (2.12) when applying the BnC method, and that the proposed branching priorities (2.43) and (2.45) are very effective in reducing the computational complexity of the BnC method.

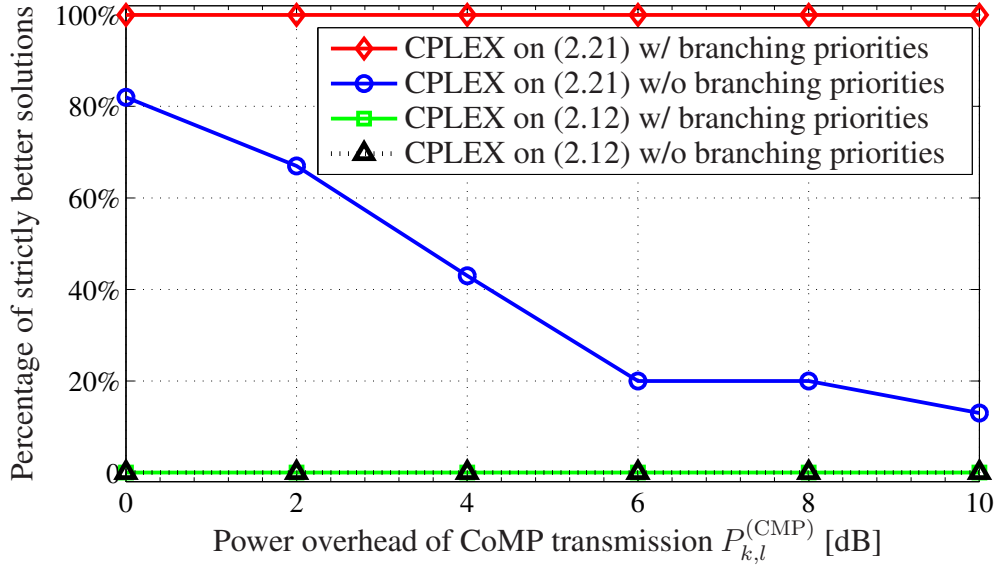


Figure 2.9: The percentage of solutions *strictly better* than the initial solutions obtained from the defl. proc. employing incentive (2.41) vs. the system parameter $P_{k,l}^{(CMP)}$.

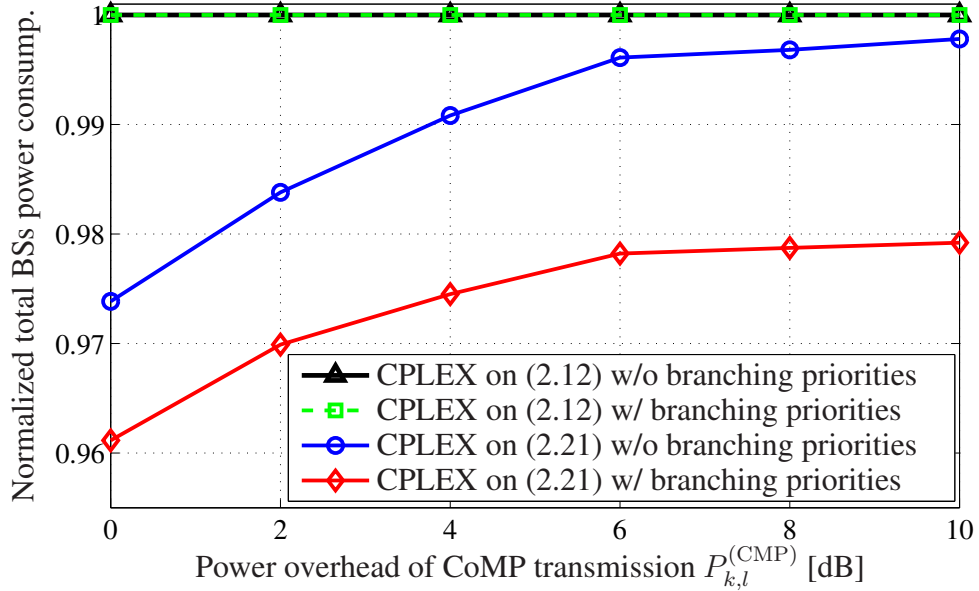


Figure 2.10: The *normalized* total BSs power consumption vs. the system parameter $P_{k,l}^{(CMP)}$.

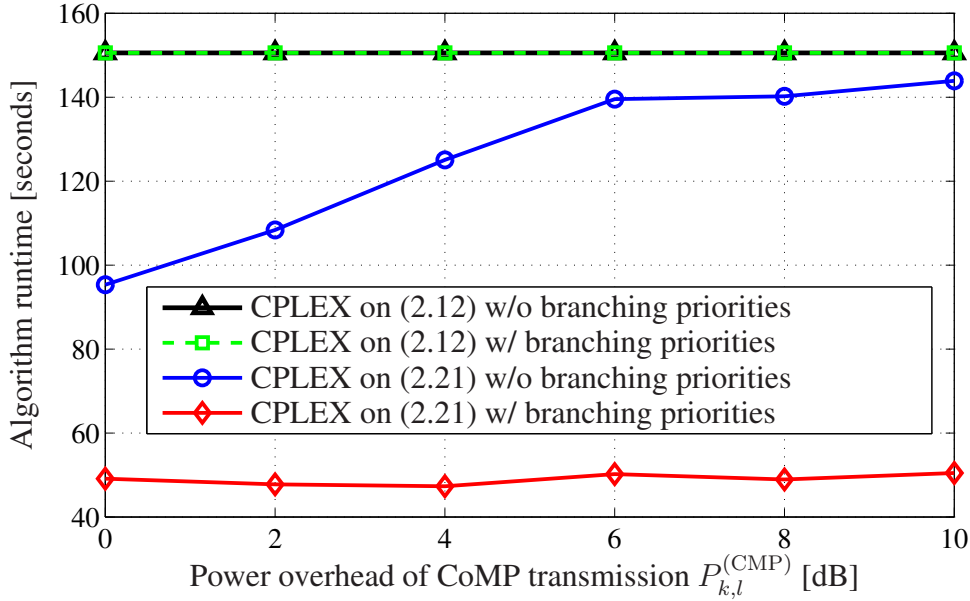


Figure 2.11: The algorithm run-time vs. the system parameter $P_{k,l}^{(CMP)}$.

2.8 Summary

We have considered in this chapter the JNOB problem aiming to balance the benefits and operational cost of CoMP transmission and to minimize the overall network power consumption. The standard big-M MISOCP formulation (2.12) and the extended MISOCP formulation (2.21) have been developed. The advantages (e.g., admitting tighter continuous relaxations) of the latter over the former have been confirmed by analytic studies and numerical results. Several techniques have been introduced to customize the BnC method implemented in the solver CPLEX when applying it on the JNOB problem. We have also developed low-complexity heuristic algorithms in Alg. 2.1 and Alg. 2.2 to compute near-optimal solutions of the JNOB problem for applications in large-scale networks. The simulation results show that Alg. 2.1 and Alg. 2.2 yield with very low computational complexity the total BSs power consumptions that are very close to the lower bounds. Our numerical results have also confirmed the reduction of computational complexity of the extended formulation (2.21) over the big-M formulation (2.12) and the effectiveness of the proposed customizing strategies. Finally, it has been observed that balancing the gain and operational overhead of CoMP transmission results in partial BS cooperation and sparse network topologies. Further, the PAs of some of the BSs are switched off when possible to reduce the overall BSs power consumption in the proposed sparse network design.

Chapter 3

Discrete rate adaptation, admission control, and downlink beamforming

3.1 Introduction

The on-going wireless data explosion drives the mobile network operators to employ spectrum- and energy-efficient wireless communications technologies in current and future cellular networks [1–11]. As we have discussed in Chapter 1, multiuser downlink beamforming, in which multiple mobile stations (MSs) are jointly served on the same time and frequency resources, represents one of the promising technologies for achieving spectrum- and energy-efficient wireless communications.

Multiuser downlink beamforming has been intensively investigated in the literature (see, e.g., [12, 13, 18, 24–33, 49–53, 55–58]) and has already been adopted in the latest cellular standard, e.g., in 3GPP LTE-A [7, 8]. Particularly, the problem of optimizing the beamformers to maximize the (weighted) sum-rate of the downlink system under the transmission power budget of the base station (BS) has been examined in, e.g., [13, 49–53, 55–58], where the problem has been proved to be NP-hard. In those existing works, the instantaneous data rates of the MSs are assumed to be *continuous and strictly increasing* functions of the received SINRs at the MSs, e.g., employing Shannon’s capacity formula [13, 49–53, 55–58]. As a result, the instantaneous data rates and the received SINRs of the MSs resulted from the sum-rate maximization problem may take any arbitrary continuous values.

In practical cellular networks, to accommodate the variations in wireless channels, discrete rate adaptation in the form of adaptive modulation and coding (AMC) is widely adopted for controlling the block error rate (BLER) or to meet the prescribed BLER requirement specified by the cellular standards [7, 8, 19, 20]. In this dissertation, discrete rate adapta-

tion refers to the procedure of assigning an achievable data rate, i.e., a specific modulation and coding scheme (MCS), to each MS according to their channel conditions [7, 8, 20, 85–90, 107, 108]. With AMC, the achievable physical-layer instantaneous data rates of the MSs are determined by the specific MCSs assigned to them and thus take *discrete* values [7, 8, 20, 85–90, 107, 108]. As a result, under AMC, the data rate of a MS is not a continuous function of the received SINRs and it is different from the Shannon’s capacity formula. For instance, in LTE systems, discrete data rate adaptation in the form of AMC is employed. The instantaneous data rates of the MSs are determined by the assigned MCSs and attain *discrete* values, rather than arbitrary continuous values, as shown in Fig. 3.1. Further, assigning a specific data rate (i.e., a specific MCS) to a MS in practical cellular systems generally requires the received SINR at the MS to be above a predetermined threshold for guaranteeing the prescribed block error rate (BLER) requirement of the wireless link, see, e.g., Fig. 3.1.

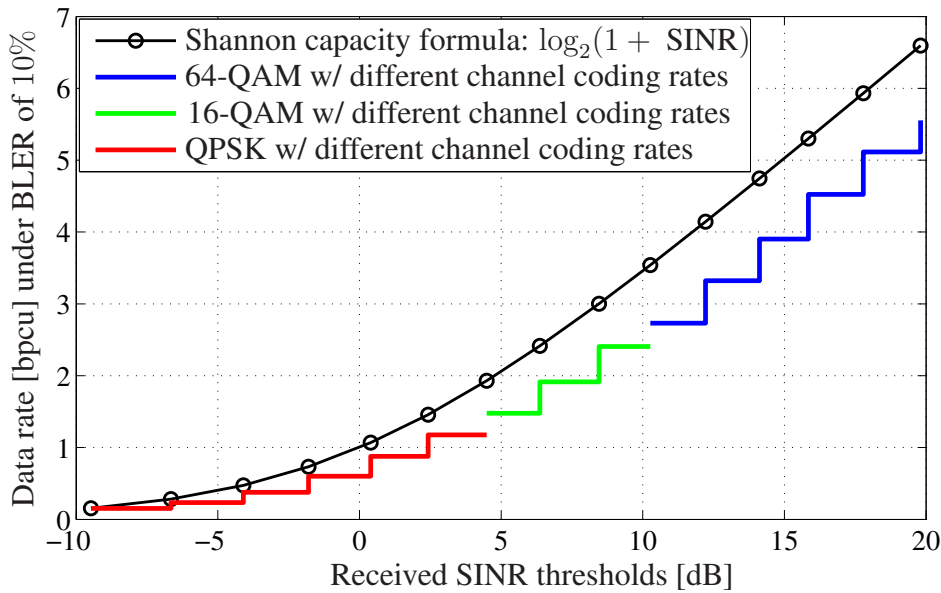


Figure 3.1: The achievable data rates vs. the thresholds of the received SINRs in LTE systems [7, 8, 20, 85–87].

To promote practical applications that employ discrete rate adaptation in the form of AMC and multiuser downlink beamforming, e.g., in LTE and LTE-A systems [7, 8, 20, 85–87], we consider in this chapter the joint optimization of discrete rate adaptation and multiuser downlink beamforming (DRAB) to achieve the maximum sum-rate of the downlink system with minimum total transmitted BS power. In our discrete rate adaptation framework, it is allowed that a zero data rate is assigned to a MS in a given time-slot, practically meaning that the MS is not admitted in that particular time-slot. As a result, user admission control is embedded in

the discrete rate assignment procedure. Furthermore, minimum received SINR requirements corresponding to the assigned data rates (i.e., the assigned MCSs) of the admitted MSs are included in the DRAB problem to meet the BLER targets prescribed by the wireless standards, e.g., by LTE [7, 8, 20, 85–90]. The DRAB problem that we consider in this chapter can be interpreted as a nontrivial extension of the conventional sum-rate maximization problem (with continuous rate adaptation) [13, 49–53, 55–58], and it includes as special cases the joint downlink beamforming and admission control problem (with fixed rate and SINR requirements) [83, 109–112], as well as the problem of joint rate adaptation and power control (with fixed transmit beamformers) [85–90, 107, 108]. Note that inspired by our preliminary work in [113], joint discrete rate adaptation and multiuser downlink beamforming has also been studied in [114]. However, the practical minimum SINR requirements for ensuring the prescribed BLER targets were *not* considered in [114].

Since the admitted MSs are coupled through the co-channel interference in the downlink SINR constraints and the MCS assignment (i.e., the discrete data rate allocation) procedure involves binary decision variables, the DRAB problem naturally leads to a non-convex mixed integer nonlinear program (MINLP) [67–69]. That is, the DRAB remains a non-convex program even after relaxing the integer constraints and thus cannot be efficiently solved [67–69]. Similar to Chapter 2, instead of treating it as a general non-convex MINLP, we address the DRAB problem using the mixed-integer second-order cone program (MISOCP) framework [82]. We reformulate the SINR constraints in our discrete data rate adaptation framework using the big-M approach [67–69] and develop a standard big-M MISOCP formulation of the DRAB problem, which supports the convex continuous relaxation based BnC method [67–69, 81, 82]. Based on the big-M formulation, we introduce auxiliary optimization variables and develop an improved extended MISOCP formulation [68, 82] of the DRAB problem. The extended formulation exhibits several interesting structural properties that are exploited in the algorithmic solutions, e.g., in the BnC method. We provide in-depth theoretical analysis to show that the extended formulation generally admits strictly tighter continuous relaxations than that of the standard big-M formulation (and thus yields significantly reduced computational complexity when applying the BnC method). Based on the analysis, several efficient strategies, e.g., customized node selection and branching rules, are proposed to customize the standard BnC method implemented in the MISOCP solver IBM ILOG CPLEX for further computational complexity reduction. We also develop low-complexity second-order cone program (SOCP) based inflation and deflation procedures [83, 84] to compute the close-to-optimal solutions of the DRAB problem for practical application in large-scale systems.

Monte Carlo simulations are carried out to verify the analytic studies and to demonstrate

the performance of the heuristic algorithms. The parallel BnC method implemented in the MISOCP solver CPLEX [81], which are customized according to the DRAB problem and our proposed customizing strategies, is applied to both DRAB problem formulations for reference. Our simulation results show that the average sum-rates of the downlink system achieved by the proposed fast inflation and deflation procedures are very close to that of the optimal solutions computed by the BnC method in CPLEX, while the computational complexity of the heuristic algorithms is much less than that of the customized BnC method. Furthermore, the simulation results confirm that the extended MISOCP formulation yields a significant reduction in computational complexity, as compared to the standard big-M MISOCP formulation, when applying the customized BnC method on the two formulations. Particularly, the numerical results show that the percentages of the certified optimal solutions (cf. Section 5.5.1) when applying the BnC method on the extended MISOCP formulation are significantly larger than that of the standard big-M MISOCP formulation for the considered settings. This confirms the improvement of the extended formulation over the standard big-M formulation in terms of computational complexity.

This chapter is based on my original work that has been submitted in [115] and my original work that has been published in [113].

3.2 System model

For the ease of presentation, we consider a cellular downlink system comprising one cell, with one BS and $K > 1$ single-antenna MSs. The BS is equipped with $M > 1$ antennas. The K MSs are admissible under the predefined minimum data rate requirements (cf. Section 3.3.1). Denote $\mathbf{h}_k^H \in \mathbb{C}^{1 \times M}$ and $\mathbf{w}_k \in \mathbb{C}^{M \times 1}$ as the frequency-flat channel vector and the beamformer of the k th MS, respectively, $\forall k \in \mathcal{K} \triangleq \{1, 2, \dots, K\}$. The received signal $y_k \in \mathbb{C}$ at the k th MS is given by (see, e.g., [12, 13, 18, 25–28, 55–57])

$$y_k = \mathbf{h}_k^H \mathbf{w}_k x_k + \sum_{j=1, j \neq k}^K \mathbf{h}_k^H \mathbf{w}_j x_j + z_k, \forall k \in \mathcal{K} \quad (3.1)$$

where $x_k \in \mathbb{C}$ represents the normalized data symbol, i.e., $\mathbb{E}\{|x_k|^2\} = 1$, designated for the k th MS, and $z_k \in \mathbb{C}$ denotes the additive circularly-symmetric white Gaussian noise [19] at the k th MS, with zero mean and variance σ_k^2 , $\forall k \in \mathcal{K}$. Note that the signal model in (3.1) has the same form as that given in Eq. (2.1) of Chapter 2.1.

Similar to the existing works [12, 13, 18, 24–33, 49–53, 55–58, 83, 109–112], it is assumed that the data symbols of the MSs are mutually independent and independent from the noise.

With single user detection at the MSs, i.e., when the co-channel interference in Eq. (3.1) is treated as noise, the received SINR at the k th MS, denoted by SINR_k , can then be expressed as (see, e.g., [12, 13, 28])

$$\text{SINR}_k \triangleq \frac{|\mathbf{h}_k^H \mathbf{w}_k|^2}{\sum_{j=1, j \neq k}^K |\mathbf{h}_k^H \mathbf{w}_j|^2 + \sigma_k^2}, \forall k \in \mathcal{K}. \quad (3.2)$$

Note that the term SINR_k expressed in (3.2) has the same form as the one given in Eq. (2.2) of Chapter 2.1.

Table 3.1: The candidate MCSs and data rates, and the corresponding SINR requirements of LTE systems [7, 8, 20, 85–87]

Modulation Order	Code Rate ($\times 1024$)	Data Rate R_l [bits/symbol]	SINR Level $\Gamma_l^{(\text{MIN})}$ [dB]
QPSK	78	78/512	-9.478
QPSK	120	120/512	-6.658
QPSK	193	193/512	-4.098
QPSK	308	308/512	-1.798
QPSK	449	449/512	0.399
QPSK	602	602/512	2.424
16-QAM	378	756/512	4.489
16-QAM	490	980/512	6.367
16-QAM	616	1232/512	8.456
64-QAM	466	1398/512	10.266
64-QAM	567	1701/512	12.218
64-QAM	666	1998/512	14.122
64-QAM	772	2316/512	15.849
64-QAM	873	2619/512	17.786
64-QAM	948	2844/512	19.809

To exploit the diversity of the channel vectors $\{\mathbf{h}_k^H, \forall k \in \mathcal{K}\}$, discrete data rate adaptation in the form of AMC is widely adopted in practical wireless systems, e.g., in LTE networks [7, 8, 20, 85–87]. With rate adaptation, the data rate of the k th MS is determined by the specific MCS that is assigned to the MS and therefore takes *discrete* values [7, 8, 20, 85–87]. For instance, Tab. 3.1 lists the set of candidate MCSs and the resulting data rates defined in the cellular standard LTE [7, 8, 20]. Corresponding to each MCS and data rate, there

exists a minimum received SINR requirement for guaranteeing the target BLER prescribed by the wireless standards, e.g., by 3GPP LTE [7, 8, 20, 85–87]. While the candidate MCSs and the resulting data rates are defined in cellular standards, the corresponding minimum received SINR requirements are generally equipment and implementation dependent. For instance, typical SINR requirements in LTE systems are also listed in Tab. 3.1. These SINR thresholds in Tab. 3.1 are obtained from extensive simulations under the target BLER of 10% [7, 8, 20, 85–87]. The candidate data rates and the corresponding SINR thresholds listed in Tab. 3.1 are also displayed in Fig. 3.1.

We consider in this chapter the scenario that the BS assigns at most one specific MCS out of the $L > 1$ candidate MCSs $\{MCS_1, MCS_2, \dots, MCS_L\}$ to each MS in \mathcal{K} . In the case that no MCS (i.e., a zero data rate) is assigned to the k th MS, then the k th MS is *not* admitted in the current time-slot. The problem of interest is to optimize the discrete data rate adaptation and multiuser downlink beamforming jointly to achieve the maximum sum-rate of the downlink system with minimum total transmitted BS power. To model the MCS assignment procedure, we introduce the *binary* variable $a_{k,l} \in \{0, 1\}$, with $a_{k,l} = 1$ meaning that the l th candidate MCS (i.e., the l th candidate data rate) is allocated to the k th MS, and $a_{k,l} = 0$ otherwise, $\forall k \in \mathcal{K}, \forall l \in \mathcal{L} \triangleq \{1, 2, \dots, L\}$. Since at most one MCS (i.e., one specific data rate) needs to be assigned to the k th MS in one particular time-slot, we apply the following *multiple-choice* constraints on the binary variables $\{a_{k,l}, \forall k \in \mathcal{K}, \forall l \in \mathcal{L}\}$ in our DRAB problem:

$$\sum_{l=1}^L a_{k,l} \leq 1, \forall k \in \mathcal{K}. \quad (3.3)$$

Under Eq. (3.3), the instantaneous (physical layer [7, 8, 20]) data rate of the k th MS, denoted by r_k , can be expressed as

$$r_k = \sum_{l=1}^L a_{k,l} R_l, \forall k \in \mathcal{K} \quad (3.4)$$

where the constant R_l represents the data rate corresponding to the l th candidate MCS (see, e.g., Tab. 3.1), $\forall l \in \mathcal{L}$. If a nonzero data rate is assigned to the k th MS, i.e., if $\sum_{l=1}^L a_{k,l} = 1$, then the received SINR at the k th MS is required to be above a certain threshold to guarantee the BLER target, as specified in, e.g., Tab. 3.1 of LTE systems [7, 8, 20, 85–87]. Under Eq. (3.3), the minimum SINR requirements of the K MSs for ensuring the predefined BLER

target can be formulated as

$$\text{SINR}_k \geq \sum_{l=1}^L a_{k,l} \Gamma_l^{(\text{MIN})}, \forall k \in \mathcal{K} \quad (3.5)$$

where SINR_k is given in Eq. (3.2) and the constant $\Gamma_l^{(\text{MIN})}$ denotes the SINR requirement corresponding to the l th candidate MCS (see, e.g., Tab. 3.1), $\forall l \in \mathcal{L}$. Note that the MCS assignments $\{a_{k,l}, \forall k \in \mathcal{K}, \forall l \in \mathcal{L}\}$ and the beamformers $\{\mathbf{w}_k, \forall k \in \mathcal{K}\}$ are coupled in the SINR constraints in (3.5) in the DRAB problem.

Similar to Chapter 2, it is assumed throughout this chapter that the BS has full knowledge of the instantaneous channel vectors $\{\mathbf{h}_k^H, \forall k \in \mathcal{K}\}$. The assumption of perfect CSI known at the BS is commonly adopted in the existing works (see, e.g., [7, 12, 13, 18, 19, 25, 26, 49–53, 55–58]), which is practically realizable in time-division duplex (TDD) systems [7, 19]. Note that the results presented in this chapter can directly be extended to a multi-cell downlink system.

3.3 The standard big-M formulation of the DRAB problem

3.3.1 The big-M MISOCP formulation

The problem of interest is to jointly optimize the discrete rate adaptation (i.e., the MCS assignment and admission control) and the beamformer design for the K MSs. The objective is to maximize the system utility function $f(\{a_{k,l}\}, \{\mathbf{w}_k\})$, which is defined as

$$f(\{a_{k,l}\}, \{\mathbf{w}_k\}) \triangleq \sum_{k=1}^K \sum_{l=1}^L a_{k,l} R_l - \rho \sum_{k=1}^K \|\mathbf{w}_k\|_2^2 \quad (3.6)$$

where the terms $\sum_{k=1}^K \sum_{l=1}^L a_{k,l} R_l$ and $\sum_{k=1}^K \|\mathbf{w}_k\|_2^2$ represent the downlink sum-rate and the total transmitted power of the BS, respectively. Taking into account the per-BS sum-power constraint, which is given by [49–53, 55–58]:

$$\sum_{k=1}^K \|\mathbf{w}_k\|_2^2 \leq P^{(\text{MAX})} \quad (3.7)$$

where $P^{(\text{MAX})}$ denotes the maximum allowable transmission power of the BS. The constant weighting factor ρ can be configured to ensure that among all feasible data rate assignments having the same maximum sum-rate, the ones with the least total transmitted BS power are

selected as the optimal solutions. That is, there exists a constant ρ such that maximizing the utility function $f(\{a_{k,l}\}, \{\mathbf{w}_k\})$ yields the maximum sum-rate with the minimum total transmitted BS power. For instance, for the discrete data rates listed in Tab. 3.1, we can simply choose $\rho = 1 / (1 + 512P^{(\text{MAX})})$ [83, 110, 111].

The SINR constraints in the form of Eq. (3.5) are non-convex constraints even after the binary variables $\{a_{k,l}, \forall k \in \mathcal{K}, \forall l \in \mathcal{L}\}$ are relaxed to be continuous variables taking values in the closed interval $[0, 1]$. To derive more tractable equivalent expressions of the SINR constraints in (3.5), we rewrite the K SINR constraints (3.5) into the following KL SINR constraints:

$$\left(\sum_{j=1, j \neq k}^K |\mathbf{h}_k^H \mathbf{w}_j|^2 + \sigma_k^2 \right) a_{k,l} \Gamma_l^{(\text{MIN})} \leq |\mathbf{h}_k^H \mathbf{w}_k|^2, \forall k \in \mathcal{K}, \forall l \in \mathcal{L}. \quad (3.8)$$

Note that due to Eq. (3.3) and the fact that $a_{k,l} \in \{0, 1\}, \forall k \in \mathcal{K}, \forall l \in \mathcal{L}$, the SINR constraints in (3.8) are equivalent to that in (3.5). However, the products of the binary variables $\{a_{k,l}, \forall k \in \mathcal{K}, \forall l \in \mathcal{L}\}$ and the beamformers $\{\mathbf{w}_k, \forall k \in \mathcal{K}\}$ in the SINR constraints in (3.8) still impose non-convexity, besides the integer constraints on the indicators $\{a_{k,l}, \forall k \in \mathcal{K}, \forall l \in \mathcal{L}\}$. To cope with this difficulty, we adopt the so-called big-M approach [67–69] to further rewrite the KL SINR constraints in (3.8) as

$$\sum_{j=1}^K |\mathbf{h}_k^H \mathbf{w}_j|^2 + \sigma_k^2 \leq (1 - a_{k,l})^2 U_k^2 + \gamma_l^2 |\mathbf{h}_k^H \mathbf{w}_k|^2, \forall k \in \mathcal{K}, \forall l \in \mathcal{L} \quad (3.9)$$

where the big-M constant $U_k > 0$ and the constant $\gamma_l > 0$ are defined, respectively, as

$$U_k \triangleq \sqrt{\|\mathbf{h}_k\|_2^2 P^{(\text{MAX})} + \sigma_k^2}, \forall k \in \mathcal{K} \quad (3.10)$$

$$\gamma_l \triangleq \sqrt{1 + 1/\Gamma_l^{(\text{MIN})}}, \forall l \in \mathcal{L}. \quad (3.11)$$

Taking into account the Cauchy-Schwarz inequality [34, 116] and the per-BS sum-power constraint in (3.7), we have that

$$\sum_{j=1}^K |\mathbf{h}_k^H \mathbf{w}_j|^2 + \sigma_k^2 \leq \|\mathbf{h}_k\|_2^2 \sum_{j=1}^K \|\mathbf{w}_j\|_2^2 + \sigma_k^2 \leq U_k^2, \forall k \in \mathcal{K}. \quad (3.12)$$

As a result, due to Eq. (3.12), when $a_{k,l} = 0$, i.e., when the l th candidate MCS is not assigned to the k th MS, the resulting (k, l) th constraint in (3.9) is automatically satisfied, and the resulting (k, l) th constraint in (3.8) is also automatically satisfied. When $a_{k,l} = 1$, i.e.,

when the l th candidate MCS is assigned to the k th MS, the resulting (k, l) th SINR constraint in (3.9) is the same as that in (3.8). Hence, the SINR constraints in (3.9) are equivalent to that of (3.8), which follows immediately from Eq. (3.12) and the fact that $a_{k,l} \in \{0, 1\}$.

It is well-known that the beamformers exhibit a phase-invariance property in the sense that the beamformers $\{\mathbf{w}_k, \forall k \in \mathcal{K}\}$ and the beamformers $\{\mathbf{w}_k e^{j\theta_k \sqrt{-1}}, \forall k \in \mathcal{K}\}$ result in the same received SINRs at the MSs and the same total transmitted BS power, $\forall \theta_k \in [0, 2\pi)$. As a result, we can choose the phase of the beamformer \mathbf{w}_k such that the term $\mathbf{h}_k^H \mathbf{w}_k$ is real and non-negative [12, 13, 83]. In other words, the SINR constraints in Eq. (3.9) can be equivalently rewritten as (see, e.g., [12, 13, 83]):

$$\text{Im} \{ \mathbf{h}_k^H \mathbf{w}_k \} = 0, \text{Re} \{ \mathbf{h}_k^H \mathbf{w}_k \} \geq 0, \forall k \in \mathcal{K} \quad (3.13a)$$

$$\| [\mathbf{h}_k^H \mathbf{W}, \sigma_k] \|_2 \leq (1 - a_{k,l}) U_k + \gamma_l \text{Re} \{ \mathbf{h}_k^H \mathbf{w}_k \}, \forall k \in \mathcal{K}, \forall l \in \mathcal{L} \quad (3.13b)$$

where the beamformer matrix $\mathbf{W} \in \mathbb{C}^{M \times K}$, i.e., the collection of the K beamformers of the K MSs, is defined as

$$\mathbf{W} \triangleq [\mathbf{w}_1, \mathbf{w}_2, \dots, \mathbf{w}_K]. \quad (3.14)$$

Note that the SINR constraints in (3.13b) become second-order cone (SOC) constraints when the binary variables $\{a_{k,l}, \forall k \in \mathcal{K}, \forall l \in \mathcal{L}\}$ are relaxed to be continuous variables that take values in the closed interval $[0, 1]$ [34, 105].

With the system utility function $f(\{a_{k,l}\}, \{\mathbf{w}_k\})$ defined in (3.6) and the reformulated SINR constraints in (3.13), the joint discrete rate adaptation and multiuser downlink beam-

forming (DRAB) problem can be cast as the following MISOCP:

$$\Phi^{(\text{BMI})} \triangleq \max_{\{a_{k,l}, \mathbf{w}_k\}} f(\{a_{k,l}\}, \{\mathbf{w}_k\}) \quad (3.15a)$$

$$\text{s.t. (3.3): } \sum_{l=1}^L a_{k,l} \leq 1, \forall k \in \mathcal{K}$$

$$(3.7): \sum_{k=1}^K \|\mathbf{w}_k\|_2^2 \leq P^{(\text{MAX})}$$

$$(3.13a): \text{Im}\{\mathbf{h}_k^H \mathbf{w}_k\} = 0, \text{Re}\{\mathbf{h}_k^H \mathbf{w}_k\} \geq 0, \forall k \in \mathcal{K}$$

$$(3.13b): \|\left[\mathbf{h}_k^H \mathbf{W}, \sigma_k\right]\|_2 \leq (1 - a_{k,l})U_k + \gamma_l \text{Re}\{\mathbf{h}_k^H \mathbf{w}_k\}, \forall k \in \mathcal{K}, \forall l \in \mathcal{L}$$

$$r_k \triangleq \sum_{l=1}^L a_{k,l} R_l \geq r_k^{(\text{MIN})} \sum_{l=1}^L a_{k,l}, \forall k \in \mathcal{K} \quad (3.15b)$$

$$\sigma_k \sum_{l=1}^L a_{k,l} \sqrt{\Gamma_l^{(\text{MIN})}} \leq \text{Re}\{\mathbf{h}_k^H \mathbf{w}_k\}, \forall k \in \mathcal{K} \quad (3.15c)$$

$$a_{k,l} \in \{0, 1\}, \forall k \in \mathcal{K}, \forall l \in \mathcal{L} \quad (3.15d)$$

where the constraint in (3.15b) is included to guarantee the quality-of-service (QoS) of the k th MS if it is admitted, i.e., if $\sum_{l=1}^L a_{k,l} = 1$, with $r_k^{(\text{MIN})}$ denoting the minimum data rate requirement of the k th MS when it is admitted. The constraints in (3.15c) represent problem-specific cuts (cf. Section 2.3.2), which are derived from the SINR constraints in (3.8) by dropping the co-channel interference. The DRAB problem formulation in (3.15) is referred to as the big-M integer (BMI) formulation in the sequel. Note that it is of great practical interest to include the SINR constraints in (3.13) in the DRAB problem (3.15) for guaranteeing the prescribed BLER targets in practical cellular networks [7, 8, 20]. The SINR constraints in (3.13) were considered in our preliminary work [113], however, *not* in the follow-up work of [114].

We remark that in contrast to the conventional QoS-constrained multiuser downlink beamforming problem [12, 13, 28], the considered DRAB problem in the form of the MISOCP (3.15) is always feasible. For instance, the point described by the parameter tuple $\{a_{k,l} = 0, \mathbf{w}_k = \mathbf{0}, \forall k \in \mathcal{K}, \forall l \in \mathcal{L}\}$ is a (trivial) feasible solution of problem (3.15). As user admission control is embedded in the discrete rate assignment procedure via the multiple-choice constraints in (3.3), the DRAB problem (3.15) contains as a special case the problem of joint downlink beamforming and admission control [83, 109–112]. The formulated DRAB problem (3.15) represents a MISOCP, which is commonly solved with the convex continuous relaxation based BnC method [67–69, 81, 82].

3.3.2 The continuous relaxation of the big-M formulation

We know from Section 2.3.2 that the BnC method relying on solving the convex continuous relaxation of the DRAB problem (3.15). The convex continuous relaxation of the DRAB problem (3.15), which is the convex SOCP resulted from relaxing all integer constraints in the DRAB problem (3.15), is given by

$$\Phi^{(\text{BMC})} \triangleq \max_{\{a_{k,l}, \mathbf{w}_k\}} f(\{a_{k,l}\}, \{\mathbf{w}_k\}) \quad (3.16a)$$

$$\text{s.t. (3.3): } \sum_{l=1}^L a_{k,l} \leq 1, \forall k \in \mathcal{K}$$

$$(3.7): \sum_{k=1}^K \|\mathbf{w}_k\|_2^2 \leq P^{(\text{MAX})}$$

$$(3.13a): \text{Im}\{\mathbf{h}_k^H \mathbf{w}_k\} = 0, \text{Re}\{\mathbf{h}_k^H \mathbf{w}_k\} \geq 0, \forall k \in \mathcal{K}$$

$$(3.13b): \|[\mathbf{h}_k^H \mathbf{W}, \sigma_k]\|_2 \leq (1 - a_{k,l})U_k + \gamma_l \text{Re}\{\mathbf{h}_k^H \mathbf{w}_k\}, \forall k \in \mathcal{K}, \forall l \in \mathcal{L}$$

$$(3.15b): r_k \triangleq \sum_{l=1}^L a_{k,l} R_l \geq r_k^{(\text{MIN})} \sum_{l=1}^L a_{k,l}, \forall k \in \mathcal{K}$$

$$(3.15c): \sigma_k \sum_{l=1}^L a_{k,l} \sqrt{\Gamma_l^{(\text{MIN})}} \leq \text{Re}\{\mathbf{h}_k^H \mathbf{w}_k\}, \forall k \in \mathcal{K}$$

$$0 \leq a_{k,l} \leq 1, \forall k \in \mathcal{K}, \forall l \in \mathcal{L} \quad (3.16b)$$

where the variables $\{a_{k,l}, \forall k \in \mathcal{K}, \forall l \in \mathcal{L}\}$, which are originally constrained in the discrete set $\{0, 1\}$ as in Eq. (3.15d), are relaxed to be continuous variables taking values in the closed interval $[0, 1]$ in Eq. (3.16b). The SOCP in (3.16) is referred to as the big-M continuous relaxation (BMC) in this chapter.

Since every feasible solution of the DRAB problem in (3.15) is also feasible for the associated continuous relaxation in (3.16), it holds that

$$\Phi^{(\text{BMC})} \geq \Phi^{(\text{BMI})}. \quad (3.17)$$

That is the optimal objective value of the SOCP in (3.16) provides an upper bound on the optimal objective value of the MISOCP in (3.15). The gap between the two optimal objective values, i.e., the term $(\Phi^{(\text{BMC})} - \Phi^{(\text{BMI})})$, represents the measure of the *tightness* of the continuous relaxation in (3.16). A smaller gap $(\Phi^{(\text{BMC})} - \Phi^{(\text{BMI})})$ corresponds to a tighter continuous relaxation in (3.16).

3.4 The extended formulation and analytic studies

3.4.1 The extended MISOCP formulation

While the standard big-M formulation (3.15) represents a straightforward formulation of the DRAB problem, it results in loose continuous relaxations (2.13) and very large BnC search trees [67–69]. In order to develop an enhanced MISOCP formulation of the DRAB problem (3.15), we introduce the vector $\mathbf{v}_{k,l} \in \mathbb{C}^{M \times 1}$ to represent the *virtual* beamformer of the k th MS that corresponds to the l th candidate MCS (i.e., the l th candidate data rate R_l), and we denote accordingly $\phi_{k,l} \geq 0$ as the virtual transmission power, i.e., the term $\|\mathbf{v}_{k,l}\|_2^2$, $\forall k \in \mathcal{K}, \forall l \in \mathcal{L}$. Considering the multiple-choice constraints in (3.3) and the actual beamformer \mathbf{w}_k of the k th MS, we impose the following constraints:

$$\mathbf{w}_k \triangleq \sum_{l=1}^L a_{k,l} \mathbf{v}_{k,l} = \sum_{l=1}^L \mathbf{v}_{k,l}, \forall k \in \mathcal{K} \quad (3.18)$$

$$\|\mathbf{v}_{k,l}\|_2^2 \leq a_{k,l} \phi_{k,l}, \forall k \in \mathcal{K}, \forall l \in \mathcal{L} \quad (3.19)$$

$$0 \leq \phi_{k,l} \leq a_{k,l} P^{(\text{MAX})}, \forall k \in \mathcal{K}, \forall l \in \mathcal{L} \quad (3.20)$$

$$\sum_{k=1}^K \sum_{l=1}^L \phi_{k,l} \leq P^{(\text{MAX})} \quad (3.21)$$

where Eq. (3.21) represents the per-BS sum-power constraint as that of Eq. (3.7). We use the big-M method [67–69] in Eqs. (3.19) and (3.20) to ensure that $\phi_{k,l} = 0$ and $\mathbf{v}_{k,l} = \mathbf{0}$ when $a_{k,l} = 0$. Furthermore, due to Eq. (3.21), Eqs. (3.19) and (3.20) are automatically satisfied when $a_{k,l} = 1$. Eq. (3.19) can further be rewritten as

$$\| [2\mathbf{v}_{k,l}^T, (a_{k,l} - \phi_{k,l})] \|_2 \leq a_{k,l} + \phi_{k,l}, \forall k \in \mathcal{K}, \forall l \in \mathcal{L} \quad (3.22)$$

which become SOC constraints when the binary variables $\{a_{k,l}, \forall k \in \mathcal{K}, \forall l \in \mathcal{L}\}$ are relaxed to be continuous variables taking values in the closed interval $[0, 1]$ [34, 105].

For notational convenience, we define the binary integer variable $b_k \in \{0, 1\}$ as (cf. Eq. (3.3)):

$$b_k \triangleq \sum_{l=1}^L a_{k,l}, \forall k \in \mathcal{K}. \quad (3.23)$$

That is, the variable b_k can be considered as the *indicator for admission control* of the k th MS, with $b_k = 1$ indicating that the k th MS is admitted, and $b_k = 0$ otherwise.

With Eqs. (3.20) – (3.23), the SINR constraints in (3.13) can be rewritten as

$$\text{Im} \{ \mathbf{h}_k^H \mathbf{v}_{k,l} \} = 0, \text{Re} \{ \mathbf{h}_k^H \mathbf{v}_{k,l} \} \geq 0, \forall k \in \mathcal{K}, \forall l \in \mathcal{L} \quad (3.24a)$$

$$\| [\mathbf{h}_k^H \mathbf{W}, \sigma_k] \|_2 \leq (1 - b_k) U_k + \sum_{l=1}^L \gamma_l \text{Re} \{ \mathbf{h}_k^H \mathbf{v}_{k,l} \}, \forall k \in \mathcal{K}, \forall l \in \mathcal{L}. \quad (3.24b)$$

Since now the term $\sum_{k=1}^K \sum_{l=1}^L \phi_{k,l}$ represents the total transmitted BS power, similar to the system utility function $f(\{a_{k,l}\}, \{\mathbf{w}_k\})$ defined in Eq. (3.6), we redefine a new system utility function $g(\{a_{k,l}\}, \{\phi_{k,l}\})$ as

$$g(\{a_{k,l}\}, \{\phi_{k,l}\}) \triangleq \sum_{k=1}^K \sum_{l=1}^L a_{k,l} R_l - \rho \sum_{k=1}^K \sum_{l=1}^L \phi_{k,l}. \quad (3.25)$$

The DRAB problem (3.15) can then be equivalently reformulated as the following MISOCP, which is referred to as the extended integer (EXI) formulation in the sequel:

$$\Phi^{(\text{EXI})} \triangleq \max_{\{a_{k,l}, \mathbf{v}_{k,l}, \phi_{k,l}, b_k\}} g(\{a_{k,l}\}, \{\phi_{k,l}\}) \quad (3.26a)$$

$$\text{s.t. (3.3): } \sum_{l=1}^L a_{k,l} \leq 1, \forall k \in \mathcal{K}$$

$$(3.15b): r_k \triangleq \sum_{l=1}^L a_{k,l} R_l \geq r_k^{(\text{MIN})} \sum_{l=1}^L a_{k,l}, \forall k \in \mathcal{K}$$

$$(3.20): 0 \leq \phi_{k,l} \leq a_{k,l} P^{(\text{MAX})}, \forall k \in \mathcal{K}, \forall l \in \mathcal{L}$$

$$(3.21): \sum_{k=1}^K \sum_{l=1}^L \phi_{k,l} \leq P^{(\text{MAX})}$$

$$(3.22): \| [2\mathbf{v}_{k,l}^T, (a_{k,l} - \phi_{k,l})] \|_2 \leq a_{k,l} + \phi_{k,l}, \forall k \in \mathcal{K}, \forall l \in \mathcal{L}$$

$$(3.23): b_k \triangleq \sum_{l=1}^L a_{k,l}, \forall k \in \mathcal{K}$$

$$(3.24a): \text{Im} \{ \mathbf{h}_k^H \mathbf{v}_{k,l} \} = 0, \text{Re} \{ \mathbf{h}_k^H \mathbf{v}_{k,l} \} \geq 0, \forall k \in \mathcal{K}, \forall l \in \mathcal{L}$$

$$(3.24b): \| [\mathbf{h}_k^H \mathbf{W}, \sigma_k] \|_2 \leq (1 - b_k) U_k + \sum_{l=1}^L \gamma_l \text{Re} \{ \mathbf{h}_k^H \mathbf{v}_{k,l} \}, \forall k \in \mathcal{K}, \forall l \in \mathcal{L}$$

$$\sigma_k a_{k,l} \sqrt{\Gamma_l^{(\text{MIN})}} \leq \text{Re} \{ \mathbf{h}_k^H \mathbf{v}_{k,l} \}, \forall k \in \mathcal{K}, \forall l \in \mathcal{L} \quad (3.26b)$$

$$\gamma_l \text{Re} \{ \mathbf{h}_k^H \mathbf{v}_{k,l} \} \leq U_k a_{k,l}, \forall k \in \mathcal{K}, \forall l \in \mathcal{L} \quad (3.26c)$$

$$a_{k,l} \in \{0, 1\}, b_k \in \{0, 1\}, \forall k \in \mathcal{K}, \forall l \in \mathcal{L} \quad (3.26d)$$

where the constraints in (3.26b) represent the problem-specific cuts similar to that of (3.15c), which are derived from the SINR constraints in (3.24b) by dropping the co-channel interference. The constraints in (3.26c) also represent the problem-specific cuts, as shown in the following lemma.

Lemma 3.1 (Valid Cuts). *Under the integer constraints in (3.26d), the constraints in (3.26c) in the DRAB problem (3.26) are automatically satisfied. That is, the constraints in (3.26c) represent valid problem-specific cuts (cf. Section 2.3.2).*

Proof 3.1. *Please refer to Appendix A.4 for the proof.*

Note that the devised extended MISOCP formulation in (3.26) is also known as perspective formulation and lifting in the mixed-integer programming literature [68, 82, 97].

We further remark that the extended MISOCP formulation (3.26) and the standard big-M MISOCP formulation (3.15) are equivalent in terms of the optimal objective value, i.e. $\Phi^{(\text{EXI})} = \Phi^{(\text{BMI})}$, and the optimal solution set due to the fact that $a_{k,l} \in \{0, 1\}, \forall k \in \mathcal{K}, \forall l \in \mathcal{L}$. However, the extended formulation (3.26) generally admits strictly tighter continuous relaxations than that of the standard big-M formulation (3.15), as analyzed in next subsection. Due to the tighter continuous relaxations, the computational complexity of solving the extended formulation (3.26) when applying the BnC method is significantly less than that of the big-M formulation (3.15), which will be demonstrated with numerical results in Section 3.7.

3.4.2 Analytic comparison of the two formulations

In this subsection, we analytically show that the extended MISOCP formulation (3.26) generally admits strictly tighter continuous relaxations than that of the standard big-M formulation (3.15). The convex continuous relaxation of the extended MISOCP formulation (3.26) can be expressed as the following SOCP, which is referred to as the extended continuous

relaxation (EXC) in this chapter:

$$\begin{aligned}
\Phi^{(\text{EXC})} &\triangleq \max_{\{a_{k,l}, \mathbf{v}_{k,l}, \phi_{k,l}, b_k\}} g(\{a_{k,l}\}, \{\phi_{k,l}\}) & (3.27a) \\
\text{s.t. (3.3): } &\sum_{l=1}^L a_{k,l} \leq 1, \forall k \in \mathcal{K} \\
(3.15b): r_k &\triangleq \sum_{l=1}^L a_{k,l} R_l \geq r_k^{(\text{MIN})} \sum_{l=1}^L a_{k,l}, \forall k \in \mathcal{K} \\
(3.20): &0 \leq \phi_{k,l} \leq a_{k,l} P^{(\text{MAX})}, \forall k \in \mathcal{K}, \forall l \in \mathcal{L} \\
(3.21): &\sum_{k=1}^K \sum_{l=1}^L \phi_{k,l} \leq P^{(\text{MAX})} \\
(3.22): &\| [2\mathbf{v}_{k,l}^T, (a_{k,l} - \phi_{k,l})] \|_2 \leq a_{k,l} + \phi_{k,l}, \forall k \in \mathcal{K}, \forall l \in \mathcal{L} \\
(3.23): &b_k \triangleq \sum_{l=1}^L a_{k,l}, \forall k \in \mathcal{K} \\
(3.24a): &\text{Im} \{ \mathbf{h}_k^H \mathbf{v}_{k,l} \} = 0, \text{Re} \{ \mathbf{h}_k^H \mathbf{v}_{k,l} \} \geq 0, \forall k \in \mathcal{K}, \forall l \in \mathcal{L} \\
3.24b: &\| [\mathbf{h}_k^H \mathbf{W}, \sigma_k] \|_2 \leq (1 - b_k) U_k + \sum_{l=1}^L \gamma_l \text{Re} \{ \mathbf{h}_k^H \mathbf{v}_{k,l} \}, \forall k \in \mathcal{K}, \forall l \in \mathcal{L} \\
(3.26b): &\sigma_k a_{k,l} \sqrt{\Gamma_l^{(\text{MIN})}} \leq \text{Re} \{ \mathbf{h}_k^H \mathbf{v}_{k,l} \}, \forall k \in \mathcal{K}, \forall l \in \mathcal{L} \\
(3.26c): &\gamma_l \text{Re} \{ \mathbf{h}_k^H \mathbf{v}_{k,l} \} \leq U_k a_{k,l}, \forall k \in \mathcal{K}, \forall l \in \mathcal{L} \\
&0 \leq a_{k,l} \leq 1, 0 \leq b_k \leq 1, \forall k \in \mathcal{K}, \forall l \in \mathcal{L} & (3.27b)
\end{aligned}$$

where the variables $\{a_{k,l}, b_k, \forall k \in \mathcal{K}, \forall l \in \mathcal{L}\}$, which are originally constrained to take binary values as in Eq. (3.26d), are relaxed to be continuous variables constrained in the closed interval $[0, 1]$ in Eq. (3.27b). Similar to the continuous relaxation in (3.16) that is associated with the standard big-M formulation (3.15), the continuous relaxation in (3.27) offers an upper bound on the optimal objective value of the extended MISOCP formulation (3.26), i.e., $\Phi^{(\text{EXC})} \geq \Phi^{(\text{EXI})}$, since every feasible solution of the MISOCP (3.26) is also feasible for the associated continuous relaxation in (3.27).

Assume that the point $\{a_{k,l}^{(\text{EXC})}, \mathbf{v}_{k,l}^{(\text{EXC})}, \phi_{k,l}^{(\text{EXC})}, b_k^{(\text{EXC})}, \forall k \in \mathcal{K}, \forall l \in \mathcal{L}\}$ is an optimal (not necessarily unique) solution of the SOCP in (3.27). We define according to Eqs. (3.18)

and (3.14) the vector $\mathbf{w}_k^{(\text{EXC})} \in \mathbb{C}^{M \times 1}$ and the matrix $\mathbf{W}^{(\text{EXC})} \in \mathbb{C}^{M \times K}$, respectively, as

$$\mathbf{w}_k^{(\text{EXC})} \triangleq \sum_{l=1}^L \mathbf{v}_{k,l}^{(\text{EXC})}, \forall k \in \mathcal{K} \quad (3.28)$$

$$\mathbf{W}^{(\text{EXC})} \triangleq \left[\mathbf{w}_1^{(\text{EXC})}, \mathbf{w}_2^{(\text{EXC})}, \dots, \mathbf{w}_K^{(\text{EXC})} \right]. \quad (3.29)$$

Taking into account the SINR constraints in (3.24b) and the problem-specific cuts in (3.26c), the following results can readily be derived.

Lemma 3.2 (Dominated Constraints). *The optimal solution $\{a_{k,l}^{(\text{EXC})}, \mathbf{v}_{k,l}^{(\text{EXC})}, \phi_{k,l}^{(\text{EXC})}, b_k^{(\text{EXC})}, \forall k \in \mathcal{K}, \forall l \in \mathcal{L}\}$ of the continuous relaxation in (3.27) satisfies that:*

$$\| [\mathbf{h}_k^H \mathbf{W}^{(\text{EXC})}, \sigma_k] \|_2 \leq \left(1 - a_{k,l}^{(\text{EXC})}\right) U_k + \gamma_l \text{Re} \left\{ \mathbf{h}_k^H \mathbf{v}_{k,l}^{(\text{EXC})} \right\}, \forall k \in \mathcal{K}, \forall l \in \mathcal{L}. \quad (3.30)$$

Proof 3.2. *Please refer to Appendix A.5 for the proof.*

We know from Lemma 3.2 and its proof in Appendix A.5 that the constraints in (3.30) are dominated by that of (3.24b), i.e.,

$$\begin{aligned} \| [\mathbf{h}_k^H \mathbf{W}^{(\text{EXC})}, \sigma_k] \|_2 &\leq \left(1 - b_k^{(\text{EXC})}\right) U_k + \sum_{l=1}^L \gamma_l \text{Re} \left\{ \mathbf{h}_k^H \mathbf{v}_{k,l}^{(\text{EXC})} \right\} \\ &\leq \left(1 - a_{k,l}^{(\text{EXC})}\right) U_k + \gamma_l \text{Re} \left\{ \mathbf{h}_k^H \mathbf{v}_{k,l}^{(\text{EXC})} \right\}. \end{aligned} \quad (3.31)$$

Considering the constraints given in (3.22) and the fact that the objective function in (3.27a) is maximized, we can straightforwardly prove by contradicting argument that the constraints in (3.22) are active at optimal solutions, i.e.,

$$\| \mathbf{v}_{k,l}^{(\text{EXC})} \|_2^2 = a_{k,l}^{(\text{EXC})} \phi_{k,l}^{(\text{EXC})}, \forall k \in \mathcal{K}, \forall l \in \mathcal{L}. \quad (3.32)$$

Making use of Eqs. (3.30) and (3.32), we can make the following analytic statement regarding the tightness of the continuous relaxations in (3.16) and (3.27).

Theorem 3.1 (Tighter Continuous Relaxation). *The point characterized by the parameter tuple $\{a_{k,l}^{(\text{EXC})}, \mathbf{w}_k^{(\text{EXC})}, \forall k \in \mathcal{K}, \forall l \in \mathcal{L}\}$, which is directly constructed from the optimal solution $\{a_{k,l}^{(\text{EXC})}, \mathbf{v}_{k,l}^{(\text{EXC})}, \phi_{k,l}^{(\text{EXC})}, b_k^{(\text{EXC})}, \forall k \in \mathcal{K}, \forall l \in \mathcal{L}\}$ of the continuous relaxation in (3.27), is a feasible solution of the continuous relaxation in (3.16), and it further holds*

that

$$\Phi^{(\text{EXC})} = g\left(\left\{a_{k,l}^{(\text{EXC})}\right\}, \left\{\phi_{k,l}^{(\text{EXC})}\right\}\right) \leq f\left(\left\{a_{k,l}^{(\text{EXC})}\right\}, \left\{\mathbf{w}_k^{(\text{EXC})}\right\}\right) \leq \Phi^{(\text{BMC})}. \quad (3.33)$$

Proof 3.3. Please refer to Appendix A.6 for the proof.

We know from *Theorem 3.1* that the SOCP in (3.27), i.e., the continuous relaxation of the extended MISOCP formulation (3.26), generally offers a tighter (smaller) upper bound on the optimal objective value of the DRAB problem (3.15) than that of the SOCP in (3.16), i.e., the continuous relaxation of the standard big-M MISOCP formulation (3.15). Further, as a direct consequence of Eqs. (3.28) and (3.32), and *Theorem 3.1*, the following special case can readily be established.

Corollary 3.1 (Special Case). *If the SOCPs in (3.16) and in (3.27) achieve the same optimal objective value, i.e., if*

$$\Phi^{(\text{BMC})} = \Phi^{(\text{EXC})} \quad (3.34)$$

then the following properties must hold:

$$a_{k,l}^{(\text{EXC})} \in \{0, 1\}, b_k^{(\text{EXC})} \in \{0, 1\}, \forall k \in \mathcal{K}, \forall l \in \mathcal{L} \quad (3.35)$$

$$\Phi^{(\text{BMI})} = \Phi^{(\text{BMC})} = \Phi^{(\text{EXC})} = \Phi^{(\text{EXI})}. \quad (3.36)$$

We know from *Corollary 3.1* that if $\Phi^{(\text{BMC})} = \Phi^{(\text{EXC})}$, then all the *relaxed* binary variables $\{a_{k,l}^{(\text{EXC})}, b_k^{(\text{EXC})}, \forall k \in \mathcal{K}, \forall l \in \mathcal{L}\}$ precisely attain *integer* values. As a result, in the case that $\Phi^{(\text{BMC})} = \Phi^{(\text{EXC})}$, the points $\{a_{k,l}^{(\text{EXC})}, \mathbf{w}_k^{(\text{EXC})}, \forall k \in \mathcal{K}, \forall l \in \mathcal{L}\}$ and $\{a_{k,l}^{(\text{EXC})}, \mathbf{v}_{k,l}^{(\text{EXC})}, \phi_{k,l}^{(\text{EXC})}, b_k^{(\text{EXC})}, \forall k \in \mathcal{K}, \forall l \in \mathcal{L}\}$ are respectively the optimal solutions of the standard big-M formulation in (3.15) and the extended formulation in (3.26), and therefore $\Phi^{(\text{BMI})} = \Phi^{(\text{BMC})} = \Phi^{(\text{EXC})} = \Phi^{(\text{EXI})}$. Further, *Corollary 3.1* suggests that the SOCP in (3.27) provides *strictly tighter (smaller)* upper bounds of the optimal objective value $\Phi^{(\text{BMI})}$ than that of the SOCP in (3.16), unless all the four problems in (3.15), (3.16), (3.26), and (3.27) achieve the same optimal objective value.

We remark that although the extended formulation (3.26) involves more optimization variables than the standard big-M formulation (3.15), the former has significantly reduced computational complexity as compared to the latter when applying the customized BnC method (cf. Section 3.5). This is because the former generally admits *strictly tighter* continuous relaxations than the latter, as analytically shown in *Theorem 3.1* and *Corollary 3.1*. The reduction in computational complexity of the extended MISOCP formulation in (3.26)

as compared to the standard big-M MISOCP formulation in (3.15) will further be verified with numerical examples in Section 3.7.

3.5 Techniques for customizing the BnC method

3.5.1 Customized optimality criterion

We denote $\Psi^{(\text{BIF})}$ and $\Psi^{(\text{GUB})}$ as the objective value of the incumbent solution (i.e., the best-known integer-feasible solution) and the smallest global upper bound (GUB) of the optimal objective value $\Phi^{(\text{EXI})}$ of the DRAB problem, respectively, that are computed in the BnC procedure. Since $\Psi^{(\text{BIF})}$ and $\Psi^{(\text{GUB})}$ are the best-known global lower bound (GLB) and GUB of the optimal objective value $\Phi^{(\text{EXI})}$, respectively, it holds that

$$0 \leq \Psi^{(\text{BIF})} \leq \Phi^{(\text{EXI})} \leq \Psi^{(\text{GUB})}. \quad (3.37)$$

As discussed in Section 2.5.1, an incumbent solution computed in the BnC procedure is declared as an optimal solution of the DRAB problem (3.26) if it satisfies [69, 81]:

$$\text{Relative MIP gap} \triangleq \frac{\Psi^{(\text{GUB})}}{\Psi^{(\text{BIF})}} - 1 \leq \eta \quad (3.38)$$

where the constant $\eta \geq 0$ denotes the predetermined relative optimality tolerance, which can be customized for the DRAB problem in specific practical applications [69, 81].

3.5.2 Customized node selection and branching rules

As in Section 2.5.2, we employ the *best-bound search* rule for node selection in the BnC procedure when applying CPLEX on the DRAB problem. The best-bound search rule can speed up the process of computing the optimality certificate defined in (3.38) [67–69].

Recall that the point $\{a_{k,l}^{(\text{EXC})}, \mathbf{v}_{k,l}^{(\text{EXC})}, \phi_{k,l}^{(\text{EXC})}, b_k^{(\text{EXC})}, \forall k \in \mathcal{K}, \forall l \in \mathcal{L}\}$ represents an optimal solution of the SOCP in (3.27). We observe from Eqs. (3.3) and (3.23) that the variables $\{a_{k,l}^{(\text{EXC})}, \forall k \in \mathcal{K}, \forall l \in \mathcal{L}\}$ and $\{b_k^{(\text{EXC})}, \forall k \in \mathcal{K}\}$ are coupled and it follows from Eq. (3.32) that there exists scalar ambiguity between the variables $a_{k,l}^{(\text{EXC})}$ and $\phi_{k,l}^{(\text{EXC})}$, $\forall k \in \mathcal{K}, \forall l \in \mathcal{L}$. As a result, the variables $\{a_{k,l}^{(\text{EXC})}, b_k^{(\text{EXC})}, \forall k \in \mathcal{K}, \forall l \in \mathcal{L}\}$ are not appropriate for determining the branching priorities of the (relaxed) binary variables. We propose here to relate the branching priorities of the (relaxed) binary variables $\{a_{k,l}, b_k, \forall k \in \mathcal{K}, \forall l \in \mathcal{L}\}$ to the channel gains $\{\|\mathbf{h}_k\|_2, \forall k \in \mathcal{K}\}$ and the candidate data rates $\{R_l, \forall l \in \mathcal{L}\}$. Since

the branching priorities are predefined and do not depend on the optimal solutions of the continuous relaxations, the proposed prioritizing scheme facilitates parallel implementations.

Denote the set $\overline{\mathcal{K}}$ as the collection of the \overline{K} ($0 \leq \overline{K} \leq K$) MSs that have the \overline{K} largest channel gains among $\{\|\mathbf{h}_k\|_2, \forall k \in \mathcal{K}\}$, and denote the integers $\overline{\Omega}_k$ and $\overline{\Upsilon}_{k,l}$ as the branching priorities of the (relaxed) binary variables b_k and $a_{k,l}$, respectively. For simplicity of presentation, we introduce here the principles for determining the branching priorities, rather than providing exact definitions as done in Section 2.5.2. We partition the (relaxed) binary variables into three disjoint groups, namely $\mathcal{G}_1 \triangleq \{b_k, \forall k \in \overline{\mathcal{K}}\}$, $\mathcal{G}_2 \triangleq \{a_{k,l}, \forall k \in \mathcal{K}, \forall l \in \mathcal{L}\}$, and $\mathcal{G}_3 \triangleq \{b_k, \forall k \in \mathcal{K} \setminus \overline{\mathcal{K}}\}$. The proposed prioritizing principles are as follows.

(P1) We prioritize firstly admitting the MSs in the set $\overline{\mathcal{K}}$, secondly data rate assignment, and then admitting the MSs in the set $\mathcal{K} \setminus \overline{\mathcal{K}}$. In other words, the branching priorities of the variables in \mathcal{G}_1 are strictly larger than that of \mathcal{G}_2 , which are strictly larger than that of \mathcal{G}_3 , i.e.,

$$\min_{k \in \overline{\mathcal{K}}} \overline{\Omega}_k > \max_{k \in \mathcal{K}, l \in \mathcal{L}} \overline{\Upsilon}_{k,l} \geq \min_{k \in \mathcal{K}, l \in \mathcal{L}} \overline{\Upsilon}_{k,l} > \max_{k \in \mathcal{K} \setminus \overline{\mathcal{K}}} \overline{\Omega}_k. \quad (3.39)$$

(P2) The branching priorities of the variables in \mathcal{G}_1 and \mathcal{G}_3 are sorted according to the channel gains, i.e.,

$$\overline{\Omega}_j \geq \overline{\Omega}_k, \text{ if } \|\mathbf{h}_j\|_2 \geq \|\mathbf{h}_k\|_2, \forall j, k \in \mathcal{K}. \quad (3.40)$$

(P3) The branching priorities of the variables in \mathcal{G}_2 are determined by considering firstly the channel gains and secondly the candidate data rates, i.e.,

$$\min_{l \in \mathcal{L}} \overline{\Upsilon}_{j,l} \geq \max_{l \in \mathcal{L}} \overline{\Upsilon}_{k,l}, \text{ if } \|\mathbf{h}_j\|_2 \geq \|\mathbf{h}_k\|_2, \forall j \neq k, \forall j, k \in \mathcal{K} \quad (3.41a)$$

$$\overline{\Upsilon}_{k,l} \geq \overline{\Upsilon}_{k,m}, \text{ if } R_l \geq R_m, \forall k \in \mathcal{K}, \forall l \neq m, l, m \in \mathcal{L}. \quad (3.41b)$$

Appendix A.7 presents exemplary mathematical definitions of the branching priorities $\overline{\Omega}_k$ and $\overline{\Upsilon}_{k,l}$ following the proposed prioritizing principles (P1) – (P3), assuming that the candidate data rates $\{R_l, \forall l \in \mathcal{L}\}$ and the associated SINR thresholds $\{\Gamma_l^{(\text{MIN})}, \forall l \in \mathcal{L}\}$ can be ordered as (see, e.g., Tab. 3.1)

$$R_1 \leq R_2 \leq \dots \leq R_L \quad (3.42)$$

$$\Gamma_1^{(\text{MIN})} \leq \Gamma_2^{(\text{MIN})} \leq \dots \leq \Gamma_L^{(\text{MIN})}. \quad (3.43)$$

3.5.3 Preprocessing

We know from the SINR constraints in (3.8) and the minimum data rate requirements in (3.15b) that the *necessary* conditions for assigning the l th candidate rate R_l to the k th MS are:

$$R_l \geq r_k^{(\text{MIN})} \quad (3.44)$$

$$\|\mathbf{h}_k\|_2^2 P^{(\text{MAX})} \geq \sigma_k^2 \Gamma_l^{(\text{MIN})} \quad (3.45)$$

where the necessary condition in (3.45) is obtained by dropping the co-channel interference in the SINR constraints (3.5). As a result, not all the candidate data rates $\{R_l, \forall l \in \mathcal{L}\}$ can be assigned to the k th MS and a preprocessing step can be performed to reduce the number of candidate data rates. Denote \mathcal{L}_k as the set of indices of the candidate data rates that can possibly be assigned to the k th MS. According to the necessary conditions in (3.44) and (3.45), the set \mathcal{L}_k can be defined as

$$\mathcal{L}_k \triangleq \left\{ l \mid l \in \mathcal{L}, R_l \geq r_k^{(\text{MIN})}, \|\mathbf{h}_k\|_2^2 P^{(\text{MAX})} \geq \sigma_k^2 \Gamma_l^{(\text{MIN})} \right\}. \quad (3.46)$$

To reduce the computational complexity, the preprocessing step should be performed before applying the customized BnC method to the two DRAB problem formulations in (3.15) and in (3.26). Specifically, the following cuts shall be added to the extended MISOCP formulation (3.26):

$$a_{k,l} = 0, \forall k \in \mathcal{K}, \forall l \in \mathcal{L} \setminus \mathcal{L}_k \quad (3.47)$$

$$\phi_{k,l} = 0, \mathbf{v}_{k,l} = \mathbf{0}, \forall k \in \mathcal{K}, \forall l \in \mathcal{L} \setminus \mathcal{L}_k \quad (3.48)$$

Accordingly, the problem-specific cuts defined in Eq. (3.47) shall be added to the standard big-M MISOCP formulation in (3.15).

Furthermore, the BnC method can be initialized with high-quality integer-feasible solutions of the DRAB problem. The high-quality integer-feasible initializations can be computed by low-complexity heuristic algorithms, which are discussed in the next section.

3.6 The low-complexity heuristic algorithms

3.6.1 The SOCP based inflation procedure

We propose in this subsection a fast SOCP based inflation procedure [83, 84] to compute near-optimal solutions of the DRAB problem. The inflation procedure is initialized with the zero data rate assigned to all MSs (i.e., none of the MSs is admitted). In each iteration, one of the non-admitted MSs is selected and tentatively assigned a nonzero data rate. The selected MS is admitted with the assigned data rate if the data rate assignments obtained in the previous iteration together with the new data rate assignment are feasible. The performance of the inflation procedure depends on which one of the non-admitted MSs is chosen and what data rate is assigned to the chosen MS in each iteration. We propose here to select the candidate MS and the data rate according to the branching priorities $\{\bar{\Upsilon}_{k,l}, \forall k \in \mathcal{K}, \forall l \in \mathcal{L}\}$ presented in Section 3.5.2 and Appendix A.7. Denote $\mathcal{K}^{(n)}$ and $\mathcal{L}_k^{(n)}$ as the set of the indices of the admitted MSs and the set of the indices of the candidate (assigned) MCSs of the k th MS, respectively, generated in the n th iteration, with $\mathcal{K}^{(0)} = \emptyset$ (the empty set), and $\mathcal{L}_k^{(0)} = \mathcal{L}_k$ (which is defined in (3.46)), $\forall k \in \mathcal{K}$. In the n th iteration, the following step:

$$(\bar{k}, \bar{l}) = \underset{k \in \mathcal{K} \setminus \mathcal{K}^{(n-1)}, l \in \mathcal{L}_k^{(n-1)}}{\operatorname{argmax}} \bar{\Upsilon}_{k,l} \quad (3.49)$$

is carried out. If no valid index pair (\bar{k}, \bar{l}) can be found from Eq. (3.49), the inflation procedure terminates and returns the results obtained in the previous iteration. Otherwise, we tentatively update the sets $\mathcal{K}^{(n)} = \mathcal{K}^{(n-1)} \cup \{\bar{k}\}$, $\mathcal{L}_{\bar{k}}^{(n)} = \{\bar{l}\}$, and $\mathcal{L}_k^{(n)} = \mathcal{L}_k^{(n-1)}$, $\forall k \in \mathcal{K} \setminus \{\bar{k}\}$. Then, in the n th iteration, the following convex SOCP:

$$\left\{ \mathbf{w}_k^{(n)} \right\} \triangleq \underset{\{\mathbf{w}_k\}}{\operatorname{argmin}} \sum_{k=1}^K \|\mathbf{w}_k\|_2^2 \quad (3.50a)$$

$$\text{s.t. (3.7): } \sum_{k=1}^K \|\mathbf{w}_k\|_2^2 \leq P^{(\text{MAX})}$$

$$(3.13a): \operatorname{Im} \{ \mathbf{h}_k^H \mathbf{w}_k \} = 0, \operatorname{Re} \{ \mathbf{h}_k^H \mathbf{w}_k \} \geq 0, \forall k \in \mathcal{K}$$

$$\| [\mathbf{h}_k^H \mathbf{W}, \sigma_k] \|_2 \leq \gamma_l \operatorname{Re} \{ \mathbf{h}_k^H \mathbf{w}_k \}, \forall k \in \mathcal{K}^{(n)}, \forall l \in \mathcal{L}_k^{(n)} \quad (3.50b)$$

is solved using, e.g., the interior-point method [34, 105] or fast specialized algorithms that are built on the downlink-uplink duality theory [12, 13, 25, 26, 28]. If the SOCP in (3.50) is feasible, the inflation procedure proceeds to the next iteration. Otherwise, one step backtracking is performed, i.e., we reset $\mathcal{K}^{(n)} = \mathcal{K}^{(n-1)}$, and $\mathcal{L}_{\bar{k}}^{(n)} = \mathcal{L}_{\bar{k}}^{(n-1)} \setminus \{\bar{l}\}$ to exclude the

index pair (\bar{k}, \bar{l}) from future consideration. Since one of the candidate data rates is tested for one of the non-admitted MSs in each iteration, the worst-case computational complexity of the inflation procedure consists in solving $\sum_{k=1}^K L_k$ instances of the SOCP in (3.50), with the cardinality $L_k \triangleq |\mathcal{L}_k|, \forall k \in \mathcal{K}$. The fast inflation procedure is summarized in Alg. 3.1.

Init.: Initialize $\mathcal{K}^{(0)} = \emptyset$, and $\mathcal{L}_k^{(0)} = \mathcal{L}_k, \forall k \in \mathcal{K}$, and set the iteration number $n = 1$.
Step 1: Compute (\bar{k}, \bar{l}) according to Eq. (3.49). If no index pair (\bar{k}, \bar{l}) can be found from Eq. (3.49), *stop* and return $\mathcal{K}^{(n-1)}$ and $\{\mathcal{L}_k^{(n-1)}, \forall k \in \mathcal{K}^{(n-1)}\}$. Otherwise, update the sets $\mathcal{K}^{(n)} = \mathcal{K}^{(n-1)} \cup \{\bar{k}\}$, $\mathcal{L}_k^{(n)} = \{\bar{l}\}$, and $\mathcal{L}_k^{(n)} = \mathcal{L}_k^{(n-1)}, \forall k \in \mathcal{K} \setminus \{\bar{k}\}$.
Step 2: Solve the SOCP in (3.50) with the obtained sets $\mathcal{K}^{(n)}$ and $\{\mathcal{L}_k^{(n)}, \forall k \in \mathcal{K}^{(n)}\}$.
Step 3: If the SOCP in (3.50) is infeasible, set $\mathcal{K}^{(n)} = \mathcal{K}^{(n-1)}$ and $\mathcal{L}_k^{(n)} = \mathcal{L}_k^{(n-1)} \setminus \{\bar{l}\}$. Otherwise, update the iteration number $n \leftarrow n + 1$ and go back to **Step 1** and repeat.

Algorithm 3.1: The proposed SOCP based inflation procedure

3.6.2 The SOCP based deflation procedure

In this subsection we propose a low-complexity SOCP based deflation procedure, which represents a non-trivial extension of the SOCP based deflation procedure presented in [83]. The deflation procedure yields integer-feasible solutions of the DRAB problem with better objective function values than that of the inflation procedure in Alg. 3.1 (see Section 3.7), at slightly increased computational complexity. Denote the binary variables $\{a_{k,l}^{(n)}, \forall k \in \mathcal{K}, \forall l \in \mathcal{L}\}$ as the data rate assignments for the K MSs obtained in the n th iteration. The deflation procedure is initialized with $a_{k,l}^{(0)} = 1, \forall k \in \mathcal{K}, \forall l \in \mathcal{L}_k$, and $a_{k,l}^{(0)} = 0, \forall k \in \mathcal{K}, \forall l \in \mathcal{L} \setminus \mathcal{L}_k$, with the set \mathcal{L}_k defined in (3.46). In the n th iteration, we firstly copy $a_{k,l}^{(n)} = a_{k,l}^{(n-1)}, \forall k \in \mathcal{K}, \forall l \in \mathcal{L}$, and solve the following feasibility problem, which represents a convex SOCP, using, e.g., the interior-point method [34, 105]:

$$\left\{ \mathbf{v}_{k,l}^{(n)}, s_{k,l}^{(n)}, c_k^{(n)} \right\} \triangleq \underset{\{\mathbf{v}_{k,l}, s_{k,l}, c_k\}}{\operatorname{argmin}} \sum_{k=1}^K \sum_{l=1}^L \|\mathbf{v}_{k,l}\|_2^2 + \mu \sum_{k=1}^K \sum_{l=1}^L s_{k,l} \quad (3.51a)$$

$$\text{s.t. (3.7): } \sum_{k=1}^K \|\mathbf{w}_k\|_2^2 \leq P^{(\text{MAX})}$$

$$(3.24a): \operatorname{Im} \{ \mathbf{h}_k^H \mathbf{v}_{k,l} \} = 0, \operatorname{Re} \{ \mathbf{h}_k^H \mathbf{v}_{k,l} \} \geq 0, \forall k \in \mathcal{K}, \forall l \in \mathcal{L}$$

$$\| [\mathbf{h}_k^H \mathbf{W}, \sigma_k] \|_2 \leq c_k, \text{ if } \sum_{l=1}^L a_{k,l}^{(n)} \geq 1 \quad (3.51b)$$

$$c_k \leq s_{k,l} + \gamma_l \operatorname{Re} \{ \mathbf{h}_k^H \mathbf{v}_{k,l} \}, \text{ if } a_{k,l}^{(n)} = 1 \quad (3.51c)$$

$$s_{k,l} \geq 0, \forall k \in \mathcal{K}, \forall l \in \mathcal{L} \quad (3.51d)$$

where the auxiliary optimization variables $\{s_{k,l}, \forall k \in \mathcal{K}, \forall l \in \mathcal{L}\}$ are introduced in problem (3.51) to ensure that it is always feasible. In the objective function (3.51a), the constant $\mu > 0$ represents a large penalty factor for the *total infeasibility measure*, i.e., the term $\sum_{k=1}^K \sum_{l=1}^L s_{k,l}$. As shall be shown in Section 3.7, the performance of the deflation procedure is *not* sensitive to the penalty factor μ and thus it can easily be configured. The auxiliary optimization variables $\{c_k, \forall k \in \mathcal{K}\}$ are employed to simplify the formulation of the relaxed SINR constraints in Eqs. (3.51b) and (3.51c). In the n th iteration, if the obtained total infeasibility measure satisfies that $\sum_{k=1}^K \sum_{l=1}^L s_{k,l}^{(n)} < \beta$, with the constant $\beta > 0$ denoting the predefined infeasibility tolerance, the deflation procedure terminates. Otherwise, the following step:

$$\left(\tilde{k}, \tilde{l}\right) \triangleq \underset{k \in \mathcal{K}, l \in \mathcal{L}}{\operatorname{argmax}} s_{k,l}^{(n)} \quad (3.52)$$

is carried out to find the index pair $\left(\tilde{k}, \tilde{l}\right)$, and we set $a_{\tilde{k}, \tilde{l}}^{(n)} = 0$ to *exclude* assigning the \tilde{l} th MCS to the \tilde{k} th MS. If two index pairs correspond to the same maximum infeasibility measure in Eq. (3.52), i.e., if $s_{\tilde{k}_1, \tilde{l}_1}^{(n)} = s_{\tilde{k}_2, \tilde{l}_2}^{(n)} = \max_{k \in \mathcal{K}, l \in \mathcal{L}} s_{k,l}^{(n)}$, we then choose the index pair with the *smaller* branching priority, i.e., we choose $\left(\tilde{k}, \tilde{l}\right) = \left(\tilde{k}_1, \tilde{l}_1\right)$ if $\bar{\Upsilon}_{\tilde{k}_1, \tilde{l}_1} \leq \bar{\Upsilon}_{\tilde{k}_2, \tilde{l}_2}$. Otherwise, we choose $\left(\tilde{k}, \tilde{l}\right) = \left(\tilde{k}_2, \tilde{l}_2\right)$. That is we consider the infeasibility measures, the channel gains, and the candidate data rates jointly when determining the index pair $\left(\tilde{k}, \tilde{l}\right)$.

Denote $\{a_{k,l}^{(\text{DFL})}, \forall k \in \mathcal{K}, \forall l \in \mathcal{L}\}$ and $\{\mathbf{v}_{k,l}^{(\text{DFL})}, \forall k \in \mathcal{K}, \forall l \in \mathcal{L}\}$ as the data rate assignments and the virtual beamformers, respectively, obtained from the deflation procedure. The deflation procedure may lead to that more than one variables in the set $\{a_{k,l}^{(\text{DFL})}, \forall l \in \mathcal{L}\}$ are set to one for the k th MS, i.e., more than one data rates are assigned to the k th MS. In case that $\sum_{l=1}^L a_{k,l}^{(\text{DFL})} > 1$, a post-processing step shall be performed to assign the largest possible data rate to the k th MS based on the indicators $\{a_{k,l}^{(\text{DFL})}, \forall l \in \mathcal{L}\}, \forall k \in \mathcal{K}$. Assuming that the candidate data rates are ordered as in Eq. (3.42), we obtain the final data rate assignments $\{\tilde{a}_{k,l}^{(\text{DFL})}, \forall k \in \mathcal{K}, \forall l \in \mathcal{L}\}$ and the beamformers $\{\tilde{\mathbf{w}}_k^{(\text{DFL})}, \forall k \in \mathcal{K}\}$, respectively, as

$$\tilde{a}_{k,l}^{(\text{DFL})} = \begin{cases} a_{k,l}^{(\text{DFL})}, & \text{if } l = \underset{m \in \mathcal{L}_k}{\operatorname{argmax}} a_{k,m}^{(\text{DFL})} R_m \\ 0, & \text{otherwise} \end{cases}, \forall k \in \mathcal{K}, \forall l \in \mathcal{L} \quad (3.53)$$

$$\tilde{\mathbf{w}}_k^{(\text{DFL})} = \sum_{l=1}^L \tilde{a}_{k,l}^{(\text{DFL})} \mathbf{v}_{k,l}^{(\text{DFL})}, \forall k \in \mathcal{K}. \quad (3.54)$$

Similar to the proposed inflation procedure in Alg. 3.1, the worst-case computational

complexity of the proposed deflation procedure consists in solving $\sum_{k=1}^K L_k$ instances of the SOCP in (3.51), since one of the candidate data rate assignments is excluded in each iteration. The proposed low-complexity deflation procedure is summarized in Alg. 3.2.

Init.: Initialize $a_{k,l}^{(0)} = 1, \forall k \in \mathcal{K}, \forall l \in \mathcal{L}_k$, and set $a_{k,l}^{(0)} = 0, \forall k \in \mathcal{K}, \forall l \in \mathcal{L} \setminus \mathcal{L}_k$. Specify the infeasibility tolerance β , and set the iteration number $n = 1$.

Step 1: Set $a_{k,l}^{(n)} = a_{k,l}^{(n-1)}, \forall k \in \mathcal{K}, \forall l \in \mathcal{L}$, and solve the feasibility problem (3.51).

Step 2: If $\sum_{k=1}^K \sum_{l=1}^L s_{k,l}^{(n)} < \beta$, go to **Post-step**. Otherwise, compute the index pair (\tilde{k}, \tilde{l}) according to Eq. (3.52). If $s_{\tilde{k}_1, \tilde{l}_1}^{(n)} = s_{\tilde{k}_2, \tilde{l}_2}^{(n)} = \max_{k \in \mathcal{K}, l \in \mathcal{L}} s_{k,l}^{(n)}$, set $(\tilde{k}, \tilde{l}) = (\tilde{k}_1, \tilde{l}_1)$ if $\bar{\Upsilon}_{\tilde{k}_1, \tilde{l}_1} \leq \bar{\Upsilon}_{\tilde{k}_2, \tilde{l}_2}$. Otherwise, set $(\tilde{k}, \tilde{l}) = (\tilde{k}_2, \tilde{l}_2)$. Fix $a_{\tilde{k}, \tilde{l}}^{(n)} = 0$.

Step 3: Set $n \leftarrow n + 1$ and go back to **Step 1** and repeat.

Post-step: Compute the data rate assignments $\{a_{k,l}^{(\text{DFL})}, \forall k \in \mathcal{K}, \forall l \in \mathcal{L}\}$ and the beamformers $\{\tilde{\mathbf{w}}_k^{(\text{DFL})}, \forall k \in \mathcal{K}\}$ according to Eqs. (3.53) and (3.54), respectively.

Algorithm 3.2: The proposed SOCP based deflation procedure

3.7 Simulation results

As in Chapter 2, we adopt in the simulations the following channel model [106]: (i) the 3GPP LTE pathloss (PL) mode: $PL = 148.1 + 37.6 \log_{10}(d)$ (in dB), with d (in km) denoting the BS-MS distance; (ii) log-norm shadowing with zero mean, 8 dB variance; (iii) Rayleigh fading with zero mean and unit variance; and (iv) transmit antenna power gain of 9 dB; (v) the noise power $\sigma_k^2 = -143$ dB, $\forall k \in \mathcal{K}$. The BS is equipped with $M = 4$ transmit antennas, and the distances between the BS and the K MSs are uniformly and randomly generated in the interval $[0.05, 1]$ km. The data rates and SINR requirements listed in Tab. 1 are used. We choose the weighting factor $\rho = 1 / (1 + 512P^{(\text{MAX})})$ (c.f Eqs. (3.6) and (3.25)), the relative optimality tolerance $\eta = 0.5\%$ (cf. Eq. (3.38)), the parameter $\bar{K} = 12$ (cf. Eq. A.17) and the infeasibility tolerance $\beta = 10^{-5}$ in Alg. 3.2. The maximum transmission power $P^{(\text{MAX})}$ of the BS, the penalty parameter μ (cf. Eq. (3.51a)), and the number of admissible MSs K are listed under (or in) the figures. For comparison, the MIP solver CPLEX [81] is applied to the DRAB problem formulations in (3.15) and in (3.26). All simulation results are averaged over 600 Monte Carlo runs (MCRs).

3.7.1 Performance of the low-complexity algorithms

We first investigate the performance of the proposed low-complexity algorithms in Alg. 3.1 and Alg. 3.2. For all simulation results presented in this subsection, the runtime limit of the

solver CPLEX is set as $T = 720$ seconds

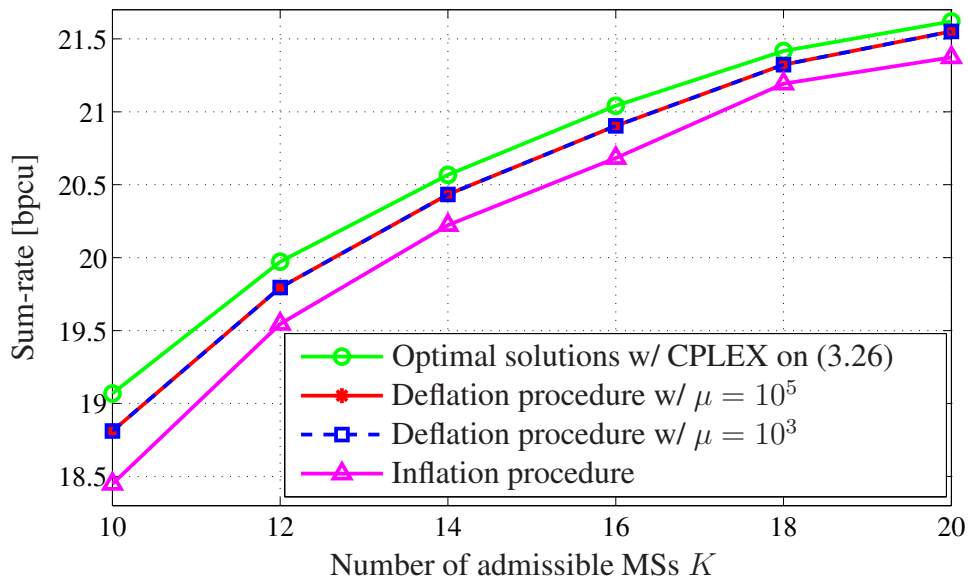


Figure 3.2: The sum-rate vs. the parameter K , with $P^{(\text{MAX})} = 14$ dB.

Fig. 3.2 displays the average sum-rate in bits-per-channel-use (bpcu) versus (vs.) the number of *admissible* MSs K , i.e., the total number of MSs available to be admitted, with the maximum transmission power of the BS $P^{(\text{MAX})} = 14$ dB. Fig. 3.2 shows that the deflation procedure in Alg. 3.2 yields sum-rates that are very close to that of the optimal solutions satisfying the optimality criterion in (3.38). For instance, the relative gap is less than 0.7% for $K \geq 14$. The deflation procedure is *not* sensitive to the penalty factor μ (cf. Eq. (3.51a)) since choosing $\mu = 10^5$ and $\mu = 10^3$ yield almost identical sum-rates. Furthermore, the inflation procedure in Alg. 3.1 also demonstrates good performance compared to the optimal solutions computed by CPLEX. For example, the relative gap of the sum-rates achieved by Alg. 3.1 and that of the optimal solutions is less than 1.7% for $K \geq 14$. The inflation and deflation procedures have much less computational complexity than that of the BnC method (cf. Fig. 3.4).

Fig. 3.3 depicts the average total transmitted power vs. the number of admissible MSs K . We observe from Fig. 3.3 that the excess in the total transmitted BS power achieved by the deflation procedure in Alg. 3.2 is negligible, compared to that of the optimal solutions computed by CPLEX. The inflation procedure in Alg. 3.1 yields the BS power consumption that exceeds that of the optimal solutions by less than 0.4 dB for all considered values of K . Further, Fig. 3.2 and Fig. 3.3 together suggest that the multiuser diversity gain in terms of increased sum-rate and reduced total transmitted BS power is achieved from MS admission control in the proposed design.

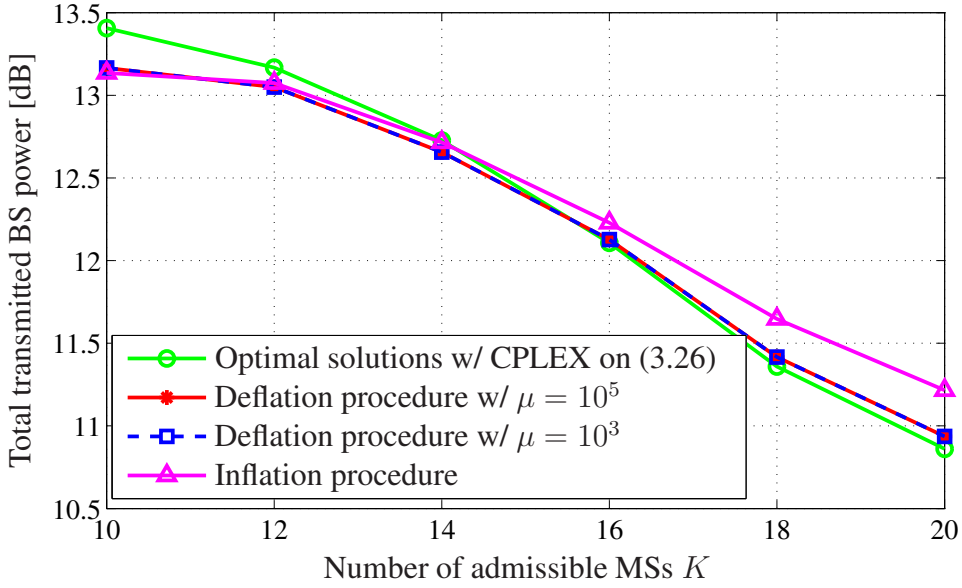


Figure 3.3: The total transmitted BS power vs. the parameter K , with $P^{(\text{MAX})} = 14$ dB.

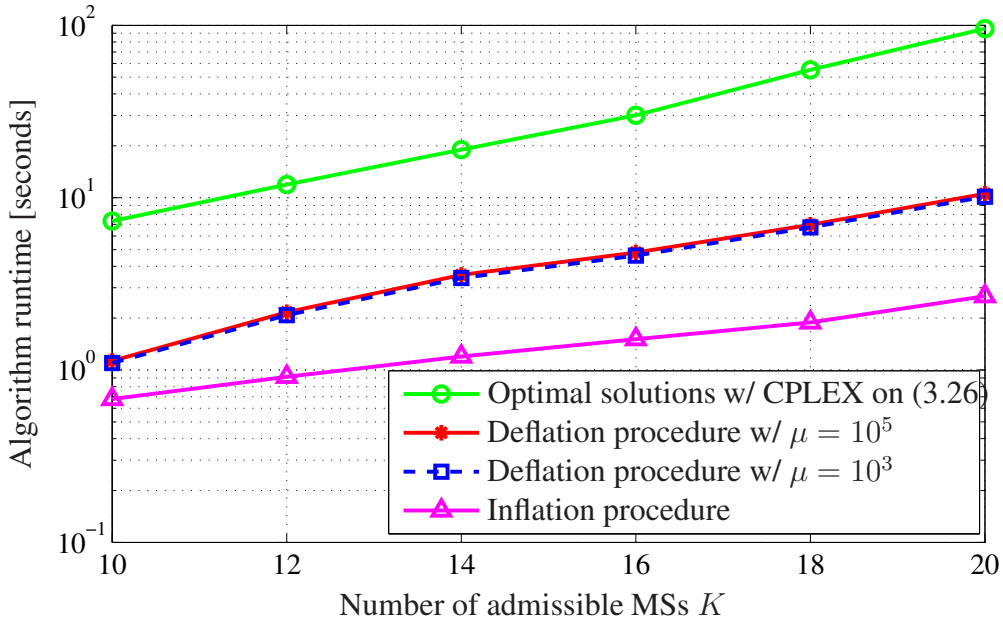


Figure 3.4: The algorithm runtime vs. the parameter K , with $P^{(\text{MAX})} = 14$ dB.

The runtime of the considered schemes vs. the number of admissible MSs K is plotted in Fig. 3.4. Fig. 3.4 clearly shows that the heuristic algorithms in Alg. 3.1 and Alg. 3.2 admit significantly less computational complexity than that of the customized BnC method. While the deflation procedure yields larger sum-rates with less BS power consumption than the inflation procedure, the former has a slightly more computational complexity. In practice, when employing application-specific hardware and software, the required runtime can be

significantly reduced [67–69, 81, 82].

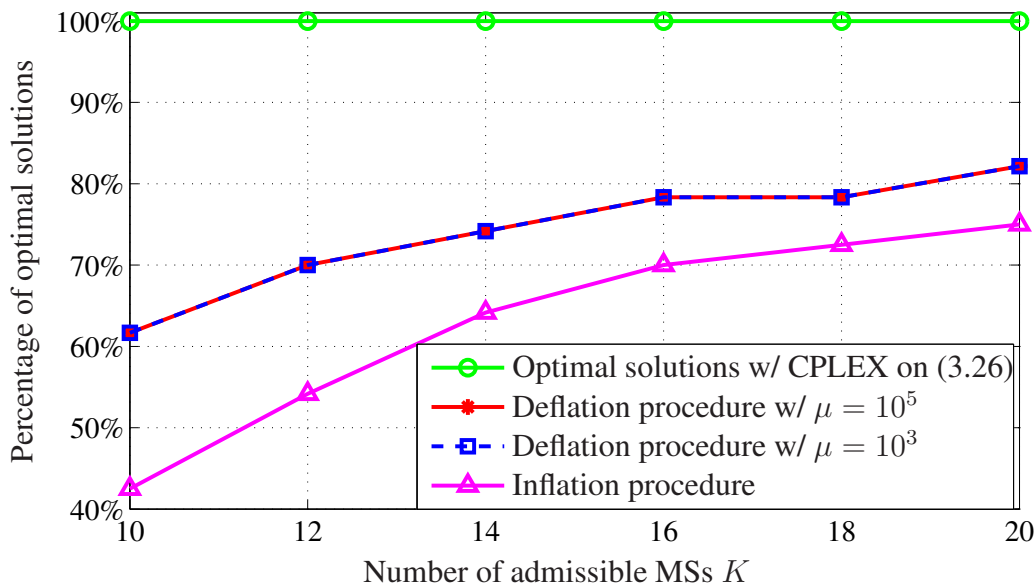


Figure 3.5: The percentage of optimal solutions vs. the parameter K , with $P^{(\text{MAX})} = 14$ dB.

The percentage of certified optimal (with respect to the optimality certificate defined in (3.38)) solutions vs. the number of admissible MSs K is shown in Fig. 3.5. It can be seen from Fig. 3.5 that the proposed deflation procedure yields optimal solutions in more than 62% of the MCRs for all considered values of K , and it generates optimal solutions in more than 83% of the MCRs with $K = 20$. The proposed inflation procedure computes optimal solutions in more than 43% of the MCRs for all considered values of K , and it achieves optimal solutions in more than 75% of the MCRs with $K = 20$.

3.7.2 Comparison of the two MISOCP formulations

We next compare the performance of the two DRAB problem formulations. As reference, the performance of the deflation procedure in Alg. 3.2 is also presented. For all simulation results presented in this subsection, the runtime limit of the solver CPLEX is set as $T = 50$ seconds.

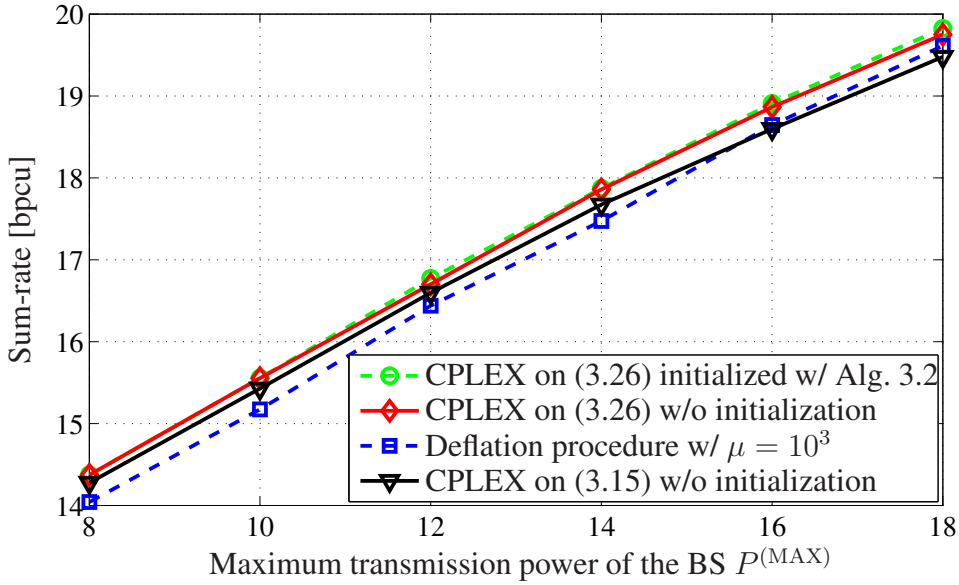


Figure 3.6: The sum-rate vs. the parameter $P^{(MAX)}$, with $K = 10$.

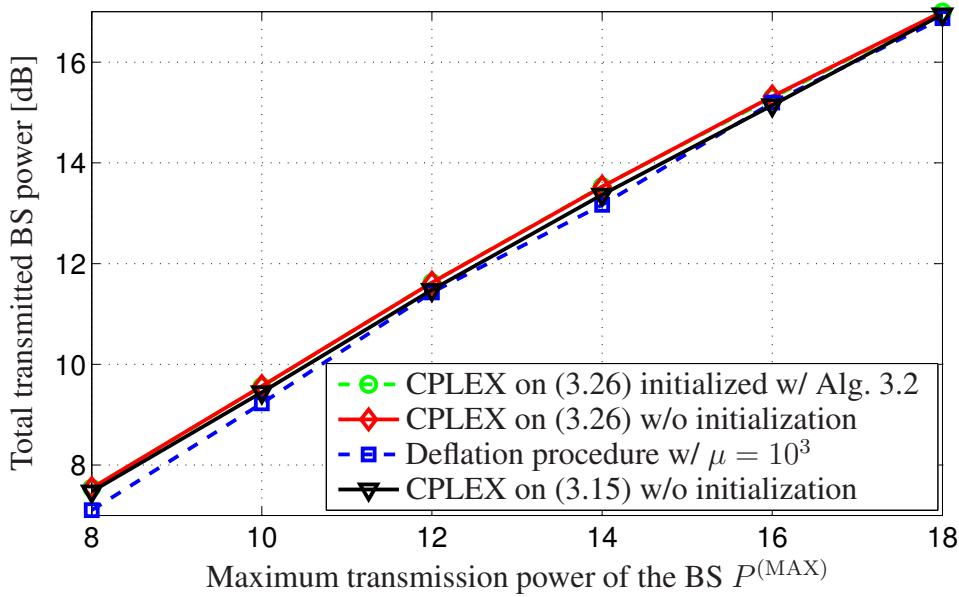


Figure 3.7: The total transmitted BS power vs. the parameter $P^{(MAX)}$, with $K = 10$.

We plot in Fig. 3.6 the average sum-rate vs. the maximum transmission power of the BS $P^{(MAX)}$, with the number of admissible MSs $K = 10$. The dotted curve with circles represents the results obtained by applying the solver CPLEX to the extended formulation (3.26) and CPLEX is initialized with the integer-feasible solutions computed by the proposed deflation procedure in Alg. 3.2. We observe from Fig. 3.6 that all considered methods achieve almost the same sum-rates. Furthermore, all considered schemes achieve almost the same total transmitted power of the BS, which is displayed in Fig. 3.7.

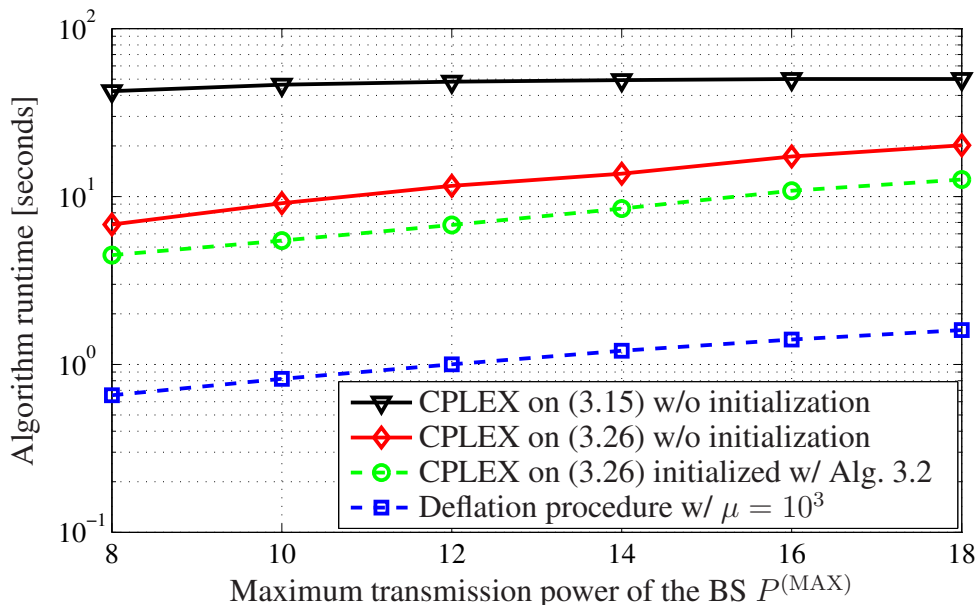


Figure 3.8: The algorithm runtime vs. the parameter $P^{(MAX)}$, with $K = 10$.

The average runtime of the considered methods vs. the maximum transmission power of the BS $P^{(MAX)}$ is depicted in Fig. 3.8. Note that the runtime represented by the solid curve with down-triangles, i.e., the method applying CPLEX on the standard big-M formulation (3.15) without initialization, is about 50 seconds, which corresponds to the chosen runtime limit. We see from Fig. 3.8 that the extended formulation (3.26) admits less computational complexity than that of the big-M formulation (3.15) when applying the customized BnC method (cf. Section 3.5), and the computational complexity of the customized BnC method applied to problem (3.26) is further reduced when it is initialized with the integer-feasible solutions found by the proposed deflation procedure in Alg. 3.2.

Fig. 3.9 displays the percentage of certified optimal (under the optimality criterion in (3.38)) solutions vs. the maximum transmission power of the BS $P^{(MAX)}$. Fig. 3.8 and Fig. 3.9 together clearly show that the extended formulation (3.26) admits less computational complexity for computing the optimality certificate in (3.38) than that of the big-M formulation (3.15) when applying the customized BnC method in CPLEX.

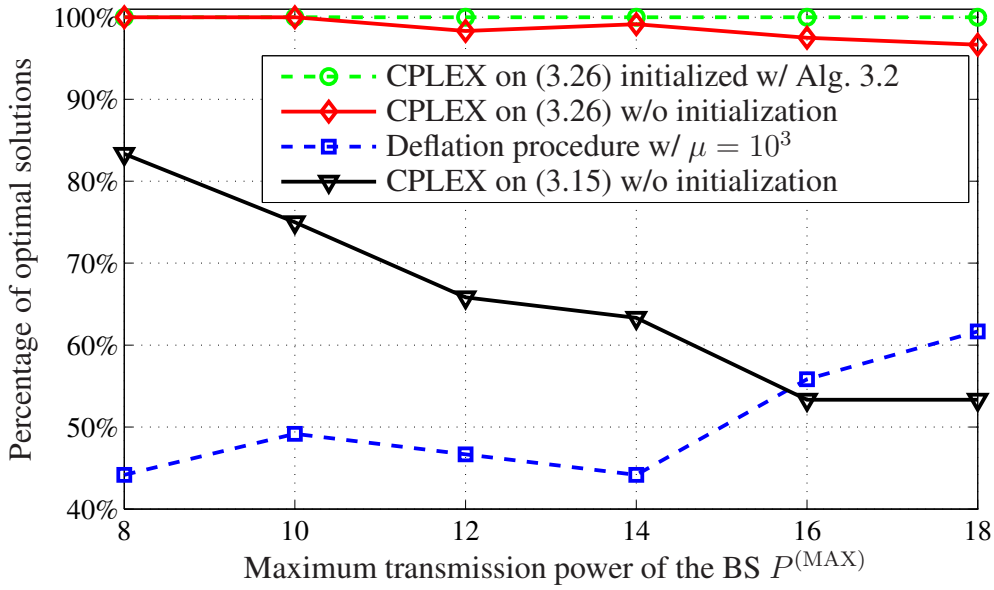


Figure 3.9: The percentage of optimal solutions vs. the parameter $P^{(\text{MAX})}$, with $K = 10$.

3.8 Summary

Similar to the contributions presented in Chapter 3, we have developed in this chapter two MISOCP formulations for the considered DRAB problem. It has also been analytically proved that the extended formulation (3.26) generally admits strictly tighter continuous relaxations than that of the standard big-M formulation (3.15). Several efficient strategies have been proposed to customize the standard BnC method implemented in CPLEX for solving the DRAB problem. We have furthermore developed the low-complexity SOCP based inflation and deflation procedures in Alg. 3.1 and Alg. 3.2, respectively, to compute near-optimal solutions of the DRAB problem for applications in large-scale networks. Our simulation results have shown that the proposed inflation and deflation procedures yield with very low computational complexity average sum-rates and BS power consumptions that are very close to that of the optimal solutions computed by CPLEX for the considered simulation settings. The numerical results have also confirmed the significant reduction in computational complexity of the extended MISOCP formulation over the standard big-M MISOCP formulation when applying the customized BnC method in CPLEX.

Chapter 4

Codebook-based downlink beamforming and channel predistortion

4.1 Introduction

In modern cellular standards, e.g., in 3GPP LTE/LTE-A [7, 8, 20], both non-codebook-based (i.e., adaptive) and codebook-based (i.e., switched) multiuser downlink beamforming schemes are defined. In non-codebook-based multiuser downlink beamforming, after computing the (optimal) beamformers (including transmission power allocations), the BS applies these beamformers to transmit *user-specific reference signals* (URSs) to inform the MSs about the composite (precoded) channels (i.e., the inner products of the beamformers and the original channels). The MSs estimate the composite channels using the known URSs. In contrast to this, in codebook-based multiuser downlink beamforming (also known as single-layer-per-user precoding), the BS assigns the precoding vectors from the predefined precoding vector codebook that consists of a finite number of predetermined precoding vectors, to the MSs, along with proper transmission power allocations. The BS then signals the indices of the assigned precoding vectors and the allocated transmission powers to the MSs [7, 8, 14, 20–22, 117, 118]. The multiuser downlink beamforming schemes presented in Chapters 2 and 3, in which the beamforming vectors are chosen from the continuous vector spaces, represent non-codebook-based beamforming techniques [12, 13, 24]. In Chapters 4 and 5, we consider codebook-based multiuser downlink beamforming schemes [7, 8, 14, 20–22, 117–120]. Similar to Chapter 2, we employ in this chapter also the QoS-constrained approach when optimizing codebook-based multiuser downlink beamforming, where the QoS targets of the admitted MSs are expressed through the minimum received SINR requirements [23].

We consider first the joint optimization of precoding vector assignment and transmission power allocation in the standard codebook-based multiuser downlink beamforming (SCBF) problem. While it is well-known that the QoS based beamformer design problem in non-codebook-based multiuser downlink beamforming can be efficiently solved using either convex optimization techniques or customized iterative algorithms [12, 13, 25–31, 121], the SINR-constrained SCBF problem represents a combinatorial mixed-integer program (MIP) and is significantly more challenging. This is because in the SCBF problem precoding vector assignments involve *binary* decision makings, and the precoding vector assignments and transmission power allocations of multiple MSs are coupled through co-channel interference in the downlink SINR constraints. To facilitate algorithmic solutions of the SCBF problem, we develop a mixed-integer linear program (MILP) reformulation of the SCBF problem, which can be solved using, e.g., the standard BnC method [67–69, 81, 82]. The computational complexity of the BnC method when applying to the SCBF problem may not be affordable for practical applications. To develop more efficient solutions, we follow a similar idea as presented in [12, 13, 25–30] and introduce a virtual uplink (VUL) problem, in which the precoding vector assignments of different MSs are naturally decoupled. We establish the uplink-downlink duality between the VUL problem and the downlink SCBF problem, and develop a customized power iteration algorithm to optimally solve the VUL problem and hence the SCBF problem. Only very simple algebraic operations are performed in each iteration of the proposed power iteration method. Resorting to the standard interference function (SIF) approach [35, 36, 122, 123], we show analytically that the proposed power iteration algorithm yields either the optimal (within the prescribed numerical accuracy) solutions of the SCBF problem (when it is feasible), or the infeasibility certificates (when it is infeasible).

Since the beamformers are confined in the predefined precoding vector codebook consisting of a small number of fixed precoding vectors, codebook-based downlink beamforming inherently exhibits performance degradation in terms of, e.g., increased transmitted BS power required to guarantee the QoS targets of the admitted MSs, as compared to non-codebook-based downlink beamforming (cf. Section 4.5). To improve the performance of codebook-based downlink beamforming, we introduce a channel predistortion procedure in the standard codebook-based multiuser downlink beamforming [7, 8, 14, 20–22, 117–120]. The channel predistortion scheme consists in a common linear transformation of the downlink channel vectors using one common channel predistortion matrix. The channel predistortion mechanism introduces additional degrees of freedom for beamformer design in the standard codebook-based downlink beamforming. As shall be discussed further in Section 4.4.1, the channel predistortion scheme involves minor modifications in the transmission procedures of the *cell-specific* reference signals and user payload data. As a result,

the channel predistortion scheme does not introduce any additional signaling overhead or modifications of the mobile receivers. That is, the proposed channel predistortion mechanism can be straightforwardly applied in current third generation (3G) and fourth generation (4G) cellular standards, e.g., in 3GPP LTE/LTE-A [7, 8, 20]. To ensure that the predistorted channel vectors can still be tracked in the channel estimation procedures performed at the MSs, smoothness constraints are imposed on the predistorted channel processes. The SINR-constrained codebook-based beamforming and channel predistortion (CBCP) problem represents a *non-convex* MIP, which remains a *non-convex* program even after relaxing the integer constraints, and efficient optimal algorithmic solutions for non-convex MIPs are not available in the literature [67, 68].

We develop an alternating optimization algorithm (ATOA) to approximately solve the CBCP problem. The ATOA iterates between solving two subproblems: (i) optimizing the precoding vector assignments and the power allocations under a *fixed* channel predistortion matrix, which represents a MILP that can be efficiently solved using, e.g., the BnC method and/or the proposed customized power iteration method, and (ii) optimizing the channel predistortion matrix and the transmission power allocations under *fixed* precoding vector assignments, which can be closely approximated by a second-order cone program (SOCP) that can be efficiently solved using, e.g., the interior-point method [34]. Since either one of the two subproblems in the ATOA may become infeasible even if the original CBCP problem is feasible, an alternating feasibility search algorithm (AFSA), which follows a similar procedure as the ATOA, is also developed to compute feasible solutions of the CBCP problem, which are used to initialize the ATOA. Convergence properties of the proposed ATOA and AFSA are discussed.

The simulation results show that, for the SCBF problem, the proposed customized power iteration method yields with a few low-complexity iterations, either the same total transmitted BS power as that of the optimal solutions computed by the BnC method (when the SCBF problem is feasible), or the infeasibility certificates (when it is infeasible). Our numerical results also demonstrate that the proposed channel predistortion design achieves significant reductions in the total transmitted BS power and tremendous increases in the percentage of feasible cases out of all Monte Carlo runs, as compared to the standard codebook-based downlink beamforming (without channel predistortion).

This chapter is based on my original work that has been published in [124–126], and new simulation results are presented in this chapter.

4.2 System model

Similar to Chapter 3, we consider in this chapter a cellular downlink system with one BS equipped with $M > 1$ transmit antennas, and $K > 1$ single-antenna MSs. All the K MSs are admitted with the prescribed QoS requirements. We denote $\mathbf{h}_k^H \in \mathbb{C}^{1 \times M}$, $\mathbf{u}_k \in \mathbb{C}^{M \times 1}$, and $p_k > 0$ as the frequency-flat channel vector, the normalized beamformer (precoding vector), i.e., $\|\mathbf{u}_k\|_2 = 1$, and the allocated transmission power, respectively, of the k th MS, $\forall k \in \mathcal{K} \triangleq \{1, 2, \dots, K\}$. The received signal $y_k \in \mathbb{C}$ at the k th MS can be written as (see, e.g., [12, 13, 18, 25–33])

$$y_k = \mathbf{h}_k^H \mathbf{u}_k \sqrt{p_k} x_k + \mathbf{h}_k^H \sum_{j=1, j \neq k}^K \mathbf{u}_j \sqrt{p_j} x_j + z_k, \forall k \in \mathcal{K} \quad (4.1)$$

where $x_k \in \mathbb{C}$ denotes the normalized data symbol, i.e., $\mathbb{E}\{|x_k|^2\} = 1$, of the k th MS, and $z_k \in \mathbb{C}$ represents the additive circularly-symmetric white Gaussian noise [19] at the k th MS, with zero mean and variance σ_k^2 , $\forall k \in \mathcal{K}$. Note that the beamforming vector \mathbf{w}_k discussed in Chapters 2 and 3, e.g., in Eqs. (2.1) and (3.1), corresponds to the term $\sqrt{p_k} \mathbf{u}_k$ in the signal model (4.1), $\forall k \in \mathcal{K}$.

We consider in this chapter the codebook-based multiuser downlink beamforming as defined in modern wireless standards, e.g., in 3GPP LTE/LTE-A [7, 8, 20]. In codebook-based multiuser downlink beamforming, the normalized beamformer \mathbf{u}_k is assigned from one of the predetermined precoding vectors in the predefined precoding vector codebook \mathcal{B} that consists of $L > 1$ unit-norm precoding vectors, i.e.,

$$\mathbf{u}_k \in \mathcal{B} \triangleq \{\mathbf{v}_1, \mathbf{v}_2, \dots, \mathbf{v}_L\}, \forall k \in \mathcal{K} \quad (4.2)$$

where the predetermined precoding vector $\mathbf{v}_l \in \mathbb{C}^{M \times 1}$ and $\|\mathbf{v}_l\|_2 = 1$, $\forall l \in \mathcal{L} \triangleq \{1, 2, \dots, L\}$.

Assume that the data symbols of the MSs are mutually independent and are independent from the noise. Under single-user detection, i.e., treating co-channel interference as noise at the receivers, the downlink (DL) received SINR at the k th MS, denoted by $\text{SINR}_k^{(\text{DL})}$, can then be expressed as (see, e.g., [12, 13, 18, 25–33])

$$\text{SINR}_k^{(\text{DL})} \triangleq \frac{p_k |\mathbf{u}_k^H \mathbf{h}_k|^2}{\sum_{j=1, j \neq k}^K p_j |\mathbf{u}_j^H \mathbf{h}_k|^2 + \sigma_k^2}, \forall k \in \mathcal{K}. \quad (4.3)$$

As in Chapters 2 and 3, we also assume in this chapter that the instantaneous downlink channel vectors $\{\mathbf{h}_k^H, \forall k \in \mathcal{K}\}$ are known at the BS, which is practically realizable in, e.g.,

TDD systems by exploiting channel reciprocity [7, 19].

4.3 The standard codebook-based downlink beamforming problem

4.3.1 The SCBF problem formulation

Following the SINR-constrained approach [12, 13, 18, 25–33], we consider the joint optimization of precoding vector assignment and transmission power allocation to minimize the total transmitted power of the BS while guaranteeing the prescribed SINR target $\Gamma_k^{(\text{MIN})}$, representing the subscribed QoS requirement of the k th MS [23], $\forall k \in \mathcal{K}$. The standard codebook-based multiuser downlink beamforming (SCBF) problem can be formulated as the following *discrete* optimization problem:

$$\Phi^{(\text{SCBF})} \triangleq \min_{\{\mathbf{u}_k, p_k\}} \sum_{k=1}^K p_k \quad (4.4a)$$

$$\text{s.t. } \mathbf{u}_k \in \mathcal{B}, \forall k \in \mathcal{K} \quad (4.4b)$$

$$p_k \geq 0, \forall k \in \mathcal{K} \quad (4.4c)$$

$$\sum_{k=1}^K p_k \leq P^{(\text{MAX})} \quad (4.4d)$$

$$\text{SINR}_k^{(\text{DL})} = \frac{p_k |\mathbf{u}_k^H \bar{\mathbf{h}}_k|^2}{\sum_{j=1, j \neq k}^K p_j |\mathbf{u}_j^H \bar{\mathbf{h}}_k|^2 + 1} \geq \Gamma_k^{(\text{MIN})}, \forall k \in \mathcal{K} \quad (4.4e)$$

where the term $\text{SINR}_k^{(\text{DL})}$ is defined in Eq. (4.3). Eq. (4.4d) represents the per-BS sum-power constraint, with the constant $P^{(\text{MAX})} > 0$ denoting the maximum transmission power of the BS. The normalized downlink channel vector $\bar{\mathbf{h}}_k^H \in \mathbb{C}^{1 \times M}$ in Eq. (4.4e) is defined as

$$\bar{\mathbf{h}}_k^H \triangleq \mathbf{h}_k^H / \sigma_k, \forall k \in \mathcal{K}. \quad (4.5)$$

Note that the conventional QoS-constrained non-codebook-based downlink beamforming problem can be efficiently solved to optimality using convex optimization techniques or specialized iterative algorithms [12, 13, 25–28, 121]. In contrast to this, efficient convex optimization techniques cannot be applied to solve the SCBF problem (4.4) due to the *discrete* constraints defined in (4.4b). To facilitate computing the optimal solutions of the SCBF problem (4.4) using, e.g., the BnC method [67–69, 81, 82], we propose next a MILP

reformulation of the SCBF problem (4.4).

We introduce the *binary* integer variable $\{a_{k,l} \in \{0, 1\}, \forall k \in \mathcal{K}, \forall l \in \mathcal{L}\}$ to model the assignments of precoding vectors from the precoding vector codebook as defined in Eq. (4.4b). We indicate with $a_{k,l} = 1$ that the l th precoding vector $\mathbf{v}_l \in \mathcal{B}$ is assigned to the k th MS, and $a_{k,l} = 0$ otherwise. Accordingly, we introduce the variable $\phi_{k,l} \geq 0$ to model the allocated transmission power corresponding to the l th precoding vector $\mathbf{v}_l \in \mathcal{B}$ when it is assigned to the k th MS, $\forall k \in \mathcal{K}, \forall l \in \mathcal{L}$. To derive a MILP formulation, we impose the following constraints in the SCBF problem:

$$\sum_{k=1}^K \sum_{l=1}^L \phi_{k,l} \leq P^{(\text{MAX})} \quad (4.6)$$

$$0 \leq \phi_{k,l} \leq a_{k,l} P^{(\text{MAX})}, \forall k \in \mathcal{K}, \forall l \in \mathcal{L} \quad (4.7)$$

$$\sum_{l=1}^L a_{k,l} = 1, \forall k \in \mathcal{K} \quad (4.8)$$

where Eq. (4.6) represents the reformulation of the per-BS sum-power constraint as that given in (4.4d). Eq. (4.7) implements the big-M method [67–69] to ensure that $\phi_{k,l} = 0$ when $a_{k,l} = 0$. Furthermore, Eq. (4.7) is automatically satisfied when $a_{k,l} = 1$ due to Eq. (4.6). Eqs. (4.7) and (4.8) together imply that one and only one binary variable in the set $\{a_{k,l}, \forall l \in \mathcal{L}\}$ is one, and one and only one variable in the set $\{\phi_{k,l}, \forall l \in \mathcal{L}\}$ is non-zero for the k th MS. As a result, we can express the transmission power p_k and the beamformer \mathbf{u}_k of the k th MS, respectively, as

$$p_k = \sum_{l=1}^L a_{k,l} \phi_{k,l} = \sum_{l=1}^L \phi_{k,l}, \forall k \in \mathcal{K} \quad (4.9)$$

$$\mathbf{u}_k = \sum_{l=1}^L a_{k,l} \mathbf{v}_l, \forall k \in \mathcal{K}. \quad (4.10)$$

Eqs. (4.9) and (4.10) together further imply that

$$p_j |\mathbf{u}_j^H \bar{\mathbf{h}}_k|^2 = \sum_{l=1}^L \phi_{j,l} |\mathbf{v}_l^H \bar{\mathbf{h}}_k|^2, \forall j, k \in \mathcal{K}. \quad (4.11)$$

Making use of Eq. (4.11), the term SINR_k given in Eq. (4.4e) can be rewritten as

$$\text{SINR}_k^{(\text{DL})} = \frac{\sum_{m=1}^L \phi_{k,m} |\mathbf{v}_m^H \bar{\mathbf{h}}_k|^2}{\sum_{j=1, j \neq k}^K \sum_{l=1}^L \phi_{j,l} |\mathbf{v}_l^H \bar{\mathbf{h}}_k|^2 + 1}, \forall k \in \mathcal{K}. \quad (4.12)$$

We obtain from the downlink SINR constraints in (4.4e) the following *necessary* condition for assigning the l th precoding vector $\mathbf{v}_l \in \mathcal{B}$ to the k th MS:

$$P^{(\text{MAX})} |\mathbf{v}_l^H \bar{\mathbf{h}}_k|^2 > \Gamma_k^{(\text{MIN})}. \quad (4.13)$$

The necessary condition defined in (4.13) is derived from the downlink SINR constraints in (4.4e) by dropping the co-channel interference. Denote the set \mathcal{L}_k as the indices of the precoding vectors that can possibly be assigned to the k th MS. According to the necessary condition in (4.13), the set \mathcal{L}_k can be defined as

$$\mathcal{L}_k \triangleq \left\{ l \mid l \in \mathcal{L}, P^{(\text{MAX})} |\mathbf{v}_l^H \bar{\mathbf{h}}_k|^2 > \Gamma_k^{(\text{MIN})} \right\}, \forall k \in \mathcal{K}. \quad (4.14)$$

With Eqs. (4.6) – (4.8), and (4.12), and the set \mathcal{L}_k defined in (4.14), the SCBF problem (4.4) can be equivalently reformulated as the following MILP:

$$\Phi^{(\text{SCBF})} \triangleq \min_{\{a_{k,l}, \phi_{k,l}\}} \sum_{k=1}^K \sum_{l=1}^L \phi_{k,l} \quad (4.15a)$$

$$\text{s.t. (4.6): } \sum_{k=1}^K \sum_{l=1}^L \phi_{k,l} \leq P^{(\text{MAX})}$$

$$(4.7): 0 \leq \phi_{k,l} \leq a_{k,l} P^{(\text{MAX})}, \forall k \in \mathcal{K}, \forall l \in \mathcal{L}$$

$$(4.8): \sum_{l=1}^L a_{k,l} = 1, \forall k \in \mathcal{K}$$

$$\text{SINR}_k^{(\text{DL})} = \frac{\sum_{m=1}^L \phi_{k,m} |\mathbf{v}_m^H \bar{\mathbf{h}}_k|^2}{\sum_{j=1, j \neq k}^K \sum_{l=1}^L \phi_{j,l} |\mathbf{v}_l^H \bar{\mathbf{h}}_k|^2 + 1} \geq \Gamma_k^{(\text{MIN})}, \forall k \in \mathcal{K} \quad (4.15b)$$

$$a_{k,l} \in \{0, 1\}, \forall k \in \mathcal{K}, \forall l \in \mathcal{L} \quad (4.15c)$$

$$a_{k,l} = 0, \forall k \in \mathcal{K}, \forall l \in \mathcal{L} \setminus \mathcal{L}_k. \quad (4.15d)$$

The MILP formulation in (4.15) of the SCBF problem can be solved using, e.g., the standard BnC method [67–69, 81, 82] that is implemented in, e.g., the commercial MIP solver IBM ILOG CPLEX [81].

4.3.2 The customized power iteration method

The computational complexity of the standard BnC method [67–69, 81, 82] when applying to the MILP formulation (4.15) of the SCBF problem may be prohibitive for practical systems with large numbers of MSs and/or candidate precoding vectors. We propose in this subsection a low-complexity customized iterative algorithm to more efficiently solve the SCBF problem in the form of (4.15).

Similar to the existing contributions [12, 13, 25–30] that consider the conventional non-codebook-based multiuser downlink beamforming, we introduce here the following codebook-based *virtual* uplink (VUL) beamforming problem:

$$\Phi^{(\text{VUL})} \triangleq \min_{\{\mathbf{u}_k, q_k\}} \sum_{k=1}^K q_k \quad (4.16a)$$

$$\text{s.t. } \mathbf{u}_k \in \mathcal{B}, \forall k \in \mathcal{K} \quad (4.16b)$$

$$q_k \geq 0, \forall k \in \mathcal{K} \quad (4.16c)$$

$$\sum_{k=1}^K q_k \leq P_{\max} \quad (4.16d)$$

$$\text{SINR}_k^{(\text{VUL})} \triangleq \frac{q_k |\mathbf{u}_k^H \bar{\mathbf{h}}_k|^2}{\sum_{j=1, j \neq k}^K q_j |\mathbf{u}_k^H \bar{\mathbf{h}}_j|^2 + 1} \geq \Gamma_k^{(\text{MIN})}, \forall k \in \mathcal{K} \quad (4.16e)$$

where the variable q_k and the term $\text{SINR}_k^{(\text{VUL})}$ denote the VUL transmission power and the VUL received SINR of the k th MS, respectively, $\forall k \in \mathcal{K}$.

Leveraging the results regarding the uplink-downlink duality in the conventional non-codebook-based multiuser downlink beamforming problem presented in [13, 27–30], the following property can readily be proved.

Proposition 4.1 (Feasibility). *The SINR-constrained downlink SCBF problem (4.4) is feasible if and only if (iff) the virtual uplink problem (4.16) is feasible [13, Section 27.2.4].*

Assume for now that the VUL problem (4.16) is feasible and that the vectors $\{\tilde{\mathbf{u}}_k, \forall k \in \mathcal{K}\}$ are the optimal (not necessarily unique) beamformers of the VUL problem (4.16). We define the beamformer matrix $\tilde{\mathbf{U}} \in \mathbb{C}^{M \times K}$, the *coupling* matrix $\mathbf{C}(\tilde{\mathbf{U}}) \in \mathbb{R}^{K \times K}$, and the

diagonal matrix $\mathbf{D}(\tilde{\mathbf{U}}) \in \mathbb{R}^{K \times K}$, respectively, as

$$\tilde{\mathbf{U}} \triangleq [\tilde{\mathbf{u}}_1, \tilde{\mathbf{u}}_2, \dots, \tilde{\mathbf{u}}_K] \quad (4.17)$$

$$[\mathbf{C}(\tilde{\mathbf{U}})]_{k,j} \triangleq \begin{cases} 0, & \text{if } k = j \\ \tilde{\mathbf{u}}_j^H \bar{\mathbf{Q}}_k \tilde{\mathbf{u}}_j, & \text{otherwise} \end{cases}, \forall k, j \in \mathcal{K} \quad (4.18)$$

$$[\mathbf{D}(\tilde{\mathbf{U}})]_{k,j} \triangleq \begin{cases} \frac{\Gamma_k^{(\text{MIN})}}{\tilde{\mathbf{u}}_k^H \bar{\mathbf{Q}}_k \tilde{\mathbf{u}}_k}, & \text{if } k = j \\ 0, & \text{otherwise} \end{cases}, \forall k, j \in \mathcal{K} \quad (4.19)$$

where the matrix $\bar{\mathbf{Q}}_k \in \mathbb{C}^{M \times M}$ is defined as

$$\bar{\mathbf{Q}}_k \triangleq \bar{\mathbf{h}}_k \bar{\mathbf{h}}_k^H, \forall k \in \mathcal{K}. \quad (4.20)$$

With the definitions given in (4.17) - (4.19), the following statements regarding the uplink-downlink duality between the VUL problem (4.16) and the combinatorial downlink SCBF problem (4.4) can readily be concluded [13, Section 27.2.4].

(D1) The beamformers $\{\tilde{\mathbf{u}}_k, \forall k \in \mathcal{K}\}$ are optimal (not necessarily unique) for both the VUL problem (4.16) and the downlink SCBF problem (4.4).

(D2) Both the optimal VUL transmission power vector $\tilde{\mathbf{q}} \triangleq [\tilde{q}_1, \tilde{q}_2, \dots, \tilde{q}_K]^T$ and the optimal downlink transmission power vector $\tilde{\mathbf{p}} \triangleq [\tilde{p}_1, \tilde{p}_2, \dots, \tilde{p}_K]^T$ are *unique* and are respectively given by

$$\tilde{\mathbf{q}} = \left((\mathbf{D}(\tilde{\mathbf{U}}))^{-1} - (\mathbf{C}(\tilde{\mathbf{U}}))^T \right)^{-1} \mathbf{1} \quad (4.21)$$

$$\tilde{\mathbf{p}} \triangleq \left((\mathbf{D}(\tilde{\mathbf{U}}))^{-1} - \mathbf{C}(\tilde{\mathbf{U}}) \right)^{-1} \mathbf{1} \quad (4.22)$$

with the all-ones vector $\mathbf{1} \triangleq [1, 1, \dots, 1]^T \in \mathbb{R}^{K \times 1}$.

(D3) The same minimum total transmitted BS power is achieved both in the VUL problem (4.16) and the downlink SCBF problem (4.4), i.e.,

$$\Phi^{(\text{VUL})} = \mathbf{1}^T \tilde{\mathbf{q}} = \mathbf{1}^T \tilde{\mathbf{p}} = \Phi^{(\text{SCBF})}. \quad (4.23)$$

We know from *Proposition 4.1* and the uplink-downlink duality properties (D1) – (D3) that we can focus on the VUL problem (4.16) when solving the downlink SCBF problem (4.4). Note that the VUL problem (4.16) is much easier to solve since the precoding vector assignments in the VUL SINR constraints in (4.16e) are naturally decoupled.

Following the idea of the power iteration method that was originally proposed for solving

the conventional non-codebook-based multiuser downlink beamforming problem [12, 25, 26], we propose here a customized iterative algorithm to compute the optimal solutions of the SCBF problem (4.4) (when it is feasible). The algorithm also yields the infeasibility certificates (when problem (4.4) is infeasible). In the initialization of the customized power iteration algorithm, the following *necessary* conditions:

$$P^{(\text{MAX})} \max_{l \in \mathcal{L}} \mathbf{v}_l^H \overline{\mathbf{Q}}_k \mathbf{v}_l > \Gamma_k^{(\text{MIN})}, \forall k \in \mathcal{K} \quad (4.24)$$

are evaluated. The necessary conditions given in (4.24) are derived from the necessary condition defined in (4.13). If any one of the necessary conditions in (4.24) is violated, the SCBF problem (4.4) is clearly infeasible and the algorithm terminates. Otherwise, in the n th ($n \geq 1$) iteration, the VUL power vector $\mathbf{q}^{(n)} \triangleq [q_1^{(n)}, q_2^{(n)}, \dots, q_K^{(n)}]^T$ is computed according to the following *power iteration* process (see, e.g., [12, 25, 26]):

$$\mathbf{q}^{(n)} = \mathbf{f}(\mathbf{q}^{(n-1)}) \quad (4.25)$$

where the vector function $\mathbf{f}(\mathbf{q}^{(n)}) : \mathbb{R}^{K \times 1} \mapsto \mathbb{R}^{K \times 1}$ is defined as

$$\mathbf{f}(\mathbf{q}^{(n-1)}) \triangleq [f_1(\mathbf{q}^{(n-1)}), f_2(\mathbf{q}^{(n-1)}), \dots, f_K(\mathbf{q}^{(n-1)})]^T \quad (4.26a)$$

$$f_k(\mathbf{q}^{(n-1)}) \triangleq \max_{l \in \mathcal{L}_k} f_{k,l}(\mathbf{q}^{(n-1)}), \forall k \in \mathcal{K} \quad (4.26b)$$

$$f_{k,l}(\mathbf{q}^{(n-1)}) \triangleq \frac{\Gamma_k^{(\text{MIN})} + \Gamma_k^{(\text{MIN})} \sum_{j=1, j \neq k}^K (\mathbf{v}_l^H \overline{\mathbf{Q}}_j \mathbf{v}_l) q_j^{(n-1)}}{\mathbf{v}_l^H \overline{\mathbf{Q}}_k \mathbf{v}_l}, \forall k \in \mathcal{K}, \forall l \in \mathcal{L}_k \quad (4.26c)$$

If it holds that $\mathbf{1}^T \mathbf{q}^{(n)} > P^{(\text{MAX})}$ in the n th iteration, the algorithm declares that the downlink SCBF problem (4.4) is infeasible and terminates. Otherwise, the beamforming (precoding) vector of the k th MS is updated according to

$$\mathbf{u}_k^{(n)} = \mathbf{v}_{l_k^{(n)}}, \forall k \in \mathcal{K} \quad (4.27)$$

where the precoding vector index $l_k^{(n)}$ is given by

$$l_k^{(n)} \triangleq \operatorname{argmax}_{l \in \mathcal{L}} f_{k,l}(\mathbf{q}^{(n-1)}), \forall k \in \mathcal{K}. \quad (4.28)$$

The proposed iterative algorithm starts with the all-zeros vector $\mathbf{q}^{(0)} = \mathbf{0}$, and iterates until $\mathbf{1}^T \mathbf{q}^{(n)} - \mathbf{1}^T \mathbf{q}^{(n-1)} < \epsilon$ (when the SCBF problem (4.4) is feasible), or $\mathbf{1}^T \mathbf{q}^{(n)} > P^{(\text{MAX})}$ (when it is infeasible). Here, ϵ denotes the prescribed numerical accuracy. The proposed

customized power iteration method is summarized in Alg. 4.1. Note that each iteration of Alg. 4.1 only involves simple algebraic operations. The convergence and optimality analysis of Alg. 4.1 is presented in the next subsection.

Init.: (i) If *not* all conditions in Eq. (4.24) are satisfied, declare infeasibility and stop.
(ii) Specify the numerical accuracy ϵ , initialize $q_k^{(0)} = 0, \forall k \in \mathcal{K}$, and set the iteration number $n = 1$.

Step 1: Compute $\mathbf{q}^{(n)}$ according to Eq. (4.25).

Step 2: If $\mathbf{1}^T \mathbf{q}^{(n)} > P^{(\text{MAX})}$, *declare infeasibility* of the SCBF problem (4.4) and terminate.

Step 3: Compute $\{\mathbf{u}_k^{(n)}, \forall k \in \mathcal{K}\}$ according to Eq. (4.27).

Step 4: If $\mathbf{1}^T \mathbf{q}^{(n)} - \mathbf{1}^T \mathbf{q}^{(n-1)} < \epsilon$, go to **Post-step**. Otherwise, set $n \leftarrow n + 1$ and go back to **Step 1** and repeat.

Post-step: Set the beamformer matrix $\tilde{\mathbf{U}} = [\mathbf{u}_1^{(n)}, \mathbf{u}_2^{(n)}, \dots, \mathbf{u}_K^{(n)}]$ and compute the downlink power vector $\tilde{\mathbf{p}}$ according to Eq. (4.22).

Algorithm 4.1: The proposed customized power iteration method

4.3.3 Optimality of the power iteration method

We study in this subsection the convergence and optimality of the proposed customized power iteration procedure in Alg. 4.1 using the standard interference function (SIF) approach [35, 36, 122, 123]. The SIF approach is well-known to be a very effective and elegant way to prove the convergence and optimality of the power iteration method [35, 36, 122, 123]. We first revisit the definition of a SIF [35, 36].

Definition 4.1. *The vector function $\mathbf{g}(\mathbf{q}) : \mathbb{R}^{K \times 1} \mapsto \mathbb{R}^{K \times 1}$ defined on the VUL power vector $\mathbf{q} \triangleq [q_1, q_2, \dots, q_K]^T$ is called a SIF if it satisfies the following properties [36, Definition 1], where the inequalities between vectors are element-wise inequalities:*

- (P1) *Positivity:* $\mathbf{g}(\mathbf{q}) > \mathbf{0}$ (the all-zeros vector).
- (P2) *Monotonicity:* if $\mathbf{q}^{(1)} \geq \mathbf{q}^{(2)}$, then $\mathbf{g}(\mathbf{q}^{(1)}) \geq \mathbf{g}(\mathbf{q}^{(2)})$.
- (P3) *Scalability:* for all $\alpha > 1$, $\alpha \mathbf{g}(\mathbf{q}) > \mathbf{g}(\alpha \mathbf{q})$.

We next show that the function $\mathbf{f}(\mathbf{q}^{(n-1)})$ defined in Eq. (4.26a), which is used in the proposed power iteration procedure in (4.25), represents a SIF.

Lemma 4.1 (SIF). *The vector interference function $\mathbf{f}(\mathbf{q}^{(n-1)})$ defined in (4.26a) and used in the power iteration procedure of (4.25) represents a SIF.*

Proof 4.1 (Sketch of the Proof). *It can directly be verified that the function $f_{k,l}(\mathbf{q}^{(n-1)})$ defined in (4.26c) satisfies (P1) – (P3) of Definition 4.1 and thus it is a SIF, $\forall l \in \mathcal{L}_k$. According*

to [36, Theorem 5], the function $f_k(\mathbf{q}^{(n)})$ defined in (4.26b) is also a SIF, $\forall k \in \mathcal{K}$. As a result, the vector interference function $\mathbf{f}(\mathbf{q}^{(n-1)})$ defined in (4.26a) represents a SIF.

Since the vector interference function $\mathbf{f}(\mathbf{q}^{(n)})$ used in the power iteration process in (4.25) represents a SIF, the following two propositions can readily be established. The proofs of the propositions can be found in the reference [36].

Proposition 4.2 (Monotonicity). *The sequence of the VUL power vectors $\{\mathbf{q}^{(n)}\}$ generated by the proposed Alg. 4.1 (when it is initialized with the all-zeros vector) is element-wisely non-decreasing [36, Lemma 2].*

Proposition 4.3 (Feasible Case). *If the VUL problem in (4.16) is feasible, then the following results hold [36, Theorem 2]:*

(i) *The SIF $\mathbf{f}(\mathbf{q}^{(n-1)})$ defined in (4.26a) has a unique fixed point [36], which is the unique optimal VUL power vector $\tilde{\mathbf{q}}$, i.e.,*

$$\tilde{\mathbf{q}} = \mathbf{f}(\tilde{\mathbf{q}}). \quad (4.29)$$

(ii) *From any non-negative starting vector, the power iteration process in (4.25) converges to the unique fixed point $\tilde{\mathbf{q}}$ as $n \rightarrow \infty$.*

(iii) *The proposed power iteration method in Alg. 4.1 yields the optimal beamformer matrix $\tilde{\mathbf{U}}$ (not necessarily unique), and the unique optimal power vectors $\tilde{\mathbf{q}}$ and $\tilde{\mathbf{p}}$ (within the prescribed numerical accuracy ϵ) as $n \rightarrow \infty$.*

Proposition 4.2 further implies the following conclusions.

Corollary 4.1 (Infeasible Case). *If the SCBF problem (4.4) is infeasible (but all the necessary conditions in Eq. (4.24) are satisfied), there exists an iteration number $\check{n} \geq 1$ such that $\mathbf{1}^T \mathbf{q}^{(\check{n})} > P^{(\text{MAX})}$. In other words, the proposed customized power iteration method in Alg. 4.1 yields the infeasibility certificates when the SCBF problem (4.4) is infeasible.*

We know from *Proposition 4.3* and *Corollary 4.1* that the proposed customized power iteration method in Alg. 4.1 yields either optimal (within the prescribed numerical accuracy) solutions of the SCBF problem (4.4) (when it is feasible) or the infeasibility certificates (when it is infeasible). That is, the proposed Alg. 4.1 optimally solves the SCBF problem (4.4). Note that in contrast to the standard BnC method [67–69, 81, 82], the proposed Alg. 4.1 represents a low-complexity optimal algorithm for the combinatorial SCBF problem (4.4) and it can easily be implemented in practice (see, e.g., [25, 36]).

4.4 Channel predistortion for performance improvement

4.4.1 The CBCP problem formulation

The codebook-based multiuser downlink beamforming naturally admits performance degradation in terms of, e.g., increased transmitted BS power required for guaranteeing the SINR targets of the admitted MSs [7, 8, 14, 20–22], as compared to non-codebook-based multiuser downlink beamforming [12]. To improve the performance of codebook-based downlink beamforming, e.g., to reduce the transmitted power of the BS, we propose in this section an adaptive channel predistortion scheme. The proposed channel predistortion procedure applies a common linear transformation of the downlink channel vectors $\{\mathbf{h}_k^H, \forall k \in \mathcal{K}\}$ using *one common* channel predistortion matrix $\mathbf{G} \in \mathbb{C}^{M \times M}$. With the linear channel predistortion, we define the *predistorted* channel vector $\check{\mathbf{h}}_k^H \in \mathbb{C}^{1 \times M}$ as

$$\check{\mathbf{h}}_k^H \triangleq \mathbf{h}_k^H \mathbf{G}, \forall k \in \mathcal{K} \quad (4.30)$$

where \mathbf{h}_k^H represents the original downlink channel vector of the k th MS (cf. Section 4.2), $\forall k \in \mathcal{K}$.

Following the expression of the downlink received SINR of the k th MS, i.e., $\text{SINR}_k^{(\text{DL})}$, given in (4.3), with channel predistortion the downlink received SINR at the k th MS, denoted by $\text{SINR}_k^{(\text{CP})}$, can be expressed as

$$\text{SINR}_k^{(\text{CP})} \triangleq \frac{p_k |\mathbf{u}_k^H \check{\mathbf{h}}_k|^2}{\sum_{j=1, j \neq k}^K p_j |\mathbf{u}_j^H \check{\mathbf{h}}_k|^2 + \sigma_k^2} = \frac{p_k |\mathbf{u}_k^H \mathbf{G}^H \mathbf{h}_k|^2}{\sum_{j=1, j \neq k}^K p_j |\mathbf{u}_j^H \mathbf{G}^H \mathbf{h}_k|^2 + \sigma_k^2}, \forall k \in \mathcal{K}. \quad (4.31)$$

It is important to note that the channel predistortion procedure can be embedded in the transmitter chains of the cell-specific reference signals and user payload data. Instead of transmitting $\sum_{j=1}^K \mathbf{u}_j^H \sqrt{p_j} x_j$, the BS transmits $\sum_{j=1}^K \mathbf{u}_j^H \mathbf{G}^H \sqrt{p_j} x_j$ when the channel predistortion scheme is applied, as illustrated in Fig. 4.1. The k th MS directly estimates the *predistorted* channel vector $\check{\mathbf{h}}_k^H$ with the help of *cell-specific reference signals* that are transmitted by the BS, e.g., in every downlink subframe in LTE systems [7, 8]. The k th MS then uses the predistorted channel vector $\check{\mathbf{h}}_k^H$ for coherent data symbols detection. As a result, the proposed predistortion mechanism does *not* introduce additional signalling overhead or modifications of the mobile receivers.

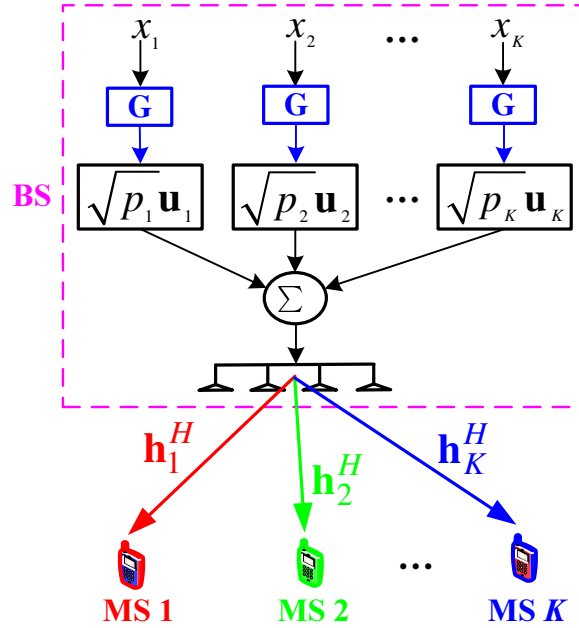


Figure 4.1: Illustration of embedding the channel predistortion procedure in the transmitter chains, e.g., the k th MS sees the effective composite channel $\mathbf{h}_k^H \mathbf{G} \mathbf{u}_k$.

To ensure that the channel estimation procedure carried out at the k th MS, which is designed for the original channel process $\{\mathbf{h}_k^H(\tau)\}$, is not adversely affected and can be equivalently performed on the predistorted channel process $\{\check{\mathbf{h}}_k^H(\tau)\}$, we impose the following smoothness-constraints on the predistorted channel vectors:

$$\|\mathbf{G}^H(\tau)\mathbf{h}_k(\tau) - \mathbf{h}_k(\tau)\|_2 \leq \delta_k(\tau), \forall k \in \mathcal{K} \quad (4.32)$$

where $\delta_k(\tau)$ denotes a small constant at the τ th ($\tau \geq 1$) time-slot. Note that we omit the time-slot index τ for succinctness of presentation when it is clear from the context.

Eq. (4.32) further implies that

$$\begin{aligned} \|\check{\mathbf{h}}_k(\tau) - \check{\mathbf{h}}_k(\tau - 1)\|_2 &= \|\mathbf{G}^H(\tau)\mathbf{h}_k(\tau) - \mathbf{G}^H(\tau - 1)\mathbf{h}_k(\tau - 1)\|_2 \\ &= \|\mathbf{G}^H(\tau)\mathbf{h}_k(\tau) - \mathbf{h}_k(\tau) + \mathbf{h}_k(\tau) - \mathbf{h}_k(\tau - 1) + \mathbf{h}_k(\tau - 1) - \\ &\quad \mathbf{G}^H(\tau - 1)\mathbf{h}_k(\tau - 1)\|_2 \\ &\leq \delta_k(\tau) + \zeta_k(\tau) + \delta_k(\tau - 1), \forall k \in \mathcal{K}. \end{aligned} \quad (4.33)$$

with the constant $\zeta_k(\tau) \triangleq \|\mathbf{h}_k(\tau) - \mathbf{h}_k(\tau - 1)\|_2, \forall k \in \mathcal{K}$. Eq. (4.33) suggests that the norm of the change of the predistorted channel process $\{\check{\mathbf{h}}_k^H(\tau)\}$ in two consecutive time-slots is bounded and the parameter $\delta_k(\tau)$ can be configured so that the k th MS can successfully estimate the predistorted channel process $\{\check{\mathbf{h}}_k^H(\tau)\}, \forall k \in \mathcal{K}$.

We know from Eqs. (4.32) and (4.33) that the smoothness-constraints defined in (4.32) not only limit the deviation of the predistorted channel vector $\check{\mathbf{h}}_k^H(\tau)$ from the original channel vector $\mathbf{h}_k^H(\tau)$, but also restrict the changes of the predistorted channel process $\{\check{\mathbf{h}}_k^H(\tau)\}$ in two consecutive time-slots, $\forall k \in \mathcal{K}$.

When applying channel predistortion, i.e., when the BS transmits $\sum_{j=1}^K \mathbf{u}_j^H \mathbf{G}^H \sqrt{p_j} x_j$, the actual transmission power allocated to the k th MS, denoted by \check{p}_k , is given by

$$\check{p}_k = \mathbb{E} \left\{ \left\| \mathbf{G} \mathbf{u}_k \sqrt{p_k} x_k \right\|_2^2 \right\} = p_k \left\| \mathbf{G} \mathbf{u}_k \right\|_2^2 = \sum_{k=1}^K \sum_{l=1}^L \phi_{k,l} \left\| \mathbf{G} \mathbf{v}_l \right\|_2^2, \forall k \in \mathcal{K} \quad (4.34)$$

where we have used the constraints in (4.8) and (4.10) to obtain the last equality in Eq. (4.34). Correspondingly, to take into account the channel predistortion procedure, the constraints in (4.6) and (4.7) shall be reformulated, respectively, as

$$\sum_{k=1}^K \check{p}_k = \sum_{k=1}^K \sum_{l=1}^L \phi_{k,l} \left\| \mathbf{G} \mathbf{v}_l \right\|_2^2 \leq P^{(\text{MAX})} \quad (4.35)$$

$$0 \leq \phi_{k,l} \left\| \mathbf{G} \mathbf{v}_l \right\|_2^2 \leq a_{k,l} P^{(\text{MAX})}, \forall k \in \mathcal{K}, \forall l \in \mathcal{L} \quad (4.36)$$

where Eq. 4.35 represents the per-BS sum-power constraint. Eq. (4.36) implements the celebrated big-M method [67–69] to ensure that $\phi_{k,l} \left\| \mathbf{G} \mathbf{v}_l \right\|_2^2 = 0$ and $\phi_{k,l} = 0$, when $a_{k,l} = 0$. Furthermore, Eq. (4.36) is automatically satisfied when $a_{k,l} = 1$ due to Eq. (4.35). Eqs. (4.8), (4.10), and (4.36) together further imply that

$$p_j \left| \mathbf{u}_j^H \mathbf{G}^H \mathbf{h}_k \right|^2 = \sum_{l=1}^L \phi_{j,l} \left| \mathbf{v}_l^H \mathbf{G}^H \mathbf{h}_k \right|^2, \forall j, k \in \mathcal{K}. \quad (4.37)$$

Substituting Eq. (4.37) into Eq. (4.31), we obtain that

$$\text{SINR}_k^{(\text{CP})} = \frac{\sum_{m=1}^L \phi_{k,m} \left| \mathbf{v}_m^H \mathbf{G}^H \mathbf{h}_k \right|^2}{\sum_{j=1, j \neq k}^K \sum_{l=1}^L \phi_{j,l} \left| \mathbf{v}_l^H \mathbf{G}^H \mathbf{h}_k \right|^2 + \sigma_k^2}, \forall k \in \mathcal{K}. \quad (4.38)$$

To improve the performance (e.g., to reduce the total transmitted BS power) of the standard codebook-based downlink beamforming, i.e., the SCBF problem in (4.15), we incorporate the channel predistortion procedure in the SCBF problem and consider the joint optimization of codebook-based beamforming and channel predistortion (CBCP). Specifically,

based on the SCBF problem (4.15), the CBCP problem can be formulated as

$$\Phi^{(\text{CBCP})} \triangleq \min_{\{a_{k,l}, \phi_{k,l}, \mathbf{G}\}} \sum_{k=1}^K \sum_{l=1}^L \phi_{k,l} \|\mathbf{G}\mathbf{v}_l\|_2^2 \quad (4.39a)$$

$$\text{s.t. (4.8): } \sum_{l=1}^L a_{k,l} = 1, \forall k \in \mathcal{K}$$

$$(4.15d): a_{k,l} = 0, \forall k \in \mathcal{K}, \forall l \in \mathcal{L} \setminus \mathcal{L}_k$$

$$(4.32): \|\mathbf{G}^H \mathbf{h}_k - \mathbf{h}_k\|_2 \leq \delta_k, \forall k \in \mathcal{K}$$

$$(4.35): \sum_{k=1}^K \sum_{l=1}^L \phi_{k,l} \|\mathbf{G}\mathbf{v}_l\|_2^2 \leq P^{(\text{MAX})}$$

$$(4.36): 0 \leq \phi_{k,l} \|\mathbf{G}\mathbf{v}_l\|_2^2 \leq a_{k,l} P^{(\text{MAX})}, \forall k \in \mathcal{K}, \forall l \in \mathcal{L}$$

$$\text{SINR}_k^{(\text{CP})} = \frac{\sum_{m=1}^L \phi_{k,m} |\mathbf{v}_m^H \mathbf{G}^H \mathbf{h}_k|^2}{\sum_{j=1, j \neq k}^K \sum_{l=1}^L \phi_{j,l} |\mathbf{v}_l^H \mathbf{G}^H \mathbf{h}_k|^2 + \sigma_k^2} \geq \Gamma_k^{(\text{MIN})}, \forall k \in \mathcal{K} \quad (4.39b)$$

$$a_{k,l} \in \{0, 1\}, \forall k \in \mathcal{K}, \forall l \in \mathcal{L}. \quad (4.39c)$$

We remark that it can straightforwardly be shown that when the number of admitted MSs is less than the number of transmit antennas at the BS and the smoothness constraints in (4.32) are not presented, i.e., when $K \leq M$ and $\delta_k \rightarrow +\infty, \forall k \in \mathcal{K}$, the CBCP problem (4.39) reduces to the conventional non-codebook-based multiuser downlink beamforming problem [12, 13, 18, 28]. In this case, the proposed channel predistortion scheme improves the performance of codebook-based downlink beamforming to be the same as that of non-codebook-based downlink beamforming.

It is further observed that the CBCP problem in (4.39) is reduced to the SCBF problem (4.15) when setting $\mathbf{G} = \mathbf{I}$ (the identity matrix). Hence, the total transmitted BS power achieved in the CBCP problem (4.39) is no larger than that of the SCBF problem (4.15) (when the SCBF problem (4.15) is feasible), i.e., it always holds that

$$\Phi^{(\text{CBCP})} \leq \Phi^{(\text{SCBF})}. \quad (4.40)$$

Due to the constraints in (4.35), (4.36), (4.38), and the integer constraints in (4.39c), the CBCP problem (4.39) represents a non-convex MIP, which remains a non-convex program even after relaxing the integer constraints (4.39c) and it can not be efficiently solved to global optimality [67–69].

However, we observe that when the channel predistortion matrix \mathbf{G} is fixed, e.g., when setting $\mathbf{G} = \mathbf{I}$, the CBCP problem (4.39) reduces to a MILP that has the same structure

as the SCBF problem (4.15) and it can be efficiently solved using the proposed customized power iteration method in Alg 4.1. In addition, when the precoding vector assignments $\{a_{k,l}, \forall k \in \mathcal{K}, \forall l \in \mathcal{L}\}$ are fixed, the CBCP problem (4.39) reduces to a difference-of-convex (DC) program [54, 60, 127] that can be closely approximated by a convex SOCP [126] and the SOCP approximation can be efficiently solved using, e.g., the interior-point method [34, 105]. This observation motivates us to consider the alternating optimization (AO) based approach, as elaborated in detail in the next two subsections.

4.4.2 The alternating optimization algorithm

We propose in this subsection an alternating optimization algorithm (ATOA) to solve approximately the CBCP problem (4.39). In each alternation of the ATOA, one MILP and one SOCP are solved, where the MILP can be efficiently solved using the proposed customized power iteration method in Alg. 4.1.

We first consider optimizing the precoding vector assignments and the transmission power allocations under a *fixed* channel predistortion matrix. Denote $\mathbf{G}^{(n-1)}$ as the channel predistortion matrix used to initialize the n th ($n \geq 1$) alternation stage, e.g., choosing $\mathbf{G}^{(0)} = \mathbf{I}$ in the first alternation stage. With $\mathbf{G} = \mathbf{G}^{(n-1)}$, The constraints in (4.35) and (4.36), and the SINR constraints in (4.39b) can be rewritten, respectively, as

$$\sum_{k=1}^K \sum_{l=1}^L \phi_{k,l} \|\mathbf{G}^{(n-1)} \mathbf{v}_l\|_2^2 \leq P^{(\text{MAX})} \quad (4.41)$$

$$0 \leq \phi_{k,l} \|\mathbf{G}^{(n-1)} \mathbf{v}_l\|_2^2 \leq a_{k,l} P^{(\text{MAX})}, \forall k \in \mathcal{K}, \forall l \in \mathcal{L} \quad (4.42)$$

$$\left(\sum_{j=1, j \neq k}^K \sum_{l=1}^L \phi_{j,l} |\mathbf{h}_k^H \mathbf{G}^{(n-1)} \mathbf{v}_l|^2 + \sigma_k^2 \right) \bar{\gamma}_k \leq \sum_{m=1}^L \phi_{k,m} |\mathbf{h}_k^H \mathbf{G}^{(n-1)} \mathbf{v}_m|^2, \forall k \in \mathcal{K} \quad (4.43)$$

where the constant $\bar{\gamma}_k$ is defined as

$$\bar{\gamma}_k \triangleq 1/\Gamma_k^{(\text{MIN})}, \forall k \in \mathcal{K}. \quad (4.44)$$

With the fixed channel predistortion matrix $\mathbf{G}^{(n-1)}$, the constraints in (4.41) – (4.43) become linear constraints in the variables $\{a_{k,l}, \phi_{k,l}, \forall k \in \mathcal{K}, \forall l \in \mathcal{L}\}$ and therefore the

CBCP problem (4.39) reduces to the following MILP:

$$\{a_{k,l}^{(n)}, \phi_{k,l}^{(n)}\} \triangleq \underset{\{b_{k,l}, \phi_{k,l}\}}{\operatorname{argmin}} \sum_{k=1}^K \sum_{l=1}^L \phi_{k,l} \|\mathbf{G}^{(n-1)} \mathbf{v}_l\|_2^2 \quad (4.45a)$$

$$(4.8): \sum_{l=1}^L a_{k,l} = 1, \forall k \in \mathcal{K}$$

$$(4.39c): a_{k,l} \in \{0, 1\}, \forall k \in \mathcal{K}, \forall l \in \mathcal{L}$$

$$(4.41): \sum_{k=1}^K \sum_{l=1}^L \phi_{k,l} \|\mathbf{G}^{(n-1)} \mathbf{v}_l\|_2^2 \leq P^{(\text{MAX})}$$

$$(4.42): 0 \leq \phi_{k,l} \|\mathbf{G}^{(n-1)} \mathbf{v}_l\|_2^2 \leq a_{k,l} P^{(\text{MAX})}, \forall k \in \mathcal{K}, \forall l \in \mathcal{L}$$

$$(4.43): \left(\sum_{j=1, j \neq k}^K \sum_{l=1}^L \phi_{j,l} |\mathbf{h}_k^H \mathbf{G}^{(n-1)} \mathbf{v}_l|^2 + \sigma_k^2 \right) \bar{\gamma}_k \leq \sum_{m=1}^L \phi_{k,m} |\mathbf{h}_k^H \mathbf{G}^{(n-1)} \mathbf{v}_m|^2, \forall k \in \mathcal{K}.$$

We further define the virtual precoding vector $\check{\mathbf{v}}_l$, the virtual precoding vector codebook $\check{\mathcal{B}}$, and the virtual beamformer $\check{\mathbf{u}}_k$, respectively, as

$$\check{\mathbf{v}}_l \triangleq \begin{cases} \frac{\mathbf{G}^{(n-1)} \mathbf{v}_l}{\|\mathbf{G}^{(n-1)} \mathbf{v}_l\|_2}, & \text{if } \|\mathbf{G}^{(n-1)} \mathbf{v}_l\|_2 > 0 \\ 0, & \text{otherwise} \end{cases}, \forall l \in \mathcal{L} \quad (4.46)$$

$$\check{\mathcal{B}} \triangleq \{\check{\mathbf{v}}_1, \check{\mathbf{v}}_2, \dots, \check{\mathbf{v}}_L\} \quad (4.47)$$

$$\check{\mathbf{u}}_k \triangleq \begin{cases} \frac{\mathbf{G}^{(n-1)} \mathbf{u}_k}{\|\mathbf{G}^{(n-1)} \mathbf{u}_k\|_2}, & \text{if } \|\mathbf{G}^{(n-1)} \mathbf{u}_k\|_2 > 0 \\ 0, & \text{otherwise} \end{cases}, \forall k \in \mathcal{K}. \quad (4.48)$$

With the channel predistortion matrix $\mathbf{G}^{(n-1)}$ and the newly defined vector $\check{\mathbf{u}}_k$, the term $\text{SINR}_k^{(\text{CP})}$ defined in (4.31) can be rewritten as

$$\text{SINR}_k^{(\text{CP})} = \frac{\check{p}_k |\check{\mathbf{u}}_k^H \mathbf{h}_k|^2}{\sum_{j=1, j \neq k}^K \check{p}_j |\check{\mathbf{u}}_j^H \mathbf{h}_k|^2 + \sigma_k^2}, \forall k \in \mathcal{K}. \quad (4.49)$$

The reduced MILP (4.45) can then be equivalently reformulated as

$$\left\{ \check{\mathbf{u}}_k^{(n)}, \check{p}_k^{(n)} \right\} \triangleq \min_{\{\check{\mathbf{u}}_k, \check{p}_k\}} \sum_{k=1}^K \check{p}_k \quad (4.50a)$$

$$\text{s.t. } \check{\mathbf{u}}_k \in \check{\mathcal{B}}, \forall k \in \mathcal{K} \quad (4.50b)$$

$$\check{p}_k \geq 0, \forall k \in \mathcal{K} \quad (4.50c)$$

$$\sum_{k=1}^K \check{p}_k \leq P^{(\text{MAX})} \quad (4.50d)$$

$$\text{SINR}_k^{(\text{CP})} = \frac{\check{p}_k |\check{\mathbf{u}}_k^H \bar{\mathbf{h}}_k|^2}{\sum_{j=1, j \neq k}^K \check{p}_j |\check{\mathbf{u}}_j^H \bar{\mathbf{h}}_k|^2 + 1} \geq \Gamma_k^{(\text{MIN})}, \forall k \in \mathcal{K}. \quad (4.50e)$$

Problem (4.50) has exactly the same structure as the SCBF problem in (4.4). Therefore, problem (4.50) and hence the reduced MILP in (4.45) can be solved to global optimality using the proposed power iteration method in Alg. 4.1. From an optimal solution of problem (4.50), e.g., $\left\{ \check{\mathbf{u}}_k^{(n)}, \check{p}_k^{(n)}, \forall k \in \mathcal{K} \right\}$, an optimal solution of problem (4.45) can directly be computed according to

$$a_{k,l}^{(n)} = \begin{cases} 1, & \text{if } \check{\mathbf{u}}_k^{(n)} = \check{\mathbf{v}}_l \\ 0, & \text{otherwise} \end{cases}, \forall k \in \mathcal{K}, \forall l \in \mathcal{L} \quad (4.51)$$

$$\phi_{k,l}^{(n)} = \begin{cases} \frac{\check{p}_k}{\|\mathbf{G}^{(n-1)} \check{\mathbf{u}}_k^{(n)}\|_2^2}, & \text{if } a_{k,l}^{(n)} = 1 \\ 0, & \text{otherwise} \end{cases}, \forall k \in \mathcal{K}, \forall l \in \mathcal{L}. \quad (4.52)$$

We next consider optimizing the predistortion matrix and the transmission power allocations under *fixed* precoding vector assignments. In the n th alternation stage, for fixed precoding vector assignments, i.e., for the given integers $\{a_{k,l}^{(n)}, \forall k \in \mathcal{K}, \forall l \in \mathcal{L}\}$, we define the auxiliary optimization vector $\mathbf{g}_k \in \mathbb{C}^{M \times 1}$ as

$$\mathbf{g}_k \triangleq \sum_{l=1}^L a_{k,l}^{(n)} \mathbf{G} \mathbf{v}_l, \forall k \in \mathcal{K} \quad (4.53)$$

which is linear in the channel predistortion matrix \mathbf{G} . We further define the auxiliary optimization variable $d_k > 0$ as

$$d_k \triangleq 1 / \sum_{l=1}^L \phi_{k,l}, \forall k \in \mathcal{K}. \quad (4.54)$$

Eqs. (4.8), (4.36), and (4.38) together suggest that *one and only one* of the variables in the set $\{\phi_{k,l}, \forall l \in \mathcal{L}\}$ is non-zero for the k th MS. As a result, with Eqs. (4.53) and (4.54), the per-BS sum-power constraint in (4.35) and the SINR constraints in (4.38) can be rewritten, respectively, as

$$\sum_{k=1}^K \sum_{l=1}^L \phi_{k,l} \|\mathbf{G}\mathbf{v}_l\|_2^2 = \sum_{k=1}^K \frac{\|\mathbf{g}_k\|_2^2}{d_k} \leq P^{(\text{MAX})} \quad (4.55)$$

$$\left(\sum_{j=1, j \neq k}^K \frac{|\mathbf{h}_k^H \mathbf{g}_j|^2}{d_j} + \sigma_k^2 \right) \bar{\gamma}_k \leq \frac{|\mathbf{h}_k^H \mathbf{g}_k|^2}{d_k}, \forall k \in \mathcal{K}. \quad (4.56)$$

Since the quadratic-over-linear function $|\mathbf{h}_k^H \mathbf{g}_j|^2/d_j$ is jointly convex in the variables d_j and \mathbf{g}_j , $\forall j, k \in \mathcal{K}$ [34], the SINR constraints in (4.56) represent DC constraints [54, 60, 127]. A common approach to deal with such DC constraints as that of (4.56) is to linearize the right-hand-side (RHS) of Eq. (4.56), which results in strengthened SINR constraints [54, 60, 127]. Define respectively the constant variable $\check{d}_k^{(n)}$ and the constant vector $\check{\mathbf{g}}_k^{(n)}$ in the n th alternation stage as

$$\check{d}_k^{(n)} \triangleq 1 / \sum_{l=1}^L \phi_{k,l}^{(n)}, \forall k \in \mathcal{K} \quad (4.57)$$

$$\check{\mathbf{g}}_k^{(n)} \triangleq \sum_{l=1}^L a_{k,l}^{(n)} \mathbf{G}^{(n-1)} \mathbf{v}_l, \forall k \in \mathcal{K}. \quad (4.58)$$

The first-order Taylor expansion of the function $|\mathbf{h}_k^H \mathbf{g}_k|^2/d_k$, i.e., the linearization of the RHS of the SINR constraints in (4.56), at the given point $[\check{d}_k^{(n)}, (\check{\mathbf{g}}_k^{(n)})^T]^T$, which is denoted by $\xi_k(\check{d}_k^{(n)}, \check{\mathbf{g}}_k^{(n)})$, is given by [128–130]:

$$\xi_k(\check{d}_k^{(n)}, \check{\mathbf{g}}_k^{(n)}) \triangleq \frac{2\text{Re} \left\{ \mathbf{g}_k^H \mathbf{Q}_k \check{\mathbf{g}}_k^{(n)} \right\}}{\check{d}_k^{(n)}} - \frac{|\mathbf{h}_k^H \check{\mathbf{g}}_k^{(n)}|^2 d_k}{(\check{d}_k^{(n)})^2}, \forall k \in \mathcal{K} \quad (4.59)$$

where the matrix $\mathbf{Q}_k \in \mathbb{C}^{M \times M}$ is defined as

$$\mathbf{Q}_k \triangleq \mathbf{h}_k \mathbf{h}_k^H, \forall k \in \mathcal{K}. \quad (4.60)$$

Replacing the RHS of Eq. (4.56) with the linear approximation $\xi_k(\check{d}_k^{(n)}, \check{\mathbf{g}}_k^{(n)})$ given in (4.59), we obtain the following *strengthened* SINR constraints under the given precoding vector as-

signments $\{a_{k,l}^{(n)}, \forall k \in \mathcal{K}, \forall l \in \mathcal{L}\}$:

$$\left(\sum_{j=1, j \neq k}^K \frac{|\mathbf{h}_k^H \mathbf{u}_j|^2}{d_j} + \sigma_k^2 \right) \bar{\gamma}_k \leq \xi_k \left(\check{d}_k^{(n)}, \check{\mathbf{g}}_k^{(n)} \right), \forall k \in \mathcal{K}. \quad (4.61)$$

Since convex constraints involving the quadratic-over-linear functions can be implemented as second-order cone (SOC) constraints [34, 105], with the given precoding vector assignments $\{a_{k,l}^{(n)}, \forall k \in \mathcal{K}, \forall l \in \mathcal{L}\}$ and the strengthened SINR constraints in (4.61), the CBCP problem (4.39) can be approximated by the following convex SOCP:

$$\left\{ \mathbf{G}^{(n)}, d_k^{(n)}, \mathbf{g}_k^{(n)} \right\} \triangleq \underset{\{\mathbf{G}, d_k, \mathbf{g}_k\}}{\operatorname{argmin}} \sum_{k=1}^K \frac{\|\mathbf{g}_k\|_2^2}{d_k} \quad (4.62a)$$

$$(4.32): \left\| \mathbf{G}^H(\tau) \mathbf{h}_k(\tau) - \mathbf{h}_k(\tau) \right\|_2 \leq \delta_k(\tau), \forall k \in \mathcal{K}$$

$$(4.53) \mathbf{g}_k \triangleq \sum_{l=1}^L a_{k,l}^{(n)} \mathbf{G} \mathbf{v}_l, \forall k \in \mathcal{K}$$

$$(4.55): \sum_{k=1}^K \sum_{l=1}^L \phi_{k,l} \|\mathbf{G} \mathbf{v}_l\|_2^2 = \sum_{k=1}^K \frac{\|\mathbf{g}_k\|_2^2}{d_k} \leq P^{(\text{MAX})}$$

$$(4.59): \xi_k \left(\check{d}_k^{(n)}, \check{\mathbf{g}}_k^{(n)} \right) \triangleq \frac{2 \operatorname{Re} \left\{ \mathbf{g}_k^H \mathbf{Q}_k \check{\mathbf{g}}_k^{(n)} \right\}}{\check{d}_k^{(n)}} - \frac{|\mathbf{h}_k^H \check{\mathbf{g}}_k^{(n)}|^2 d_k}{\left(\check{d}_k^{(n)} \right)^2}, \forall k \in \mathcal{K}$$

$$(4.61): \left(\sum_{j=1, j \neq k}^K \frac{|\mathbf{h}_k^H \mathbf{u}_j|^2}{d_j} + \sigma_k^2 \right) \bar{\gamma}_k \leq \xi_k \left(\check{d}_k^{(n)}, \check{\mathbf{g}}_k^{(n)} \right), \forall k \in \mathcal{K}$$

$$d_k > 0, \forall k \in \mathcal{K} \quad (4.62b)$$

which can be efficiently solved using, e.g., the primal-dual interior-point method [34, 105]. Note that the transmission power allocations $\{\phi_{k,l}, \forall k \in \mathcal{K}, \forall l \in \mathcal{L}\}$ are further optimized through the auxiliary variables $\{d_k, \forall k \in \mathcal{K}\}$ in the SOCP approximation (4.62) in the n th alternation stage of the ATOA.

Since the point $\{\mathbf{G}^{(n-1)}, \check{d}_k^{(n)}, \check{\mathbf{g}}_k^{(n)}, \forall k \in \mathcal{K}\}$ is a feasible solution of the SOCP approximation (4.62), problem (4.62) is feasible as long as problem (4.45) is feasible. The proposed ATOA iterates between solving problem (4.50), which is equivalent to problem (4.45), and problem (4.62) until the reduction of the total transmitted BS power is less than the predefined numerical accuracy $\epsilon > 0$, or until the maximum number of allowable alternations $N^{(\text{MAX})}$ is reached. Since the total transmitted BS power resulted from solving problems (4.50) and (4.62) does not increase in the alternations and it is positive, the total trans-

mitted BS power computed in the alternating procedure converges and hence the proposed ATOA converges (not necessarily to optimal solutions of the CBCP problem (4.39)). The computational complexity of the proposed ATOA can easily be controlled by configuring the parameters ϵ and/or $N^{(\text{MAX})}$. The proposed ATOA is summarized in Alg. 4.2.

Init.: Specify ϵ and $N^{(\text{MAX})}$, and set the *alternation* number $n = 1$.

Step 1: Set $\mathbf{G}^{(0)} = \mathbf{I}$ and solve problem (4.50) using Alg. 4.1 to obtain the total transmitted BS power $\Phi^{(n)} \triangleq \sum_{k=1}^K \check{p}_k^{(n)}$. If problem (4.50) is feasible with $\mathbf{G}^{(0)} = \mathbf{I}$, go to "Step 4".

Step 2: Compute $\mathbf{G}^{(0)}$ with the AFSA in Alg. 4.3 presented in Section 4.4.3. If no feasible $\mathbf{G}^{(0)}$ is found by Alg. 4.3, *terminate*.

Step 3: Solve problem (4.50) with $\mathbf{G}^{(n-1)}$ to obtain the total transmitted BS power $\check{\Phi}^{(n)} \triangleq \sum_{k=1}^K \check{p}_k^{(n)}$.

Step 4: Compute $a_{k,l}^{(n)}$ and $\phi_{k,l}^{(n)}$ according to Eqs. (4.51) and (4.52), respectively, $\forall k \in \mathcal{K}, \forall l \in \mathcal{L}$.

Step 5: Solve problem (4.62) with $\{a_{k,l}^{(n)}, \phi_{k,l}^{(n)}, \forall k \in \mathcal{K}, \forall l \in \mathcal{L}\}$ to obtain the total transmitted BS power $\Phi^{(n)} \triangleq \sum_{k=1}^K \|\mathbf{g}_k^{(n)}\|_2^2 / d_k^{(n)}$.

Step 6: If $\check{\Phi}^{(n)} - \Phi^{(n)} < \epsilon$, or if $n = N^{(\text{MAX})}$, stop and return $\{a_{k,l}^{(n)}, \forall k \in \mathcal{K}, \forall l \in \mathcal{L}\}$, $\{d_k^{(n)}, \forall k \in \mathcal{K}\}$, and $\mathbf{G}^{(n)}$. Otherwise, update $n \leftarrow n + 1$ and go back to "Step 3" and repeat.

Algorithm 4.2: The proposed alternating optimization algorithm (ATOA)

In the first alternation stage of the proposed ATOA in Alg. 4.2, i.e., "Step 1" of Alg. 4.2, the simple choice of the channel predistortion matrix $\mathbf{G}^{(0)} = \mathbf{I}$ may not be feasible for problem (4.45) even if the original CBCP problem (4.39) is feasible. We develop in the next subsection an alternating feasibility search algorithm (AFSA) to compute feasible initializations of the channel predistortion matrix $\mathbf{G}^{(0)}$.

4.4.3 The alternating feasibility search algorithm

As mentioned in the previous subsection, the simple choice of $\mathbf{G}^{(0)} = \mathbf{I}$ may result in an infeasible problem (4.45) in the first alternation stage in Alg. 4.2, i.e., "Step 1" of Alg. 4.2, even if the original CBCP problem (4.39) is feasible. In this case, an alternating feasibility search algorithm (AFSA) can be applied to compute a feasible initialization $\mathbf{G}^{(0)}$, i.e., "Step 2" of Alg. 4.2. The AFSA follows a similar procedure as the ATOA Alg. 4.2. How-

ever, in the AFSA, instead of problem (4.45), the following MILP feasibility problem:

$$\left\{ a_{k,l}^{(n)}, \phi_{k,l}^{(n)}, s_k^{(n)} \right\} \triangleq \underset{\{a_{k,l}, \phi_{k,l}, s_k\}}{\operatorname{argmin}} \sum_{k=1}^K s_k \quad (4.63a)$$

$$\text{s.t. (4.8): } \sum_{l=1}^L a_{k,l} = 1, \forall k \in \mathcal{K}$$

$$(4.39c): a_{k,l} \in \{0, 1\}, \forall k \in \mathcal{K}, \forall l \in \mathcal{L}$$

$$(4.41): \sum_{k=1}^K \sum_{l=1}^L \phi_{k,l} \|\mathbf{G}^{(n-1)} \mathbf{v}_l\|_2^2 \leq P^{(\text{MAX})}$$

$$(4.42): 0 \leq \phi_{k,l} \|\mathbf{G}^{(n-1)} \mathbf{v}_l\|_2^2 \leq a_{k,l} P^{(\text{MAX})}, \forall k \in \mathcal{K}, \forall l \in \mathcal{L}$$

$$\left(\sum_{j=1, j \neq k}^K \sum_{l=1}^L \phi_{j,l} |\mathbf{h}_k^H \mathbf{G}^{(n-1)} \mathbf{v}_l|^2 + \sigma_k^2 \right) \bar{\gamma}_k \leq \sum_{m=1}^L \phi_{k,m} |\mathbf{h}_k^H \mathbf{G}^{(n-1)} \mathbf{v}_m|^2 + s_k, \forall k \in \mathcal{K} \quad (4.63b)$$

$$s_k \geq 0, \forall k \in \mathcal{K} \quad (4.63c)$$

is solved using, e.g., the BnC method [67–69, 81, 82], with $\mathbf{G}^{(0)}$ fixed to \mathbf{I} . The auxiliary optimization variables $\{s_k, \forall k \in \mathcal{K}\}$ are introduced into problem (4.63) to guarantee that problem (4.63) is always feasible. The optimal objective value $\sum_{k=1}^K s_k^{(n)}$ obtained from solving problem (4.63) represents the measure of total infeasibility [34]. If the term $\sum_{k=1}^K s_k^{(n)}$ is less than the predefined infeasibility tolerance $\beta > 0$, the point $\{\mathbf{G}^{(n-1)}, a_{k,l}^{(n)}, \phi_{k,l}^{(n)}, \forall k \in \mathcal{K}, \forall l \in \mathcal{L}\}$ is declared as a feasible solution of the original CBCP problem (4.39).

Note that since the objective of problem (4.63) is not to minimize the total transmitted BS power and problem (4.63) is always feasible due to the auxiliary optimization variables $\{s_k, \forall k \in \mathcal{K}\}$, the proposed power iteration method in Alg. 4.1 cannot be applied to solve problem (4.63). That is, we have to apply the BnC method [67–69, 81, 82] to solve problem (4.63).

Accordingly, in the AFSA, instead of problem (4.62), the following SOCP feasibility

problem:

$$\left\{ \mathbf{G}^{(n)}, d_k^{(n)}, \mathbf{g}_k^{(n)}, \check{s}_k^{(n)} \right\} \triangleq \underset{\{\mathbf{G}, d_k, \mathbf{g}_k, \check{s}_k\}}{\operatorname{argmin}} \sum_{k=1}^K \check{s}_k \quad (4.64a)$$

$$\text{s.t. (4.32): } \|\mathbf{G}^H(\tau)\mathbf{h}_k - \mathbf{h}_k\|_2 \leq \delta_k, \forall k \in \mathcal{K}$$

$$(4.53): \mathbf{g}_k \triangleq \sum_{l=1}^L a_{k,l}^{(n)} \mathbf{G}\mathbf{v}_l, \forall k \in \mathcal{K}$$

$$(4.55) \sum_{k=1}^K \sum_{l=1}^L \phi_{k,l} \|\mathbf{G}\mathbf{v}_l\|_2^2 = \sum_{k=1}^K \frac{\|\mathbf{g}_k\|_2^2}{d_k} \leq P^{(\text{MAX})}$$

$$\left(\sum_{j=1, j \neq k}^K \frac{|\mathbf{h}_k^H \mathbf{g}_j|^2}{d_j} + \sigma_k^2 \right) \bar{\gamma}_k \leq \xi_k \left(\check{d}_k^{(n)}, \check{\mathbf{g}}_k^{(n)} \right) + \check{s}_k, \forall k \in \mathcal{K} \quad (4.64b)$$

$$\check{s}_k \geq 0, \forall k \in \mathcal{K} \quad (4.64c)$$

is solved using, e.g., the interior-point method [34, 105]. If the total infeasibility measure $\sum_{k=1}^K \check{s}_k^{(n)}$ is less than β , then the point $\{\mathbf{G}^{(n)}, a_{k,l}^{(n)}, \phi_{k,l}^{(n)}, \forall k \in \mathcal{K}, \forall l \in \mathcal{L}\}$ is declared as a feasible solution of the CBCP problem (4.39). The AFSA algorithm iterates between solving problems (4.63) and (4.64) until a feasible (under the feasibility tolerance β) solution of the CBCP problem (4.39) is found, or until the reduction in the total infeasibility measure, i.e., $\sum_{k=1}^K s_k^{(n)} - \sum_{k=1}^K \check{s}_k^{(n)}$, is less than ϵ , or until the maximum number of allowable alternations $\check{N}^{(\text{MAX})}$ is reached. The proposed AFSA algorithm is summarized in Alg. 4.3.

Init.: Specify ϵ , β , and $\check{N}^{(\text{MAX})}$. Set $\mathbf{G}^{(0)} = \mathbf{I}$ and the alternation number $n = 1$.

Step 1: Solve problem (4.63). If $\sum_{k=1}^K s_k^{(n)} < \beta$, stop and return $\mathbf{G}^{(n-1)}$.

Step 2: Solve problem (4.64). If $\sum_{k=1}^K \check{s}_k^{(n)} < \beta$, stop and return $\mathbf{G}^{(n)}$.

Step 3: If $\sum_{k=1}^K s_k^{(n)} - \sum_{k=1}^K \check{s}_k^{(n)} < \epsilon$, or if $n = \check{N}^{(\text{MAX})}$, terminate. Otherwise, update $n \leftarrow n + 1$ and go back to "Step 1" and repeat.

Algorithm 4.3: The proposed alternating feasibility search algorithm (AFSA)

Similar to the proposed ATOA in Alg. 4.2, the developed AFSA in Alg. 4.3 converges. However, the proposed AFSA is not guaranteed to yield a feasible solution of the original CBCP problem (4.39) even if problem (4.39) is indeed feasible. In such cases, user admission control mechanisms may be applied to select a subset of the MSs to be served.

We remark that the proposed alternating optimization approach represents a *two-phase* (suboptimal) algorithmic solution for the CBCP problem (4.39). In the first phase, the AFSA in Alg. 4.3 is applied to compute a feasible solution of problem (4.39), which is used to initialize the ATOA in Alg. 4.2 in the second phase.

4.5 Simulation results

We simulate a downlink system with $K = 4$ MSs, and $M = 4$ antennas and the maximum transmission power $P^{(\text{MAX})} = 15$ dB at the BS. As in Chapters 2 and 3, we adopt the following channel model [106]: (i) 3GPP LTE path-loss mode: $PL = 148.1 + 37.6 \log_{10}(d)$ (in dB), with d (in kilo-meter) denoting the BS-MS distance; (ii) log-norm shadowing with zero mean, 8 dB variance; (iii) Rayleigh fading with zero mean and unit variance; and (iv) transmit antenna power gain of 9 dB, and (v) the receiver noise power $\sigma_k^2 = -143$ dB, $\forall k \in \mathcal{K}$. The distances between the BS and the MSs are randomly and uniformly generated in the interval $[0.05, 1]$ (in kilometer).

The precoding vector codebook with $L = 16$ precoding vectors defined in 3GPP LTE [7, 8, 20] is used, where the precoding vectors are normalized to have unit norm in our simulations. We choose the numerical accuracy $\epsilon = 10^{-3}$, the infeasibility tolerance $\beta = 10^{-5}$, and the maximum number of allowable alternations $N^{(\text{MAX})} = \check{N}^{(\text{MAX})} = 5$ in the simulations. For the smoothness constraints in Eq. (4.32), we choose the constant $\delta_k(\tau)$ according to

$$\delta_k(\tau) = \delta \|\mathbf{h}_k(\tau)\|_2, \forall k \in \mathcal{K} \quad (4.65)$$

with $\delta \in \{0, 0.1, 0.2, 0.3, 0.4\}$, $\forall k \in \mathcal{K}$. Note that the special case of $\delta = 0$, i.e., the special case of $\mathbf{G} = \mathbf{I}$, in the CBCP problem (4.39) corresponds to the standard codebook-based beamforming problem, i.e., the SCBF problem in (4.4). The SINR targets of the MSs are chosen to be identical and are listed in the tables and figures. The MIP solver IBM ILOG CPLEX [81] is applied on the MILPs in (4.15) and (4.63). The relative optimality tolerance (cf. Section 2.5.1) in CPLEX is set as $\eta = 0.1\%$ [69, 81]. The simulation results are averaged over 5000 Monte Carlo runs (MCRs).

4.5.1 Performance of the power iteration method

We study in this subsection the performance of the proposed power iteration method in Alg. 4.1 when applying to the SCBF problem in (4.4). Tab. 4.1 lists the total transmitted BS power vs. the SINR target $\Gamma_k^{(\text{MIN})}$, averaged over feasible MCRs. Tab. 4.1 clearly shows that the proposed power iteration method in Alg. 4.1 achieves the same total transmitted BS power as that of the optimal solutions computed by the BnC method in CPLEX, as has been analytically proved in Section 4.3.3.

Table 4.1: Total transmitted BS power [watts] vs. the SINR target $\Gamma_k^{(\text{MIN})}$

$\Gamma_k^{(\text{MIN})}$ [dB]	-6	-4	-2	0	2	4
BnC in CPLEX	0.3429	0.6636	1.4833	4.3163	7.8895	11.2708
Alg. 4.1	0.3429	0.6636	1.4833	4.3163	7.8895	11.2708

Tab. 4.2 lists the average number of proved infeasible MCRs vs. the SINR target $\Gamma_k^{(\text{MIN})}$. We see from Tab. 4.2 that the proposed Alg. 4.1 obtains the infeasibility certificates when the SCBF problem (4.4) is infeasible, as concluded in *Corollary 4.1*.

Table 4.2: Average number of proved infeasible MCRs vs. the SINR target $\Gamma_k^{(\text{MIN})}$

$\Gamma_k^{(\text{MIN})}$ [dB]	-6	-4	-2	0	2	4
BnC in CPLEX	0	1	11	467	3815	4938
Alg. 4.1	0	1	11	467	3815	4938

Tab. 4.3 displays the algorithm runtime (i.e., CPU time) vs. the SINR target $\Gamma_k^{(\text{MIN})}$, averaged over all MCRs. We observe from Tab. 4.3 that the proposed Alg. 4.1 takes much less CPU time than that of the BnC method. This certifies that the proposed Alg. 4.1 admits much less computational complexity than the BnC method in CPLEX.

Table 4.3: Average algorithm runtime [seconds] vs. the SINR target $\Gamma_k^{(\text{MIN})}$

$\Gamma_k^{(\text{MIN})}$ [dB]	-6	-4	-2	0	2	4
BnC in CPLEX	0.3586	0.3601	0.3620	0.3644	0.3725	0.3775
Alg. 4.1	0.0010	0.0012	0.0018	0.0045	0.0042	0.0012

Tab. 4.4 lists the average number of iterations of Alg. 4.1 vs. the SINR target $\Gamma_k^{(\text{MIN})}$, averaged over all MCRs. We see from Tab. 4.4 that the proposed Alg. 4.1 takes only a small number of iterations to compute the optimal solutions of the SCBF problem (4.4), or to reach the infeasibility certificates. Recall that only simple algebraic operations are performed in each iteration of the proposed customized power iteration method in Alg. 4.1.

Table 4.4: Average number of iterations of Alg. 4.1 vs. the SINR target $\Gamma_k^{(\text{MIN})}$

$\Gamma_k^{(\text{MIN})}$ [dB]	-6	-4	-2	0	2	4
No. of iterations	4.85	6.66	10.63	29.33	61.98	88.05

Tab. 4.5 shows the percentage of MCRs that Alg. 4.1 and the BnC method in CPLEX achieve the *same* optimal solutions of the SCBF problem (4.4) vs. the SINR target $\Gamma_k^{(\text{MIN})}$, averaged over feasible MCRs. Tab. 4.5 shows that it is possible that the optimal solutions of the SCBF problem (4.4) computed by Alg. 4.1 and the BnC method are different. This is because the optimal solution of the SCBF problem (4.4) is generally not unique.

Table 4.5: Percentage of MCRs that Alg. 4.1 and the BnC method achieve the same optimal solutions vs. the SINR target $\Gamma_k^{(\text{MIN})}$

$\Gamma_k^{(\text{MIN})}$ [dB]	-6	-4	-2	0	2	4
Percentage	95.22%	97.78%	99%	99.65%	100%	100%

4.5.2 Performance of the alternating optimization approach

We investigate in this subsection the performance of the proposed ATOA in Alg. 4.2 and the AFSA in Alg. 4.3 when applying to the CBCP problem in (4.39). As references, the performance of the SCBF problem (4.4), which corresponds to $\delta = 0$ and $\mathbf{G} = \mathbf{I}$ in the CBCP problem (4.39), and the performance of the conventional non-codebook-based downlink beamforming [12, 13, 25–31] are also displayed.

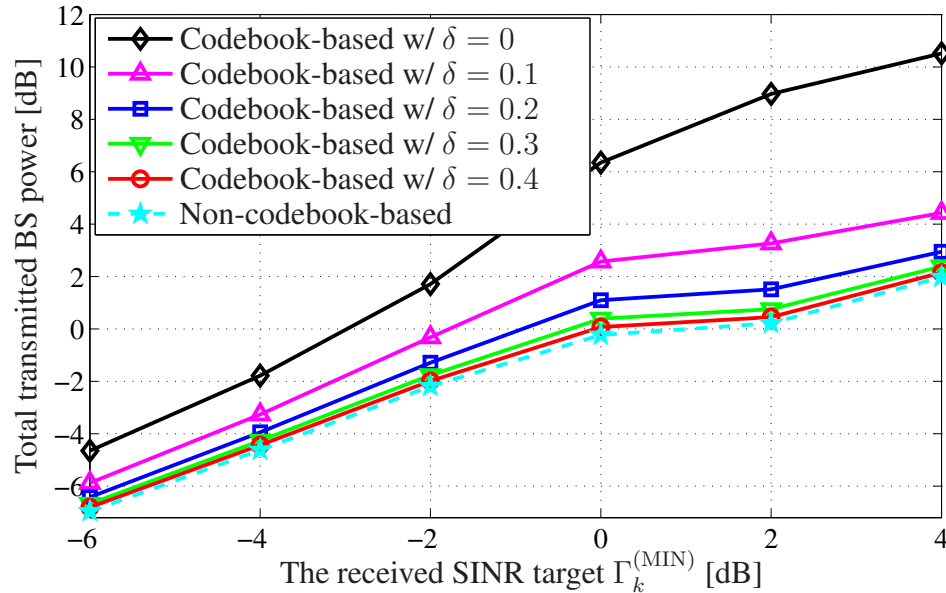


Figure 4.2: The total transmitted BS power vs. the SINR target $\Gamma_k^{(\text{MIN})}$.

Fig. 4.2 displays the total transmitted BS power vs. the SINR target $\Gamma_k^{(\text{MIN})}$. It can be observed from Fig. 4.2 that the proposed channel pre-distortion design achieves significantly reductions of the total transmitted BS power, as compared to the standard codebook-based

downlink beamforming, e.g., a reduction of 7.4 dB with $\Gamma_k^{(\text{MIN})} = 2$ dB and $\delta = 0.2$. Furthermore, the proposed design yields total transmitted BS powers that are very close to the lower bounds set by the non-codebook-based downlink beamforming.

Fig. 4.3 depicts the percentage of feasible MCRs vs. the SINR target $\Gamma_k^{(\text{MIN})}$. We observe that the percentage of feasible cases is tremendously increased with the proposed channel predistortion design, as compared to the standard codebook-based downlink beamforming, e.g., an improvement from 23.7% to 86% with $\Gamma_k^{(\text{MIN})} = 2$ dB and $\delta = 0.2$.

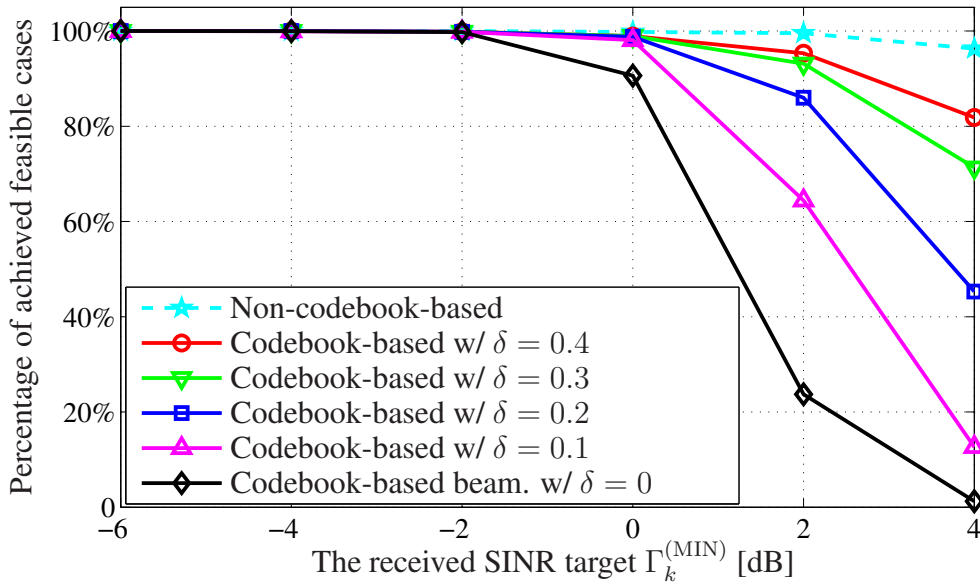


Figure 4.3: The percentage of achieved feasible cases vs. the SINR target $\Gamma_k^{(\text{MIN})}$.

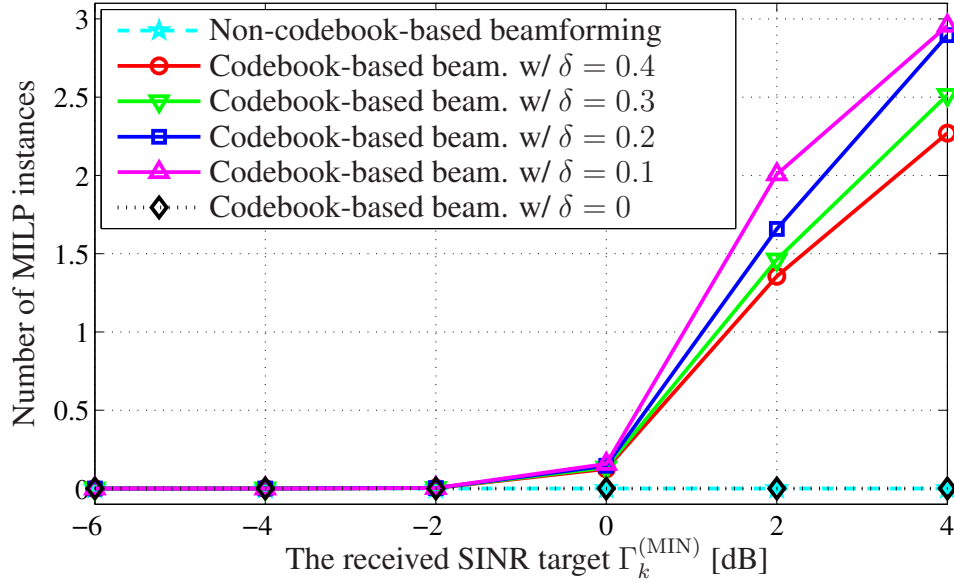


Figure 4.4: The average number of instances of the MILP (4.63) solved in the considered schemes vs. the SINR target $\Gamma_k^{(\text{MIN})}$.

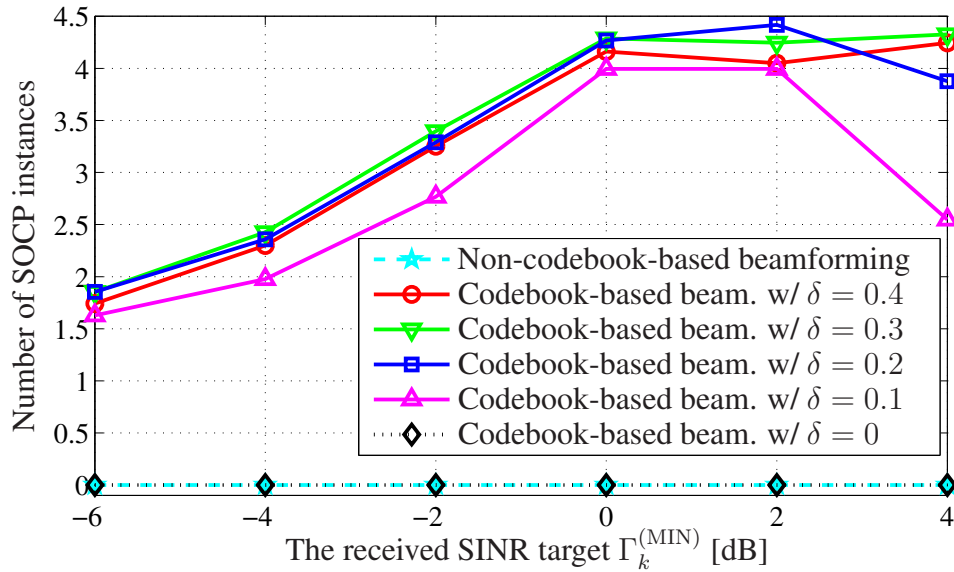


Figure 4.5: The average number of instances of the SOCP (4.64) solved in the considered schemes vs. the SINR target $\Gamma_k^{(\text{MIN})}$.

Fig. 4.4 and Fig. 4.5 display the average number of instances of the MILP in (4.63) and the average number of instances of the SOCP in (4.64) that are solved in the considered schemes, respectively. We observe from Figs. 4.4 and 4.5 that only a very small number of instances of the MILP (4.63) and the SOCP (4.64) are required to be solved in the proposed channel predistortion design. For instance, on average 1.7 instances of the MILP (4.63) and

4.4 instances of the SOCP (4.64) are solved with $\Gamma_k^{(\text{MIN})} = 2$ dB and $\delta = 0.2$, while significant performance improvement is achieved by the proposed channel predistortion mechanism (cf. Figs. 4.2 and 4.3). This shows that the proposed channel predistortion scheme is very computationally efficient for improving the performance of the standard codebook-based downlink beamforming.

4.6 Summary

In this chapter, we have considered codebook-based multiuser downlink beamforming problem. We have developed a customized power iteration method in Alg. 4.1 to solve the combinatorial standard codebook-based downlink beamforming problem in (4.4). The proposed Alg. 4.1 is built on the uplink-downlink duality between the VUL problem (4.16) and the SCBF problem (4.4) and the convenient property that the beamformer assignments in the VUL problem are nicely decoupled. It has been analytically shown that Alg. 4.1 yields either the optimal (within the desired numerical accuracy) solutions of the SCBF problem (when it is feasible), or the infeasibility certificates (when it is infeasible). To improve the performance of the standard codebook-based downlink beamforming, we have proposed an adaptive linear channel predistortion procedure that is applied on the downlink channel vectors $\{\mathbf{h}_k, \forall k \in \mathcal{K}\}$. The proposed channel predistortion scheme does not incur additional signaling overhead or modifications of the mobile receivers, and hence it can straightforwardly be incorporated into current 3G and 4G cellular standards. We developed the ATOA in Alg. 4.2 and the AFSA in Alg. 4.3 to approximately solve the joint codebook-based beamforming and channel predistortion problem in (4.39). The simulation results have shown that the proposed customized power iteration method in Alg. 4.1 is very efficient for solving the SCBF problem and have confirmed the analytic studies of Alg. 4.1. Our numerical results have also demonstrated that the proposed channel predistortion mechanism achieves significant performance improvement over the standard codebook-based downlink beamforming in terms of, e.g., significant reductions of the total transmitted BS power, and the channel predistortion matrix can be efficiently computed.

Chapter 5

Robust codebook-based downlink beamforming and admission control

5.1 Introduction

In Chapter 4, it is assumed that the instantaneous downlink channel vectors are perfectly known at the BS for optimizing codebook-based multiuser downlink beamforming and channel predistortion. The design presented in Chapter 4 is mainly applicable in time-division duplex (TDD) systems with slow-fading channels, in which the BS can track the downlink channel vectors by exploiting the reciprocity of downlink and uplink channels [7]. In this chapter, we consider codebook-based multiuser downlink beamforming in the scenarios, e.g., in frequency-division duplex (FDD) systems and/or in TDD systems with fast-fading channels, where only estimated (and hence erroneous) channel covariance matrix (CCM) information is available at the BS. As in Chapters 2 and 4, we adopt here the standard SINR-constrained approach (see, e.g., [12, 13, 18, 25–33]).

To achieve robustness against the CCM estimation errors in guaranteeing the SINR requirements of the admitted mobile stations (MSs), the worst-case robust design is employed (see, e.g., [12, 37–42, 131–135]). In this dissertation, robustness refers to the property of the downlink beamformer design that the minimum SINR requirements of the admitted MSs are guaranteed to be satisfied regardless of the quality of the channel state information (CSI) that is known at the base station (BS). Hence, in our robust design, the SINR targets of the admitted MSs are guaranteed even if only erroneous CSI is available at the BS. That is, robustness against erroneous CSI.

Similar to the conventional and the worst-case robust multiuser downlink beamforming problems [12, 13, 18, 24–33, 37–42, 131–134], the robust codebook-based multiuser downlink

beamforming problem can easily become infeasible when the number of admitted MSs is large and/or the prescribed SINR targets of the admitted MSs are high. To ensure a feasible design and to exploit multiuser diversity [19], we consider in this chapter robust codebook-based downlink beamforming jointly with user admission control. Similar to the work on joint non-codebook-based downlink beamforming and admission control [83, 109–112], in the robust codebook-based downlink beamforming and admission control (RCBA) problem, we intend to attain the maximum number of concurrently supported MSs with the minimum total transmitted BS power under the prescribed SINR requirements of the admissible MSs and the per-BS sum-power constraint. The work of this chapter can be seen as an extension of the prior contributions presented in [12, 37, 38], i.e., extending the existing works of [12, 37, 38] to incorporate joint robust codebook-based downlink beamforming and user admission control.

As we have seen in Chapter 4, precoding vector assignments and transmission power allocations of multiple MSs are coupled in the downlink SINR constraints. In addition, the worst-case SINR constraints involve (inner) optimization procedures. As a result, the RCBA problem naturally leads to a non-convex bi-level mixed-integer program (BL-MIP) [60, 136], with the *inner* optimization problems appearing in the worst-case SINR constraints. The BL-MIP formulation cannot be efficiently solved to global optimality due to the inner optimization steps and the integer optimization variables [60, 136]. We first adopt the conservative approach as presented in [12, 37] to cope with the *inner* optimization steps in the worst-case SINR constraints. That is, we first propose conservative approximations of the worst-case SINR constraints, which gives rise to the *strengthened* worst-case SINR constraints, and develop a MILP approximation of the RCBA problem. While the MILP approximation can be efficiently solved using, e.g., the BnC method, it results in unnecessarily increased total transmitted BS power required to ensure the SINR targets of the admitted MSs due to the conservative approximations (see, e.g., [12, 37, 38], and Section 5.7).

To achieve a more power-efficient design, we reformulate the RCBA problem into an equivalent mixed-integer second-order cone program (MISOCP) [82], which can be solved using, e.g. the BnC method [67–69]. Similar to the work of [38], the exact MISOCP reformulation of the RCBA problem is developed through transforming the inner optimization problems in the worst-case SINR constraints into independent convex semidefinite programs (SDPs) and applying the strong Lagrange duality theory [34] to the resulting inner SDPs. As discussed in Chapters 2 and 3, to reduce the computational complexity of the BnC method when applying it to the MILP approximation and the exact MISOCP reformulation of the RCBA problem, we introduce several customizing techniques to adapt the solution process of the standard BnC method implemented in the MIP solver IBM ILOG CPLEX [81]. The

customizing strategies are derived from the properties of the RCBA problem and mainly include adding problem-specific cuts and employing customized node selection rules and branching priorities [81].

Since the computational complexity associated with the standard BnC method for solving the exact MISOCP reformulation may not be practically affordable in large-scale networks, we develop a low-complexity second-order cone programming (SOCP) based inflation procedure (i.e., a greedy algorithm) [83,84] to compute the near-optimal solutions of the RCBA problem. Different from the inflation procedures presented in Chapters 2 and 3, we invoke a sub-enumeration procedure (see Alg. 5.1) and solve a sequence of SOCPs to determine which one of the non-admitted MSs is the best candidate to admit in each iteration of the inflation procedure. The best candidate MS in each iteration is the one that results in the largest increase in the system utility if it is admitted. The inflation procedure proposed in this chapter represents a greedy algorithm.

The simulations results show that the MILP based approach, the MISOCP based approach, and the inflation procedure yield almost the same average number of admitted MSs. However, the MILP based approach requires much more total transmitted BS power to guarantee the SINR targets of the admitted MSs than that of the MISOCP based approach and the inflation procedure. The numerical results also demonstrate that the inflation procedure has much less computational complexity than the MILP based approach and the MISOCP based approach when the number of admissible MSs is large. While the MISOCP based approach achieves the largest system utility on average, it also admits the highest computational complexity among the three methods.

This chapter is based on my original work that has been published in [124,125,137], and the MILP based approach is added and new simulation results are presented in this chapter.

5.2 System model and problem statement

As in Chapters 3 and 4, in this chapter we focus on the downlink of a cellular network with one BS equipped with M transmit antennas, and K single-antenna MSs. The K MSs are admissible under the prescribed minimum received SINR targets (representing QoS requirements [23]). As in Chapter 4, we denote $\mathbf{h}_k^H \in \mathbb{C}^{1 \times M}$, $\mathbf{u}_k \in \mathbb{C}^{M \times 1}$, and $p_k > 0$ as the frequency-flat channel vector, the unit-norm precoding vector, and the allocated transmission power, respectively, of the k th MS, $\forall k \in \mathcal{K} \triangleq \{1, 2, \dots, K\}$. The received signal

$y_k \in \mathbb{C}$ at the k th MS can then be written as (see, e.g., [12, 13, 18, 28])

$$y_k = \mathbf{h}_k^H \mathbf{u}_k \sqrt{p_k} x_k + \sum_{j=1, j \neq k}^K \mathbf{h}_k^H \mathbf{u}_j \sqrt{p_j} x_j + z_k, \forall k \in \mathcal{K} \quad (5.1)$$

where $x_k \in \mathbb{C}$ denotes the normalized data symbol, i.e., $\mathbb{E}\{|x_k|^2\} = 1$, intended to the k th MS, and $z_k \in \mathbb{C}$ stands for the additive circularly-symmetric white Gaussian noise [19] at the k th MS, with zero mean and variance σ_k^2 , $\forall k \in \mathcal{K}$. Note that the signal model in (5.1) is identical to that given in Eq. (4.1) of Chapter 4. However, different from Chapter 4, it is assumed in this chapter that the downlink channel vectors $\{\mathbf{h}_k, \forall k \in \mathcal{K}\}$ are *not* known at the BS. That is, we assume in this chapter that the downlink channel vectors $\{\mathbf{h}_k^H, \forall k \in \mathcal{K}\}$ are random vectors.

As in Chapter 4 (cf. Eq. (4.2)), we consider in this chapter the codebook-based multiuser downlink beamforming. That is, the normalized precoding vector \mathbf{u}_k is assigned from the predefined precoding vector codebook \mathcal{B} consisting of $L > 1$ fixed precoding vectors, i.e.,

$$\mathbf{u}_k \in \mathcal{B} \triangleq \{\mathbf{v}_1, \mathbf{v}_2, \dots, \mathbf{v}_L\}, \forall k \in \mathcal{K} \quad (5.2)$$

where the precoding vector $\mathbf{v}_l \in \mathbb{C}^{M \times 1}$ and $\|\mathbf{v}_l\|_2 = 1$, $\forall l \in \mathcal{L} \triangleq \{1, 2, \dots, L\}$. Assume that the data symbols of the MSs are mutually independent and independent from the noise. With single-user detection at the receivers, the *average* received SINR at the k th MS, denoted by SINR_k , can then be expressed as (see, e.g., [12, 37–42])

$$\text{SINR}_k \triangleq \frac{p_k \mathbf{u}_k^H \mathbf{R}_k \mathbf{u}_k}{\sum_{j=1, j \neq k}^K p_j \mathbf{u}_j^H \mathbf{R}_k \mathbf{u}_j + \sigma_k^2}, \forall k \in \mathcal{K} \quad (5.3)$$

where the matrix $\mathbf{R}_k \triangleq \mathbb{E}\{\mathbf{h}_k \mathbf{h}_k^H\} \in \mathbb{C}^{M \times M}$ represents the *true* CCM of the k th MS, $\forall k \in \mathcal{K}$. Note that the term SINR_k defined in (5.3) represents the average received SINR at the k th MS, while the expression SINR_k given in Eq. (4.3) of Chapter 4 refers to the instantaneous received SINR at the k th MS [12].

Similar to Chapter 4, to model the precoding vector assignment procedure, we introduce the *binary* integer variable $a_{k,l} \in \{0, 1\}$ to indicate with $a_{k,l} = 1$ that the l th precoding vector $\mathbf{v}_l \in \mathcal{B}$ is assigned to the k th MS, and $a_{k,l} = 0$ otherwise. Accordingly, we introduce the continuous variable $\phi_{k,l} \geq 0$ to model the transmission power allocated to the l th precoding vector $\mathbf{v}_l \in \mathcal{B}$ for the k th MS, $\forall k \in \mathcal{K}, \forall l \in \mathcal{L}$. Since at most one precoding vector may be assigned to a MS in codebook-based downlink beamforming (also known as single-layer-

per-user precoding [7]), we impose the following constraints in the RCBA problem:

$$\sum_{k=1}^K \sum_{l=1}^L \phi_{k,l} \leq P^{(\text{MAX})} \quad (5.4)$$

$$0 \leq \phi_{k,l} \leq a_{k,l} P^{(\text{MAX})}, \forall k \in \mathcal{K}, \forall l \in \mathcal{L} \quad (5.5)$$

$$\sum_{l=1}^L a_{k,l} \leq 1, \forall k \in \mathcal{K} \quad (5.6)$$

where Eq. (5.4) represents the per-BS sum-power constraint, with the constant $P^{(\text{MAX})} > 0$ denoting the maximum transmission power of the BS. Eq. (5.5) implements the so-called big-M method [67,68] to ensure that $\phi_{k,l} = 0$ when $a_{k,l} = 0$. Furthermore, due to the per-BS sum-power constraint in (5.4), Eq. (5.5) is automatically satisfied when $a_{k,l} = 1$. Note that for the precoding vector selection constraints, i.e., the multiple-choice constraints in (5.6), if $\sum_{l=1}^L a_{k,l} = 0$, i.e., if no precoding vector is assigned to the k th MS, the k th MS is not admitted in the current time-slot. Hence, with the multiple-choice constraints in (5.6), user admission control is naturally embedded in the precoding vector assignment procedure.

As in Chapter 4 (cf. Eqs. (4.9) and (4.10)), under the constraints in Eqs. (5.5) and (5.6), we can express the transmission power p_k and the beamformer \mathbf{u}_k of the k th MS, respectively, as

$$p_k = \sum_{l=1}^L a_{k,l} \phi_{k,l} = \sum_{l=1}^L \phi_{k,l}, \forall k \in \mathcal{K} \quad (5.7)$$

$$\mathbf{u}_k = \sum_{l=1}^L a_{k,l} \mathbf{v}_l, \forall k \in \mathcal{K}. \quad (5.8)$$

Eqs. (5.7) and (5.8) together further imply that

$$(\sqrt{p_j} \mathbf{u}_j)^H \mathbf{R}_k (\sqrt{p_j} \mathbf{u}_j) = \sum_{l=1}^L \phi_{j,l} \mathbf{v}_l^H \mathbf{R}_k \mathbf{v}_l = \sum_{l=1}^L \phi_{j,l} \text{Tr}\{\mathbf{R}_k \mathbf{V}_l\}, \forall j, k \in \mathcal{K} \quad (5.9)$$

where the constant matrix $\mathbf{V}_l \in \mathbb{C}^{M \times M}$ is defined as

$$\mathbf{V}_l \triangleq \mathbf{v}_l \mathbf{v}_l^H \succeq \mathbf{0}, \forall l \in \mathcal{L}. \quad (5.10)$$

Making use of Eq. (5.9), the term SINR_k defined in Eq. (5.3) can be rewritten as

$$\text{SINR}_k = \frac{\sum_{m=1}^L \phi_{k,m} \text{Tr}\{\mathbf{R}_k \mathbf{V}_m\}}{\sum_{j=1, j \neq k}^K \sum_{l=1}^L \phi_{j,l} \text{Tr}\{\mathbf{R}_k \mathbf{V}_l\} + \sigma_k^2}, \forall k \in \mathcal{K}. \quad (5.11)$$

Due to limited channel training resources, channel variations, channel estimation errors, and channel feedback errors and delay, the *true* CCM \mathbf{R}_k is usually not available at the BS, e.g., in FDD systems [7, 19]. In this case, only the *estimated* CCM of the k th MS, denoted by $\widehat{\mathbf{R}}_k \in \mathbb{C}^{M \times M}$, is known to the BS [12, 37–40]. In practical systems, the estimated CCM $\widehat{\mathbf{R}}_k$ is generally different from the true CCM \mathbf{R}_k . Following the approach presented in [12, 37–40], we model in this chapter the estimated (erroneous) CCM $\widehat{\mathbf{R}}_k$ as

$$\widehat{\mathbf{R}}_k = \mathbf{R}_k + \mathbf{\Delta}_k, \forall k \in \mathcal{K} \quad (5.12)$$

where the matrix $\mathbf{\Delta}_k \in \mathbb{C}^{M \times M}$ denotes the estimation errors in the estimated CCM $\widehat{\mathbf{R}}_k$, i.e., the matrix $\mathbf{\Delta}_k$ represents the mismatch matrix. We know from practical considerations that the matrices \mathbf{R}_k and $\widehat{\mathbf{R}}_k$ are positive semidefinite, i.e., $\mathbf{R}_k \succeq \mathbf{0}$ and $\widehat{\mathbf{R}}_k \succeq \mathbf{0}$, and the mismatch matrix $\mathbf{\Delta}_k$ is Hermitian, i.e., $\mathbf{\Delta}_k = \mathbf{\Delta}_k^H$. Further, it is commonly assumed in the literature that the Frobenius norm of the mismatch matrix $\mathbf{\Delta}_k$ is upper-bounded by a known constant $\delta_k \geq 0$ (see, e.g., [12, 37, 38]), i.e.,

$$\|\mathbf{\Delta}_k\|_F \leq \delta_k, \forall k \in \mathcal{K}. \quad (5.13)$$

In this chapter, we consider the problem of precoding vector assignment and power allocation for the K MSs to maximize the system utility function $f(\{a_{k,l}\}, \{\phi_{k,l}\})$, which is defined as

$$f(\{a_{k,l}\}, \{\phi_{k,l}\}) \triangleq \sum_{k=1}^K \sum_{l=1}^L a_{k,l} - \rho \sum_{k=1}^K \sum_{l=1}^L \phi_{k,l} \quad (5.14)$$

where the constant weighting factor $\rho > 0$ is adopted to guarantee that maximizing the system utility function $f(\{a_{k,l}\}, \{\phi_{k,l}\})$ will result in the maximum number of admitted MSs (i.e., the term $\sum_{k=1}^K \sum_{l=1}^L a_{k,l}$) with the minimum total transmitted BS power (i.e., the term $\sum_{k=1}^K \sum_{l=1}^L \phi_{k,l}$) [83, 110, 111]. As in Chapter 3, taking into account the per-BS sum-power constraint in (5.4), we can simply choose the weighting factor ρ as $\rho = 1 / (1 + P^{(\text{MAX})})$ [83, 110, 111].

Similarly as in the conventional QoS-constrained designs [12, 13, 18, 24–33, 37–42, 131–133], if the k th MS is admitted, i.e., if $\sum_{l=1}^L a_{k,l} = 1$, then the average received SINR of the

k th MS must exceed or equal to a prescribed threshold $\Gamma_k^{(\text{MIN})}$ to guarantee the QoS that the k th MS is subscribed to. To achieve robustness against the CCM estimation errors $\{\Delta_k, \forall k \in \mathcal{K}\}$, we adopt here the worst-case robust design approach (see, e.g., [12, 37, 38, 131–134]). Specifically, we define in this chapter the following worst-case SINR constraints for the K admissible MSs:

$$\begin{aligned} \min_{\Delta_k \in \mathcal{E}_k} \text{SINR}_k &= \min_{\Delta_k \in \mathcal{E}_k} \frac{\sum_{m=1}^L \phi_{k,m} \text{Tr}\{(\widehat{\mathbf{R}}_k - \Delta_k) \mathbf{V}_m\}}{\sum_{j=1, j \neq k}^K \sum_{l=1}^L \phi_{j,l} \text{Tr}\{(\widehat{\mathbf{R}}_k - \Delta_k) \mathbf{V}_l\} + \sigma_k^2} \\ &\geq \Gamma_k^{(\text{MIN})} \sum_{l=1}^L a_{k,l}, \forall k \in \mathcal{K} \end{aligned} \quad (5.15)$$

where the estimation error set \mathcal{E}_k is defined as

$$\mathcal{E}_k \triangleq \left\{ \Delta_k \mid \mathbf{R}_k = \widehat{\mathbf{R}}_k - \Delta_k \succeq 0, \text{ and } \|\Delta_k\|_F^2 \leq \delta_k^2 \right\}, \forall k \in \mathcal{K}. \quad (5.16)$$

Note that the CCM estimation error sets $\{\mathcal{E}_k, \forall k \in \mathcal{K}\}$ defined in (5.16) are mutually independent among the K admissible MSs.

With the system utility function $f(\{a_{k,l}\}, \{\phi_{k,l}\})$ defined in (5.14) and the worst-case SINR constraints defined in Eqs. (5.15) and (5.16), the robust joint codebook-based downlink beamforming and admission control (RCBA) problem can be stated as

$$\Phi^{(\text{RCBA})} \triangleq \max_{\{a_{k,l}, \phi_{k,l}\}} f(\{a_{k,l}\}, \{\phi_{k,l}\}) \quad (5.17a)$$

$$\text{s.t. (5.4): } \sum_{k=1}^K \sum_{l=1}^L \phi_{k,l} \leq P^{(\text{MAX})}$$

$$(5.5): 0 \leq \phi_{k,l} \leq a_{k,l} P^{(\text{MAX})}, \forall k \in \mathcal{K}, \forall l \in \mathcal{L}$$

$$(5.6): \sum_{l=1}^L a_{k,l} \leq 1, \forall k \in \mathcal{K}$$

$$(5.15) \min_{\Delta_k \in \mathcal{E}_k} \frac{\sum_{m=1}^L \phi_{k,m} \text{Tr}\{(\widehat{\mathbf{R}}_k - \Delta_k) \mathbf{V}_m\}}{\sum_{j=1, j \neq k}^K \sum_{l=1}^L \phi_{j,l} \text{Tr}\{(\widehat{\mathbf{R}}_k - \Delta_k) \mathbf{V}_l\} + \sigma_k^2} \geq \Gamma_k^{(\text{MIN})} \sum_{l=1}^L a_{k,l}, \forall k \in \mathcal{K}$$

$$(5.16): \mathcal{E}_k \triangleq \left\{ \Delta_k \mid \mathbf{R}_k = \widehat{\mathbf{R}}_k - \Delta_k \succeq 0, \text{ and } \|\Delta_k\|_F^2 \leq \delta_k^2 \right\}, \forall k \in \mathcal{K}$$

$$a_{k,l} \in \{0, 1\}, \forall k \in \mathcal{K}, \forall l \in \mathcal{L}. \quad (5.17b)$$

The RCBA problem (5.17) contains the *inner* optimization problems in the worst-case SINR constraints in (5.15) and the *outer* optimization problem (5.17). As a result, the RCBA problem formulation in (5.17) represents a BL-MIP [60, 136], which is generally

intractable due to the inner optimization step in Eq. (5.15) and the integer constraints in Eq. (5.17b) [60, 136]. To facilitate the development of efficient algorithmic solutions, we derive a MILP approximation in next section and an exactly equivalent MISOCP reformulation in Section 5.4 of the RCBA problem in (5.17), respectively.

5.3 The conservative MILP approximation

We develop in this section a MILP approximation of the RCBA problem in the BL-MIP form of (5.17). We observe that for any arbitrary values of the variables $a_{k,l} \in \{0, 1\}$, $\phi_{k,l} \geq 0$, $\forall k \in \mathcal{K}, \forall l \in \mathcal{L}$, it always holds that:

$$\begin{aligned}
& \min_{\Delta_k \in \mathcal{E}_k} \frac{\sum_{m=1}^L \phi_{k,m} \text{Tr}\{(\widehat{\mathbf{R}}_k - \Delta_k) \mathbf{V}_m\}}{\sum_{j=1, j \neq k}^K \sum_{l=1}^L \phi_{j,l} \text{Tr}\{(\widehat{\mathbf{R}}_k - \Delta_k) \mathbf{V}_l\} + \sigma_k^2} \\
& \geq \frac{\min_{\Delta_k \in \mathcal{E}_k} \sum_{m=1}^L \phi_{k,m} \text{Tr}\{(\widehat{\mathbf{R}}_k - \Delta_k) \mathbf{V}_m\}}{\max_{\Delta_k \in \mathcal{E}_k} \sum_{j=1, j \neq k}^K \sum_{l=1}^L \phi_{j,l} \text{Tr}\{(\widehat{\mathbf{R}}_k - \Delta_k) \mathbf{V}_l\} + \sigma_k^2} \\
& \geq \frac{\min_{\|\Delta_k\|_F \leq \delta_k} \sum_{m=1}^L \phi_{k,m} \text{Tr}\{(\widehat{\mathbf{R}}_k - \Delta_k) \mathbf{V}_m\}}{\max_{\|\Delta_k\|_F \leq \delta_k} \sum_{j=1, j \neq k}^K \sum_{l=1}^L \phi_{j,l} \text{Tr}\{(\widehat{\mathbf{R}}_k - \Delta_k) \mathbf{V}_l\} + \sigma_k^2}, \forall k \in \mathcal{K} \quad (5.18)
\end{aligned}$$

where the CCM estimation error set \mathcal{E}_k is defined in (5.16). Based on the properties stated in Eq. (5.18), we follow a similar approach as that of [12, 37] and employ the following conservative approximations of the worst-case SINR constraints defined in Eq. (5.15):

$$\frac{\min_{\|\Delta_k\|_F \leq \delta_k} \sum_{m=1}^L \phi_{k,m} \text{Tr}\{(\widehat{\mathbf{R}}_k - \Delta_k) \mathbf{V}_m\}}{\max_{\|\Delta_k\|_F \leq \delta_k} \sum_{j=1, j \neq k}^K \sum_{l=1}^L \phi_{j,l} \text{Tr}\{(\widehat{\mathbf{R}}_k - \Delta_k) \mathbf{V}_l\} + \sigma_k^2} \geq \Gamma_k^{(\text{MIN})} \sum_{l=1}^L a_{k,l}, \forall k \in \mathcal{K}. \quad (5.19)$$

Due to Eq. (5.18), the constraints in (5.19) represent the *strengthened* worst-case SINR constraints. That is, if the k th constraint defined in (5.19) is satisfied with $\sum_{l=1}^L a_{k,l} = 1$, then the corresponding k th constraint defined in (5.15) is also satisfied with $\sum_{l=1}^L a_{k,l} = 1$.

Note that in order to obtain closed-form expressions for the conservative approximations of the worst-case SINR constraints in (5.19), we have used the constraint that $\|\Delta_k\|_F \leq \delta_k$, instead of the constraint that $\Delta_k \in \mathcal{E}_k$ in (5.19). Specifically, considering the constraints in Eqs. (5.5) and (5.6), i.e., taking into account the fact that at most one of the variables in the set $\{\phi_{k,l}, \forall l \in \mathcal{L}\}$ is non-zero, $\forall k \in \mathcal{K}$, it holds in the numerator of the left-hand-side (LHS)

of Eq. (5.19) that

$$\min_{\|\Delta_k\|_F \leq \delta_k} \sum_{m=1}^L \phi_{k,m} \text{Tr}\{(\widehat{\mathbf{R}}_k - \Delta_k) \mathbf{V}_m\} = \sum_{m=1}^L \phi_{k,m} \left(\text{Tr}\{\widehat{\mathbf{R}}_k \mathbf{V}_m\} - \delta_k \right), \forall k \in \mathcal{K} \quad (5.20)$$

where we have chosen the minimizer $\widetilde{\Delta}_k = \delta_k \mathbf{I}$ in the LHS of Eq. (5.20). Similarly, it holds in the denominator of the LHS of Eq. (5.19) that

$$\max_{\|\Delta_k\|_F \leq \delta_k} \sum_{j=1, j \neq k}^K \sum_{l=1}^L \phi_{j,l} \text{Tr}\{(\widehat{\mathbf{R}}_k - \Delta_k) \mathbf{V}_l\} = \sum_{j=1, j \neq k}^K \sum_{l=1}^L \phi_{j,l} \left(\text{Tr}\{\widehat{\mathbf{R}}_k \mathbf{V}_l\} + \delta_k \right), \forall k \in \mathcal{K} \quad (5.21)$$

where we have chosen the maximizer $\widetilde{\Delta}_k = -\delta_k \mathbf{I}$ in the LHS of Eq. (5.21).

Substituting Eqs. (5.20) and (5.21) back into the strengthened worst-case SINR constraints in (5.19), we obtain the following closed-form expressions of the strengthened worst-case SINR constraints in (5.19):

$$\frac{\sum_{m=1}^L \phi_{k,m} \left(\text{Tr}\{\widehat{\mathbf{R}}_k \mathbf{V}_m\} - \delta_k \right)}{\sum_{j=1, j \neq k}^K \sum_{l=1}^L \phi_{j,l} \left(\text{Tr}\{\widehat{\mathbf{R}}_k \mathbf{V}_l\} + \delta_k \right) + \sigma_k^2} \geq \Gamma_k^{(\text{MIN})} \sum_{l=1}^L a_{k,l}, \forall k \in \mathcal{K}. \quad (5.22)$$

We remark that the strengthened worst-case SINR constraints in (5.22) represent the well-known diagonal-loading solution for robust downlink beamforming [12, 37, 38].

The strengthened worst-case SINR constraints in (5.22) can further be equivalently rewritten as

$$\begin{aligned} & \sum_{m=1}^L \phi_{k,m} \left(\text{Tr}\{\widehat{\mathbf{R}}_k \mathbf{V}_m\} - \delta_k \right) \\ & \geq \left(\sum_{j=1, j \neq k}^K \sum_{l=1}^L \phi_{j,l} \left(\text{Tr}\{\widehat{\mathbf{R}}_k \mathbf{V}_l\} + \delta_k \right) + \sigma_k^2 \right) \Gamma_k^{(\text{MIN})} \sum_{l=1}^L a_{k,l}, \forall k \in \mathcal{K}. \end{aligned} \quad (5.23)$$

Due to the bi-linear terms involving the variables $\{\phi_{k,l}, \forall k \in \mathcal{K}, \forall l \in \mathcal{L}\}$ and $\{a_{k,l}, \forall k \in \mathcal{K}, \forall l \in \mathcal{L}\}$ in Eq. (5.23), the strengthened worst-case SINR constraints in (5.23) remain non-convex constraints even when the integer variables $\{a_{k,l}, \forall k \in \mathcal{K}, \forall l \in \mathcal{L}\}$ are relaxed to be continuous variables taking values in the closed interval $[0, 1]$. To derive more tractable equivalent reformulations of the SINR constraints in (5.23), we adopt here the well-known big-M method [67–69] to reformulate the strengthened worst-case SINR constraints

in (5.23). We define the constants $U_k > 0$ and $\bar{\gamma}_k > 0$, respectively, as

$$U_k \triangleq P^{(\text{MAX})} \left(\max_{l \in \mathcal{L}} \text{Tr}\{\widehat{\mathbf{R}}_k \mathbf{V}_l\} + \delta_k \right) + \sigma_k^2, \forall k \in \mathcal{K} \quad (5.24)$$

$$\bar{\gamma}_k = 1/\Gamma_k^{(\text{MIN})}, \forall k \in \mathcal{K}. \quad (5.25)$$

Taking into account the per-BS sum-power constraint (5.4), the constant U_k satisfies that

$$U_k \geq \sum_{j=1, j \neq k}^K \sum_{l=1}^L \phi_{j,l} (\text{Tr}\{\widehat{\mathbf{R}}_k \mathbf{V}_l\} + \delta_k) + \sigma_k^2, \forall k \in \mathcal{K}. \quad (5.26)$$

With the constants U_k and $\bar{\gamma}_k$, the strengthened worst-case SINR constraints in (5.23) can be equivalently rewritten as

$$\begin{aligned} & \bar{\gamma}_k \sum_{m=1}^L \phi_{k,m} \left(\text{Tr}\{\widehat{\mathbf{R}}_k \mathbf{V}_m\} - \delta_k \right) + \left(1 - \sum_{l=1}^L a_{k,l} \right) U_k \\ & \geq \sum_{j=1, j \neq k}^K \sum_{l=1}^L \phi_{j,l} \left(\text{Tr}\{\widehat{\mathbf{R}}_k \mathbf{V}_l\} + \delta_k \right) + \sigma_k^2, \forall k \in \mathcal{K}. \end{aligned} \quad (5.27)$$

The constraints in (5.27) are equivalent to that of (5.23). This follows because when $\sum_{l=1}^L a_{k,l} = 1$, the k th constraint in (5.27) is identical to that of the k th constraint in (5.23). Moreover, when $\sum_{l=1}^L a_{k,l} = 0$, the k th constraint in (5.27) is automatically satisfied due to the big-M constant U_k and Eq. (5.26). The k th constraint in (5.23) is also automatically satisfied when $\sum_{l=1}^L a_{k,l} = 0$. As a result, the constraints in (5.27) are equivalent to the strengthened worst-case SINR constraints in (5.23).

Replacing the worst-case SINR constraints in (5.15) with the derived closed-form conservative approximations in (5.27), we obtain the following MILP approximation of the RCBA

problem in (5.17):

$$\begin{aligned}
\Phi^{(\text{MILP})} &\triangleq \min_{\{a_{k,l}, \phi_{k,l}\}} f(\{a_{k,l}\}, \{\phi_{k,l}\}) & (5.28a) \\
\text{s.t. (5.4): } &\sum_{k=1}^K \sum_{l=1}^L \phi_{k,l} \leq P^{(\text{MAX})} \\
(5.5): &0 \leq \phi_{k,l} \leq a_{k,l} P^{(\text{MAX})}, \forall k \in \mathcal{K}, \forall l \in \mathcal{L} \\
(5.6): &\sum_{l=1}^L a_{k,l} \leq 1, \forall k \in \mathcal{K} \\
(5.17b): &a_{k,l} \in \{0, 1\}, \forall k \in \mathcal{K}, \forall l \in \mathcal{L} \\
(5.27): &\bar{\gamma}_k \sum_{m=1}^L \phi_{k,m} \left(\text{Tr}\{\widehat{\mathbf{R}}_k \mathbf{V}_m\} - \delta_k \right) + \left(1 - \sum_{l=1}^L a_{k,l} \right) U_k \\
&\geq \sum_{j=1, j \neq k}^K \sum_{l=1}^L \phi_{j,l} \left(\text{Tr}\{\widehat{\mathbf{R}}_k \mathbf{V}_l\} + \delta_k \right) + \sigma_k^2, \forall k \in \mathcal{K}
\end{aligned}$$

which can be efficiently solved using, e.g., the standard BnC method [67–69, 81, 82] that is implemented in the MIP solver IBM ILOG CPLEX [81].

We remark that due to the conservative approximations employed in (5.22), the MILP based approach (5.28) requires more total transmitted BS power to guarantee the SINR requirements of the admitted MSs (see, e.g., Section 5.7), which has also been reported in the robust non-codebook-based multiuser downlink beamforming problem [38].

5.4 The equivalent MISOCP reformulation

The main difficulties of the RCBA problem in the form of the BL-MIP in (5.17) stem from the inner optimization problems in the worst-case SINR constraints in (5.15) and the integer constraints in (5.17b). Different from the conservative approximations (5.22) proposed in the previous section, we derive here more tractable *equivalent* reformulations of the worst-case SINR constraints in (5.15) and develop an exact MISOCP reformulation of the RCBA problem (5.17). We observe that the following SINR constraints:

$$\text{SINR}_k \geq \Gamma_k^{(\text{MIN})} \sum_{l=1}^L a_{k,l}, \forall k \in \mathcal{K} \quad (5.29)$$

with the term $\text{SINR}_k^{(\text{DL})}$ given in Eq. (5.11), are equivalent to the following constraints:

$$\begin{aligned} & \bar{\gamma}_k \sum_{m=1}^L \phi_{k,m} \text{Tr}\{(\widehat{\mathbf{R}}_k - \mathbf{\Delta}_k) \mathbf{V}_m\} + \left(1 - \sum_{l=1}^L a_{k,l}\right) U_k \\ & \geq \sum_{j=1, j \neq k}^K \sum_{l=1}^L \phi_{j,l} \text{Tr}\{(\widehat{\mathbf{R}}_k - \mathbf{\Delta}_k) \mathbf{V}_l\} + \sigma_k^2, \forall k \in \mathcal{K}. \end{aligned} \quad (5.30)$$

The constraints in Eq. (5.30) can further be rewritten as

$$\text{Tr}\{(\widehat{\mathbf{R}}_k - \mathbf{\Delta}_k) \mathbf{A}_k\} \geq \sigma_k^2 + \left(\sum_{l=1}^L a_{k,l} - 1\right) U_k, \forall k \in \mathcal{K}. \quad (5.31)$$

where the auxiliary optimization matrix $\mathbf{A}_k \in \mathbb{C}^{M \times M}$ is defined as

$$\mathbf{A}_k \triangleq \bar{\gamma}_k \sum_{m=1}^L \phi_{k,m} \mathbf{V}_m - \sum_{j=1, j \neq k}^K \sum_{l=1}^L \phi_{j,l} \mathbf{V}_l, \forall k \in \mathcal{K}. \quad (5.32)$$

Considering the equivalence of the constraints in Eqs. (5.29) and (5.31), the worst-case SINR constraints defined in (5.15) can be equivalently rewritten as

$$\left(\min_{\mathbf{\Delta}_k \in \mathcal{E}_k} \text{Tr}\{(\widehat{\mathbf{R}}_k - \mathbf{\Delta}_k) \mathbf{A}_k\}\right) \geq \sigma_k^2 + \left(\sum_{l=1}^L a_{k,l} - 1\right) U_k, \forall k \in \mathcal{K}. \quad (5.33)$$

Following a similar approach as that presented in [38], for the k th MS, we treat the inner optimization problem in the LHS of the worst-case SINR constraints in (5.33) as an independent *convex* SDP, which can be written as

$$\Gamma_k^{(\text{LHS})} \triangleq \min_{\mathbf{\Delta}_k} \text{Tr}\{(\widehat{\mathbf{R}}_k - \mathbf{\Delta}_k) \mathbf{A}_k\} \quad (5.34a)$$

$$\text{s.t. } \widehat{\mathbf{R}}_k - \mathbf{\Delta}_k \succeq \mathbf{0} \quad (5.34b)$$

$$\|\mathbf{\Delta}_k\|_F^2 \leq \delta_k^2. \quad (5.34c)$$

Note that the convex SDP in (5.34) is *strictly* feasible, e.g., the point $\mathbf{\Delta}_k = -\frac{\delta_k}{2} \mathbf{I}$ is a strictly feasible solution of problem (5.34). As a result, we can apply the strong Lagrange duality theory [34] to the SDP in (5.34) and focus on the associated dual problem [34, 38]. The Lagrangian function $\mathcal{L}_k(\mathbf{\Delta}_k, \lambda_k, \mathbf{Z}_k)$ associated with the convex SDP in (5.34) can be

written as [34, 38]

$$\mathcal{L}_k(\Delta_k, \lambda_k, \mathbf{Z}_k) \triangleq \text{Tr}\{(\widehat{\mathbf{R}}_k - \Delta_k)\mathbf{A}_k\} + \lambda_k(\|\Delta_k\|_F^2 - \varepsilon_k^2) - \text{Tr}\{(\widehat{\mathbf{R}}_k - \Delta_k)\mathbf{Z}_k\} \quad (5.35)$$

where the matrix $\mathbf{Z}_k \succeq \mathbf{0}$ and the variable $\lambda_k \geq 0$ represent the Lagrange multipliers associated with the constraints in (5.34b) and (5.34c), respectively. The dual function $\mathcal{D}_k(\lambda_k, \mathbf{Z}_k)$ associated with the convex SDP in (5.34) can be expressed as [34]

$$\mathcal{D}_k(\lambda_k, \mathbf{Z}_k) \triangleq \min_{\Delta_k} \mathcal{L}_k(\Delta_k, \lambda_k, \mathbf{Z}_k). \quad (5.36)$$

Due to the constraints in (5.34c), the optimal objective function value of the convex SDP in (5.34) is *bounded*. Further, the dual function $\mathcal{D}_k(\lambda_k, \mathbf{Z}_k)$ defined in Eq. (5.36) is *unbounded* if $\lambda_k = 0$. As a result, according to the strong Lagrange duality theory [34], it must hold that $\lambda_k > 0$ so that the dual function $\mathcal{D}_k(\lambda_k, \mathbf{Z}_k)$ is also bounded. To solve the unconstrained minimization problem in the right-hand-side (RHS) of Eq. (5.36), we set the partial derivative of the Lagrangian function $\mathcal{L}_k(\Delta_k, \lambda_k, \mathbf{Z}_k)$ with respect to (w.r.t.) the mismatch matrix Δ_k to the all-zeros matrix, i.e., we set

$$\frac{\partial \mathcal{L}_k(\Delta_k, \lambda_k, \mathbf{Z}_k)}{\partial \Delta_k} = -\mathbf{A}_k + 2\lambda_k \Delta_k + \mathbf{Z}_k = \mathbf{0}. \quad (5.37)$$

We then obtain from solving Eq. (5.37) the minimizer [34, 38]

$$\widetilde{\Delta}_k = \frac{\mathbf{A}_k - \mathbf{Z}_k}{2\lambda_k} \quad (5.38)$$

of the minimization problem in the RHS of Eq. (5.36). Substituting the minimizer $\widetilde{\Delta}_k$ given in (5.38) back into the Lagrangian function $\mathcal{L}_k(\Delta_k, \lambda_k, \mathbf{Z}_k)$ in (5.35), we obtain the closed-form expression of the dual function $\mathcal{D}_k(\lambda_k, \mathbf{Z}_k)$ as [34, 38]

$$\mathcal{D}_k(\lambda_k, \mathbf{Z}_k) = \text{Tr}\{\widehat{\mathbf{R}}_k(\mathbf{A}_k - \mathbf{Z}_k) - \frac{\|\mathbf{A}_k - \mathbf{Z}_k\|_F^2}{4\lambda_k} - \lambda_k \delta_k^2\}. \quad (5.39)$$

The dual problem associated with the convex SDP in (5.34) can then be rewritten as [34, 38]

$$\Gamma_k^{(\text{LHS})} = \max_{\lambda_k > 0, \mathbf{Z}_k \succeq \mathbf{0}} \mathcal{D}_k(\lambda_k, \mathbf{Z}_k) = \max_{\mathbf{Z}_k \succeq \mathbf{0}} \max_{\lambda_k > 0} \mathcal{D}_k(\lambda_k, \mathbf{Z}_k). \quad (5.40)$$

We know from fundamental algebra that [34, 116]

$$-\frac{\|\mathbf{A}_k - \mathbf{Z}_k\|_F^2}{4\lambda_k} - \lambda_k \delta_k^2 \leq -\delta_k \|\mathbf{A}_k - \mathbf{Z}_k\|_F \quad (5.41)$$

where the equality in Eq. (5.41) is achieved if and only if $\tilde{\lambda}_k = \frac{\|\mathbf{A}_k - \mathbf{Z}_k\|_F}{2\delta_k}$. As a result, maximizing the dual function $\mathcal{D}_k(\lambda_k, \mathbf{Z}_k)$ w.r.t. the Lagrange multiplier $\lambda_k > 0$ results in the maximizer [34, 38]

$$\tilde{\lambda}_k = \frac{\|\mathbf{A}_k - \mathbf{Z}_k\|_F}{2\delta_k}. \quad (5.42)$$

Substituting the maximizer $\tilde{\lambda}_k$ back into the dual function $\mathcal{D}_k(\lambda_k, \mathbf{Z}_k)$ given in (5.39), we obtain the reduced dual problem as

$$\Gamma_k^{(\text{LHS})} = \max_{\mathbf{Z}_k \succeq \mathbf{0}} \left(\text{Tr}\{\widehat{\mathbf{R}}_k(\mathbf{A}_k - \mathbf{Z}_k)\} - \delta_k \|\mathbf{A}_k - \mathbf{Z}_k\|_F \right). \quad (5.43)$$

Making use of the equivalence between the dual problem in (5.43) and the convex SDP in (5.34), we obtain the following equivalent reformulations of the worst-case SINR constraints in (5.33):

$$\max_{\mathbf{Z}_k \succeq \mathbf{0}} \left(\text{Tr}\{\widehat{\mathbf{R}}_k(\mathbf{A}_k - \mathbf{Z}_k)\} - \delta_k \|\mathbf{A}_k - \mathbf{Z}_k\|_F \right) \geq \sigma_k^2 + \left(\sum_{l=1}^L a_{k,l} - 1 \right) U_k, \forall k \in \mathcal{K}. \quad (5.44)$$

We further observe that, for the k th MS, the worst-case SINR constraint in (5.44) is satisfied if there exists a matrix $\mathbf{Z}_k \succeq \mathbf{0}$ for which the k th constraint defined in (5.44) is satisfied. As a result, the formulated RCBA problem in (5.17) can be equivalently rewritten

as the following mixed-integer semidefinite program (MISDP):

$$\Phi^{(\text{RCBA})} = \min_{\{a_{k,l}, \phi_{k,l}, \mathbf{Z}_k\}} f(\{a_{k,l}\}, \{\phi_{k,l}\}) \quad (5.45a)$$

$$\text{s.t. (5.4): } \sum_{k=1}^K \sum_{l=1}^L \phi_{k,l} \leq P^{(\text{MAX})}$$

$$(5.5): 0 \leq \phi_{k,l} \leq a_{k,l} P^{(\text{MAX})}, \forall k \in \mathcal{K}, \forall l \in \mathcal{L}$$

$$(5.6): \sum_{l=1}^L a_{k,l} \leq 1, \forall k \in \mathcal{K}$$

$$\mathbf{Z}_k \succeq \mathbf{0}, \forall k \in \mathcal{K} \quad (5.45b)$$

$$\text{Tr}\{\widehat{\mathbf{R}}_k(\mathbf{A}_k - \mathbf{Z}_k)\} - \delta_k \|\mathbf{A}_k - \mathbf{Z}_k\|_F \geq \sigma_k^2 + \left(\sum_{l=1}^L a_{k,l} - 1 \right) U_k, \forall k \in \mathcal{K} \quad (5.45c)$$

$$a_{k,l} \in \{0, 1\}, \forall k \in \mathcal{K}, \forall l \in \mathcal{L}. \quad (5.45d)$$

We can then follow the procedure presented in [38, Appendix A] with modifications required for accommodating the integer variables to prove that, without loss of optimality of the RCBA problem in the form of (5.45), we can choose $\mathbf{Z}_k = \mathbf{0}, \forall k \in \mathcal{K}$, in problem (5.45). As a result, the MISDP formulation in (5.45) of the RCBA problem can be equivalently rewritten as the following MISOCP [38, Section IV.A]:

$$\Phi^{(\text{RCBA})} = \max_{\{a_{k,l}, \phi_{k,l}\}} f(\{a_{k,l}\}, \{\phi_{k,l}\}) \quad (5.46a)$$

$$\text{s.t. (5.4): } \sum_{k=1}^K \sum_{l=1}^L \phi_{k,l} \leq P^{(\text{MAX})}$$

$$(5.5): 0 \leq \phi_{k,l} \leq a_{k,l} P^{(\text{MAX})}, \forall k \in \mathcal{K}, \forall l \in \mathcal{L}$$

$$(5.6): \sum_{l=1}^L a_{k,l} \leq 1, \forall k \in \mathcal{K}$$

$$\text{Tr}\{\widehat{\mathbf{R}}_k \mathbf{A}_k\} - \delta_k \|\text{vec}\{\mathbf{A}_k\}\|_2 \geq \sigma_k^2 + \left(\sum_{l=1}^L a_{k,l} - 1 \right) U_k, \forall k \in \mathcal{K} \quad (5.46b)$$

$$a_{k,l} \in \{0, 1\}, \forall k \in \mathcal{K}, \forall l \in \mathcal{L} \quad (5.46c)$$

where we have used the equalities that [34]: $\mathbf{Z}_k = \mathbf{0}$ and $\|\mathbf{A}_k\|_F = \|\text{vec}\{\mathbf{A}_k\}\|_2, \forall k \in \mathcal{K}$, to obtain the worst-case SINR constraints in Eq. (5.46b).

We remark that the RCBA problem in the form of the BL-MIP (5.17) has been equivalently converted into the MISOCP formulation in (5.46), which admits convex continuous

relaxations (i.e., convex SOCPs) and can be more efficiently solved using, e.g., the convex continuous relaxation based BnC method [67–69, 81, 82]. The BnC method relies on solving the continuous relaxation (CRLX) of the RCBA problem (5.46), which is given by

$$\Phi^{(\text{CRLX})} = \min_{\{a_{k,l}, \phi_{k,l}\}} f(\{a_{k,l}\}, \{\phi_{k,l}\}) \quad (5.47a)$$

$$\text{s.t. (5.4): } \sum_{k=1}^K \sum_{l=1}^L \phi_{k,l} \leq P^{(\text{MAX})}$$

$$(5.5): 0 \leq \phi_{k,l} \leq a_{k,l} P^{(\text{MAX})}, \forall k \in \mathcal{K}, \forall l \in \mathcal{L}$$

$$(5.6): \sum_{l=1}^L a_{k,l} \leq 1, \forall k \in \mathcal{K}$$

$$(5.46b): \text{Tr}\{\widehat{\mathbf{R}}_k \mathbf{A}_k\} - \delta_k \|\text{vec}\{\mathbf{A}_k\}\|_2 \geq \sigma_k^2 + \left(\sum_{l=1}^L a_{k,l} - 1 \right) U_k, \forall k \in \mathcal{K}$$

$$0 \leq a_{k,l} \leq 1, \forall k \in \mathcal{K}, \forall l \in \mathcal{L} \quad (5.47b)$$

where the variables $\{a_{k,l}, \forall k \in \mathcal{K}, \forall l \in \mathcal{L}\}$ originally constrained in the discrete set $\{0, 1\}$ as in (5.46c) are relaxed to be continuous variables that take values in the closed interval $[0, 1]$ as given in Eq. (5.47b).

Recall that the auxiliary matrix \mathbf{A}_k defined in (5.32) is *linear* in the power allocation variables $\{\phi_{k,l}, \forall k \in \mathcal{K}, \forall l \in \mathcal{L}\}$. Hence, when the term $-\delta_k \|\text{vec}\{\mathbf{A}_k\}\|_2$ in (5.46b) is not presented, i.e., for non-robust designs, the RCBA problem in (5.46) reduces to a MILP [67–69], which requires far fewer computational efforts to solve than that of the MISOCP formulation in (5.46) [67–69, 81, 82]. Hence, for the RCBA problem in the form of (5.46), to achieve robustness against the CCM estimation errors, not only more transmitted BS power needs to be invested (see, e.g., [12, 37–42, 131–135]), but also more computational efforts are required, as compared to non-robust downlink beamforming designs.

5.5 Techniques for customizing the BnC method

Based on the structure of the RCBA problem in the form of the MISOCP in (5.46), we propose here efficient strategies to customize the parallel BnC method implemented in the MIP solver CPLEX [81]. The customizing strategies are introduced to reduce the computational efforts of the BnC method when applying CPLEX on the RCBA problem in (5.46).

5.5.1 Customized optimality criterion

We denote $\Psi^{(\text{BIF})}$ and $\Psi^{(\text{GUB})}$ as the objective value of the incumbent solution (i.e., the best-known integer-feasible solution) and the smallest global upper bound (GUB) of the optimal objective value $\Phi^{(\text{RCBA})}$ of the RCBA problem (5.46), respectively, computed in the BnC procedure. Since $\Psi^{(\text{BIF})}$ and $\Psi^{(\text{GUB})}$ are the best-known global lower bound (GLB) and the GUB of the optimal objective value $\Phi^{(\text{RCBA})}$, respectively, it holds that

$$0 \leq \Psi^{(\text{BIF})} \leq \Phi^{(\text{RCBA})} \leq \Psi^{(\text{GUB})}. \quad (5.48)$$

As presented in Sections 2.5.1 and 5.5.1, an incumbent solution computed by the BnC procedure is declared to be an optimal solution of the RCBA problem (5.46) if it satisfies that [69, 81]:

$$\text{Relative MIP gap} \triangleq \frac{\Psi^{(\text{GUB})}}{\Psi^{(\text{BIF})}} - 1 \leq \eta \quad (5.49)$$

where the constant $\eta \geq 0$ denotes the predetermined relative optimality tolerance, which can be customized according to the RCBA problem (5.46) in specific practical applications.

5.5.2 Customized node selection and branching rules

As in Chapters 2 and 3, we adopt the *best-bound search* rule [81] for node selection in the BnC procedure when applying the solver CPLEX on the RCBA problem (5.46). The best-bound search rule favors the computation of the optimality certificate defined in (5.49) [81].

As for the customized branching priorities, we propose here to relate the branching priority of the (relaxed) binary variable $a_{k,l}$ to the incentive measure $\Upsilon_{k,l}$, defined as

$$\Upsilon_{k,l} \triangleq P^{(\text{MAX})} \text{Tr}\{\widehat{\mathbf{R}}_k \mathbf{V}_l\}, \forall k \in \mathcal{K}, \forall l \in \mathcal{L} \quad (5.50)$$

which represents the maximum signal power received at the k th MS when the l th precoding vector $\mathbf{v}_l \in \mathcal{B}$ is assigned to the k th MS, $\forall k \in \mathcal{K}, \forall l \in \mathcal{L}$. That is, a larger term $P^{(\text{MAX})} \text{Tr}\{\widehat{\mathbf{R}}_k \mathbf{V}_l\}$ corresponds to a larger branching priority of the (relaxed) binary variable $a_{k,l}$. Similar to Chapter 2, we define here the branching priority, denoted by $\overline{\Upsilon}_{k,l}$, associated with the (relaxed) binary variable $a_{k,l}$ as

$$\overline{\Upsilon}_{k,l} \triangleq \sum_{j=1}^K \sum_{m=1}^L \mathcal{I}(\Upsilon_{j,m} \leq \Upsilon_{k,l}), \forall k \in \mathcal{K}, \forall l \in \mathcal{L} \quad (5.51)$$

where the indicator function $\mathcal{I}(\Upsilon_{j,m} \leq \Upsilon_{k,l})$ is defined as

$$\mathcal{I}(\Upsilon_{j,m} \leq \Upsilon_{k,l}) = \begin{cases} 1, & \text{if } \Upsilon_{j,m} \leq \Upsilon_{k,l} \\ 0, & \text{otherwise.} \end{cases} \quad (5.52)$$

5.5.3 Preprocessing

We know from the worst-case SINR constraints in (5.15) that, to assign the l th precoding vector $\mathbf{v}_l \in \mathcal{B}$ to the k th MS, it is required that:

$$P^{(\text{MAX})} \left(\min_{\Delta_k \in \mathcal{E}_k} \text{Tr}\{(\widehat{\mathbf{R}}_k - \Delta_k)\mathbf{V}_l\} \right) \geq \sigma_k^2 \Gamma_k^{(\text{MIN})}. \quad (5.53)$$

Since the minimization problem in the LHS of Eq. (5.53) represents a convex SDP [34], the necessary condition in (5.53) can easily be verified in the preprocessing step. In case that the necessary condition in (5.53) is *not* satisfied, i.e., if it is *infeasible* to assign the l th precoding vector $\mathbf{v}_l \in \mathcal{B}$ to the k th MS, we fix $a_{k,l} = 0$ in the RCBA problem (5.46).

In addition, as presented in Chapters 2 and 3, we can also introduce problem-specific cuts [67–69, 81, 82] to reduce the size of the feasible set of the continuous relaxation in (5.47). For example, the following cuts can be added to the RCBA problem (5.46):

$$\phi_{k,l} \text{Tr}\{\widehat{\mathbf{R}}_k \mathbf{V}_l\} \geq a_{k,l} \sigma_k^2 \Gamma_k^{(\text{MIN})}, \forall k \in \mathcal{K}, \forall l \in \mathcal{L}. \quad (5.54)$$

The problem-specific cuts defined in (5.54) are derived from the SINR constraints in (5.46b) by dropping the term $-\delta_k \|\text{vec}\{\mathbf{A}_k\}\|_2$ and the co-channel interference in Eq. (5.46b).

Further, high-quality integer-feasible solutions can be utilized to initialize the BnC procedure to reduce the computational efforts. We develop in the subsequent section a low-complexity inflation procedure (i.e., a heuristic greedy algorithm) [83, 84] to compute near-optimal integer-feasible solutions of the RCBA problem in (5.46).

5.6 The SOCP based inflation procedure

The computational complexity of the BnC method when applying on the MISOCP formulation of the RCBA problem in (5.46) may be prohibitive for practical applications in large-scale networks. We propose here a low-complexity SOCP based inflation procedure [83, 84] to compute close-to-optimal solutions of the RCBA problem (5.46). The integer-feasible solutions computed by the inflation procedure can be used to initialize the BnC algorithm to reduce the computational efforts required for computing the optimal solutions and/or opti-

mality certificates. The inflation procedure starts with $\{a_{k,l}^{(0)} = 0, \forall k \in \mathcal{K}, \forall l \in \mathcal{L}\}$. In the n th iteration ($1 \leq n \leq K$), the best candidate among the *zero-valued* variables in the set $\{a_{k,l}^{(n-1)}, \forall k \in \mathcal{K}, \forall l \in \mathcal{L}\}$ is chosen and fixed to *one*. To determine the best candidate in the n th iteration, a sub-enumerating process is introduced. Define $\tilde{a}_{k,l}^{(n)} \triangleq a_{k,l}^{(n-1)}, \forall k \in \mathcal{K}, \forall l \in \mathcal{L}$. In the (j, m) th ($1 \leq j \leq K, 1 \leq m \leq L$) sub-enumeration in the n th iteration of the inflation procedure, if $\tilde{a}_{j,m}^{(n)} = 0$, we set $\tilde{a}_{j,m}^{(n)} = 1$, and the following convex SOCP:

$$P_{j,m}^{(n)} \triangleq \min_{\{\phi_{k,l}\}} \sum_{k=1}^K \sum_{l=1}^L \phi_{k,l} \quad (5.55a)$$

$$\text{s.t. (5.4): } \sum_{k=1}^K \sum_{l=1}^L \phi_{k,l} \leq P^{(\text{MAX})}$$

$$\phi_{k,l} \geq 0, \forall k \in \mathcal{K}, \forall l \in \mathcal{L} \quad (5.55b)$$

$$\text{Tr}\{\widehat{\mathbf{R}}_k \mathbf{A}_k\} - \delta_k \|\text{vec}\{\mathbf{A}_k\}\|_2 \geq \sigma_k^2, \text{ if } \max_{l \in \mathcal{L}} \tilde{a}_{k,l}^{(n)} = 1, \forall k \in \mathcal{K} \quad (5.55c)$$

is solved using, e.g., the interior-point method [34, 105]. If the SOCP in (5.55) is infeasible, we set $a_{j,m}^{(n-1)} = \tilde{a}_{j,m}^{(n)} = -1$ to prevent infinite cycles, and set $P_{j,m}^{(n)} = 2P^{(\text{MAX})}$. The best candidate in the n th iteration of the inflation procedure is the *zero-valued* variable in the set $\{a_{k,l}^{(n-1)}, \forall k \in \mathcal{K}, \forall l \in \mathcal{L}\}$ that corresponds to the *smallest* entry in the set $\{P_{j,m}^{(n)}, \forall k \in \mathcal{K}, \forall l \in \mathcal{L}\}$. If $\min_{j \in \mathcal{K}, m \in \mathcal{L}} P_{j,m}^{(n)} = 2P^{(\text{MAX})}$, i.e., if no feasible precoding vector assignment is found in the n th iteration, the inflation procedure terminates. Note that in the first iteration, since no precoding vector assignment is fixed yet, we can simply compute $P_{j,m}^{(1)}$ according to

$$P_{j,m}^{(1)} = \begin{cases} \frac{\sigma_j^2 \Gamma_j^{(\text{MIN})}}{\text{Tr}\{\widehat{\mathbf{R}}_j \mathbf{V}_m\} - \delta_j}, & \text{if } \text{Tr}\{\widehat{\mathbf{R}}_j \mathbf{V}_m\} - \delta_j > 0 \\ 2P^{(\text{MAX})}, & \text{otherwise} \end{cases}, \forall j \in \mathcal{K}, \forall m \in \mathcal{K}. \quad (5.56)$$

The proposed low-complexity inflation procedure is summarized in Alg. 5.1. The worst-case computational complexity of the proposed inflation procedure in Alg. 5.1 mainly con-

sists of solving $\frac{(K-1)KL}{2}$ instances of the convex SOCP in (5.55).

Init.: Compute $P_{j,m}^{(1)}$ according to Eq. (5.56). If $\min_{j \in \mathcal{K}, m \in \mathcal{L}} P_{j,m}^{(1)} = 2P^{(\text{MAX})}$, *terminate*. Otherwise, compute $(\bar{k}, \bar{l}) = \underset{j \in \mathcal{K}, m \in \mathcal{L}}{\operatorname{argmin}} P_{j,m}^{(1)}$. Set $a_{k,l}^{(1)} = 0, \forall k \in \mathcal{K} \setminus \{\bar{k}\}, \forall l \in \mathcal{L}$, and set $a_{\bar{k},\bar{l}}^{(1)} = -1, \forall l \in \mathcal{L} \setminus \{\bar{l}\}$, and fix $a_{\bar{k},\bar{l}}^{(1)} = 1$.

for $n = 2$ to K **do**

If none of the variables in the set $\{a_{k,l}^{(n-1)}, \forall k \in \mathcal{K}, \forall l \in \mathcal{L}\}$ equals to zero, *stop* and go to **Post-step**. Otherwise, define $\tilde{a}_{k,l}^{(n)} = a_{k,l}^{(n-1)}, \forall k \in \mathcal{K}, \forall l \in \mathcal{L}$.

for $j = 1$ to K , and $m = 1$ to L **do**

If $\tilde{a}_{j,m}^{(n)} = 0$, set $\tilde{a}_{j,m}^{(n)} = 1$, solve the SOCP in (5.55).

If the SOCP in (5.55) is infeasible, set $a_{j,m}^{(n-1)} = \tilde{a}_{j,m}^{(n)} = -1$, and set $P_{j,m}^{(n)} = 2P^{(\text{MAX})}$. Otherwise, set $P_{j,m}^{(n)} = \sum_{k=1}^K \sum_{l=1}^L \phi_{k,l}^{(n)}$.

end

If $\min_{j \in \mathcal{K}, m \in \mathcal{L}} P_{j,m}^{(n)} = 2P^{(\text{MAX})}$, *stop* and go to **Post-step**. Otherwise, compute $(\bar{k}, \bar{l}) = \underset{j \in \mathcal{K}, m \in \mathcal{L}}{\operatorname{argmin}} P_{j,m}^{(n)}$. Set $a_{k,l}^{(n)} = a_{k,l}^{(n-1)}, \forall k \in \mathcal{K} \setminus \{\bar{k}\}, \forall l \in \mathcal{L}$, and set $a_{\bar{k},\bar{l}}^{(n)} = -1, \forall l \in \mathcal{L} \setminus \{\bar{l}\}$, and fix $a_{\bar{k},\bar{l}}^{(n)} = 1$.

end

Post-step: Set $a_{k,l}^{(n-1)} = \max\{a_{k,l}^{(n-1)}, 0\}, \forall k \in \mathcal{K}, \forall l \in \mathcal{L}$, and return the point $\{a_{k,l}^{(n-1)}, \phi_{k,l}^{(n-1)}, \forall k \in \mathcal{K}, \forall l \in \mathcal{L}\}$ as a feasible solution of the RCBA problem.

Algorithm 5.1: The proposed SOCP based inflation procedure

5.7 Simulation results

In the simulations, we consider a downlink system with one BS having $M = 4$ transmit antennas and the maximum transmission power of $P^{(\text{MAX})} = 15$ dB. The parameter ρ in Eq. (5.14) is chosen as $\rho = 1 / (1 + P^{(\text{MAX})})$. Following the prior works [12, 38, 121, 138], the (m, l) th entry of the *normalized* (i.e., normalized by the noise power) true CCM \mathbf{R}_k is modeled according to

$$[\mathbf{R}_k]_{m,l} = \exp\left(-(\pi(m-l)\sigma_\theta \cos \theta_k)^2 / 2\right) \times \exp\left(\sqrt{-1}\pi(m-l) \sin \theta_k\right), \forall m, l = 1, 2, \dots, M, \forall k \in \mathcal{K} \quad (5.57)$$

where $\sigma_\theta = \pi/90$ denotes the spread angle, and θ_k represents the *random* angular direction of the k th MS, $\forall k \in \mathcal{K}$. The estimation error (mismatch) matrix $\mathbf{\Delta}_k$ is uniformly generated in a sphere centered at the all-zeros matrix and with a radius of $\delta_k = 0.2$ [12, 38, 121], i.e., the

parameter δ_k in Eq. (5.13) is chosen as $\delta_k = 0.2, \forall k \in \mathcal{K}$. The noise power at the receivers is normalized to one, i.e., we set $\sigma_k^2 = 1$ watt, $\forall k \in \mathcal{K}$.

As in Chapter 4, the precoding vector codebook with $L = 16$ precoding vectors defined in 3GPP LTE [7, 8, 20] is used in the simulations. The minimum SINR requirements of the K admissible MSs are chosen to be identical. The values of $\Gamma_k^{(\text{MIN})}$ and K are listed in the tables and the figures. The MIP solver CPLEX [81] is applied on the MILP approximation (5.28) and the RCBA problem in (5.46). The relative optimality tolerance in the optimality certificate defined in (5.49) is set as $\eta = 0.1\%$. The runtime limit of the solver CPLEX is set as $T = 150$ seconds. All simulation results are averaged over 500 Monte Carlo runs (MCRs).

Recall that the MISOCP in (5.46) represents an equivalent reformulation of the original RCBA problem in (5.17). In the figures and the tables, “w/ init.” indicates that the solver CPLEX is initialized with the solutions found by the inflation procedure in Alg. 5.1. “w/ SU init.” refers to that the CPLEX is initialized with the solutions that only a single user is admitted, which can directly be identified by inspecting the cuts in (5.54). The BnC method in CPLEX is customized according to the customizing strategies presented in Section 5.5.2 for the cases labeled with “w/ init.” and “w/ SU init.”, but *not* for the cases labeled with “w/o custom.”. However, the solver CPLEX is initialized with the solutions that only a single user is admitted for the cases labeled with “w/o custom.”.

5.7.1 Performance with different SINR targets

We study in this subsection the performance of the MILP based approach (5.28), the MISOCP based approach (5.46), and the inflation procedure in Alg. 5.1, with different values of the SINR target $\Gamma_k^{(\text{MIN})}$ and the fixed number of admissible MSs $K = 10$.

Fig. 5.1 displays the system utility (cf. Eq. (5.14)) vs. the SINR target $\Gamma_k^{(\text{MIN})}$. We observe from Fig. 5.1 that the system utility achieved by the proposed inflation procedure in Alg. 5.1 is remarkably close to that of the optimal (according to the optimality certificate (5.49)) solutions computed by the solver CPLEX, e.g., the *largest* relative gap at $\Gamma_k^{(\text{MIN})} = 2$ dB is less than 5.5%. The system utility obtained by the MILP based approach (5.28) is also considerably close to that of the optimal solutions, e.g., the *largest* relative gap at $\Gamma_k^{(\text{MIN})} = -2$ dB is less than 9%. Further, under the runtime limit of $T = 150$ seconds, the larger system utility is achieved when CPLEX is customized and is initialized with the solutions of Alg. 5.1 (i.e., the dashed curve with circles), as compared to the case that CPLEX is not customized (i.e., the solid curve with triangles). This demonstrates the effectiveness of the customizing strategies presented in Section 5.5.2.

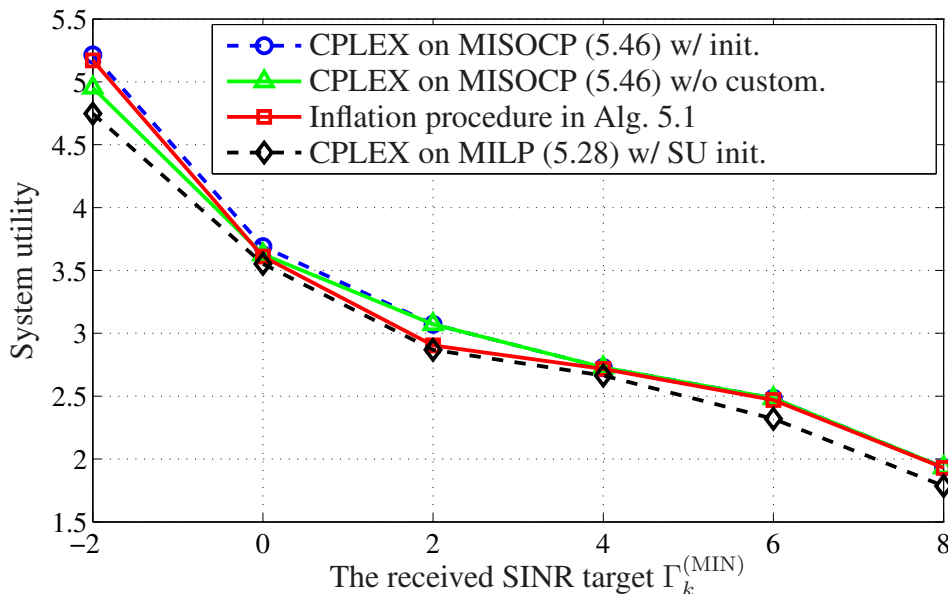


Figure 5.1: The system utility vs. the SINR target $\Gamma_k^{(\text{MIN})}$, with $K = 10$.

Table 5.1: The average number of admitted MSs (in boldface) and the total transmitted BS power [watts] vs. $\Gamma_k^{(\text{MIN})}$, with $K = 10$.

$\Gamma_k^{(\text{MIN})}$ [dB]	CPLEX on (5.46) w/ init.	Inflation procedure in Alg. 5.1	CPLEX on (5.28) w/ SU init.
-2	(5.42, 6.80)	(5.40, 7.59)	(4.99, 8.00)
0	(3.84, 4.78)	(3.75, 4.66)	(3.75, 6.34)
2	(3.27, 6.45)	(3.03, 4.14)	(3.00, 4.19)
4	(2.86, 4.39)	(2.86, 4.67)	(2.84, 5.63)
6	(2.71, 7.29)	(2.69, 7.30)	(2.62, 9.88)
8	(2.20, 8.78)	(2.20, 10.82)	(2.00, 6.99)

Tab. 5.1 lists the average number of *admitted* MSs (in boldface) and the total transmitted BS power [watts] vs. the SINR target $\Gamma_k^{(\text{MIN})}$. Note that more total transmitted BS power is required when a larger number of MSs are admitted for a given SINR target $\Gamma_k^{(\text{MIN})}$. We see from Tab. 5.1 that the MISOCP based approach (5.46) achieves a larger number of admitted MSs with less total transmitted BS power, as compared to the MILP based approach (5.28), e.g., at $\Gamma_k^{(\text{MIN})} = 6$ dB. Moreover, due to employing the conservative approximations in (5.19) for the worst-case SINR constraints in (5.15), the MILP based approach (5.28) requires more total transmitted BS power to guarantee the SINR requirements of the admitted MSs, as compared to that of the inflation procedure, e.g., at $\Gamma_k^{(\text{MIN})} = 0$ dB.

The algorithm runtime vs. the SINR target $\Gamma_k^{(\text{MIN})}$ is plotted in Fig. 5.2. It can be observed from Fig. 5.2 that, with $K = 10$, the inflation procedure and the MILP based approach (5.28) require much less runtime than that of the MISOCP based approach (5.46), while the system utility achieved by the former two is very close to that obtained by the latter (cf. Fig. 5.1). Furthermore, less runtime is required when CPLEX is customized according to the strategies presented in 5.5.2. This proves the effectiveness of the proposed customizing strategies.

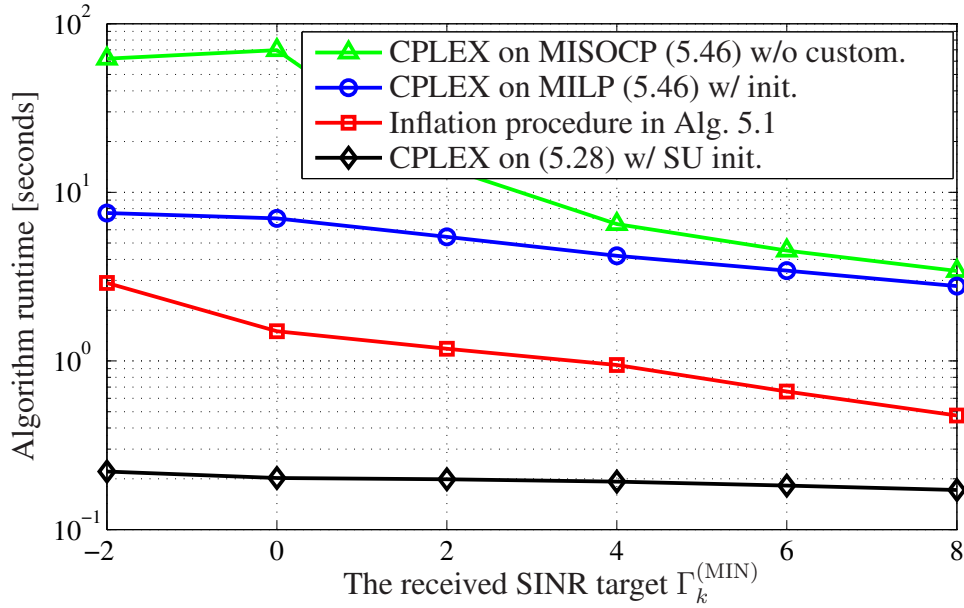


Figure 5.2: The algorithm runtime vs. the SINR target $\Gamma_k^{(\text{MIN})}$, with $K = 10$.

Fig. 5.3 depicts the percentage of optimal (according to the optimality certificate (5.49)) solutions achieved by the considered methods vs. the SINR target $\Gamma_k^{(\text{MIN})}$. We observe from Fig. 5.3 that the inflation procedure yields the optimal (under the optimality certificate (5.49)) solutions of the original RCBA problem (5.17) in most of the MCRs, e.g., more than 78.7% at $\Gamma_k^{(\text{MIN})} = 4$ dB. Further, due to the conservative approximations of the worst-case SINR constraints as given in (5.19), the MILP based approach (5.28) cannot reach the optimal solutions of the original RCBA problem (5.17) in any of the MCRs.

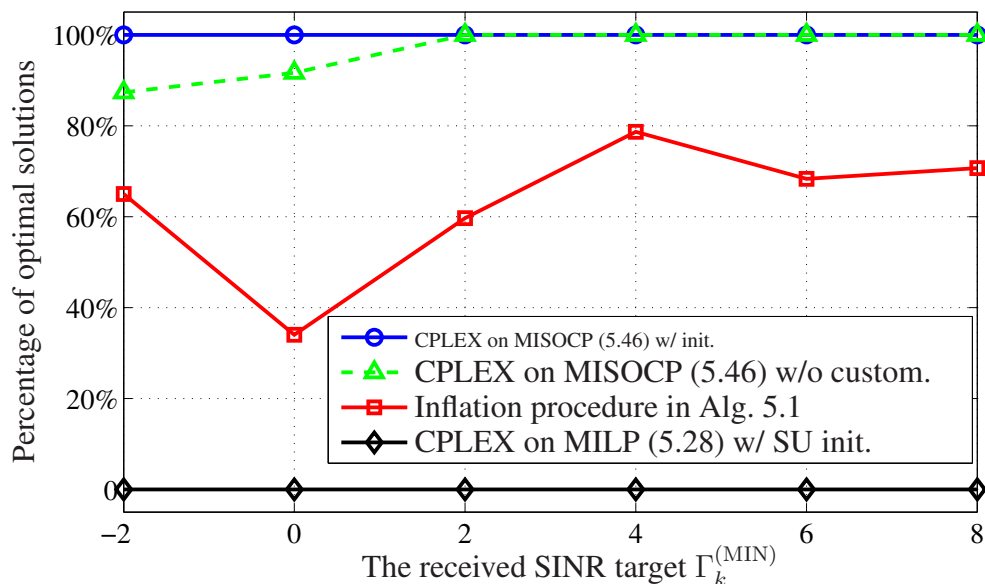


Figure 5.3: The percentage of achieved optimal solutions vs. the SINR target $\Gamma_k^{(\text{MIN})}$, with $K = 10$.

5.7.2 Performance with different numbers of admissible MSs

We investigate in this subsection the performance of the considered approaches for the original RCBA problem in (5.17), with different values of the number of admissible MSs K and the fixed SINR target $\Gamma_k^{(\text{MIN})} = 4$ dB. Since the effectiveness of the customizing strategies presented in Section 5.5.2 has already been demonstrated in Section 5.7.1 when applying the solver CPLEX on the MISOCP in (5.46), the proposed customizing strategies are not further evaluated in this subsection.

Fig. 5.4 depicts the system utility (cf. Eq. (5.14)) vs. the number of admissible MSs K . It can be seen from Fig. 5.4 that the system utility achieved by the inflation procedure in Alg. 5.1 is very close to that of the optimal (according to the optimality certificate (5.49)) solutions computed by the solver CPLEX when applying CPLEX on the MISOCP formulation (5.46), e.g., the *largest* relative gap at $K = 14$ is less than 2.8%. The system utility obtained by the MILP based approach (5.28) is also very close to that of the optimal solutions, e.g., the *largest* relative gap at $K = 12$ is less than 2.3%. Further, the system utility achieved by Alg. 5.1 is almost the same as that yielded by the MILP based approach (5.28).

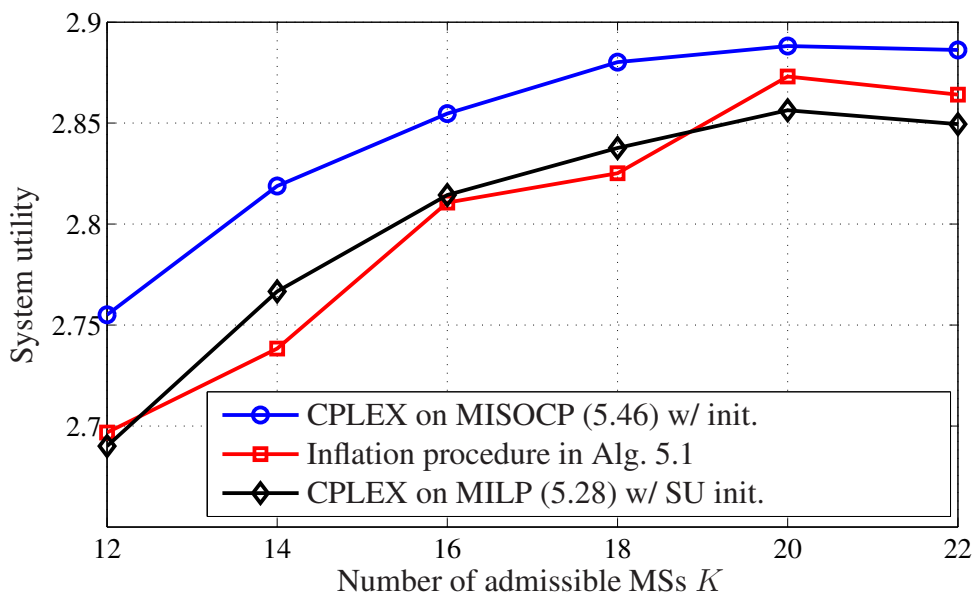


Figure 5.4: The system utility vs. the parameter K , with $\Gamma_k^{(\text{MIN})} = 4$ dB.

Table 5.2: The average number of *admitted* MSs (in boldface) and the total transmitted BS power [watts] vs. K , with $\Gamma_k^{(\text{MIN})} = 4$ dB.

K	CPLEX on (5.46) w/ init.	Inflation procedure in Alg. 5.1	CPLEX on (5.28) w/ SU init.
12	(2.89 , 4.51)	(2.85 , 5.00)	(2.88 , 6.09)
14	(2.95 , 4.17)	(2.85 , 3.75)	(2.94 , 5.55)
16	(2.97 , 3.87)	(2.92 , 3.68)	(2.97 , 5.18)
18	(3.00 , 3.91)	(2.94 , 3.75)	(2.99 , 5.08)
20	(3.00 , 3.65)	(2.99 , 3.71)	(3.00 , 4.69)
22	(3.00 , 3.71)	(2.99 , 3.67)	(3.00 , 4.91)

Tab. 5.2 lists the average number of *admitted* MSs (in boldface) and the total transmitted BS power [watts] vs. the number of admissible MSs K . Note that more total transmitted BS power is required when a larger number of MSs are admitted for the given SINR target $\Gamma_k^{(\text{MIN})} = 4$ dB. We observe from Tab. 5.2 that while the MILP based approach (5.28) achieves almost the same average number of admitted MSs as that of the MISOCP based approach (5.46) for each value of K , the former requires much more total transmitted BS power to guarantee the SINR targets of the admitted MSs than the latter, e.g., the former requires 35% more transmitted BS power at $K = 12$ than the latter. This observation is consistent with the results presented in [38] for the conventional robust non-codebook-based multiuser

downlink beamforming. Furthermore, the inflation procedure in Alg. 5.1 does not admit as many MSs as that of the MISOCP based approach (5.46) or the MILP based approach (5.28), e.g., at $K = 14$.

Fig. 5.5 displays the algorithm runtime vs. the number of admissible MSs K . Similar to Fig. 5.2, we see from Fig. 5.5 that the inflation procedure in Alg. 5.1 and the MILP based approach (5.28) require much less runtime than that of the MISOCP based approach (5.46), while the system utility achieved by the former two is very close to that of the latter (cf. Fig. 5.4). Further, when the number of admissible MSs K is small, e.g., when $K \leq 20$, the MILP based approach (5.28) requires less runtime than that of the inflation procedure. However, when $K = 22$, the former requires more runtime than that of the latter. We will further compare the performance (e.g., algorithm runtime) of the MILP based approach (5.28) and that of the inflation procedure for $20 \leq K \leq 30$ in Section 5.7.3.

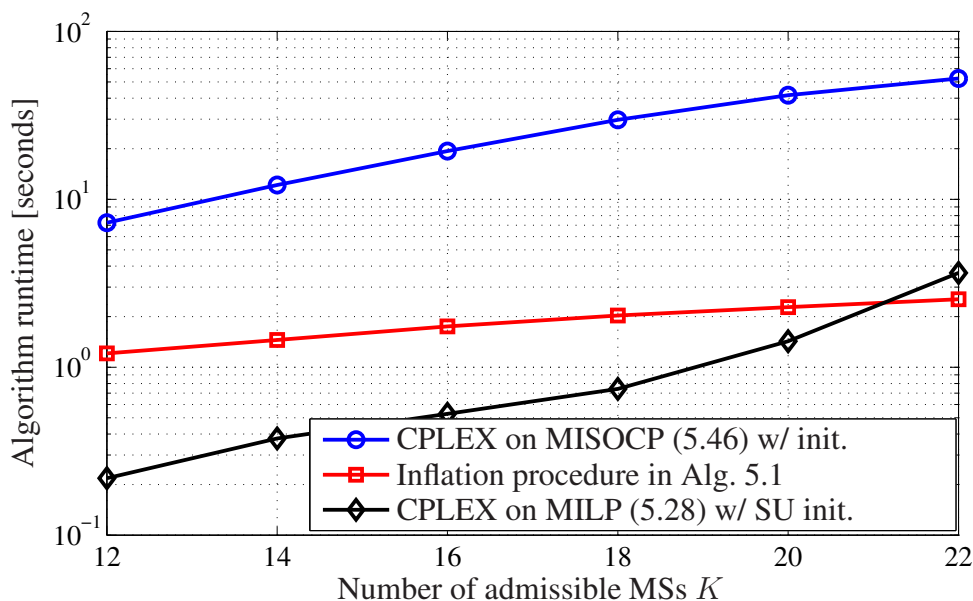


Figure 5.5: The algorithm runtime vs. the parameter K , with $\Gamma_k^{(\text{MIN})} = 4$ dB.

Fig. 5.6 displays the percentage of optimal (according to the optimality certificate (5.49)) solutions achieved by the considered methods vs. the number of admissible MSs K . Similar to Fig. 5.3, we see from Fig. 5.6 that the inflation procedure in Alg. 5.1 yields the optimal (according to the optimality certificate (5.49)) solutions of the original RCBA problem (5.17) in most of the MCRs, e.g., in more than 72% MCRs at $K = 16$. However, the MILP based approach (5.28) cannot reach the optimal solutions of the original RCBA problem (5.17) in any of the MCRs, which is due to the conservative approximations of the worst-case SINR constraints employed in the MILP based approach (5.28).

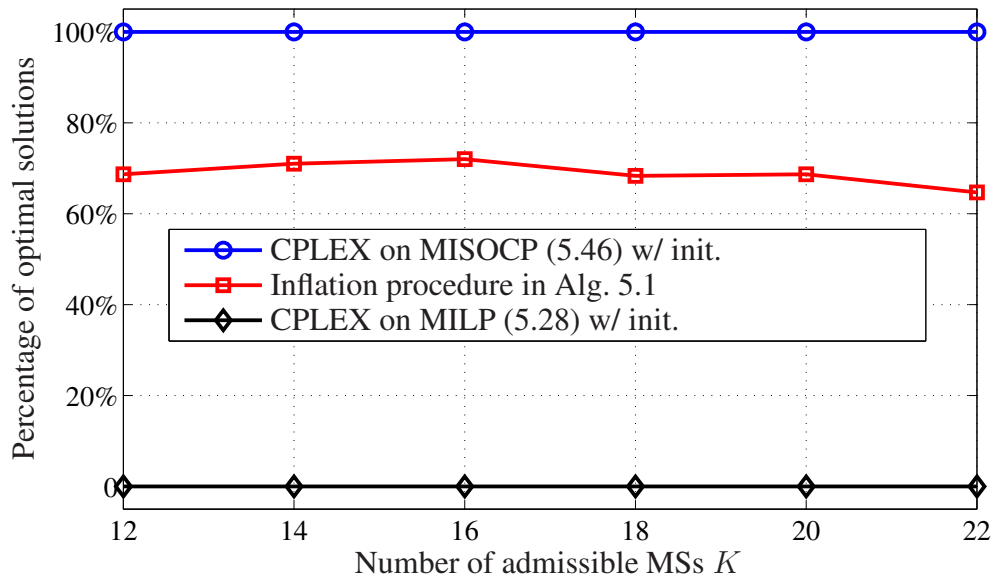


Figure 5.6: The percentage of optimal solutions achieved vs. the parameter K , with $\Gamma_k^{(\text{MIN})} = 4$ dB.

5.7.3 Further comparison with large numbers of admissible MSs

We compare in this subsection the performance of the MILP based approach (5.28) and that of the inflation procedure in Alg. 5.1 in scenarios with large numbers of admissible MSs, i.e., for $20 \leq K \leq 30$, and the fixed SINR target $\Gamma_k^{(\text{MIN})} = 4$ dB.

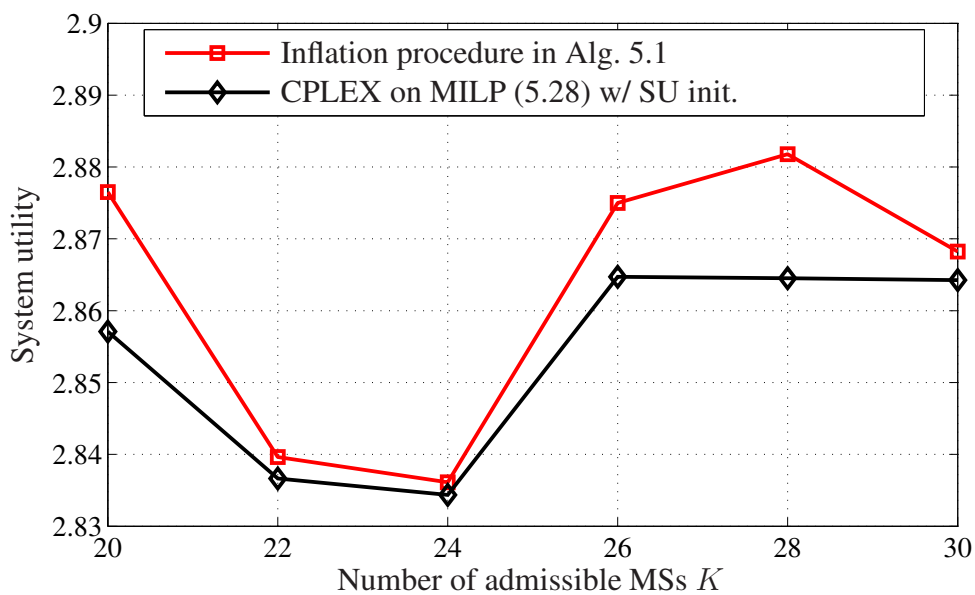


Figure 5.7: The system utility vs. the parameter K , with $\Gamma_k^{(\text{MIN})} = 4$ dB.

Fig. 5.7 depicts the system utility (cf. Eq. (5.14)) vs. the number of admissible MSs

K . Similar to Fig. 5.4, we see from Fig. 5.7 that the MILP based approach (5.28) and the inflation procedure in Alg. 5.1 achieve almost the same amount of system utility.

Table 5.3: The average number of admitted MSs (in boldface) and the total transmitted BS power [watts] vs. K , with $\Gamma_k^{(\text{MIN})} = 4$ dB.

K	Inflation procedure in Alg. 5.1	CPLEX on MILP (5.28)
20	(2.99 , 3.71)	(3.00 , 4.69)
22	(2.99 , 3.67)	(3.00 , 4.91)
24	(2.97 , 3.82)	(2.97 , 4.53)
26	(2.99 , 3.43)	(3.00 , 4.53)
28	(2.99 , 3.53)	(3.00 , 4.42)
30	(3.00 , 3.54)	(3.00 , 4.43)

Tab. 5.3 lists the average number of *admitted* MSs (in boldface) and the total transmitted BS power [watts] vs. the number of admissible MSs K . We observe from Tab. 5.3 that although the MILP based approach (5.28) achieves almost the same number of admitted MSs as that of the proposed inflation procedure in Alg. 5.1 for each considered value of K , the former requires much more total transmitted BS power to guarantee the SINR targets of the admitted MSs than the latter, e.g., the former requires 25% more transmitted BS power than the latter at $K = 30$.

The algorithm runtime vs. the number of admissible MSs K is plotted in Fig. 5.8. It can be observed from Fig. 5.8 that the inflation procedure in Alg. 5.1 requires much less runtime than that of the MILP based approach (5.28) for $K \geq 22$, e.g., the former requires only 5% the runtime of that of the latter at $K = 30$. This suggests that the inflation procedure is more efficient than the MILP based approach (5.28) for $K \geq 22$, in terms of both the yielded total transmitted BS power (cf. Tab. 5.3) and the associated computational complexity.

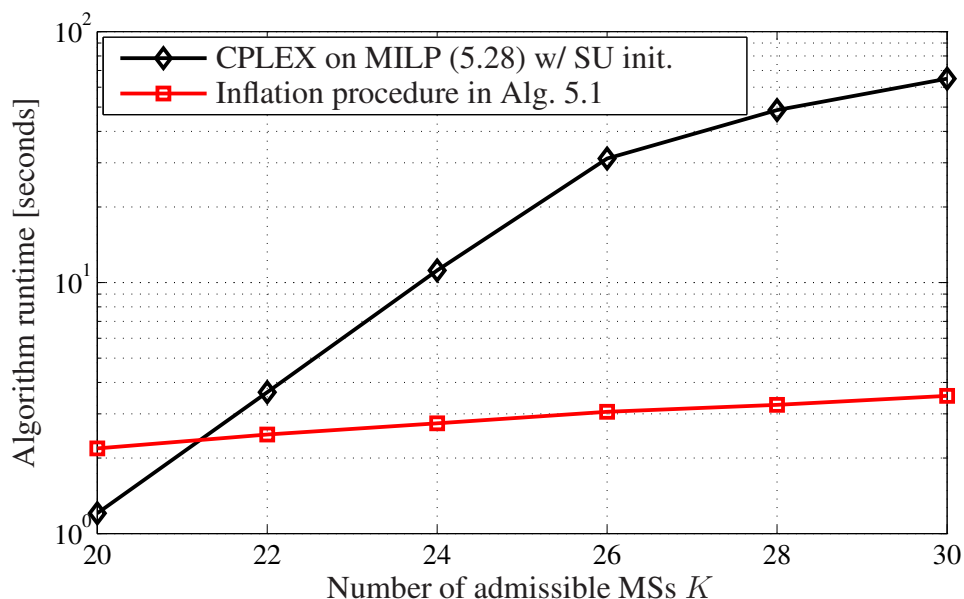


Figure 5.8: The algorithm runtime vs. the parameter K , with $\Gamma_k^{(\text{MIN})} = 4$ dB.

5.8 Summary

In this chapter, we have considered the problem of robust codebook-based multiuser downlink beamforming and admission control, with employing worst-case robust design against CCM estimation errors. The problem is of great practical interest since perfect CSI is generally difficult to obtain at the BS, especially in FDD systems. We have firstly proposed the MILP based approach (5.28), which is built on the conservative approximations of the worst-case SINR constraints. We have then devised an exact MISOCP reformulation (5.46) of the original RCBA problem 5.17. To provide a low-complexity approach for practical applications in large-scale systems, the low-complexity SOCP based inflation procedure in Alg. 5.1 has been developed. The simulation results have shown that the number of admitted MSs achieved by the inflation procedure 5.1 and the MILP based approach (5.28) is very close to that of the optimal solutions of the RCBA problem obtained through the MISOCP based approach (5.46). However, the inflation procedure 5.1 and the MILP based approach (5.28) requires much more total transmitted BS power to guarantee the SINR targets of the admitted MSs, as compared to the MISOCP based approach (5.46). Our numerical results have also demonstrated that the inflation procedure in Alg. 5.1 is more efficient in terms of, e.g., yielding significantly reduced total transmitted BS power with much less computational complexity, than that of the MILP based approach (5.28) when the number of admissible MSs K is large, e.g., when $K \geq 22$.

Chapter 6

Conclusions and outlook

Practical resource allocation problems in modern cellular networks inherently involve discrete optimization variables when taking into account the implementation restrictions and the specifications of the cellular standards. The mixed-integer programming (MIP) framework [67–69,81,82], namely mixed-integer linear program/programming (MILP) and mixed-integer second-order cone program/programming (MISOCP), is a necessary and powerful tool to exactly formulate the discrete models that arise in practical network resource allocation problems (see, e.g., [61–66]). Particularly, the MIP framework provides a realizable approach to compute the optimal solutions (performance benchmarks) of the discrete resource allocation problems. The optimal solutions are necessary and important for system performance predictions when performing network planning.

In this dissertation, we have considered five practically relevant examples regarding joint multiuser downlink beamforming and discrete resource allocation in modern cellular networks. The problems are addressed within the developed systematic MIP framework.

The MISOCP framework has been firstly developed for the joint optimization of network topology and multi-cell downlink beamforming (JNOB) in Chapter 2, where we proposed the standard big-M MISOCP formulation and the extended MISOCP formulation of the JNOB problem. Analytic studies have been carried out to compare the two formulations. The standard branch-and-cut (BnC) method [67–69, 81, 82] implemented in the MIP solver IBM ILOG CPLEX [81] was customized according to the proposed customizing techniques when applying CPLEX on the JNOB problem. We have also designed the low-complexity inflation and deflation procedures to compute near-optimal solutions of the JNOB problem for scenarios that the optimal solutions cannot be computed or certified by the BnC method in reasonable runtime. It has been observed that partial BSs cooperation schemes and sparse network topologies are deployed in the proposed design to balance the gain and the cost

of coordinated multi-point (CoMP) transmission and to minimize the total BSs power consumption.

The MISOCP framework was then applied to the joint optimization of discrete rate adaptation and downlink beamforming (DRAB) in Chapter 2. As in the JNOB problem, the standard big-M and the extended MISOCP formulations were developed for the DRAB problem, the analytic comparison was carried out, and customizing strategies for the BnC method were adopted. We have also developed the low-complexity second-order cone programming (SOCP) based inflation and deflation procedures. Our simulation results have demonstrated that the sum-rates and the total transmitted BS power achieved by the proposed inflation and deflation procedures are very close to that of the optimal solutions. It has also been shown that the practical heuristic algorithms have much less computational complexity than that of the BnC method.

We have developed the MILP formulation for the standard codebook-based downlink beamforming (SCBF) problem in Chapter 4. We have also proposed the customized power iteration method to more efficiently solve the SCBF problem. The analytic studies have remarkably shown that the proposed fast power iteration method is optimal for solving or detecting the infeasibility of the SCBF problem. The adaptive channel predistortion scheme has further been proposed to enhance the performance of the standard codebook-based beamforming in Chapter 4. Interestingly, the proposed channel predistortion procedure does not introduce any additional signaling overhead and can straightforwardly be incorporated into current and future cellular standards. The codebook-based downlink beamforming and channel predistortion (CBCP) problem was approximately solved with the proposed alternating optimization algorithm (ATO) and alternating feasibility search algorithm (AFSA). The numerical results have shown that the channel predistortion design achieves significant performance improvement over the standard codebook-based beamforming in terms of, e.g., significant reductions of the total transmitted BS power and tremendous increases of percentages of feasible Monte Carlo runs (MCRs).

Three approaches have been proposed for the robust codebook-based downlink beamforming and admission control (RCBA) problem in Chapter 5. The MILP based approach is built on the conservative approximations of the worst-case signal-to-interference-plus-noise ratio (SINR) constraints. The MISOCP based approach represents an equivalent reformulation of the RCBA problem. The inflation procedure (i.e., the greedy algorithm) is based on the exact MISOCP reformulation. Our simulation results have shown that the three approaches achieve almost the same average number of admitted mobile stations (MSs). However, the total transmitted BS power required for guaranteeing the SINR requirements of the admitted MSs in the MILP based approach is considerably larger than that of the other two

methods. We have also observed that the greedy algorithm admits much less computational complexity than the MILP based approach when the number of admissible MSs is large.

Plenty of follow-up research can be carried out by directly extending the studies and the MIP framework presented in this dissertation. Several extensions are being conducted by the author and the collaborators. For instance, the MISOCP framework and the JNOB problem are being extended to deal with interference management and load balancing in heterogeneous and small cell networks (HetSNets) [6, 139]. The MIP framework and the CBCP problem is being extended to incorporate user admission control. Further, more efficient algorithmic solutions are being developed for the CBCP problem.

While this thesis has been focused on the (multi-cell) downlink systems, the corresponding discrete resource allocation problems in the uplink systems can also be addressed within the developed MIP framework. Although the uplink problems generally belong to the class of non-convex MIPs, they can be converted into convex MIPs in the (virtual) downlink domain by exploiting uplink-downlink duality [12, 13]. For example, the problem of joint discrete rate adaptation and multiuser uplink beamforming can be closely related to (approximated by) the DRAB problem considered in Chapter 3. In addition, while this dissertation has only considered the scenarios with single-antenna MSs, it is also of practical interest to extend our work to the scenarios with multiple-antenna MSs, like the problem of discrete rate adaptation combined with joint transmit-receive beamforming in both downlink and uplink systems, where codebook-based beamforming (precoding) can readily be applied.

This dissertation has only covered a few exemplary problems regarding discrete resource allocation in modern cellular networks. There are many practical discrete resource allocation problems in wireless networks that can be addressed using the MIP framework presented in this thesis, e.g., wireless link activation [65], delay-constrained routing in multi-hop networks [66], cell site planning [140], and resource block scheduling in 3GPP LTE systems [6–8], to name but a few. Furthermore, the MIP framework developed in this dissertation can also be applied in the field of signal processing, e.g., in sparse filter design [141] and in sparse signal recovery [142]. As more advanced discrete and mixed-integer optimization techniques and algorithms are emerging and the powerful commercial MIP solvers are evolving, more and more practical discrete resource allocation problems in wireless communications and signal processing can be addressed within the developed MIP framework.

Appendix A

Appendices of Chapters 2 and 3

A.1 Proof of *Theorem 2.1*

Recall that the point $\{\mathbf{w}_{k,l}^{(\text{BMI})}, a_{k,l}^{(\text{BMI})}, b_l^{(\text{BMI})}, \forall k \in \mathcal{K}, \forall l \in \mathcal{L}\}$ represents an optimal solution of the JNOB problem (2.12). The necessary conditions in Eqs. (2.16) can be proved by contradicting argument.

Assuming that the necessary conditions in (2.16) do not hold, i.e., assuming that there exist two MSs with indices $\hat{j}, \hat{k} \in \mathcal{K}$ and two BSs with indices $\hat{m}, \hat{l} \in \mathcal{L}$ such that

$$a_{\hat{j},\hat{l}}^{(\text{BMI})} = a_{\hat{k},\hat{l}}^{(\text{BMI})} = a_{\hat{k},\hat{m}}^{(\text{BMI})} = 1. \quad (\text{A.1})$$

That is, it is assumed that the \hat{l} th BS serves the \hat{j} th and the \hat{k} th MSs jointly, and the \hat{l} th and the \hat{m} th BSs collaboratively serve the \hat{k} th MS. Since $\|\mathbf{w}_{\hat{j},\hat{l}}^{(\text{BMI})}\|_2^2 > 0$ when $a_{\hat{j},\hat{l}}^{(\text{BMI})} = 1$, we know from the per-BS power constraints in (2.12b) that:

$$\|\mathbf{w}_{\hat{k},\hat{l}}^{(\text{BMI})}\|_2^2 < P_{\hat{l}}^{(\text{MAX})} = P_{\hat{l}}^{(\text{MAX})} \left(a_{\hat{k},\hat{l}}^{(\text{BMI})} \right)^2. \quad (\text{A.2})$$

We can then define the new variable $\hat{a}_{\hat{k},\hat{l}}^{(\text{BMI})}$ as: $\hat{a}_{\hat{k},\hat{l}}^{(\text{BMI})} \triangleq \frac{\|\mathbf{w}_{\hat{k},\hat{l}}^{(\text{BMI})}\|_2}{\sqrt{P_{\hat{l}}^{(\text{MAX})}}}$, which satisfies the

following properties:

$$0 < \widehat{a}_{\widehat{k},\widehat{l}}^{(\text{BMI})} = \frac{\|\mathbf{w}_{\widehat{k},\widehat{l}}^{(\text{BMI})}\|_2}{\sqrt{P_{\widehat{l}}^{(\text{MAX})}}} < a_{\widehat{k},\widehat{l}}^{(\text{BMI})} \quad (\text{A.3})$$

$$\|\mathbf{w}_{\widehat{k},\widehat{l}}^{(\text{BMI})}\|_2^2 = P_{\widehat{l}}^{(\text{MAX})} \left(\widehat{a}_{\widehat{k},\widehat{l}}^{(\text{BMI})}\right)^2 \quad (\text{A.4})$$

$$\sum_{l \in \mathcal{L} \setminus \{\widehat{m}, \widehat{l}\}} a_{\widehat{k},l}^{(\text{BMI})} + \widehat{a}_{\widehat{k},\widehat{l}}^{(\text{BMI})} + a_{\widehat{k},\widehat{m}}^{(\text{BMI})} > 1. \quad (\text{A.5})$$

We can replace the variable $a_{\widehat{k},\widehat{l}}^{(\text{BMI})}$ in the optimal solution $\{\mathbf{w}_{k,l}^{(\text{BMI})}, a_{k,l}^{(\text{BMI})}, b_l^{(\text{BMI})}, \forall k \in \mathcal{K}, \forall l \in \mathcal{L}\}$ of the JNOB problem (2.12) with the variable $\widehat{a}_{\widehat{k},\widehat{l}}^{(\text{BMI})}$ to obtain a new feasible solution of the SOCP in (2.13), which, due to Eq. (A.3), achieves a *strictly smaller* objective value than $\Phi^{(\text{BMI})}$, i.e., $\Phi^{(\text{BMC})} < \Phi^{(\text{BMI})}$. This, however, contradicts with the condition that $\Phi^{(\text{BMC})} = \Phi^{(\text{BMI})}$. As a result, the \widehat{l} th BS cannot serve the \widehat{j} th and the \widehat{k} th MSs jointly in the case that $\Phi^{(\text{BMC})} = \Phi^{(\text{BMI})}$. Following a similar contradicting argument, we can prove that the \widehat{m} th BS must also serve exclusively the \widehat{k} th MS. Hence, cooperating BSs in CoMP transmission must serve exclusively a single MS when $\Phi^{(\text{BMC})} = \Phi^{(\text{BMI})}$, i.e., the necessary condition (2.16) must hold, in the case that $\Phi^{(\text{BMC})} = \Phi^{(\text{BMI})}$.

A.2 Proof of Theorem 2.2

We know from the constraints in (2.12d) and (2.12e), and Eqs. (2.31) and (2.32) that the point $\{\mathbf{w}_{k,l}^{(\text{EXC})}, a_{k,l}^{(\text{EXC})}, b_l^{(\text{EXC})}, \forall k \in \mathcal{K}, \forall l \in \mathcal{L}\}$, which is obtained from the projection of the point $\{\mathbf{w}_{k,l}^{(\text{EXC})}, a_{k,l}^{(\text{EXC})}, b_l^{(\text{EXC})}, t_{k,l}^{(\text{EXC})}, \forall k \in \mathcal{K}, \forall l \in \mathcal{L}\}$, is a feasible solution of the SOCP in (2.13). As a result, it holds that

$$\Phi^{(\text{BMC})} \leq f\left(\{a_{k,l}^{(\text{EXC})}\}, \{b_l^{(\text{EXC})}\}, \{\mathbf{w}_{k,l}^{(\text{EXC})}\}\right). \quad (\text{A.6})$$

Eq. (2.26) suggests that $f\left(\{a_{k,l}^{(\text{EXC})}\}, \{b_l^{(\text{EXC})}\}, \{\mathbf{w}_{k,l}^{(\text{EXC})}\}\right) \leq \Phi^{(\text{EXC})}$. Hence, we have $\Phi^{(\text{BMC})} \leq \Phi^{(\text{EXC})}$.

A.3 Proof of Theorem 2.3

Recall that the point $\{\mathbf{w}_{k,l}^{(\text{EXC})}, a_{k,l}^{(\text{EXC})}, b_l^{(\text{EXC})}, t_{k,l}^{(\text{EXC})}, \forall k \in \mathcal{K}, \forall l \in \mathcal{L}\}$ represents an optimal solution of the SOCP in (2.23). We first prove Eq. (2.34). If $\Phi^{(\text{BMC})} = \Phi^{(\text{EXC})}$, i.e., if

$\|\mathbf{w}_{k,l}^{(\text{EXC})}\|_2^2 = t_{k,l}^{(\text{EXC})}, \forall k \in \mathcal{K}, \forall l \in \mathcal{L}$, we know from Eq. (2.26) that the relaxed binary integer variables $\{a_{k,l}^{(\text{EXC})}, \forall k \in \mathcal{K}, \forall l \in \mathcal{L}\}$ take values in the discrete set $\{0, 1\}$. Due to Eq. (2.12d), this is also true for the relaxed binary variables $\{b_l^{(\text{EXC})}, \forall l \in \mathcal{L}\}$. Hence, Eq. (2.34) holds in the case that $\Phi^{(\text{BMC})} = \Phi^{(\text{EXC})}$.

We next prove Eq. (2.35). We know from Eq. (2.34) that the point $\{\mathbf{w}_{k,l}^{(\text{EXC})}, a_{k,l}^{(\text{EXC})}, b_l^{(\text{EXC})}, t_{k,l}^{(\text{EXC})}, \forall k \in \mathcal{K}, \forall l \in \mathcal{L}\}$ is actually an optimal solution of the JNOB problem (2.21) [67–69, 82] and therefore the projected point $\{\mathbf{w}_{k,l}^{(\text{EXC})}, a_{k,l}^{(\text{EXC})}, b_l^{(\text{EXC})}, \forall k \in \mathcal{K}, \forall l \in \mathcal{L}\}$ is an optimal solution of the JNOB problem (2.12). Hence, Eq. (2.35) holds.

Finally, we know from Eqs (2.34) and (2.35) that the projected point $\{\mathbf{w}_{k,l}^{(\text{EXC})}, a_{k,l}^{(\text{EXC})}, b_l^{(\text{EXC})}, \forall k \in \mathcal{K}, \forall l \in \mathcal{L}\}$ is an optimal solution of problem (2.12) and $\Phi^{(\text{BMC})} = \Phi^{(\text{BMI})}$ in the case that $\Phi^{(\text{BMC})} = \Phi^{(\text{EXC})}$ holds. As a result, we can directly apply the results of *Theorem 2.1* to obtain the necessary conditions in Eq. (2.36) for the special case of $\Phi^{(\text{BMC})} = \Phi^{(\text{EXC})}$.

A.4 Proof of Lemma 3.1

Recall that $a_{k,l} \in \{0, 1\}, \forall k \in \mathcal{K}, \forall l \in \mathcal{L}$ in the DRAB problem (3.26). When $a_{k,l} = 0$, we have $\mathbf{v}_{k,l} = \mathbf{0}$ due to Eq. (3.22), which is the equivalence of Eq. (3.19), and therefore the (k, l) th constraint in Eq. (3.26c) is automatically satisfied.

When $a_{k,l} = 1$, taking into account Eqs. (3.3), (3.18), and (3.19), and that the objective function in (3.26a) is maximized, it can readily be shown by contradicting argument that the SINR constraint of the k th MS defined in Eq. (3.24b) is equivalent to the following constraint (see, e.g., [12, 13, 28, 135]):

$$\|[\mathbf{h}_k^H \mathbf{W}, \sigma_k]\|_2 = \gamma_l \text{Re} \{ \mathbf{h}_k^H \mathbf{v}_{k,l} \} \quad (\text{A.7})$$

which, together with Eqs. (3.10) and (3.12), further imply that

$$\gamma_l \text{Re} \{ \mathbf{h}_k^H \mathbf{v}_{k,l} \} \leq a_{k,l} U_k \quad (\text{A.8})$$

That is the (k, l) th constraint in (3.26c) is also satisfied when $a_{k,l} = 1$. Hence, all the constraints in (3.26c) are automatically satisfied in problem (3.26), i.e. the constraints defined in Eq. (3.26c) represents valid problem-specific cuts.

A.5 Proof of Lemma 3.2

Recall that the point $\{a_{k,l}^{(\text{EXC})}, \mathbf{v}_{k,l}^{(\text{EXC})}, \phi_{k,l}^{(\text{EXC})}, b_k^{(\text{EXC})}, \forall k \in \mathcal{K}, \forall l \in \mathcal{L}\}$ denotes an optimal solution of the SOCP in (3.27). We know from the cuts in (3.26c) that

$$\begin{aligned} & \left(1 - \sum_{l=1}^L a_{k,l}^{(\text{EXC})}\right) U_k + \sum_{l=1}^L \gamma_l \text{Re} \left\{ \mathbf{h}_k^H \mathbf{v}_{k,l}^{(\text{EXC})} \right\} \\ &= \left(1 - a_{k,l}^{(\text{EXC})}\right) U_k + \gamma_l \text{Re} \left\{ \mathbf{h}_k^H \mathbf{v}_{k,l}^{(\text{EXC})} \right\} + \sum_{m=1, m \neq l}^L \left(\gamma_m \text{Re} \left\{ \mathbf{h}_k^H \mathbf{w}_{k,m}^{(\text{EXC})} \right\} - a_{k,m}^{(\text{EXC})} U_k \right) \\ &\leq \left(1 - a_{k,l}^{(\text{EXC})}\right) U_k + \gamma_l \text{Re} \left\{ \mathbf{h}_k^H \mathbf{v}_{k,l}^{(\text{EXC})} \right\}. \end{aligned} \quad (\text{A.9})$$

Eq. (A.9), together with Eq. (3.24b), imply Eq. (3.30) presented in Lemma 3.2.

A.6 Proof of Theorem 3.1

We know from Eqs. (3.24a), (3.26b), (3.28), and (3.30) that

$$\text{Im} \left\{ \mathbf{h}_k^H \mathbf{w}_k^{(\text{EXC})} \right\} = 0, \quad \text{Re} \left\{ \mathbf{h}_k^H \mathbf{w}_k^{(\text{EXC})} \right\} \geq 0, \quad \forall k \in \mathcal{K} \quad (\text{A.10})$$

$$\left\| \left[\mathbf{h}_k^H \mathbf{w}_k^{(\text{EXC})}, \sigma_k \right] \right\|_2 \leq \left(1 - a_{k,l}^{(\text{EXC})}\right) U_k + \gamma_l \text{Re} \left\{ \mathbf{h}_k^H \mathbf{w}_k^{(\text{EXC})} \right\}, \quad \forall k \in \mathcal{K}, \forall l \in \mathcal{L} \quad (\text{A.11})$$

$$\sigma_k \sum_{l=1}^L a_{k,l}^{(\text{EXC})} \sqrt{\Gamma_l} \leq \text{Re} \left\{ \mathbf{h}_k^H \mathbf{w}_k^{(\text{EXC})} \right\}, \quad \forall k \in \mathcal{K}. \quad (\text{A.12})$$

Moreover, we know from Eqs. (3.27b), (3.28), (3.32), and the triangle-inequality [34, 116] that

$$\left\| \mathbf{w}_k^{(\text{EXC})} \right\|_2^2 \leq \sum_{l=1}^L \left\| \mathbf{v}_{k,l}^{(\text{EXC})} \right\|_2^2 = \sum_{l=1}^L a_{k,l}^{(\text{EXC})} \phi_{k,l}^{(\text{EXC})} \leq \sum_{l=1}^L \phi_{k,l}^{(\text{EXC})}, \quad \forall k \in \mathcal{K} \quad (\text{A.13})$$

which, together with Eq. (3.21), further imply that

$$\sum_{k=1}^K \left\| \mathbf{w}_k^{(\text{EXC})} \right\|_2^2 \leq \sum_{k=1}^K \sum_{l=1}^L \phi_{k,l}^{(\text{EXC})} \leq P^{(\text{MAX})}. \quad (\text{A.14})$$

The constraints in (3.3) and (3.15b), together with Eqs. (A.10) – (A.12), and (A.14), suggest that the point $\{a_{k,l}^{(\text{EXC})}, \mathbf{w}_k^{(\text{EXC})}, \forall k \in \mathcal{K}, \forall l \in \mathcal{L}\}$ is a feasible solution of the SOCP in (3.16). As a result, Eq. (A.14), together with Eqs. (3.6) and (3.25), imply Eq. (3.33).

A.7 Sample branching priorities in the DRAB problem

We present here exemplary definitions of the branching priorities $\overline{\Omega}_k$ and $\overline{\Upsilon}_{k,l}$ following the principles (P1) – (P3) presented in Section 3.5.2. Denote the integer $\overline{\Theta}_k$ as the order of the channel gain $\|\mathbf{h}_k\|_2$ in the set $\{\|\mathbf{h}_k\|_2, \forall k \in \mathcal{K}\}$, i.e.,

$$\overline{\Theta}_k \triangleq \sum_{j=1}^K \mathcal{I}(\|\mathbf{h}_j\|_2 \leq \|\mathbf{h}_k\|_2), \forall k \in \mathcal{K} \quad (\text{A.15})$$

where the *indicator function* $\mathcal{I}(\|\mathbf{h}_j\|_2 \leq \|\mathbf{h}_k\|_2)$ is defined as

$$\mathcal{I}(\|\mathbf{h}_j\|_2 \leq \|\mathbf{h}_k\|_2) = \begin{cases} 1, & \text{if } \|\mathbf{h}_j\|_2 \leq \|\mathbf{h}_k\|_2 \\ 0, & \text{otherwise.} \end{cases} \quad (\text{A.16})$$

The set $\overline{\mathcal{K}}$ of the \overline{K} MSs with the \overline{K} largest channel gains among $\{\|\mathbf{h}_k\|_2, \forall k \in \mathcal{K}\}$ can then be defined as

$$\overline{\mathcal{K}} \triangleq \{k \mid k \in \mathcal{K}, \overline{\Theta}_k \geq K - \overline{K} + 1\}. \quad (\text{A.17})$$

For the variables in $\mathcal{G}_3 = \{b_k, \forall k \in \mathcal{K} \setminus \overline{\mathcal{K}}\}$, we define according to the prioritizing principle (P2) (cf. Section 3.5.2) the branching priorities $\{\overline{\Omega}_k, \forall k \in \mathcal{K} \setminus \overline{\mathcal{K}}\}$ as

$$\overline{\Omega}_k \triangleq \overline{\Theta}_k, \forall k \in \mathcal{K} \setminus \overline{\mathcal{K}}. \quad (\text{A.18})$$

Then, for the variables in $\mathcal{G}_2 = \{a_{k,l}, \forall k \in \mathcal{K}, \forall l \in \mathcal{L}\}$, we define according to the prioritizing principles (P1), (P3), and the ordering in Eq. (3.42) the branching priority $\overline{\Upsilon}_{k,l}$ as

$$\overline{\Upsilon}_{k,l} \triangleq \max_{k \in \mathcal{K} \setminus \overline{\mathcal{K}}} \overline{\Omega}_k + \overline{\Theta}_k, \forall k \in \mathcal{K}, \text{ and } l = 1 \quad (\text{A.19a})$$

$$\overline{\Upsilon}_{k,l} \triangleq \max_{k \in \mathcal{K} \setminus \overline{\mathcal{K}}} \overline{\Omega}_k + \max_{j \in \mathcal{K}} \overline{\Upsilon}_{j,l-1} + \overline{\Theta}_k, \forall k \in \mathcal{K}, \text{ and } l = 2, 3, \dots, L. \quad (\text{A.19b})$$

Finally, for the variables in $\mathcal{G}_1 = \{b_k, \forall k \in \overline{\mathcal{K}}\}$, we define according to the proposed prioritizing principles (P1) and (P2) the branching priorities $\{\overline{\Omega}_k, \forall k \in \overline{\mathcal{K}}\}$ as

$$\overline{\Omega}_k \triangleq \max_{k \in \mathcal{K}, \forall l \in \mathcal{L}} \overline{\Upsilon}_{k,l} + \overline{\Theta}_k, \forall k \in \overline{\mathcal{K}}. \quad (\text{A.20})$$

Bibliography

- [1] E. Hossain, V. K. Bhargava, and G. P. Fettweis, *Green Radio Communication Networks*. Cambridge University Press, Aug. 2012.
- [2] J.-S. Wu, S. Rangan, and H.-G. Zhang, *Green Communications: Theoretical Fundamentals, Algorithms And Applications*. CRC Press, Sep. 2012.
- [3] Rysavy Research, “Mobile broadband explosion: The 3GPP wireless evolution,” *Rysavy Research and 4G Americas*, Aug. 2012.
- [4] Cisco, “Cisco visual networking index: Global mobile data traffic forecast,” Feb. 2013. [Online]. Available: <http://goo.gl/tfzlU>
- [5] N. Ali, A. Taha, and H. Hassanein, “Quality of service in 3GPP R12 LTE-advanced,” *IEEE Commun. Mag.*, vol. 51, no. 8, pp. 103–109, Aug. 2013.
- [6] T. Q. S. Quek, G. de la Roche, I. Guvenc, and M. Kountouris, *Small Cell Networks: Deployment, PHY Techniques, and Resource Allocation*. Cambridge University Press, May 2013.
- [7] S. Sesia, I. Toufik, and M. Baker, *LTE – The UMTS Long Term Evolution: From Theory To Practice*, 2nd ed. John Wiley, Aug. 2011.
- [8] E. Dahlman, S. Parkvall, and J. Sköld, *4G: LTE/LTE-Advanced for Mobile Broadband*. Elsevier, May 2011.
- [9] D. Astely, E. Dahlman, G. Fodor, S. Parkvall, and J. Sachs, “LTE release 12 and beyond,” *IEEE Commun. Mag.*, vol. 51, no. 7, pp. 154–160, Jul. 2013.
- [10] C. Lim, T. Yoo, B. Clerckx, B. Lee, and B. Shim, “Recent trend of multiuser MIMO in LTE-Advanced,” *IEEE Commun. Mag.*, vol. 51, no. 3, pp. 127–135, Mar. 2013.
- [11] Y. Chen, S. Zhang, S. Xu, and G.-Y. Li, “Fundamental trade-offs on green wireless networks,” *IEEE Commun. Mag.*, vol. 49, no. 6, pp. 30–37, Jun. 2011.

- [12] M. Bengtsson and B. Ottersten, *Optimal and Suboptimal Transmit Beamforming*. In: Handbook of Antennas in Wireless Communications, CRC Press, Aug. 2001.
- [13] H. Boche and M. Schubert, *Duality Theory for Uplink Downlink Multiuser Beamforming*. In: Smart Antennas – State-of-the-Art, Hindawi Publishing Corporation, Dec. 2005.
- [14] K. A. Gotsis and J. N. Sahalos, *Beamforming in 3G and 4G Mobile Communications: The Switched-Beam Approach*. In: Recent Developments In Mobile Communications - A Multidisciplinary Approach, InTech, Dec. 2011.
- [15] G. Dimic and N. D. Sidiropoulos, “On downlink beamforming with greedy user selection: Performance analysis and a simple new algorithm,” *IEEE Trans. Signal Process.*, vol. 53, no. 10, pp. 3857–3868, Oct. 2005.
- [16] J.-Q. Wang, D. J. Love, and M. D. Zoltowski, “User selection with zero-forcing beamforming achieves the asymptotically optimal sum rate,” *IEEE Trans. Signal Process.*, vol. 56, no. 8, pp. 3713–3726, Aug. 2008.
- [17] L.-N. Tran, M. Juntti, M. Bengtsson, and B. Ottersten, “Beamformer designs for MISO broadcast channels with zero-forcing dirty paper coding,” *IEEE Trans. Wireless Commun.*, vol. 12, no. 3, pp. 1173–1185, Mar. 2013.
- [18] C. Farsakh and J. A. Nossek, “Spatial covariance based downlink beamforming in an SDMA mobile radio system,” *IEEE Trans. Commun.*, vol. 46, no. 11, pp. 1497–1506, Nov. 1998.
- [19] D. Tse and P. Viswanath, *Fundamentals of Wireless Communication*. Cambridge University Press, Jul. 2005.
- [20] 3GPP, *E-UTRA: Physical Channels And Modulation (Release 11)*. 3GPP TS 36.211, V11.3.0, Jun. 2013.
- [21] H. Huang, C. B. Papadias, and S. Venkatesan, *MIMO Communication For Cellular Networks*. Springer, Nov. 2011.
- [22] H. Zhu, N. Prasad, and S. Rangarajan, “Precoder design for physical layer multicasting,” *IEEE Trans. Signal Process.*, vol. 60, no. 11, pp. 5932–5947, Nov. 2012.
- [23] M. Schubert and H. Boche, *QoS-Based Resource Allocation And Transceiver Optimization*. NOW Publishers Inc., Nov. 2005.

- [24] A. B. Gershman, N. D. Sidiropoulos, S. Shahbazpanahi, M. Bengtsson, and B. Ottersten, "Convex optimization-based beamforming: From receive to transmit and network designs," *IEEE Signal Process. Mag.*, vol. 27, no. 3, pp. 62–75, May 2010.
- [25] F. Rashid-Farrokhi, K. J. R. Liu, and L. Tassiulas, "Transmit beamforming and power control for cellular wireless systems," *IEEE J. Sel. Areas Commun.*, vol. 16, no. 8, pp. 1437–1450, Oct. 1998.
- [26] F. Rashid-Farrokhi, L. Tassiulas, and K. J. R. Liu, "Joint optimal power control and beamforming in wireless networks using antenna arrays," *IEEE Trans. Commun.*, vol. 46, no. 10, pp. 1313–1324, Oct. 1998.
- [27] H. Boche and M. Schubert, "A general duality theory for uplink and downlink beamforming," in *Proc. IEEE Vehicular Technology Conf. (VTC)*, Sep. 2002, pp. 87–91.
- [28] M. Schubert and H. Boche, "Solution of the multi-user downlink beamforming problem with individual SINR constraints," *IEEE Trans. Veh. Technol.*, vol. 53, no. 1, pp. 18–28, Jan. 2004.
- [29] E. Visotsky and U. Madhow, "Optimum beamforming using transmit antenna arrays," in *Proc. IEEE Vehicular Technology Conf. (VTC)*, May 1999, pp. 851–856.
- [30] D. Tse and P. Viswanath, "Downlink-uplink duality and effective bandwidths," in *Proc. IEEE Int. Symposium on Information Theory (ISIT)*, Jun. 2002, pp. 52–52.
- [31] A. Wiesel, Y. C. Eldar, and S. Shamai, "Linear precoding via conic optimization for fixed MIMO receivers," *IEEE Trans. Signal Process.*, vol. 54, no. 1, pp. 161–176, Jan. 2006.
- [32] W. Yu and T. Lan, "Transmitter optimization for the multi-antenna downlink with per-antenna power constraints," *IEEE Trans. Signal Process.*, vol. 55, no. 6, pp. 2646–2660, Jun. 2007.
- [33] H. Dahrouj and W. Yu, "Coordinated beamforming for the multicell multi-antenna wireless system," *IEEE Trans. Wireless Commun.*, vol. 9, no. 5, pp. 1748–1759, May 2010.
- [34] S. P. Boyd and L. Vandenberghe, *Convex Optimization*. Cambridge University Press, Mar. 2004.

- [35] R. D. Yates and C.-Y. Huang, "Integrated power control and base station assignment," *IEEE Trans. Veh. Technol.*, vol. 44, no. 3, pp. 638–644, Aug. 1995.
- [36] R. D. Yates, "A framework for uplink power control in cellular radio systems," *IEEE J. Sel. Areas Commun.*, vol. 13, no. 7, pp. 1341–1347, Sep. 1995.
- [37] K. Cumanan, R. Krishna, V. Sharma, and S. Lambotharan, "Robust interference control techniques for multiuser cognitive radios using worst-case performance optimization," in *Proc. Asilomar Conf. on Signals, Systems and Computers (Asilomar)*, Oct. 2008, pp. 378–382.
- [38] I. Wajid, M. Pesavento, Y. C. Eldar, and D. Ciochina, "Robust downlink beamforming with partial channel state information for conventional and cognitive radio networks," *IEEE Trans. Signal Process.*, vol. 61, no. 14, pp. 3656–3670, Jul. 2013.
- [39] D. Ciochina, M. Pesavento, and M. K. Wong, "Worst case robust beamforming on the Riemannian manifold," in *Proc. IEEE Int. Conf. on Acoustics, Speech and Signal Process. (ICASSP)*, May 2013, pp. 3801–3805.
- [40] K. L. Law, I. Wajid, and M. Pesavento, "Robust downlink beamforming in multi-group multicasting using trace bounds on the covariance mismatches," in *Proc. IEEE Int. Conf. on Acoustics, Speech and Signal Process. (ICASSP)*, Mar. 2012, pp. 3229–3232.
- [41] M. Botros and T. N. Davidson, "Convex conic formulations of robust downlink precoder designs with quality of service constraints," *IEEE J. Sel. Topics Signal Process.*, vol. 1, no. 4, pp. 714–724, Apr. 2007.
- [42] Y.-W. Huang, D. P. Palomar, and S.-Z. Zhang, "Lorentz-positive maps and quadratic matrix inequalities with applications to robust MISO transmit beamforming," *IEEE Trans. Signal Process.*, vol. 61, no. 5, Mar. 2013.
- [43] B. K. Chalise, S. Shahbazpanahi, A. Czylwik, and A. B. Gershman, "Robust downlink beamforming based on outage probability specifications," *IEEE Trans. Wireless Commun.*, vol. 6, no. 10, pp. 3498–3503, Oct. 2007.
- [44] M. B. Shenouda and T. N. Davidson, "Probabilistically-constrained approaches to the design of the multiple antenna downlink," in *Proc. Asilomar Conf. on Signals, Systems and Computers (Asilomar)*, Oct. 2008, pp. 1120–1124.

- [45] P.-J. Chung, H.-Q. Du, and J. Gondzio, "A probabilistic constraint approach for robust transmit beamforming with imperfect channel information," *IEEE Trans. Signal Process.*, vol. 59, no. 6, pp. 2773–2782, Jun. 2011.
- [46] C. Shen, T.-H. Chang, K.-Y. Wang, Z. Qiu, and C.-Y. Chi, "Distributed robust multicell coordinated beamforming with imperfect CSI: An ADMM approach," *IEEE Trans. Signal Process.*, vol. 60, no. 6, pp. 2988–3003, Jun. 2012.
- [47] K.-Y. Wang, T.-H. Chang, W.-K. Ma, A.-M.-C. So, and C.-Y. Chi, "Probabilistic SINR constrained robust transmit beamforming: A Bernstein-type inequality based conservative approach," in *Proc. IEEE Int. Conf. on Acoustics, Speech and Signal Process. (ICASSP)*, May 2011, pp. 3080–3083.
- [48] K.-Y. Wang, A.-M.-C. So, T.-H. Chang, W.-K. Ma, and C.-Y. Chi, "Outage constrained robust transmit optimization for multiuser MISO downlinks: Tractable approximations by conic optimization," *submitted to IEEE Trans. Signal Process.*, Aug. 2013. [Online]. Available: <http://arxiv.org/abs/1108.0982>
- [49] K. Eriksson, S. Shi, N. Vucic, M. Schubert, and E. G. Larsson, "Globally optimal resource allocation for achieving maximum weighted sum-rate," in *Proc. Global Telecommunications (GLOBECOM)*, Dec. 2010, pp. 1–6.
- [50] C. W. Tan, M. Chiang, and R. Srikant, "Maximizing sum rate and minimizing MSE on multiuser downlink: Optimality, fast algorithms and equivalence via max-min SINR," *IEEE Trans. Signal Process.*, vol. 59, no. 12, pp. 6127–6143, Dec. 2011.
- [51] L. Tran, M. Hanif, A. Tölli, and M. Juntti, "Fast converging algorithm for weighted sum rate maximization in multicell MISO downlink," *IEEE Signal Process. Lett.*, vol. 19, no. 12, pp. 872–875, Dec. 2012.
- [52] Q. Zhang, C. He, and L. Jiang, "Achieving maximum weighted sum-rate in multicell downlink MISO systems," *IEEE Commun. Lett.*, vol. 16, no. 11, pp. 1808–1811, Nov. 2012.
- [53] H.-J. Choi, S.-H. Park, S.-R. Lee, and I. Lee, "Distributed beamforming techniques for weighted sum-rate maximization in MISO interfering broadcast channels," *IEEE Trans. Wireless Commun.*, vol. 11, no. 4, pp. 1314–1320, Apr. 2012.
- [54] H. Al-Shatri and T. Weber, "Achieving the maximum sum-rate using D.C. programming in cellular networks," *IEEE Trans. Signal Process.*, vol. 60, no. 3, pp. 1331–1341, Mar. 2012.

- [55] P. Weeraddana, M. Codreanu, M. Latva-aho, A. Ephremides, and C. Fischione, *Weighted Sum-Rate Maximization in Wireless Networks: A Review*. NOW Publishers Inc., Sep. 2012.
- [56] P. Weeraddana, M. Codreanu, M. Latva-aho, and A. Ephremides, “Weighted sum-rate maximization for a set of interfering links via branch and bound,” *IEEE Trans. Signal Process.*, vol. 59, no. 8, pp. 3977–3996, Aug. 2011.
- [57] —, “Multicell MISO downlink weighted sum-rate maximization: A distributed approach,” *IEEE Trans. Signal Process.*, vol. 61, no. 3, pp. 556–570, Mar. 2013.
- [58] S. Joshi, P. Weeraddana, and et al., “Weighted sum-rate maximization for MISO downlink cellular networks via branch and bound,” *IEEE Trans. Signal Process.*, vol. 60, no. 4, pp. 2090–2095, Apr. 2012.
- [59] M. F. Hanif, L.-N. Tran, A. Tölli, M. Juntti, and S. Glisic, “Efficient solutions for weighted sum rate maximization in multicellular networks with channel uncertainties,” *submitted to IEEE Trans. Signal Process.*, Aug. 2013. [Online]. Available: <http://arxiv.org/abs/1301.0178>
- [60] C. A. Floudas and P. M. Pardalos, *Encyclopedia Of Optimization*, 2nd ed. Springer, Oct. 2008.
- [61] M. G. C. Resende and P. M. Pardalos, *Handbook Of Optimization In Telecommunications*. Springer, Feb. 2006.
- [62] E. Guney, N. Aras, I. K. Altinel, and C. Ersoy, “Efficient integer programming formulations for optimum sink location and routing in heterogeneous wireless sensor networks,” *Elsevier: Computer Networks*, vol. 54, no. 11, pp. 1805–1822, Aug. 2010.
- [63] A. Tramontani, “Enhanced mixed integer programming techniques and routing problems,” *4OR: A Quarterly Journal of Operations Research*, vol. 9, no. 3, pp. 325–328, Sep. 2011.
- [64] D. Yuan, *Integer Programming and Discrete Optimization with Applications to Telecommunications Networks*. PhD Course at National ICT Australia, Feb. 2012.
- [65] D. Yuan, V. Angelakis, L. Chen, E. Karipidis, and E. G. Larsson, “On optimal link activation with interference cancelation in wireless networking,” *IEEE Trans. Veh. Technol.*, vol. 62, no. 2, pp. 939–945, 2013.

- [66] H. Hijazi, P. Bonami, and A. Ouerou, "Robust delay-constrained routing in telecommunications," *Annals of Operations Research*, vol. 206, no. 1, pp. 163–181, Jul. 2013.
- [67] D.-S. Chen, R. G. Batson, and Y. Dang, *Applied Integer Programming: Modeling and Solution*. John Wiley, Sep. 2011.
- [68] J. Lee and S. Leyffer, *Mixed Integer Nonlinear Programming*. The IMA Volumes in Math. and its Applications, Springer, Jan. 2012.
- [69] Y. Pochet and L. A. Wolsey, *Production Planning by Mixed Integer Programming*. Springer, May 2006.
- [70] D. Gesbert, S. Hanly, and et al., "Multi-cell MIMO cooperative networks: A new look at interference," *IEEE J. Sel. Areas Commun.*, vol. 28, no. 9, pp. 1380–1408, Dec. 2010.
- [71] P. Marsch and G. P. Fettweis, *Coordinated Multi-Point in Mobile Communications: From Theory to Practice*. Cambridge University Press, Jul. 2011.
- [72] A. Papadogiannis, D. Gesbert, and E. Hardouin, "A dynamic clustering approach in wireless networks with multi-cell cooperative processing," in *Proc. IEEE Int. Conf. on Communications (ICC)*, May 2008, pp. 4033–4037.
- [73] J. Zhang, J. Andrews, A. Ghosh, and R. W. Heath Jr., "Networked MIMO with clustered linear precoding," *IEEE Trans. Wireless Commun.*, vol. 8, no. 4, pp. 1910–1921, Apr. 2009.
- [74] J.-M. Moon and D.-H. Cho, "Inter-cluster interference management based on cell-clustering in network MIMO systems," in *Proc. IEEE Vehicular Technology Conf. (VTC)*, May 2011, pp. 1–6.
- [75] Y. Zeng, E. Gunawan, Y. L. Guan, and J. Liu, "Joint base station selection and linear precoding for cellular networks with multi-cell processing," in *Proc. IEEE TENCON*, Nov. 2010, pp. 1976–1981.
- [76] S.-J. Kim, S. Jain, and G. B. Giannakis, "Backhaul-constrained multi-cell cooperation using compressive sensing and spectral clustering," in *Proc. IEEE Int. Workshop on Signal Process. Advances in Wireless Commun. (SPAWC)*, Jun. 2012, pp. 65–69.
- [77] M.-Y. Hong, R. Sun, H. Baligh, and Z.-Q. Luo, "Joint base station clustering and beamformer design for partial coordinated transmission in heterogeneous networks," *IEEE J. Sel. Areas Commun.*, vol. 31, no. 2, pp. 226–240, Feb. 2013.

- [78] C. T. K. Ng and H. Huang, "Linear precoding in cooperative MIMO cellular networks with limited coordination clusters," *IEEE J. Sel. Areas Commun.*, vol. 28, no. 9, pp. 1446–1454, Dec. 2010.
- [79] H.-T. Wai and W.-K. Ma, "A decentralized method for joint admission control and beamforming in coordinated multicell downlink," in *Proc. Asilomar Conf. on Signals, Systems and Computers (Asilomar)*, Nov. 2012, pp. 559–563.
- [80] W. Yu, T. Kwon, and C. Shin, "Multicell coordination via joint scheduling, beamforming, and power spectrum adaptation," *IEEE Trans. Wireless Commun.*, vol. 12, no. 7, pp. 1–14, Jul. 2013.
- [81] IBM, "IBM ILOG CPLEX optimization studio – CPLEX users manual v12.5.1," Jun. 2013.
- [82] S. Drewes, *Mixed Integer Second Order Cone Programming*. PhD thesis, Technische Universität Darmstadt, 2009.
- [83] E. Matakani, N. D. Sidiropoulos, Z.-Q. Luo, and L. Tassiulas, "Convex approximation techniques for joint multiuser downlink beamforming and admission control," *IEEE Trans. Wireless Commun.*, vol. 7, no. 7, pp. 2682–2693, Jul. 2008.
- [84] Y.-F. Liu, Y.-H. Dai, and Z.-Q. Luo, "Joint power and admission control via linear programming deflation," *IEEE Trans. Signal Process.*, vol. 61, no. 6, pp. 1327–1338, Mar. 2013.
- [85] J. Fan, Q. Yin, G. Y. Li, B. Peng, and X. Zhu, "MCS selection for throughput improvement in downlink LTE systems," in *Proc. ICCCN*, Aug. 2011.
- [86] A. Alexiou, C. Bouras, V. Kokkinos, A. Papazois, and G. Tsihrizis, "Modulation and coding scheme selection in multimedia broadcast over a single frequency network-enabled long-term evolution networks," *Int. J. Commun. Syst.*, vol. 8, no. 8, pp. 1–17, Aug. 2011.
- [87] F.-T. Chen and G.-L. Tao, "A novel MCS selection criterion for supporting AMC in LTE system," in *Proc. Int. Conf. on Computer Application and Syst. Modeling (IC-CASM)*, Oct. 2010.
- [88] D. I. Kim, E. Hossain, and V. K. Bhargava, "Dynamic rate and power adaptation for forward link transmission using high-order modulation and multicode formats in

- cellular wcdma networks,” *IEEE Trans. Wireless Commun.*, vol. 4, no. 5, pp. 2361–2372, Sep. 2005.
- [89] J. Tang and X. Zhang, “Quality-of-service driven power and rate adaptation over wireless links,” *IEEE Trans. Wireless Commun.*, vol. 6, no. 8, pp. 3058–3068, Aug. 2007.
- [90] L. Ding, F. Tong, Z. Chen, and Z. Liu, “A novel MCS selection criterion for VoIP in LTE,” in *Proc. Int. Conf. on Wireless Commun., Netw., and Mobile Computing (WiCOM)*, Sept. 2011.
- [91] S. Shamai and B. M. Zaidel, “Enhancing the cellular downlink capacity via co-processing at the transmitting end,” in *Proc. IEEE Vehicular Technology Conf. (VTC)*, May 2001, pp. 1745–1749.
- [92] G. J. Foschini, K. Karakayali, and R. A. Valenzuela, “Coordinating multiple antenna cellular networks to achieve enormous spectral efficiency,” *IEE Proc. of Commun.*, vol. 153, no. 4, pp. 548–555, Aug. 2006.
- [93] 3GPP, *E-UTRA: Further Advancements for E-UTRA Physical Layer Aspects (Release 9)*. 3GPP TS 36.814, V9.0.0, Mar. 2010.
- [94] R. Irmer, H.-P. Mayer, and et al., “Multisite field trial for LTE and advanced concepts,” *IEEE Commun. Mag.*, vol. 47, no. 2, pp. 92–98, Feb. 2009.
- [95] R. Irmer, H. Droste, and et al., “Coordinated multipoint: Concepts, performance, and field trial results,” *IEEE Commun. Mag.*, vol. 49, no. 2, pp. 102–111, Feb. 2011.
- [96] A. Tölli, H. Pennanen, and P. Komulainen, “Decentralized minimum power multi-cell beamforming with limited backhaul signaling,” *IEEE Trans. Wireless Commun.*, vol. 10, no. 2, pp. 570–580, Feb. 2011.
- [97] O. Gnuk and J. Linderoth, “Perspective reformulations of mixed integer nonlinear programs with indicator variables,” *Mathematical Programming*, vol. 124, pp. 183–205, Jul. 2010.
- [98] Y. Cheng, M. Pesavento, and A. Philipp, “Joint network optimization and downlink beamforming for CoMP transmissions using mixed integer conic programming,” *IEEE Trans. Signal Process.*, vol. 61, no. 16, pp. 3972–3987, Aug. 2013.

- [99] Y. Cheng, S. Drewes, A. Philipp, and M. Pesavento, "Joint network optimization and beamforming for coordinated multi-point transmission using mixed integer programming," in *Proc. IEEE International Conf. on Acoustics, Speech and Signal Process. (ICASSP)*, May 2012, pp. 3217–3220.
- [100] —, "Joint network topology optimization and multicell beamforming using mixed integer programming," in *Proc. International ITG Workshop on Smart Antennas (WSA)*, Mar. 2012, pp. 187–192.
- [101] G. Micallef, P. Mogensen, and H.-O. Sheck, "Cell size breathing and possibilities to introduce cell sleep mode," in *European Wireless Conf. (EWC)*, Apr. 2010, pp. 111–115.
- [102] E. Oh and B. Krishnamachari, "Energy savings through dynamic base station switching in cellular wireless access networks," in *Proc. IEEE Global Telecommunications Conf. (GLOBECOM)*, Dec. 2010, pp. 1–5.
- [103] A. Chatzipapas, S. Alouf, and V. Mancuso, "On the minimization of power consumption in base stations using on-off power amplifiers," in *Proc. IEEE Online Conf. on Green Commun. (GreenCom)*, Sep. 2011, pp. 18–23.
- [104] O. Arnold, F. Richter, G. P. Fettweis, and O. Blume, "Power consumption modeling of different base station types in heterogeneous cellular networks," in *Proc. Future Network and Mobile Summit*, Jun. 2010, pp. 1–8.
- [105] M. S. Lobo, L. Vandenberghe, S. P. Boyd, and H. Lebert, "Applications of second-order cone programming," *Linear Algebra and its Applications*, vol. 284, no. 1, pp. 193–228, Nov. 1998.
- [106] H. Holma and A. Toskala, *LTE for UMTS: OFDMA and SC-FDMA Based Radio Access*. John Wiley, Apr. 2009.
- [107] K. Leung and L. Wang, "Integrated link adaptation and power control to improve error and throughput performance in wireless packet networks," *IEEE Trans. Wireless Commun.*, vol. 1, no. 4, pp. 619–629, Oct. 2002.
- [108] A. M. Gjendemsjø, *Rate Adaptation, Power Control, and Diversity Combining in Wireless Systems*. PhD thesis, Norwegian Univ. of Science and Technol., 2007.

- [109] M. Butussi and M. Bengtsson, “Low complexity admission in downlink beamforming,” in *Proc. IEEE Int. Conf. on Acoustics, Speech and Signal Process. (ICASSP)*, 2006.
- [110] K. Cumanan, R. Krishna, L. Musavian, and S. Lambotharan, “Joint beamforming and user maximization techniques for cognitive radio networks based on branch and bound method,” *IEEE Trans. Wireless Commun.*, vol. 9, no. 10, pp. 3082–3092, Oct. 2010.
- [111] L. Yu, E. Karipidis, and E. G. Larsson, “Coordinated scheduling and beamforming for multicell spectrum sharing networks using branch and bound,” in *Proc. European Signal Process. Conf. (EUSIPCO)*, Aug. 2012, pp. 819–823.
- [112] D. Ciochina and M. Pesavento, “Joint user selection and beamforming in interference limited cognitive radio networks,” in *Proc. European Signal Process. Conf. (EUSIPCO)*, Aug. 2012, pp. 1389–1393.
- [113] Y. Cheng, A. Philipp, and M. Pesavento, “Dynamic rate adaptation and multiuser downlink beamforming using mixed integer conic programming,” in *Proc. European Signal Process. Conf. (EUSIPCO)*, Aug. 2012, pp. 824–828.
- [114] H.-T. Wai, Q. Li, and W.-K. Ma, “A convex approximation method for multiuser MISO sum rate maximization under discrete rate constraints,” in *Proc. IEEE Int. Conf. Acoustics, Speech and Signal Process. (ICASSP)*, May 2013, pp. 4759–4763.
- [115] Y. Cheng and M. Pesavento, “Joint rate adaptation and downlink beamforming using mixed integer conic programming,” *submitted to IEEE Trans. Signal Process.*, Jun. 2013.
- [116] W. F. Trench, *Introduction to Real Analysis*. Free Hyperlinked Edition, Nov. 2012.
- [117] C.-B. Chae, D. Mazzarese, T. Inoue, and R. W. Heath Jr., “Coordinated beamforming for the multiuser MIMO broadcast channel with limited feedforward,” *IEEE Trans. Signal Process.*, vol. 56, no. 12, pp. 6044–6056, 2008.
- [118] L. Soriano-Equigua, J. Sanchez-Garcia, J. Flores-Troncoso, and R. W. Heath Jr., “Noniterative coordinated beamforming for multiuser MIMO systems with limited feedforward,” *IEEE Signal Process. Lett.*, vol. 18, no. 12, pp. 701–704, 2011.
- [119] H.-H. Lee and Y.-C. Ko, “Low complexity codebook-based beamforming for MIMO-OFDM systems in millimeter-wave WPAN,” *IEEE Trans. Wireless Commun.*, vol. 10, no. 11, pp. 3607–3612, Nov. 2011.

- [120] J. Zhu and H.-C. Yang, "Sum-rate analysis of multiuser MIMO systems with codebook-based incremental beamforming," in *Proc. IEEE Vehicular Technology Conf. (VTC)*, Sep. 2010, pp. 1–5.
- [121] M. Bengtsson and B. Ottersten, "Optimal downlink beamforming using semidefinite optimization," in *Proc. Annual Allerton Conf. on Commun. Control and Computing (Allerton)*, vol. 37, Sep. 1999, pp. 987–996.
- [122] M. Chiang, P. Hande, T. Lan, and C. W. Tan, *Power Control in Wireless Cellular Networks*. NOW Publishers Inc., Jul. 2008, vol. 2, no. 4.
- [123] H. R. Feyzmahdavian, M. Johansson, and T. Charalambous, "Contractive interference functions and rates of convergence of distributed power control laws," *IEEE Trans. Wireless Commun.*, vol. 11, no. 12, pp. 4494–4502, Dec. 2012.
- [124] Y. Cheng and M. Pesavento, "An optimal iterative algorithm for codebook-based downlink beamforming," *IEEE Signal Process. Lett.*, vol. 20, no. 8, pp. 775–778, Aug. 2013.
- [125] ———, "Predistortion and precoding vector assignment in codebook-based downlink beamforming," in *Proc. IEEE International Workshop on Signal Process. Advances for Wireless Commun. (SPAWC)*, Jun. 2013, pp. 440–444.
- [126] ———, "Joint optimization of source power allocation and distributed relay beamforming in multiuser peer-to-peer relay networks," *IEEE Trans. Signal Process.*, vol. 60, no. 6, pp. 2962–2973, Jun. 2012.
- [127] R. Horst and N. V. Thoai, "DC programming: Overview," *J. Optim. Theory Appl.*, vol. 103, no. 1, pp. 1–43, Oct. 1999.
- [128] D. H. Brandwood, "A complex gradient operator and its application in adaptive array theory," *IEE Proceedings of Commun., Radar and Signal Process.*, vol. 130, no. 1, pp. 11–16, Feb. 1983.
- [129] S. Haykin, *Adaptive Filter Theory*, 4th ed. Prentice-Hall, Sep. 2001.
- [130] H. Li and T. Adali, "Complex-valued adaptive signal processing using nonlinear functions," *EURASIP Journal on Advances in Signal Process.*, vol. 2008, pp. 1–9, Feb. 2008.

- [131] N. Vucic and H. Boche, "Robust QoS-constrained optimization of downlink multiuser MISO systems," *IEEE Trans. Signal Process.*, vol. 57, no. 2, pp. 714–725, Feb. 2009.
- [132] G. Zheng, K. K. Wong, and B. Ottersten, "Robust cognitive beamforming with bounded channel uncertainties," *IEEE Trans. Signal Process.*, vol. 57, no. 12, pp. 4871–4881, Dec. 2009.
- [133] L. Zhang, Y. C. Liang, Y. Xin, and H. V. Poor, "Robust cognitive beamforming with partial channel state information," *IEEE Trans. Wireless Commun.*, vol. 8, no. 8, pp. 4143–4153, Aug. 2009.
- [134] E. A. Gharavol, Y. C. Liang, and K. Moutaan, "Robust downlink beamforming in multiuser MISO cognitive radio networks with imperfect channel-state information," *IEEE Trans. Veh. Technol.*, vol. 59, no. 6, pp. 2852–2860, Jun. 2010.
- [135] M. Biguesh, S. Shahbazpanahi, and A. B. Gershman, "Robust downlink power control in wireless cellular systems," *EURASIP J. Wireless Commun. and Netw.*, vol. 2004, no. 2, pp. 261–272, Dec. 2004.
- [136] J. F. Bard, *Practical Bilevel Optimization: Algorithms and Applications*. Springer, Feb. 1999.
- [137] Y. Cheng and M. Pesavento, "Robust codebook-based downlink beamforming using mixed integer conic programming," in *Proc. Proc. IEEE International Conf. on Acoustics, Speech and Signal Process. (ICASSP)*, May 2013, pp. 4187–4191.
- [138] N. Bornhorst and M. Pesavento, "Beamforming for multi-group multicasting with statistical channel state information using second-order cone programming," in *Proc. IEEE Int. Conf. on Acoustics, Speech and Signal Process. (ICASSP)*, Mar. 2012, pp. 3237–3240.
- [139] J. G. Andrews, S. Singh, Q. Ye, X. Lin, and H. Dhillon, "An overview of load balancing in HetNets: Old myths and open problems," *submitted to IEEE Commun. Mag.*, Jul. 2013. [Online]. Available: <http://arxiv.org/abs/1307.7779>
- [140] I. Siomina, D. Yuan, and F. Gunnarsson, *Automated Optimization In HSDPA Radio Network Planning*. In: Handbook of HSDPA/HSUPA Technology, CRC press, Oct. 2010.

- [141] D. Wei and A. V. Oppenheim, “A branch-and-bound algorithm for quadratically-constrained sparse filter design,” *IEEE Trans. Signal Process.*, vol. 61, no. 4, pp. 1006–1018, Feb. 2013.
- [142] Y. C. Eldar and G. Kutyniok, *Compressed Sensing: Theory and Applications*. Cambridge University Press, May 2012.

List of abbreviations

3G	Third generation (cellular networks)
3GPP	Third generation partnership project
4G	Fourth generation
AMC	Adaptive modulation and coding
AFSA	Alternating feasibility search algorithm
AO	Alternating optimization
ATOA	Alternating optimization algorithm
BI-MIP	Bi-level mixed-integer program (programming)
BLER	Block error rate
BMC	Big-M continuous relaxation
BMI	Big-M integer (formulation)
BnB	Branch-and-bound
BnC	Branch-and-cut
bpcu	Bits per channel use
BS	Base station
CAPEX	Capital expenditures
CBCP	Codebook-based downlink beamforming and channel predistortion
CCM	Channel covariance matrix
CoMP	Coordinated multi-point
CPN	Central processing node
CSI	Channel state information
DRAB	Discrete rate adaptation and downlink beamforming
DL	Downlink
EMC	Extended continuous relaxation
EMI	Extended integer (formulation)
Eq.	Equation
Eqs.	Equations

FDD	Frequency-division duplex
GLB	Global lower bound
GUB	Global upper bound
ICI	Inter-cell interference
ICT	Information and communications technology
JNOB	Joint network optimization and multi-cell downlink beamforming
LHS	Left-hand-side
LTE	Long-term evolution
LTE-A	Long-term evolution advanced
MCS	Modulation and coding scheme
MILP	Mixed-integer linear program/programming
MINLP	Mixed-integer nonlinear program/programming
MIP	Mixed-integer program/programming
MISDP	Mixed-integer semidefinite program/programming
MISOCP	Mixed-integer second-order cone program/programming
MS	Mobile station
NP hard	Non-deterministic polynomial-time hard
OPEX	Operational expenditures
PA	Power amplifier
PC	Personal computer
PSD	Positive semidefinite
QAM	Quadrature amplitude modulation
QoS	Quality-of-service
QPSK	Quadrature phase-shift keying
RCBA	Robust codebook-based downlink beamforming and admission control
RHS	Right-hand-side
SCBF	Standard codebook-based downlink beamforming
SDMA	Space-division multiple access
SIF	Standard interference function
SINR	Signal-to-interference-plus-noise ratio
SDP	Semidefinite program/programming
SOC	Second-order cone
SOCP	Second-order cone program/programming
s.t.	Subject to
TDD	Time-division duplex
UL	Uplink
VUL	Virtual uplink

Curriculum vitae

Personal information

Full name: Yong Cheng
Date of birth: Sep. 03, 1983
Nationality: P. R. China
Marital status: Married

Educations

Nov. 2010 – Present Ph.D. student in the Communication Systems Group,
Technische Universität Darmstadt, Germany
Aug. 2008 – Jun. 2010 M.Phil. in the Dept. of Elec. & Computer Eng.,
Hong Kong University of Science & Technology, Hong Kong
Oct. 2002 – Jun. 2006 B.Eng. (1st honors) in the Dept. of Info. Science & Elec. Eng.,
Zhejiang University, Hangzhou, P. R. China

Work experiences

Nov. 2010 – Present Research Assistant in the Communication Systems Group,
Technische Universität Darmstadt, Germany
Apr. 2009 – Jun. 2010 Research Assistant in the Huawei-HKUST Innovation Lab,
Hong Kong University of Science & Technology, Hong Kong
Jul. 2006 – Jul. 2008 Research Assistant in the Dept. of Info. Science & Elec. Eng.,
Zhejiang University, Hangzhou, P. R. China

Supervision and teaching

Master theses supervised:

- Ganapati Hegde, “Coordinated Interference Management and Load Balancing in Heterogeneous Cellular Networks”, Dept. of Electrical Engineering and Information Technology, Technische Universität Darmstadt, Feb. 2014 (expected).
- Nagasubramanian Viswanathan, “Coordinated Beamforming in Heterogeneous Networks with Limited CSI Feedback”, Dept. of Electrical Engineering and Information Technology, Technische Universität Darmstadt, Jun. 2013.
- Sufyan Siddique, “Distributed Beamforming in OFDM Peer-to-Peer Relay Networks”, Dept. of Electrical Engineering and Information Technology, Technische Universität Darmstadt, May 2012.

Bachelor theses supervised:

- Kilian Kiekenap, “Precoding Vector Assignment, Power Allocation, and Channel Pre-distortion in Codebook-based Downlink Beamforming”, Dept. of Electrical Engineering and Information Technology, Technische Universität Darmstadt, Proseminar report, Dec. 2013.

Teaching experiences:

- Teaching assistant of the lecture “Information Theory II”, Dept. of Electrical Engineering and Information Technology, Technische Universität Darmstadt, Summer Semester, 2013.
- Teaching assistant of the lecture “Information Theory II”, Dept. of Electrical Engineering and Information Technology, Technische Universität Darmstadt, Summer Semester, 2012.

